THE EFFECT OF CONFINING PRESSURE ON THE POST-YIELD DEFORMATION CHARACTERISTICS OF ROCKS

A Thesis submitted for the degree of
Doctor of Philosophy in Engineering
in the
University of Newcastle upon Tyne

by

A. M. PRICE, B.Sc. (Hons.)

SEPTEMBER 1979

To my wife, on our Anniversary

- something paper.

* * *

"There are mines where silver is dug;
There are places where gold is refined.
Men dig iron out of the ground
And melt copper out of the stones.
Men explore the deepest darkness
They search the depths of the earth
And dig for rocks in the darkness.
Far from where anyone lives
Or human feet ever travel,
Men dig the shafts of mines.
They work in loneliness,
Clinging to ropes in the pits.
Food grows out of the earth,
But underneath the same earth
All is torn up and crushed.
The stones of the earth contain sapphires,
And its dust contains gold.
No hawk sees the roads to the mines,
And no vulture ever flies over them.
No lion or other fierce beast
Ever travels those lonely roads.
Men dig the hardest rocks,
Dig mountains away at their base.
As they tunnel through the rocks,
They discover precious stones.
They dig to the sources of rivers
And bring to light what is hidden.
But where can wisdom be found?
Where can we learn to understand?"

- Job 28 : 1-12 (G.N.B.)

* * *

ACKNOWLEDGEMENTS

I would like to thank:

- Professor E.L.J. Potts for providing the opportunity and facilities for carrying out the research described in this thesis.

- Dr. I.W. Farmer for his advice and encouragement throughout the period of this research, and especially in the preparation of this thesis.

- The National Coal Board and Science Research Council for finance.

- Mr. King and Mr. Errington of Woodhorn Colliery, Mr. Findlay of the Nature Conservancy, and Dr. Ashwin of M.R.D.E.

- Mr. A. Szeki and Dr. E.K.S. Passaris for their interest and advice.

- The Department's technical staff for their help and constant advice, and, especially, the late Mr. T. Pollock.

- My postgraduate colleagues: N.Wise, M.Gilbert, R. Fauvel, S. Horseman and J. Armstrong, for their help in various matters, and, especially, S. Watson, for the use of his P.A.D.A.S. computing package.

- Mrs. Edna Gannie for typing the script and Mr. Rob Liddell for its reproduction.

- My wife for her patience and constant encouragement.

* * *

THE EFFECT OF CONFINING PRESSURE ON THE POST-YIELD DEFORMATION CHARACTERISTICS OF ROCKS

ADDENDUM

A.M.PRICE

TEXT

Page 6.3, section 6.2.4, line 11 "offeres" should read "offers".

Page 9.6, parag. 3, line 2 "Scholtz" should read "Scholz".

Page 9.7, parag. 1, line 8/9 "plots data" should read "both plots".

Page 10.2, eqn. 10.1 should read "$\sigma_1+\sigma_3=2q$" (also in fig. 10.1)

Page 10.5, eqn. 10.9 should read "$\sigma_1=k\sigma_3+\sigma_c$"

Page 13.2, line 2 "mineral" should read "Mining"

Throughout "MN/m^{-2}" should read "$MN\ m^{-2}$"

FIGURES

1.1	"Peak Stregth" should read "Peak Strength"
8.3	The top curve is "$\sigma_3=28\ MN/m^2$"
8.7-8.12 A6 - A7	"Sacroidal" should read "Saccharoidal"
8.7	The top curve is "$\sigma_3=42\ MN/m^2$"
8.10	"$\sigma_3=25$" should read "$\sigma_3=28$"
8.11	"16" on the $\Delta v/v$ axis should read "-16"
8.14	the bottom curve is "$\sigma_3=0$" and "$\sigma_3=0$" should read "$\sigma_3=4$"
8.20	Y axis: "Lateral Strain (%)" X axis: "Axial Strain (%)" The curves from top to bottom are "$\sigma_3=0,4,7,21$ and 36" respectively.
8.23 8.26	should read "All values of σ_3 are in MN/m^2"
8.27	should include "All values of σ_3 are in MN/m^2"
8.34	Y axis: "Poisson's Ratio"
9.5	P has units "N/mm^2", "$\sigma_1=\sigma_3$" should read "$\sigma_1=2\sigma_3$"
9.6	Top curve: "$\sigma_1=3\sigma_3$" Bottom curve: "$\sigma_1=2\sigma_3$"
9.9b	Y axis: "q"
11.3	"-0.5" and "-0.25" should be exchanged.

CONTENTS

* * *

ABSTRACT

A research program into the dilatancy of Coal Measures and Coal Measures type rocks, deformed beyond the elastic range, both up to, at and beyond the point of rupture, is outlined. Detailed descriptions of a 500 ton servo-controlled testing machine, and an apparatus for the laboratory measurement of volumetric strains in rock are given. The results of triaxial, compressive tests, conducted on specimens of seven rock types, compressed axially to strains in excess of ten percent, using this equipment, are presented. A review of the critical state model for soils is given, and a similar model for rocks is proposed, based on the experimental results obtained. The application of the measured volumetric changes of the rocks to the prediction of roadway closure, using yield zone analysis, is considered and the limitations of such analyses when considering stratified deposits discussed in conjunction with several case studies.

* * *

LIST OF ILLUSTRATIONS

PLATES

CHAPTER FIVE

CHAPTER SIX

CHAPTER SEVEN

CHAPTER EIGHT

* * *

FIGURES

CHAPTER ONE

CHAPTER THREE

CHAPTER FOUR

CHAPTER FIVE

CHAPTER SIX

CHAPTER EIGHT (Portland Stone)

Saccharoidal Limestone

Sandstone

Silty Sandstone

Mudstone

APPENDIX A (contd) (Portland Stone)

Fig. A.4 Volumetric versus axial strain at a confining pressure of 14 MN m^{-2}.

Fig. A.5 Volumetric versus axial strain for confining pressures of 21 and 28 MN m^{-2}.

Saccharoidal Limestone

Fig. A.6 Comparison of lateral versus axial strains for different confining pressures.

Fig. A.7 Comparison of Poisson's ratio versus axial strains for confining pressures of 35 and 42 MN m^{-2}.

Sandstone

Fig. A.8 Comparison of axial stress versus strain for confining pressures of 7 and 14 MN m^{-2}.

Fig. A.9 Comparison of volumetric versus axial strain for confining pressures of 7 and 14 MN m^{-2}.

Fig. A.10 Comparison of lateral versus axial strain for confining pressures of 7 and 14 MN m^{-2}.

Fig. A.11 Comparison of Poisson's ratio versus axial strain for confining pressures of 14 and 7 MN m^{-2}.

Silty Sandstone

Fig. A.12 Comparison of volumetric versus axial strain for confining pressures of 29 and 42 MN m^{-2}.

Fig. A.13 Comparison of lateral versus axial strain for confining pressures of 42 and 29 MN m^{-2}.

Fig. A.14 Comparison of Poisson's ratio versus axial strain for confining pressures of 29 and 42 MN m^{-2}

Mudstone

Fig. A.15 Volumetric versus axial strain for different confining pressures.

Fig. A.16 Comparison of lateral versus axial strain for different confining pressures.

Fig. A.17 Comparison of Poisson's ratio versus axial strain for confining pressures of 21, 28 and 35 MN m^{-2}.

Rock Salt

Fig. A.18 Comparison of lateral versus axial strains for confining pressures of 21, 28 and 35 MN m^{-2}.

Fig. A.19 Poisson's ratio versus axial strain for confining pressures of 14 and 35 MN m^{-2}.

* * *

INTRODUCTION

Almost a century ago Reynolds (1885) observed that, if a granular mass, such as sand, was distorted, it experienced a definite "change of shape or distortional strain" – this property he termed dilatancy. Since then, there have been several studies into the dilatant behaviour of granular masses and rocks. Research concerned with the latter has been limited to the pre-failure and post-failure, strain hardening cases only and applications of the findings generally only concerned with earthquake prediction.

As mine workings have increased in depth in search of new reserves and increased production, it has become impossible to avoid stress levels sufficient to cause rock failure and thus dilation. It was for this reason that Kirmani (1972) recommended that laboratory studies be undertaken into the behaviour and stability of failed rock around roadways. Since the advent of stiff and servo-controlled testing machines, monitoring of the post-failure behaviour of rocks has become a possibility, and much work has been carried out in this field. In May 1973, a 500 ton servo-controlled testing machine was installed in the Department of Mining Engineering of the University of Newcastle upon Tyne.

In 1976 the Department was approached by M.R.D.E. to undertake a research program into the dilatancy of Coal Measure rocks, deformed beyond the elastic range, both up to, at, and beyond the point of rupture. The knowledge gained from this work was to be related, if possible, to the expansion of rock into an underground opening, due

to its failure. The opening was assumed to be a circular, horizontal roadway in a homogeneous, isotropic rock mass. The program involved the measurement of volumetric changes in a variety of coal measures and coal measures type rocks, deformed axially by approximately 10 percent strain, under conditions of triaxial confinement. Its main aim was to gain a greater understanding of the mechanism of dilatancy, especially in strain softening rocks, and to apply it to the closure of mine roadways due to the failure of the surrounding rock.

Seven rock types were tested: sandstone, silty sandstone, mudstone, Portland stone, saccharoidal limestone, marl and rock salt. However, due to the limited number of specimens obtainable, the results must be regarded as qualitative rather than quantitative in nature. The rock salt and marl specimens were tested in order to simulate the behaviour of the more 'plastic' coal measure rocks.

The research program included the 'setting up' and 'debugging' of the Department's servo-controlled testing machine, and the design of triaxial testing system allowing the measurement of large and sudden volume changes. This thesis describes the testing system and the design of the triaxial apparatus, and outlines the advantages and disadvantages of both. The mechanism of rock failure is reviewed, as is the available literature on laboratory testing, especially the existing information on dilatancy and its measurement. The experiments and results are described, and are applied to the formulation of a critical state model for rocks, based upon Schofield and Wroth's original model for soils, and to yield zone analysis and roadway closure.

Finally, the limitations of the latter, when considering stratified deposits, are discussed and illustrated with case studies.

* * *

CHAPTER ONE

MECHANISM OF ROCK FAILURE

1.0 Introduction

Rocks, both on a laboratory and massive scale, deform and fracture through the extension of flaws which exist in the original rock fabric. Griffith (1921), through studies on the tensile loading of glass, developed the classical theoretical model for the process, proposing that:

(a) crack extension would be initiated by high tensile stresses at the tips of flaws,

(b) cracks would extend in a direction normal to the direction of maximum tensile stress and

(c) cracks would extend when the tip stress was sufficient to satisfy the energy requirements of the newly created crack surfaces.

Since it has been shown that dilatancy is the result of this internal microfracturing prior to fracture (section 1.3) and not some periphery phenomenon, e.g. spalling (Cook, 1970), it is important to begin this thesis by outlining the mechanism of rock behaviour and breakdown up to and beyond its maximum load-bearing capacity. This is probably best done by examining a hypothetical axial stress-strain curve. Therefore, following the lead of a host of others[1], the

---

[1] Bieniawski (1967a,b); Bieniawski *et al.* (1969); Kumar (1968); Brace (1969); Brady (1969); Lane (1969); Wawersik and Fairhurst (1970); Wawersik and Brace (1971); Attewell and Farmer (1972, 1976); Bordia (1972); Peng and Podnieks (1972); Hallbauer *et al.* (1973); Hoshino and Koide (1970); Scholz (1970); Tapponier and Brace (1976).

mechanism of brittle rock fracture has been summarised in Fig. 1.1 and Table 1.1. On this stress-strain curve, six stages in the breakdown mechanism have been isolated. The stress-strain curve passes through regions I to IV prior to reaching its maximum value for the axial stress, or peak strength then region V involves the growth of macrofactures, causing division of the specimen into two or more blocks, and finally, region VI describes the mechanism of interaction between the blocks forming this new structure.

1.1 Region I

It is widely agreed (see, for example, Kumar, 1968; Brady, 1969; Bieniawski, 1967a,b; Hoshino and Koide, 1970) that when a rock specimen is initially stressed, any pre-existing microcracks or pore space orientated at suitable angles to the applied stress will close, and this is indicated by an initial non-linearity of the axial stress-strain curve. There may also be some compaction of any soft intrusions in the rock, and if the specimen is loaded unevenly, some localised fracturing.

1.2 Region II

In this stage of the breakdown, the rock has a constant elastic modulus and is assumed to deform in a perfectly elastic manner. Brady (op. cit.)sets the upper boundary of this region as the point at which internal microcracking initiates. Others (Bieniawski, 1967a,b; Hoshino and Koide, 1970), however, suggest that microcracking initiates in this region and Hoek and Bieniawski (1966) propose a mechanism of stick-slip along the previously closed microcracks (see also Morgenstern and Phukan, 1966, 1969).

1.3 Region III

This is generally accepted as the region of stable fracture propagation (Bieniawski, 1967a,b; Hallbauer et al., 1973; Attewell and Farmer, 1976), although Scholz (1970) proposes otherwise, in which microcracking events occur independently of each other, throughout the specimen. It is this microcracking which causes a volume increase of the specimen, and the onset of dilatancy, as shown in the plot of axial stress versus volumetric strain (Fig.1.1)[1]. The occurrence of these microcracking events is also reflected in the plot of frequency of seismic events (emanating from the forming microcracks) versus axial strain (also shown in Fig.1.1) (Scholz, 1968a; Cook, 1965) Therefore, region III is bounded initially by the point of microcrack initiation and latterly by the point of maximum compaction (Fig.1.1) or the point of 'critical energy release' (Bieniawski (1967a,b).

1.4 Region IV

As illustrated by all three curves in Fig.1.1 region IV is marked by a rapid acceleration of microcracking events and, consequently, volume increase. This microcracking or 'dynamic cracking'(Scholz, 1968b) activity is no longer independent, but gathers in clusters of crack arrays in the region of the resultant fault plane (Bieniawski, 1967a); Scholz, 1968b, 1970). Here, the rock sample will accelerate towards strength failure, unless the acting axial stress is reduced to below the value for the onset of this region which is, therefore, generally believed (Bieniawski, 1967a; Attewell and Farmer, 1972) to mark the long term strength of the rock. However, Sangha and Dhir (1972) deny

---

[1] Brace et al. (1966); Scholz (1967,1968,1970); Bridgeman (1949); Rothman (1975); Haimson (1974); Brady (1975); Ismail and Murrell (1976).

this and state that:

> "... for a range of stresses exceeding 'critical stress' the material is capable of forming a new microstructure which can withstand these stresses indefinitely."

They take a stress level at which the incremental Poisson's ratio becomes 0.5 as the 'critical stress'.

1.5 Region V

The rock sample has now passed its peak strength or load bearing capacity, but it is, however, still intact, even though its internal structure is highly disrupted. In this final pre-failure stage, the crack arrays fork and coalesce into macrocracks or faults.

1.6 Region VI

Once faults have formed the rock sample is better thought of as a system of 'blocks' rather than an intact structure. These 'blocks' will interact with each other and the predominant deformation mechanism will be dependent upon the friction between them. Secondary macrocracking may also occur due to differential shearing along these fault planes and possibly also as a result of bending moments acting upon some areas of the specimen. In this region the axial stress[1] acting on the rock specimen will reduce to a constant value - the residual strength of the rock. In a uniaxial test the formation of the fault might also mark the point of rupture, where the sample loses any cohesion it had as a structure or system and falls apart.

---

[1] Whilst I accept Brady et al.'s (1973) findings that it is the axial load that reduces due to the disintegration of the specimen, and not the stress, I have continued to use stress-strain values for ease of comparison between tests.

1.7 Friction in Region VI

Much work has been carried out in this area of rock breakdown and two types of frictional sliding have been identified. These are:

(a) 'stable sliding' in which the blocks slide relative to each other with a smooth movement and

(b) 'stick-slip' characterised by bursts of accelerated sliding and drops in the axial stress acting upon the specimen.

Typical examples of both forms of frictional sliding are given in Fig.1.2 (e.g. Brace, 1972; Brace and Byerlee, 1966; Engelder and Scholz, 1976; Swanson and Brown, 1971).

Various factors have been reported as influencing the frictional behaviour of rock, but often different researchers have contradicted each other in their findings. However, some general principles can be drawn from their work:

(a) At low normal stresses and in the absence of gouge, stick-slip will be favoured on smooth, rather than rough, surfaces (Dieterich, 1972).

(b) On rough surfaces, stick-slip is more likely to occur under conditions of high normal pressure (Byerlee and Brace, 1968).

(c) The influence of gouge between the sliding surfaces is more widely reported to inhibit stick-slip

behaviour (Jackson and Dunn (1974); Scholz et al. (1972); Byerlee and Summers (1976); Drennon and Handy (1972); but see also Dieterich (1972), who reports the opposite phenomenon).

(d) Increasing normal stress enhances stick-slip provided that the brittle/ductile transition is not exceeded (Brace (1972); Byerlee and Brace (1968); Drennon and Handy (1972); Engelder (1974); Engelder et al. (1975); Scholz et al. (1972)).

(e) Increased strain rate will inhibit or suppress stick-slip behaviour (Engelder et al. (1975); Scholz et al. (1972); Scholz and Engelder (1976)).

(f) There is evidence which would suggest that stick-slip is also inhibited by the presence of certain minerals (Brace (1972)).

There are other factors which influence the frictional behaviour of rock which are not covered here, such as temperature, fluids and rock properties; for example, porosity (see Brace, 1972). Normally, frictional sliding will result in the formation of gouge, varying in both distribution and quantity. Examination of both the gouge and the sliding surfaces will also reveal various other features, such as shear bands, coarse striations, slickensides and steps (Paterson, 1958; Gay, 1972; Lindstrom, 1974; Byerlee et al. 1978). Dilatancy observed with sliding surfaces, is found as a displacement normal to the

direction of sliding and is generally accepted as being caused by movement over asperities or volume changes within the gouge layers formed (Barton, 1973,1976; Schneider, 1974,1976; Scholz et al.,1972; Rengers, 1970).

1.8 Failure Mechanisms

Various workers[1] have outlined different failure mechanisms which occur in rock breakdown. These can be readily grouped under the following three classifications:

1. Cataclasis – or microcracking. This mechanism may take several forms, e.g. inter- or intra-grain microcracking, grain rotation, sliding, and microcrushing. Microcracking can be caused by simple crack extension or can result from tensile stresses created by other deformation mechanisms (see, for example, Olsson and Peng, 1976 and Tapponier and Brace, 1976).

2. Intracrystalline Gliding. This is often found upon close examination of the specimen in the form of twinning or translation gliding, and may cause distortion of the grains (e.g. Brace and Riley,1972).

3. Recrystallisation. Recrystallisation involves the displacement of dislocations within the rock structure, similar to that observed widely in metals.

---

[1] Donath and Fruth (1971); Brace and Riley (1972); Handin et al.(1957); Engelder (1974); Burdine (1963); Rummel and Fairhurst (1970).

In practice, however, the actual failure mechanism is often a complicated interaction of these three[1], and is dependent upon the imposed experimental conditions.

1.9 Failure Types

Several researchers[2] have recorded various categories of failure types for both strain-hardening and strain-softening behaviour. These can be summarised into six types:

1. Cataclasis This is characterised by an overall disintegration of the grain network within the rock structure, often leaving intact end cones and periphery splinters.

2. Columnar This type of failure is the result of tensile failure, often induced by the inclusion of friction reducers between the specimen and loading platens, and appears as one or more axial, tensile cracks dividing the specimen into distinct and separate columns.

3. Slabbing Named after the loose slabs of rock which form at the periphery of the specimen, and fall off, leaving intact end cones.

4. Brittle Fault Occuring as either a single fault plane or two or more conjugate fault planes, giving the appearance of having sheared. Under this category there is a complete loss of cohesion along the faults.

---

[1] Olsson and Peng (1976); Tapponier and Brace (1976); Montoto (1974); Engelder (1974); Donath and Fruth (1971); Goldsmith et al. (1976)

[2] Paterson (1958).

[2] Hawkes and Mellor (1970); Jaeger and Cook (1971); Kumar (1968); Jaeger (1960); Donath and Fruth (1971); Scholz (1968); Serata et al. (1968).

5. Ductile Fault This type is best described as a series of localised offsets of thin bands of cataclassed material, without a total loss of cohesion.

6. Uniform Flow Characterised by a permanent deformation, with no evidence of faulting, and no loss of cohesion.

* * *

PREFAILURE	A	Closing of pre-existing microcracks and pores plus compaction of soft inclusions. Localised fracturing if unevenly loaded.
	B	No significant changes in specimen structure.
	C	Isolated microcracking orientated in direction of maximum principal stress.
	D	Accelerating microcrack formation giving increased microcrack density.
POST FAILURE	E	Coalescence and forking of microcracks to form macrocracks - no increase in crack density. ?? W & F ?
	F	Sliding along macrofracture planes. Secondary macrocracking due to uneven shearing.

Table 1.1 Regions of Axial Stress-Strain Curve

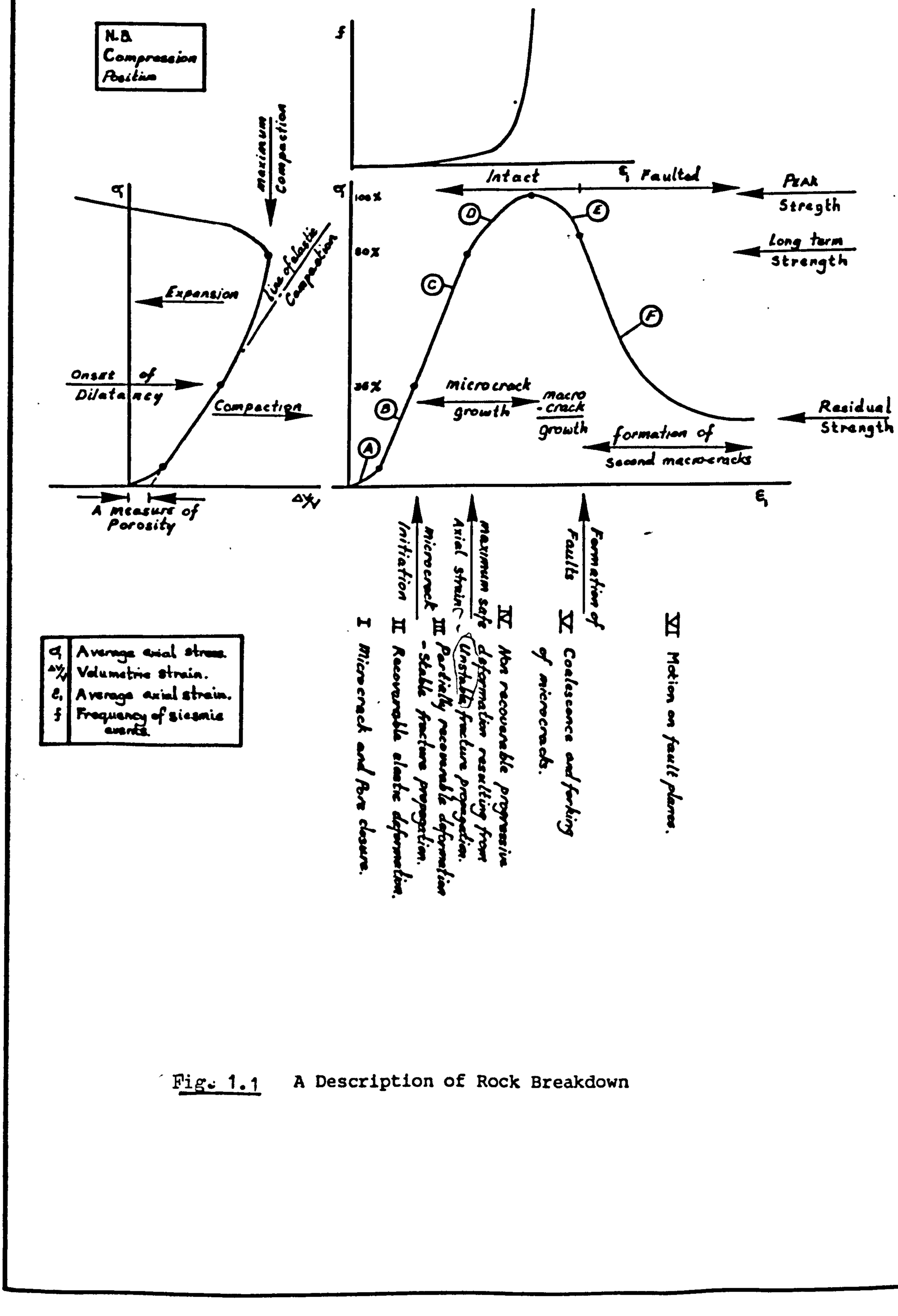

Fig. 1.1 A Description of Rock Breakdown

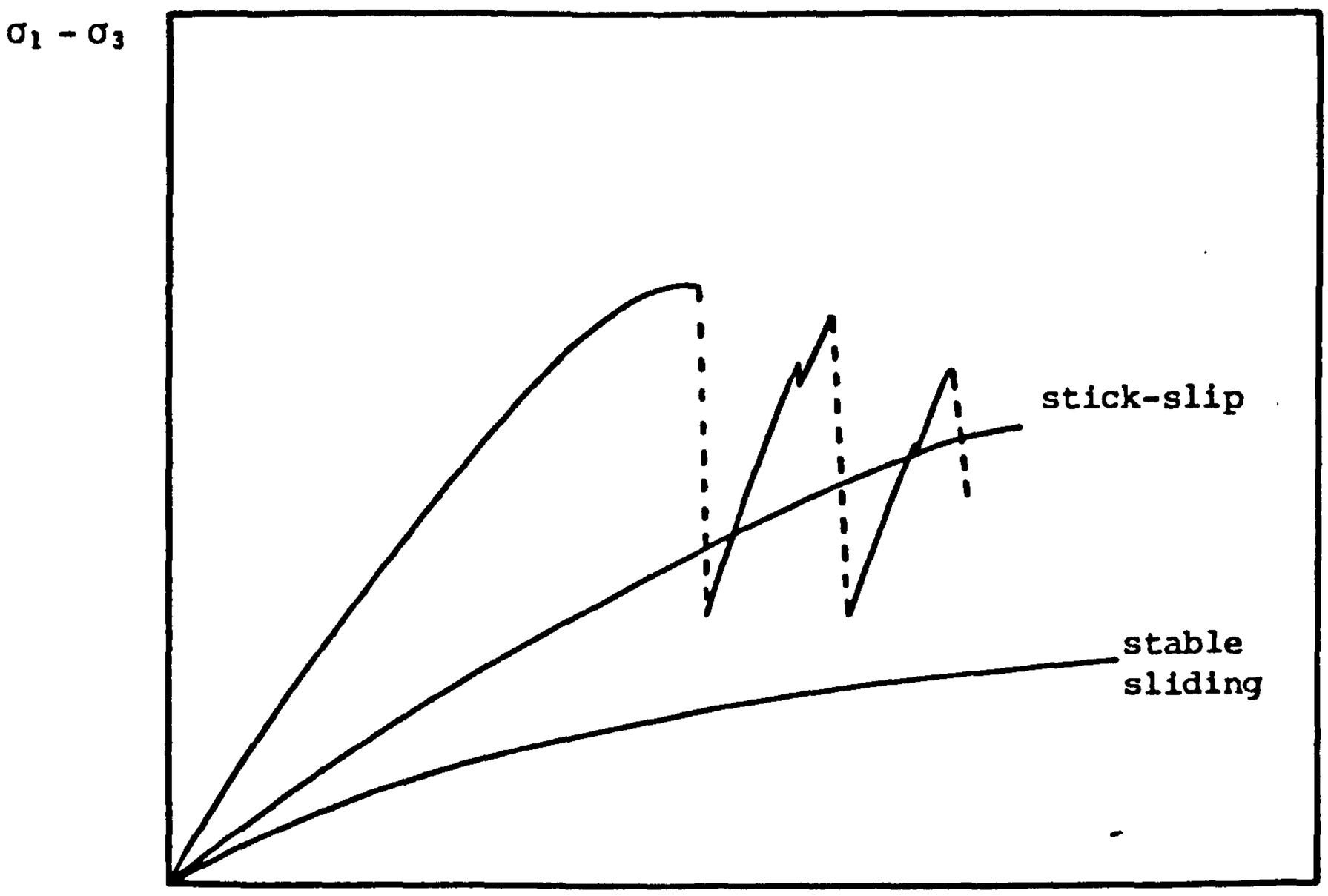

Fig. 1.2 Examples of stick-slip and stable sliding behaviour

CHAPTER TWO

FACTORS AFFECTING ROCK TESTING

2.0 Introduction

In laboratory testing of rocks there are many variables in both the rock properties and the testing environment which can alter a specimen's response to a particular test and which, therefore, need to be taken into consideration when designing an experimental programme. These include the following:

2.1 Time Effects

2.1.1 Strain Rate

The affects of strain or displacement rates on the axial stress-strain curves from laboratory compressive and tensile tests have been well documented: Paterson (1958) observed that upon increasing the strain rate during his experiments on marble, its load bearing capacity immediately increased. There is general agreement amongst workers[1] that:

(a) the shape of the pre-failure stress-strain curves is independent of the applied strain rate and

(b) that the peak strength of the rock increases with increasing strain rate.

---

[1] Grady (1977); Green et al. (1972); Kawamoto and Saito (1974); Peng and Podnieks (1972); Sangha and Dhir (1972,1975); Bieniawski (1970); Donath (1970); Donath and Fruth (1971); Hudson and Brown (1973); Goldsmith et al. (1976).

Sangha and Dhir (1975) showed (b) to be more pronounced for higher strain rates and for uniaxial tests. In an earlier paper (Sangha and Dhir, 1972),they also observed that the strain rate affected the modes of rupture in uniaxial compression, with a decrease in strain rate causing a decrease in the area of rock sliding, and an increase in the size and number of slabs. The dependence of the fracture mechanism upon the applied strain rate has been discussed by Donath (1970), who found that a fast strain rate induced a cataclastic breakdown within the specimen in preference to a mechanism of uniform flow.

With reference to the effect of strain rate on the post failure curve, various findings have been reported. For instance, Bieniawski (1970) and Hudson and Brown (1973) found that increasing strain rates gave steeper post failure curves for sandstone and marble respectively. However, quite the opposite has been reported by Rummel and Fairhurst (1970); Peng (1973) and Peng and and Podnieks (1972) for marble, sandstone and Tuff respectively. Hudson and Brown (op. cit.) suggest that this effect of strain rate might be the result of a change in the mechanism of failure, whilst Paterson (1978) proposes the possibility of it being due to "some peculiarities of machine-specimen interaction".

2.1.2 Creep

For brittle rocks at low temperature and confining pressure, creep has been shown to be the result of internal microcracking (Scholz, 1968,1970; Wu and Thomsen, 1975; Cogan, 1976). Creep has been studied for both intact and fractured rock specimens: Sangha and Dhir (1972) observed that creep tests on intact sandstone at low stress levels showed some axial creep, whilst there was recovery of the lateral

strain, which suggested to them that a greater degree of compaction would be experienced at slower strain rates. Wu and Thomsen (1975) identified three stages of creep for granite which they termed:

1. Transient Creep - involving internal microfracturing.

2. Steady State Creep - in which the axial, radial and volumetric strains increase linearly and microfracturing increases exponentially.

3. Accelerated Creep - when the axial, radial and volumetric strains increase at an accelerated rate and the microfracturing at a 'supra-exponential' rate.

Cogan (1976) reported consolidation accompanying primary creep and expansion accompanying secondary creep in limestone and shale.

Bieniawski (1969, 1970) attempted to study the creep behaviour of failed sandstone, but could not maintain a constant axial stress. He attributed this to be due to the reduction in the applied strain rate; however, it has been suggested (Hudson, 1971), that the specimen deformed along the elastic unloading characteristic of the testing machine. Peng (1973) investigated two classes of failed rock, the first in which the specimens did not have fracture planes right through them, and secondly, those that did, and thus consisted of blocks held together solely by friction. In the first case, he observed two stages of creep: a steady state, and an accelerated state, whereas in the latter, he also observed a transient creep. In both cases the creep eventually led to rupture of the specimens.

At higher temperatures and pressures, or in the case of more ductile rocks, the mechanism of creep will change from one of microfracturing to those of intra-crystalline gliding and recrystallisation.

2.1.3 Relaxation

There are consistent results from relaxation tests performed by different researchers[1] at different stages of the specimens' deformation, marked by various points along the axial force-displacement curves. If a specimen has passed the linear elastic region of its axial force-displacement (or average axial stress-strain) curve and the axial strain is held constant, the load borne by the specimen drops. This relaxation will continue until the specimen reaches an equilibrium point on some lower curve that represents the long term load bearing ability of that specimen's structure for that particular axial strain. The magnitude of this load reduction reaches its peak at a point on the post failure curve somewhere near its steepest slope.

2.2 Specimen Geometry

It is not intended to present a detailed study of the available information on the effects of specimen geometry upon the stress-strain relation here, but rather, to give an account of the work of a few researchers.

---

[1] Bieniawski (1970); Hudson (1971a, 1971b); Hudson and Brown (1973); Peng (1973); Peng and Podnieks (1972).

In short, it is generally agreed[1] that increasing a specimen's length/diameter ratio results in a decrease in the maximum stress, up to a ratio at which it reaches a nearly constant value. It is commonly accepted that this effect is due to end friction effects between specimen and platens, which, above a certain length/diameter, becomes insignificant. This effect of end friction can be demonstrated by introducing a friction reducer between the specimen and platens (Serata et al., 1968) which reduces the effect, as does applied confining pressure (Mogi, 1966). It is on the basis of these results that various workers give recommendations for specimen length/diameter ratios which are normally taken as between 2:1 and 3.5:1.[2] Hudson, Brown and Fairhurst (1972) concluded from their experiments that there was no significant variation in the compressive strength with specimen size, as did Serata et al. (op. cit.) when using friction reducers, although in underground experiments Bieniawski (1968) found that compressive strength decreased with increasing cube size. The effect of increasing length/diameter or height/width ratios upon the post-failure curves has been widely shown to make them steeper.[3]

---

[1] Mogi (1966); Serata et al. (1968); Bordia (1971); Starfield and and Wawersik (1971); Hudson, Brown and Fairhurst (1972); Hudson, Crouch and Fairhurst (1972)

[2] Hallbauer et al. (1973); Jaeger and Cook (1971); Coates (1970); Mogi (1966); Hawkes and Mellor (1970).

[3] Starfield and Wawersik (1971); Hudson, Crouch and Fairhurst (1972); Serata et al. (1968); Hudson, Brown and Fairhurst (1972).

2.3 Confining Pressure

The influence of increased confining pressure upon the stress-strain relationship for rock has been noted[1] to take several forms, including:

(a) An increase in the maximum strength of the specimen under test.

(b) A larger axial displacement before strength failure.

(c) A shallower post-failure curve.

and (d) the inflexions in the curve become less marked.

(e) An eventual transition from strain softening to strain hardening behaviour is reached.

2.4 Porosity of Pore Solutions

As will be realised from the discussion of the failure mechanism in Chapter One, the porosity of a specimen under test will vary throughout the test as microfracturing proceeds.[2] Brace and Martin (1968) report that there is ample evidence that the law of effective stress holds for many rocks (although they do quote some exceptions).

---

[1] Kovari and Tisa (1975); Sangha and Dhir (1975); Crouch (1970, 1971); Wawersik and Brace (1971); Wawersik and Fairhurst (1970); Bieniawski *et al.* (1969); Rummel (1974); Donath (1970); Bieniawski (1970).

[2] Aldrich (1969); Lane (1969); Cornet (1972); Brace and Orange (1968); Cornet and Fairhurst (1974); Handin *et al.* (1963).

Simply, the effective stress is the difference between the applied stress and pore pressure acting on a porous solid. In a drained test, the applied pore pressure is maintained at a constant value throughout, and is independent of the increased porosity due to microcracking. And, therefore, there is no influence upon the specimen behaviour in this test due to changing pore pressures.

In an undrained test, however, where the pore pressure is not controlled, the pore pressure will be dependent upon the increased porosity, and in this case, Aldrich (op. cit.) has shown that the

> "... peak strength is controlled by the effective confining pressure at failure, and that the magnitude of pore pressure rise in the specimen is governed by the initial effective confining pressure."

This relationship holds for all rocks, provided that the rate of deformation does not exceed some critical value, dependent upon the permeability of the rock, viscosity of the pore fluid and certain geometric factors (Donath, 1970; Donath and Fruth, 1971; Brace and Martin, 1968).

Aldrich (op. cit.) further reports that wet specimens are weaker than air dry specimens at all pressure levels. Pore solutions have been shown to influence rock properties; they have a direct action upon the matrix of the rock. The unit surface energy value and coefficient of friction are both altered; the matrix can be chemically dissolved and recrystallisation or weakening of certain mineral phases may be promoted (Cornet, 1972; Donath, 1970; Barton, 1973).

2.5 Other Factors

Another factor affecting the behaviour of a test specimen is its previous stress-strain history; this is clearly demonstrated in cyclic testing, for instance, where progressive cyclic loading causes cumulative disruption of the specimen structure and eventual rupture.[1] But a specimen's properties may also be modified by other aspects of its history; for example, by relief of geostatic stresses, coring and blasting, weathering, contamination, changes in moisture content or temperature and, perhaps, even in its preparation for testing (Attewell and Farmer, 1976). Reports of temperature effects upon specimen behaviour have been mixed. Some report that increased temperature results in: increased strength (Wu and Thomsen, 1975; Kumar, 1968), strength decrease (Griggs et al., 1960) and increased ductility (Donath, 1970).

Other influences upon the apparent behaviour of specimens may be purely due to experimental technique or method of measurement (see, for example, Dhir and Sangha, 1973; Wawersik, 1968 and Hudson, Brown and Fairhurst, 1972).

* * *

[1] Montoto (1974); Cain et al. (1974); Haimson (1974); Attewell and Farmer (1973); Burdine (1963), and see also Ingles et al. (1973).

CHAPTER THREE

VOLUMETRIC STRAIN MEASUREMENT - PREVIOUS WORK

3.1 Introduction

Almost a century ago, Reynolds (1885) observed that if a granular mass, such as sand, was distorted, it experienced a definite "change of shape or distortional strain" - this property he termed dilatancy. In 1925 Mead (1925) used the term dilatancy to encompass "all volume increase due to deformation" and, with particular reference to rock, he gave the term dilatation for any "increase in volume due to fracture". Since then, and more especially in recent years, there have been several similar definitions of dilatancy; for example:

> "Dilatancy means volumetric change accompanying deformation."
>
> - Goodman and Dubois (1972)

> "Dilatancy is the technical term used to describe the inelastic increase in the volume, that begins when the stress on a rock reaches half the breaking strength of the rock."
>
> - White (1976)

> "Dilatant behaviour (is defined) as an expansion when $\sigma_1 \neq \sigma_3$ with respect to the compression observed when $\sigma_1 = \sigma_3$ at the same mean stress."
>
> - Schock (1976)

The volume increase resulting from this property of dilatancy has been expressed in two forms: firstly, as dilation, which is commonly defined as the volume increase relative to elastic changes (Cook, 1970; Bonner, 1970; Scholz, 1967,1968; Zoback and Byerlee

1975) and, secondly as <u>dilatation</u>, which is the total volume increase or $\Delta V/V = \varepsilon_1 + \varepsilon_2 + \varepsilon_3$(Crouch, 1970a,70b). Hence, the degree of dilation will always be larger than that of dilatation. All measurements of volumetric strain in this thesis take no account of elastic changes and should, therefore, be regarded as a measure of dilatation.

As was shown in Chapter One, dilatancy has been proven to be the result of microcracking prior to strength failure, and not some periphery phenomenon. Although Freudenthal (1975) has made the rather dubious distinction that dilatancy is not "the <u>result</u> of cracking, but its <u>cause</u>" (his emphasis).

To date, most research carried out on dilatancy can be summarised into two classifications:

(a) <u>Earthquake Prediction</u> - in which the research into the dilatant behaviour of rock and its associated properties are assessed as precursory indications of earthquakes (e.g. Bonner, 1974; Stuart, 1974; Brady, 1975; Brace, 1975,1969; Brace and Martin, 1968; Brace and Orange, 1966,1968) and

(b) <u>A Mechanistic Approach</u> - in which the work is directed towards a greater understanding of the behaviour of rock (e.g. Bordia, 1970,1971; Bridgeman, 1949; Brown <u>et al.</u>, 1972).

3.2 Methods of Measuring Volumetric Changes

As outlined above in Chapter One, dilation is the result of extensive internal microfacturing, up to the point of fault formation, and then of frictional sliding between blocks. To date, measurements of volumetric strain in 'strain softening' rocks have mainly been confined to the intact specimen, although some measurements have been made during friction tests (Jaimson and Teufel, 1979; Mencl,1965; Goodman and Ohnishi, 1973; Millar and Martin, 1975; Goodman and Dubois, 1972). Various methods of measuring the volumetric strains of rock, both direct and indirect, have been suggested or tried.

3.2.1 Indirect Measurement

The internal microfracturing causing dilation, exerts an influence on several other rock properties. For instance, it will cause changes in rock porosity, pore pressures, p-wave velocities, resistivity and permeability and will also generate seismic events. All these factors have been examined and suggested as means of monitoring dilatancy[1], but chiefly in the earthquake prediction field. Typical variations in these properties with percentage of maximum axial stress, as reported by different workers, are presented in Fig. 3.1, for comparison with the changes in volumetric strain($\Delta V/V$). However, as a means of measuring volumetric changes in the laboratory, these properties are less than desirable, since they offer only relative differences and thus require 'calibration' against the actual volume

---

[1] Handin et al. (1963); Zoback and Byerlee (1975a, 1975b, 1976); Aldrich (1969); Brace and Orange (1966, 1968); Cornet (1972); Cornet and Fairhurst (1974); Lane (1969); Oshnishi and Goodman (1974); Bonner (1974); Brace (1969, 1975); Rummel (1974); Scholz (1967, 1970); Spetzler and Martin (1974); Scholz et al. (1973).

changes. They are also strictly limited to the pre-failure state by their very nature and the change in structure and deformation mechanism of the rock in the post-failure state.

3.2.2 Direct Measurement

By far the most commonly used direct method of measuring volumetric strains must be that of resistance strain gauges attached to the specimen[1], where both axial and lateral strains are measured and the volumetric strain computed as:

$$\Delta V = \varepsilon_l + 2\varepsilon_\theta$$

where ε_l is the axial strain (%) and ε_θ is the circumferential strain (%).

Brown et al. (1972) used a variation on the normal strain gauging configuration by having a complete circumferential strain gauge, mounted around the centre of the specimen.

Other circumferential band techniques have also been employed; for instance, Barnard (1964) tested concrete using circumferential bands connected to dial gauges to measure circumferential strain, and Ingles et al. (1973) used a similar technique, but replaced the dial gauges with linear voltage displacement transducers (L.V.D.T.s). The advantage of these techniques over the normal strain gauging configurations is that they measure over a larger area and, therefore, give more representative results for the specimen as a whole. However, they also have the disadvantage of being bulky in their construction.

---

[1] Brace et al. (1966); Green et al. (1972); Hadley (1975, 1976) Haimson (1974); Ohnishi and Goodman (1974); Rothman (1975); Scholz and Kranz (1974); Scholz (1967, 1968a); Zoback and Byerlee (1975a, 1975b); Lisk (1975); Wu and Thomsen (1975).

A few other miscellaneous methods of measuring volumetric strain have been used, including those of: Bordia (1971, 1972), who used LVDTs mounted laterally around the central circumference of his specimens; Hobbs (1971), who used a Lamb Roller Extensometer; and Murayama and Yagi (1966), who used dial gauges to measure volume increases of mudstone due to swelling.

All of the above methods have the disadvantages of:

(a) only measuring over a limited portion of the specimen and

(b) most are impractical under triaxial conditions.

There is, however, one method which has been used successfully and which does not suffer either of these two disadvantages.

Interestingly, this method was that first used in 1949 by Bridgeman (1949) to record the first volumetric strain measurements of rock. Bridgeman used a dilatometer which worked on the principle that if a specimen is immersed in a fluid, and is stressed such that its volume changes, then that change can be measured directly by recording the amount of liquid displaced in a graded capillary. Some examples of Bridgeman's results are reproduced in Fig. 3.2. Since 1949, the principal of the dilatometer has been adapted successfully to triaxial testing of both soils and rock by several researchers.[1] Edmond and Paterson (1972) adapted the principal to triaxial testing by using a triaxial cell which included a bellows and LVDT arrangement,

---

[1] Cook (1970); Crouch (1970); Cullingford et al. (1972); Edmond and Paterson (1972); Fairhurst (1973); Lewin (1971); Rowlands (1972) Darley (1973); Rummel (1974); Wawersik (1975).

facilitating the automatic logging of the specimen's volumetric behaviour. In the field of soil mechanics, Lewin (1971) developed a servo-burette system, allowing constant monitoring of volumetric strain under conditions of constant confinement (see also Rowlands (1972) and Darley (1973)). Cullingford et al. (1972) went one step further and developed a servo-controlled ram, for monitoring and maintaining constant confining pressures.

A similar approach has been used in the field of rock mechanics, where the confining pressure has been monitored by means of strain gauges and maintained constant using a pressure intensifier, manually (Cook, 1970; Crouch, 1970; Fairhurst, 1973) or within a closed-loop servo system (Rummel, 1974; Wawersik, 1975).

* * *

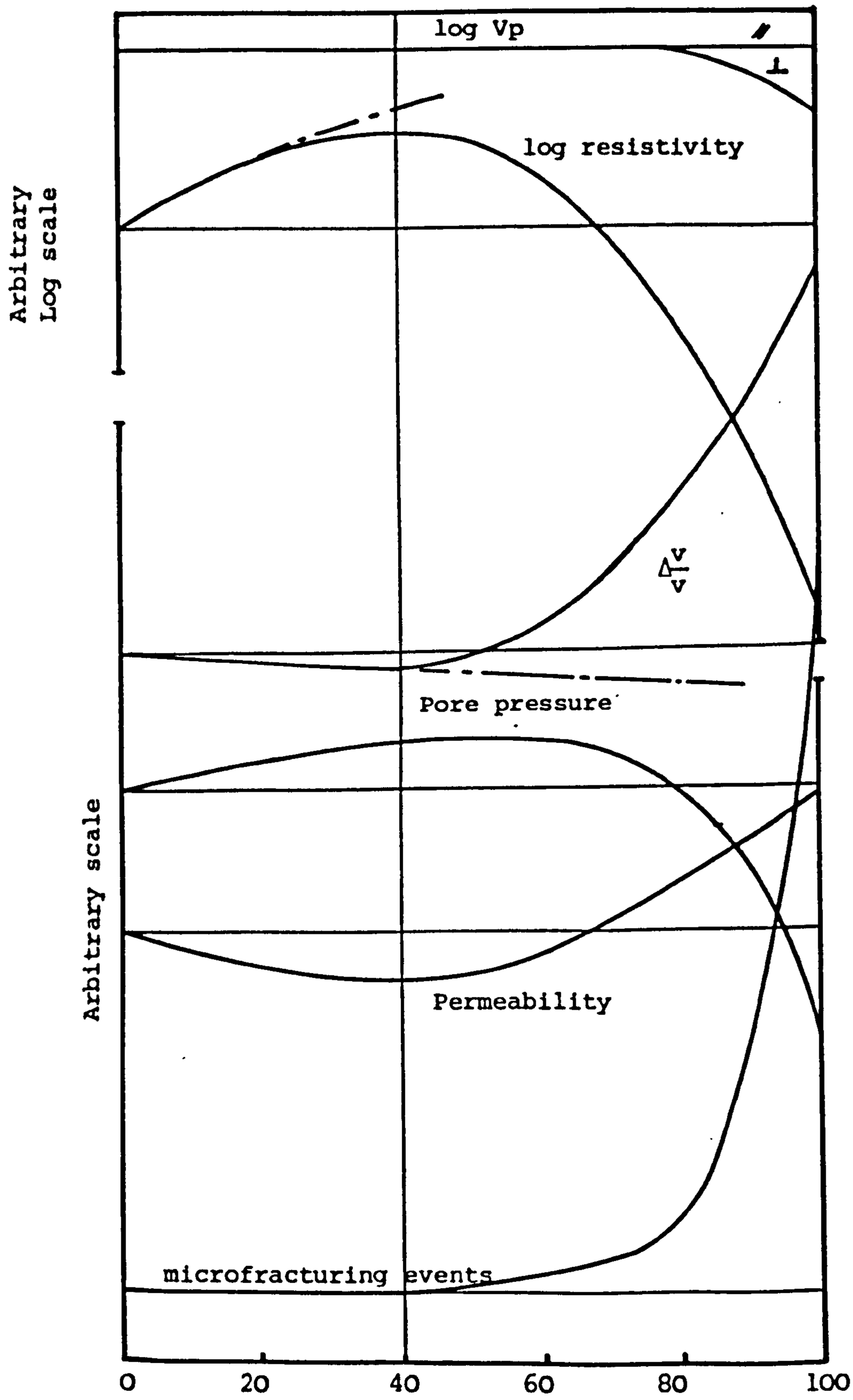

Fig. 3.1 The influence of dilation on other rock properties

often?

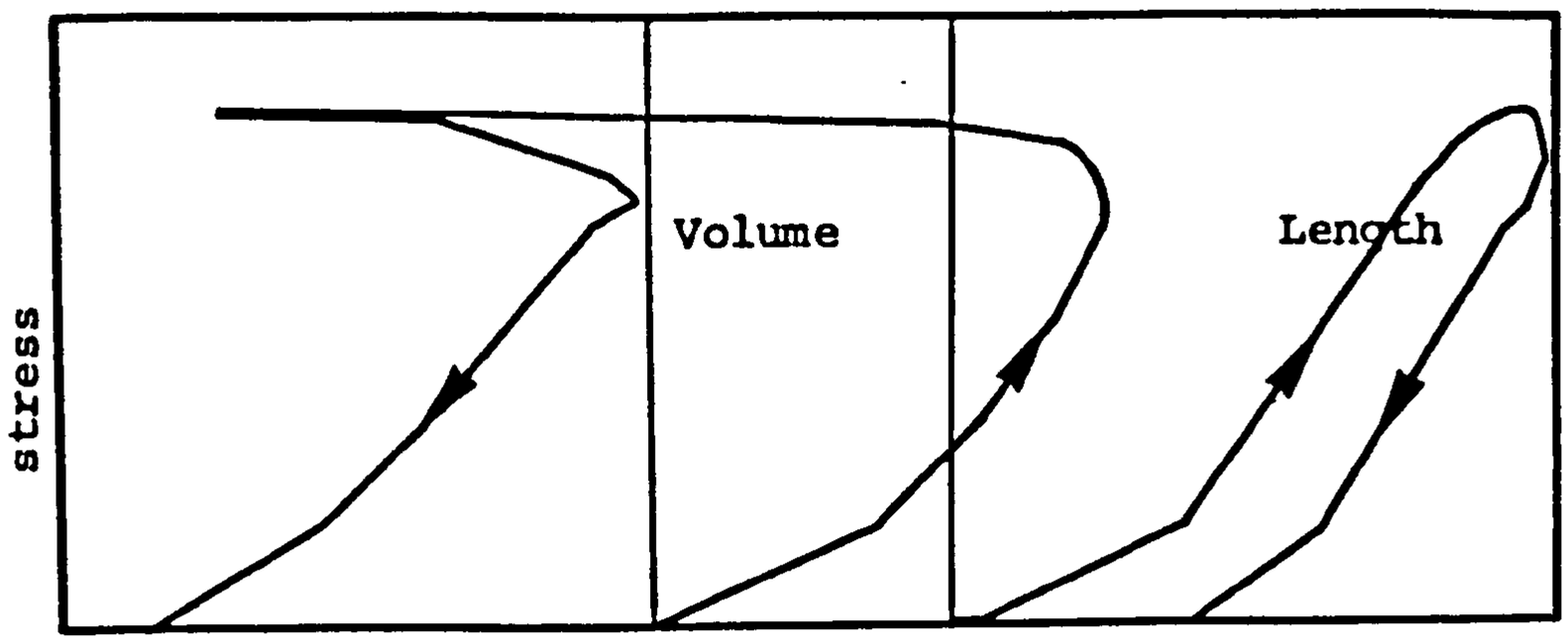

Fig. 3.2 Examples of Volumetric strains measured by Bridgeman (1949)

CHAPTER FOUR

TESTING MACHINES

4.1. Stable Rock Failure

The violent collapse of most brittle rock specimens subjected to uniaxial compression (and often triaxial compression at low confining pressures) is not necessarily a fundamental property of the rock, but is rather, a property of the testing machine. The accumulated elastic strain energy within the rock-machine system, at the point of crack coalescence, far exceeds that required to cause further disintegration. Consequently, the system becomes unstable, resulting in the violent collapse of the specimen. The rock-machine system is stable whilst the rate of elastic strain energy released from the machine during unloading is greater than that from the specimen. This concept is often illustrated by diagrams similar to Fig. 4.1,[1] in which we can see that if the specimen and machine have unloading characteristics AB and AC respectively, the system is unstable and, alternatively, that if the unloading characteristic of the machine is AD instead of AC, the system will be stable. The slopes of the unloading characteristics of the machine and specimen are a measure of their stiffness.

4.2 Factors Influencing Stability

Various factors affecting the relative stiffness of the specimen and machine (and thus stability of the system) have been reported by different workers. These include:

---

[1] Attewell and Farmer (1976); Bieniawski (1971, 1970); Hudson, Crouch and Fairhurst (1972); Rummel and Fairhurst (1970); Hojem, Cook and Heins (1975); Hudson, Brown and Fairhurst (1972); Cook and Hojem (1966); Crouch (1970).

4.2.1 Strain Rate

As outlined in 2.1.1, researchers have reported various affects of strain rate upon the post-failure stiffness of their specimens. Therefore, no set law can be adopted for choosing strain rates to help control specimen failure without some prior knowledge of how the rock under test responds to strain rate changes.

4.2.2 Confining Pressure

Similarly, 2.1.2 outlined some of the available information on the effects of confining pressure upon rock stiffness. There is general agreement that increasing confining pressure reduces specimen stiffness and thus aids control of the specimen's failure.

4.2.3 Specimen Geometry

Specimen stiffness increases with increasing length/diameter or height/width ratios. Therefore, increasing length/height ratios do not promote stability within the machine-specimen system. Hudson, Crouch and Fairhurst (op. cit) have shown that, for a particular width/height ratio, control of the failure process is favoured for specimens with small diameters. This concept is expressed mathematically by the equation:

$$k = A.E/L$$

where the length of the specimen is L, its cross-sectional area is A, its modulus of elasticity E, and its stiffness k. To encourage stability within the system we need to decrease the value of k for the specimen and increase its value for the testing machine.

4.2.4 Machine Stiffness

Apart from increasing machine stiffness through massive construction, several other methods have been used. The most popular method is that of loading steel or some other elastic material in parallel with the specimen, allowing transfer of load to the steel as the strength of the specimen decreases. (Cook (1965); Brace et al. (1966); Bieniawski et al. (1969); Brady et al. (1973)). Other systems have included the use of mercury as the hydraulic medium (Hojem et al., 1975) and the thermal contraction of preheated machine loading columns, with the loading ram locked in position (Cook and Hojem, 1966; Wawersik and Fairhurst, 1970).

4.3 Servo-Controlled Machines

An alternative method of controlling rock failure to the stiff machine is the use of a servo-controlled testing machine. The servo-controlled testing machine is programmed to follow a set loading path, and is continually monitored, allowing complete control, by comparing the machine's actual progress against its programme and correcting appropriately. This monitoring/correction may be done manually (Wawersik and Brace, 1971) or automatically.[1] Normally, the programme selected is one of constant displacement rate; that is, the loading ram of the machine compresses (or extends in the case of a tensile test) the specimen at a constant displacement rate. The magnitude of the actual specimen displacement is measured, by an LVDT for example, and the value compared with that expected by the programme. If the actual

---

[1] Hardy et al. (1971); Hudson, Brown and Fairhurst (1971, 1972); Hudson (1971 a); Hudson, Brown and Rummel (1972); Hudson, Crouch and Fairhurst (1972); Rogiers et al. (1971); Rummel and Fairhurst (1970); Attewell and Farmer (1973); Peng (1973); Peng and Podnieks (1972); Ilfelder and Wang (1979).

displacement is running ahead of, or lagging behind, that of the programme, the machine applies a corrective displacement to the ram, until the error is eliminated. A schematic diagram, illustrating this type of closed-loop system is given in Fig. 4.2. In theory, if a closed-loop servo-controlled testing machine has a fast enough response, it should be capable of controlling rock of any stiffness, given suitably monotonically changing control and feedback signals.

4.3.1 Factors affecting Control

Several factors for consideration in optimising the control of servo-controlled testing machines have been outlined by various researchers (Hudson, Brown and Fairhurst, 1971; Hudson, Crouch and Fairhurst, 1972; Rummel and Fairhurst, 1970), including:

1. The Class of Rock - In 1968, Wawersik (1968)(see also Wawersik, 1973), proposed two classes of rock behaviour in the post-failure state, based on his observations. These he termed 'stable' and 'unstable' or 'Class I' and 'Class II' respectively. A Class I rock is one in which energy must constantly be added to the rock to cause continuing failure, whilst a Class II rock will undergo violent failure unless energy is removed from it. In terms of stress-strain curves, examples of both rock types are given in Fig. 4.3. The implication for a Class II rock under test with a programme of monotonically increasing axial strain is apparent, it will follow the unloading curve ABC, rather than its true path ADC. However, Class II behaviour can be controlled and monitored, if the strain is cycled or some other suitable feedback signal is used.

2. The Feedback Signal - The control of rock failure will be optimised when the feedback signal generator is located for maximum sensitivity in detecting failure. Since specimens tend to develop microcracks perpendicular to the least principal stress, displacement transducers used as feedback signal generators should be positioned in the direction of this stress for greatest sensitivity (Hudson, Brown and Fairhurst, 1971; Hudson, Crouch and Fairhurst, 1972). Examples are given in Fig. 4.4.

3. The System Response - The response is that period of time which the machine system takes to react to the occurrence of any event within the specimen. That is, the time between the feedback signal being generated and the actuator responding to the corresponding drive signal. The response is affected by the pump capacity, valve capacity, inertia of the ram, gain setting, and so on. The gain setting governs the amount that the servo valve opens for a given error. Thus, as the gain is increased, the servo-valve opens further, correcting the error faster. There is, however, an optimim gain setting below which the machine is sluggish and above which it is unstable.

Other factors, such as those outlined earlier, affecting machine-specimen stiffness will also aid the control of the rock failure, through reducing the errors needing correction in the servo system.

* * *

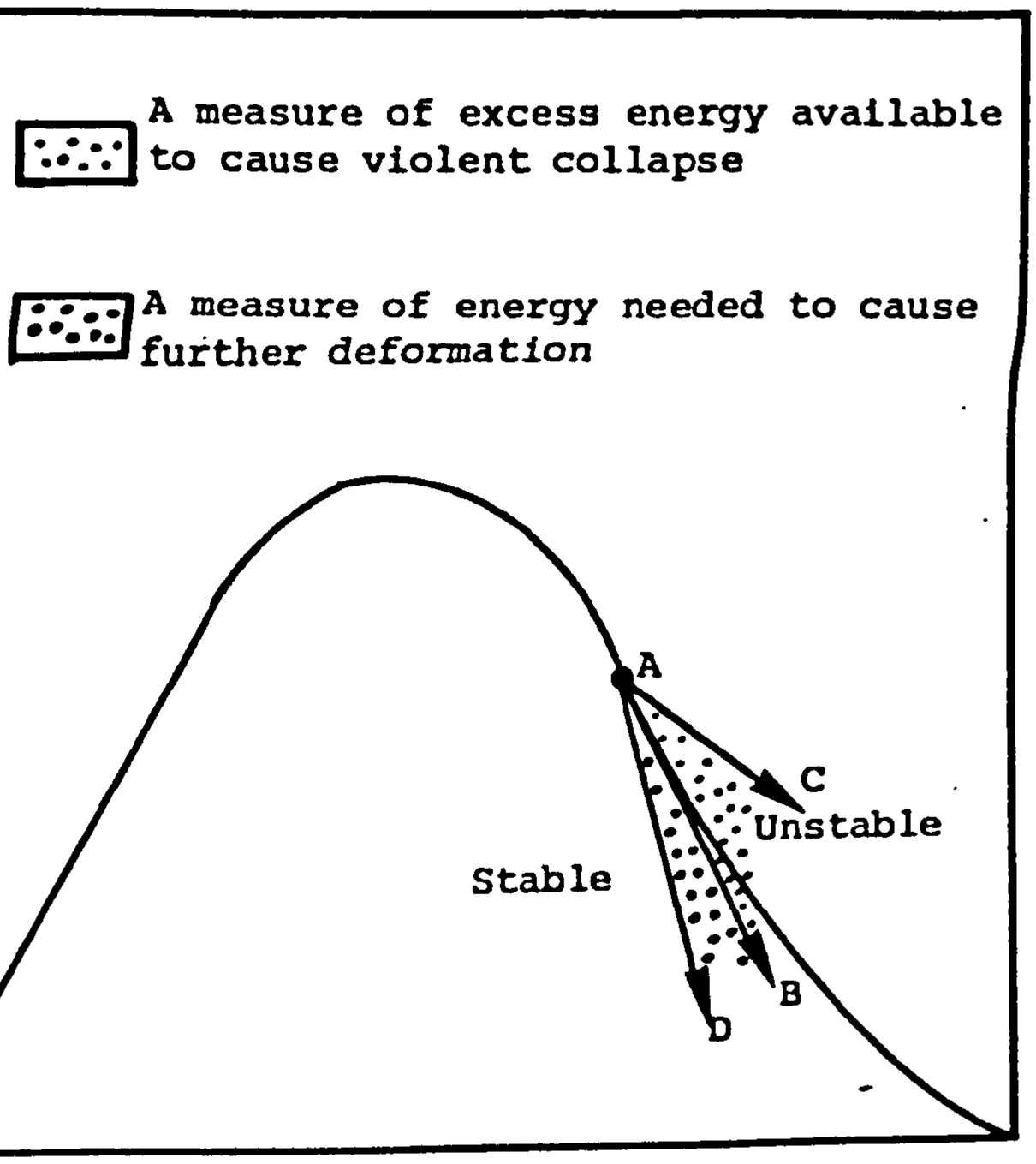

Fig.4.1 Effect of Specimen Stiffness on Stability

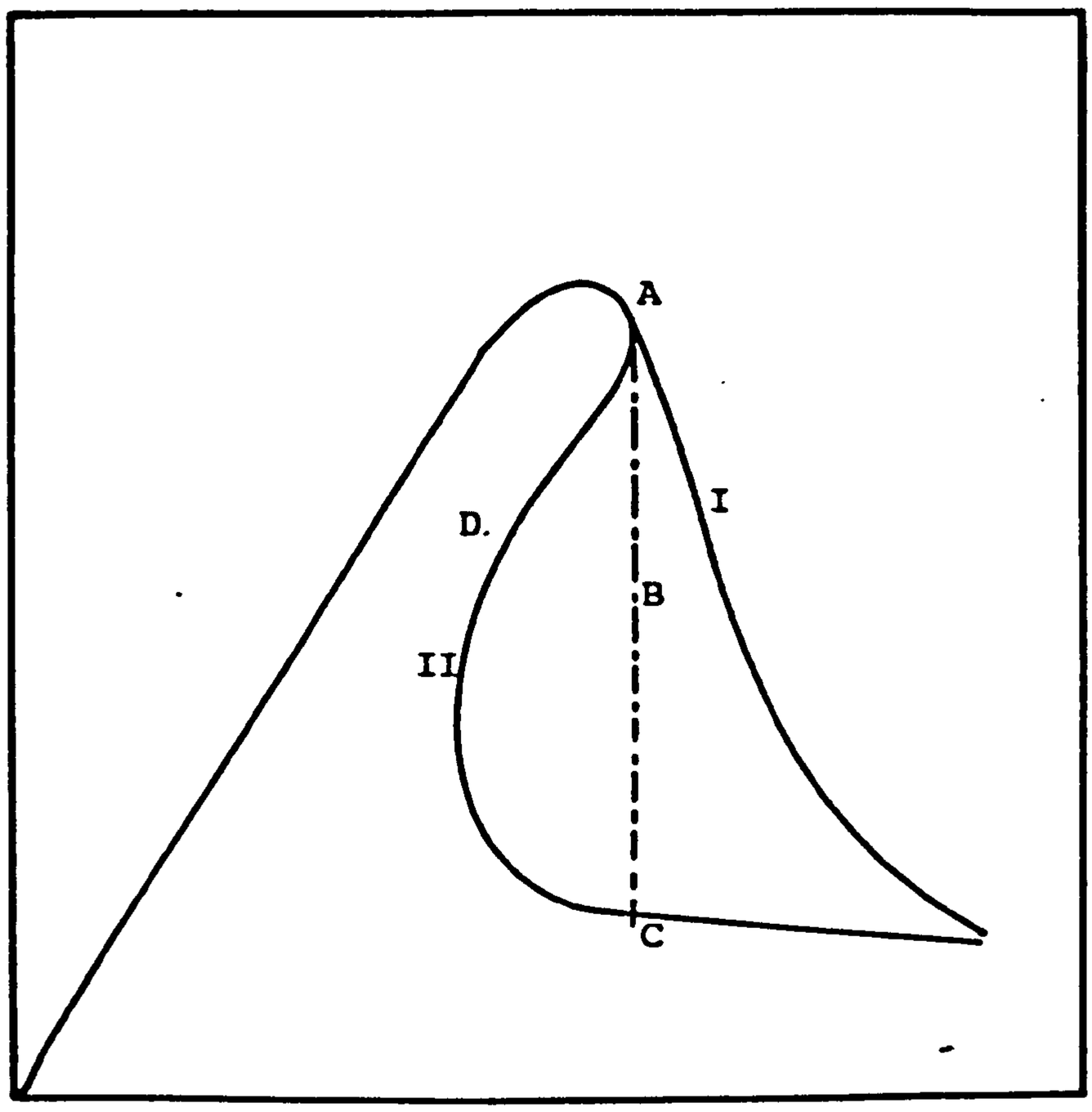

Fig.4.2 Axial stress-strain curves for Class I and II rocks

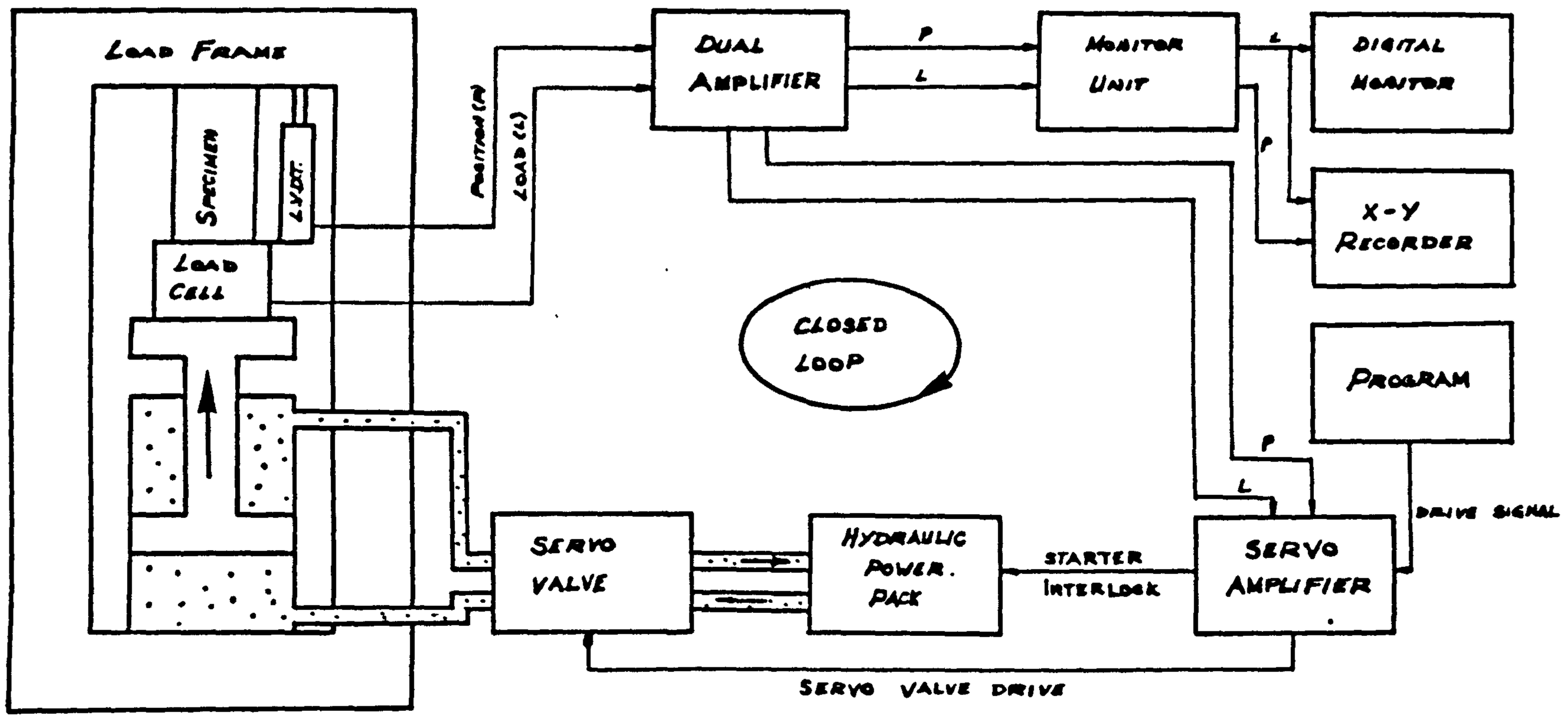

Fig.4.3A closed loop system for Servo-Controlled Testing Machines

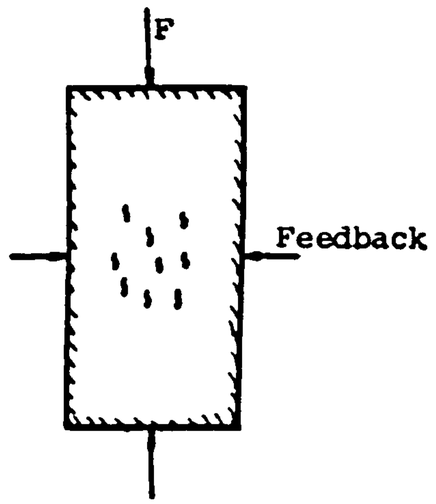

Compression

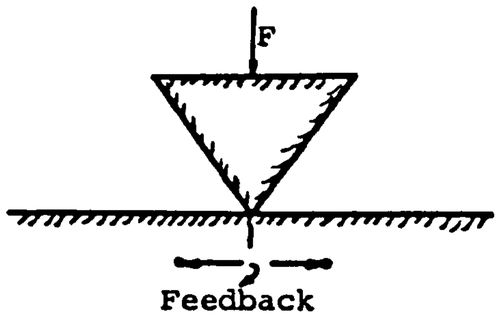

Bit Penetration

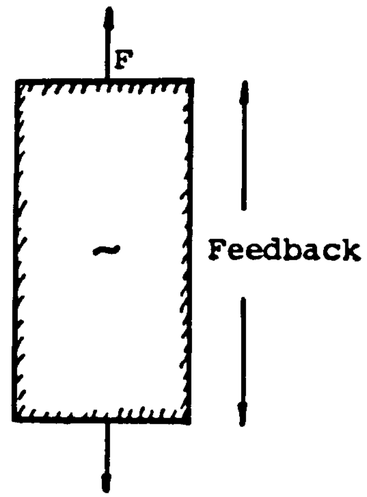

Tension

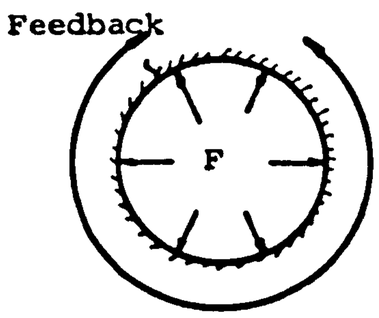

Hydraulic Fracturing

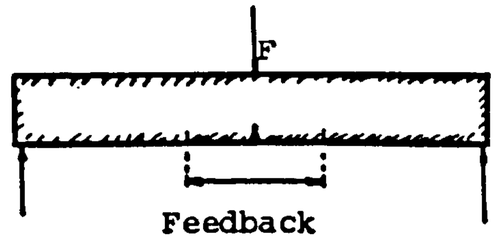

Beam Test

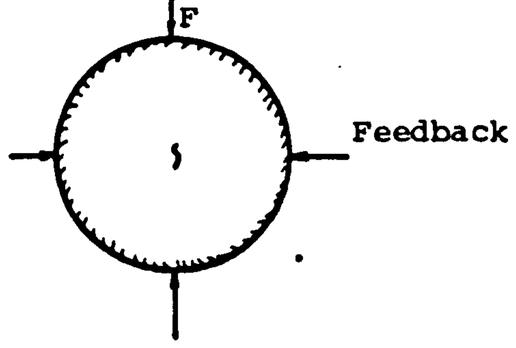

Brazilian Test

Fig.4.4 Feedback Measurement for Optimum Control

(after Hudson, Crouch & Fairhurst, 1972)

CHAPTER FIVE

A 500 TON SERVO-CONTROLLED TESTING MACHINE

5.0 History

In 1965, the rock mechanics unit of the Department of Mining Engineering of the University of Newcastle upon Tyne was re-sited in the St. Thomas' Street buildings. At that time, funds became available to increase the Department's testing facilities and it was decided to purchase a stiff testing machine. However, difficulties were experienced in deciding upon the final machine specifications. Then, following the visit of Professor Fairhurst in 1971, the Department decided to purchase a servo-controlled testing machine in favour of a stiff-machine. Specifications were agreed and tenders invited from various companies. These tenders ranged from £6000 to £60,000 and varied in their fulfilment of the given specifications. These specifications were purely mechanical and based upon the design of the Department's large-scale, creep rigs (Table 5.1). Eventually, it was decided to construct the machine in 'kit form' and contract out the various components to local firms, thus saving on transportation costs on items such as the frame. The component parts and their suppliers are given in Table 5.2.

The machine was finally constructed and installed in May, 1973. Initial experiments using the machine were conducted on gypsum and marl, plus a few brittle rocks (Lisk, 1975; Horseman - private communication), although the latter experienced difficulties and were never reported. Then, in August 1975, a new building was constructed, to house the Engineering Geology, Mining Engineering and Rock Mechanics departments. Consequently, the system was dismantled and reconstructed

in its present site. No further experiments were carried out using the machine until the present research commenced in October, 1976.

5.1 Description of the Machine

Basically, the testing facility can be sub-divided into the three systems: those of the hydraulic loading, electronic monitoring, and control and data monitoring systems. In the case of a normal uniaxial compression test, the specimen is located between the platens of the loading frame and the experiment directed and monitored by the electronic control system. During a triaxial test the specimen is seated inside a suitable triaxial cell and confining pressures are generated by independent, mobile, pressurising systems (Plate 5.1). During the experiment, both dependent and independent variables are monitored and may be permanently recorded on one or more x-y recorders.

5.1.1 The Loading System

The axial loading system can be controlled by a number of test parameters; for example, load, strain, deformation, etc., via the closed-loop control system. The hydraulic ram can be electrically programmed to apply any predetermined sequence of events corresponding to the desired control programme.

The loading frame was designed by Dr. Talbot (a previous member of staff of the Department of Mining Engineering) as a stiff frame based on his earlier large creep rig designs. The 'Hydramuscle', double acting, hydraulic actuator is mounted in the centre of, and perpendicular to, the lower platen of the loading frame. The hydraulic manifold and electrohydraulic servo-valve are mounted directly onto the side, and towards the rear of the actuator. Originally, the loading

frame was strain-gauged (and still is) allowing load measurements over the full 500 ton range. However, the system now incorporates either a departmentally built 500 tonne load cell or an N.C.B./M.R.E. 100 tonne load cell Type 440. The present system is capable of applying a top pressure of 25 MN/m^2, offering a peak loading force of 500 tons in compression and 100 tons load in tension, although a new R.D.P.Howden Ltd. 100 tonne (compression) hydraulic actuator and servo-valve have recently been purchased and will be interchangable in the frame with the existing actuator. In order to aid the response of the actuator an accumulator is included in the hydraulic circuit. Other test parameters, such as displacement, can be measured by incorporating the appropriate transducers, strain gauges, etc. within the system.

5.1.2 The Hydraulic Power Pack

The hydraulic power pack was supplied by R.D.P. Hydraulics Ltd., Wolverhampton, and is sited in one corner of the testing laboratory in its own sound-proofed container. The hydraulic power pack provides a supply of hydraulic oil (Shell Tellus 27) at a maximum confining pressure of 25 MN/m^2 (3600 psi) and a maximum flow rate of 38 L/min.(10 gals/min.). The oil is maintained at a constant temperature by means of a heat exchanger, cooled by tap water and controlled by a thermostat.

5.1.3 Electronic Control

The control electronics create the programme signal and monitor the machine's progress; then, comparing the two, it generates an error signal or servo-valve drive signal, in order to correct the difference.

In the present system the programme signal is usually generated by a digital ramp generator. This unit can be programmed to give a constant rate, increasing, decreasing or cyclic programme signal, defined by a top ramp voltage and total ramp time. The ramp voltage and time correspond to the calibration of the feedback generator and the required rate of change of the control mode, respectively. The range of ramp time available extends from 10 secs. to 9×10^9 secs. There are facilities for the use of external programme signal generators, including a punch-tape programmer and curve follower.

The system allows six signals to be monitored and any of these may be used as the feedback signal. These can be generated using load cells, displacement transducers, strain gauges, pressure transducers and so on. The choice of feedback signal is governed by the type of control required in the experiment. The feedback signal is amplified in an RDP E84 Dual Amplifier, before passing to the RDP E136 Servo-Amplifier. This signal must always be presented to the servo-amplifier as a monotonically increasing signal, since a decreasing signal results in an increasing error signal, causing excessive loading and loss of control.

The servo-amplifer constantly compares the feedback and programme signal, producing an error signal in proportion to the magnitude and polarity of their difference. This signal is the drive for the servo-valve. If there is no difference the valve is closed, otherwise the valve opens, allowing oil into or out of the actuator, in accordance with the error. The servo-amplifier also incorporates a facility for changing control modes at any predetermined point in the experiment.

Two trip limits are incorporated into the system as safety devices, which turn off the hydraulic power pack once the specified limits have been exceeded. Fig. 5.1 gives a block schematic diagram of the control electronics.

Recently the Department purchased a new electronic control console with a mobile servo-valve and pump for use with its existing soft machines. The introduction of this new control system offers greater flexibility through the opportunities for interchange with the old system. Fig. 5.2 illustrates the layout of the new system for comparison with the old. The greater flexibility lies in the improved ramp generator and servo-amplifier units. A further improvement lies in the inclusion of the RDP E221 Extensometer Amplifier allowing two displacement signals to be averaged.

5.1.4 Data Monitoring

At present, the data recording system consists of one Bryan's 26700 High Speed X-Y-T Recorder and two Philips PM 8120 X-Y-T Recorders. Contimuous plots of the required test parameters can thus be permanently recorded and if required may be transferred onto computer cards at a later stage by use of a D-Mac Digitizer.

However, it will soon be possible to record any desired test parameters directly, using a mobile data acquisition unit, which will be 'hooked' into the present departmental Hewlitt Packard 2100 series minicomputer. This will give greater accuracy and flexibility in the data acquisition and reduction processes. This system is expected to be fully operative by October 1979. A block diagram of the present data processing system is given in Fig. 5.3.

5.2 Problems Encountered

The best part of the experimental work carried out involving the servo-controlled testing machine in the academic year 1976/77 was concerned with the 'debugging' of the system. Minor errors were located and corrected in the pump's thermostat, water cooling system and safety trips. Interaction and interference between load and displacement feedbacks, between other testing machines and the servo-machine; both airborne and mains; were found and eliminated through the use of mains and amplifier filters. All three E84 Dual Amplifiers, the ramp generator, E 136 Servo-Amplifier, E86 Monitor Unit and E 92 limit trips have all needed attention of some sort; but these problems were slowly located and eliminated and a high standard of reliability eventually reached.

5.3 Summary

To summarise, the existing system, with its various modifications, has the following advantages and disadvantages:

5.3.1 Advantages

1. Two actuators of maximum loading capacities of 500 and 100 tons offer increased accuracy and flexibility in the loading system.

2. Six circuits available for amplification of test variables offer comprehensive recording and monitoring facilities.

3. A choice of load, displacement and strain control parameters plus facilities for mode changes during an experiment.

4. The ramp generator is capable of programming tests over long periods.

5. The easy recording of test variables in graphical form on X-Y-T plotters, and soon, a facility for data acquisition linked up to the departmental minicomputer.

6. The operation of the testing system is simple once calibration and preparation procedures have been completed and appropriate parameters for a particular type of test set.

7. There is a large amount of daylight between the platens, allowing large specimen and apparatus sizes.

8. A new, up-dated control console provides opportunities for interchange of units plus servo-control of two parameters during a test.

5.3.2 Disadvantages

1. The loading frame is heavy in its construction and no easy provision is made for reducing the daylight between the platens. At present, this is done by inserting spacing blocks between the top platen and the loading frame.

2. The calibration and 'setting-up' of the electronic control console is complicated and 'fiddly'.

3. There is no permanent member of staff or technician familiar with the design and operation of the system.

4. Problems have been experienced with the reliability of units, with fluctuations in electrical supplies and with airborne electrical interference.

5. The system as a whole does not seem reliable enough to match the opportunities for long term tests offered by the ramp generators.

* * *

Maximum Compressive load	...	500 tons
Maximum Tensile load	...	100 tons
Outside diameter of Actuator	...	29 inches
Axial length of Actuator	...	30 inches
Stroke of Ram	...	3 inches
Platen sizes -		
top and bottom	...	24 inches
Daylight between loading platens	...	30 inches
Overall length of Actuator to platen	...	39¼ inches
Working stresses, tension and compression	...	5T/ins^2

Table 5.1 Specifications for 500T Servo-Controlled Testing Machine

Component	Supplier
Frame	Clarke-Chapman - John Thompson Ltd., Newcastle
Actuator	HydraMuscle, Havant
Power Pack	RDP Hydraulics Limited, Wolverhampton
Servo-Valve	Dowty Servos Limited, Tewkesbury
Electronic Control Systems	RDP Electronics Limited, Wolverhampton.
Accumulator	Towlers, Leeds

Table 5.2 Suppliers of Machine Components

Plate 5.1 The 500 ton Servo-controlled Testing Machine

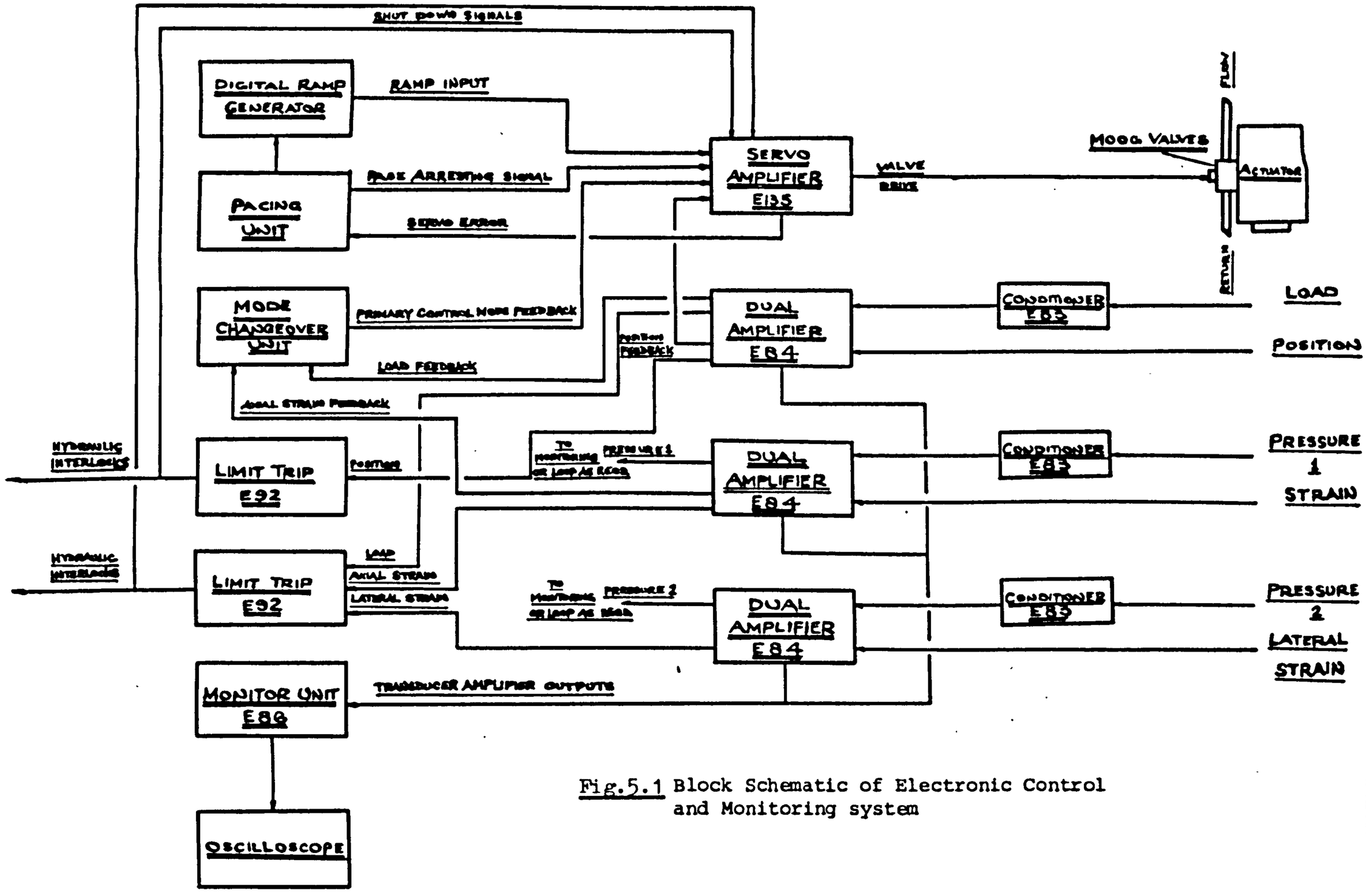

Fig.5.1 Block Schematic of Electronic Control and Monitoring system

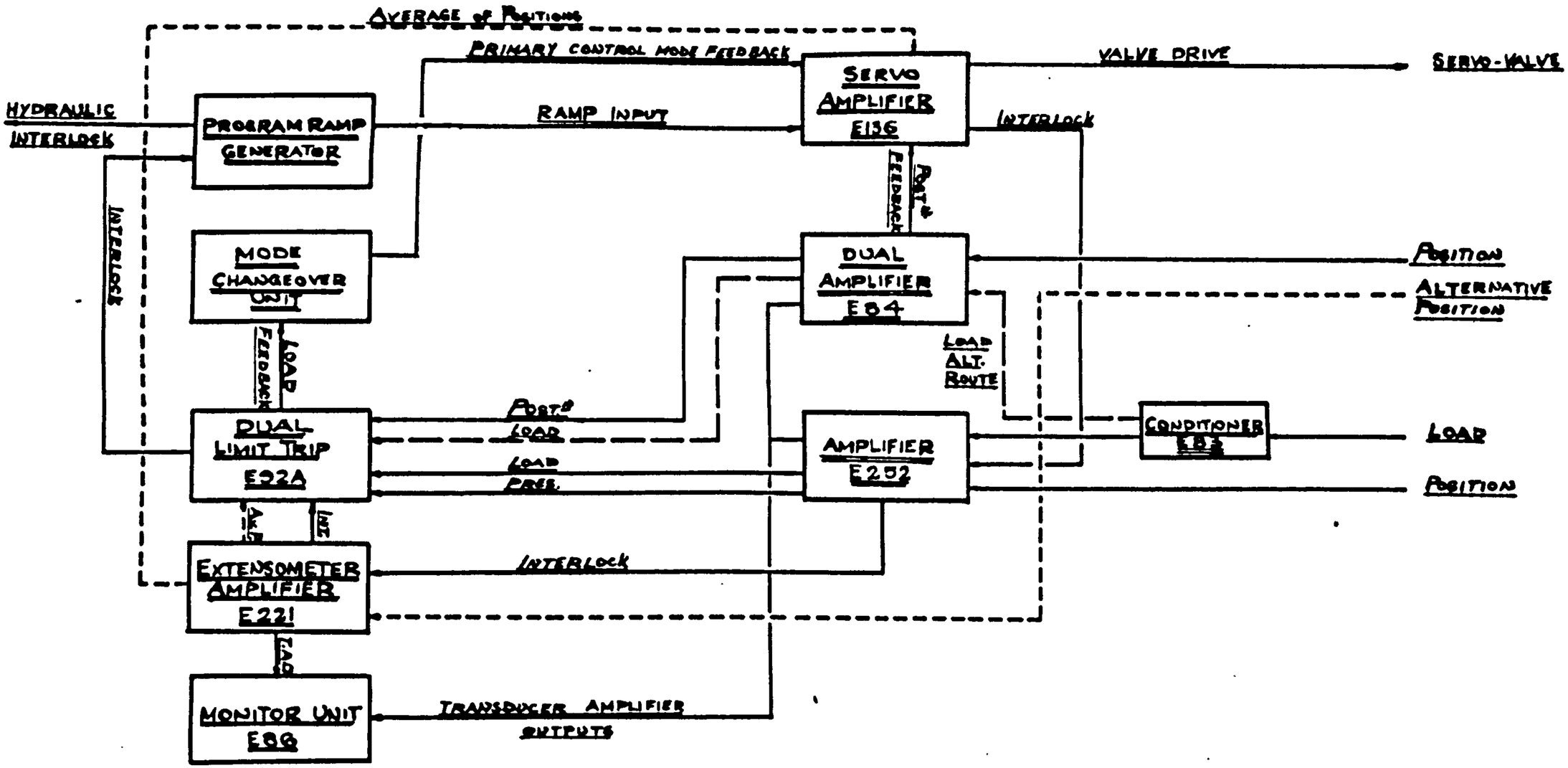

Fig.5.2 Block schematic of New Electronic control and monitoring system

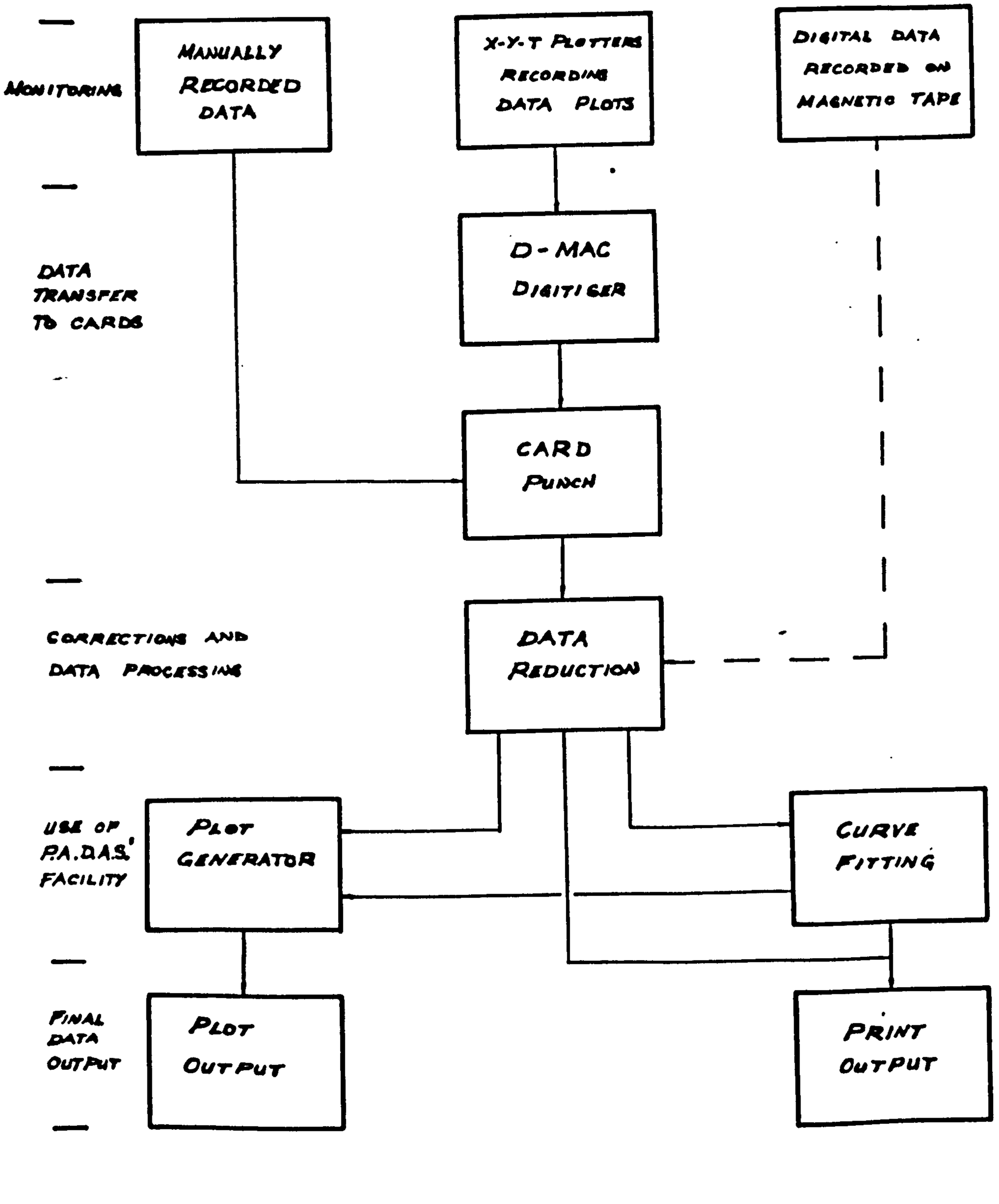

1 COURTESY OF S. WATSON

Fig.5.3 Block Schematic of Data Processing System

CHAPTER SIX

APPARATUS FOR MEASURING VOLUMETRIC CHANGES

6.1 Design Specifications

In deciding upon the design specifications for the experimental apparatus, the following requirements were taken into consideration:

1. That the triaxial cell should be capable of withstanding lateral pressures ranging from 0 to 42 MN/m^{-2}, plus a safety margin.

2. That specimens should be easy to prepare and mount inside the triaxial cell.

3. For ease of measurement the specimens should be of a size conducive to large volume changes.

4. That the apparatus should be capable of measuring large volume changes and rates of volume change.

5. That specimen compaction, as well as expansion, should also be measurable.

6. That large lateral expansions in the specimen should be possible without contact with the sides of the cell and allowing easy removal of the specimen after the test.

7. That large axial displacements should be possible.

8. That the confining pressure within the cell should be maintained at a constant, predetermined value, and should be capable of visual monitoring.

9. That both strain hardening and softening specimen behaviour should be possible.

10. That the equipment should be safe to use within a potentially lethal testing system.

6.2 The Design Principle

In examining the existing methods of measuring volumetric changes as outlined in Chapter Three, the following decisions were taken:

6.2.1 Indirect Methods of Volumetric Measurements

All the indirect methods (i.e. porosity, pore pressures, p-wave velocity, seismic events, resistivity and permeability) were rejected as a principle for the design, because:

(a) they require calibration against volumetric changes,

(b) they are not simple to 'set up' and

(c) they are rendered useless in the post-fractured state.

6.2.2 Resistant Strain Gauges and Circumferential Bands

These methods are expensive and difficult to set up for a triaxial test, although not impossible. Their main disadvantage, however, lies in the fact that they only monitor local changes, while dilatancy is itself recognised as being local in nature (Hadley, 1975; Liu and Livanos, 1976) and, therefore, these methods will give unrepresentative readings. They are also likely to give spurious readings once major fracturing or spalling has occurred (e.g. Wu and Thomsen, 1975).

6.2.3 L.V.D.T.s, Dial Gauges and Lamb Roller Extensometers

These have the same disadvantages as the above methods and are clearly impractical in a triaxial testing system.

6.2.4 Dilatometer

The methods based upon Bridgeman's dilatometer did seem to offer a suitable monitoring system, giving an 'overall' measurement of the volumetric strain, and having been adapted successfully for use in triaxial testing. It was, however, felt that the existing methods of maintaining the confining pressures and monitoring volume changes, in both soils and rock mechanics systems, would be unable to cope with the large volume changes and rates of volume change expected in the proposed experiments. All the existing research on strain-softening rocks, had been restricted to limited axial strains (in the region of 2%). Even so, the principle of the dilatometer offers distinct advantages over the other methods in that it gives an average measure of volumetric strain and is unaffected by fracturing on any scale.

6.3 The Apparatus Design

The final design chosen was one incorporating a pressure relief valve with a specified operating range of 1,000 to 10,000 psi (7 - 70 MN/m^{-2}), but which, in practice, proved capable of operating at pressures as low as 500 psi (3.5 MN/m^{-2}). This valve is mounted in series with the triaxial cell and a pressure gauge, the latter allowing the confining pressure to be monitored whilst being set and then for fluctuations (Plate 6.1). An inlet valve is used for closing

off the system from the confining pressure pump once the desired test pressure is reached.

6.3.1 Specimen Size

For ease of preparation, cylindrical specimens were chosen, and a diameter of 75mm decided upon, allowing the required large volume changes. Bearing in mind the recommendations of other workers concerning diameter: height ratios (section 2.2) a specimen length of 225mm (giving a ratio of 1:3) was considered, but abandoned since the allowable size of specimen was limited by the allowable size of apparatus which, in turn, was restricted to the amount of daylight available between the testing machine platens. Consequently, a specimen length of 150mm was chosen, giving the minimum recommended ratio of 1:2. This was also felt justifiable under triaxial testing conditions.

6.3.2 The Triaxial Cell

The design of the triaxial cell is given in Fig. 6.1 and a cut-away view of it assembled in Fig.6.2. Points to note in the design of the triaxial cell include:

1. The cell is capable of withstanding a confining pressure in excess of 70 MN/m^{-2}.

2. A simple locating point and socket arrangement allows easy central mounting of the specimen in the cell.

3. The unbalanced 250mm loading ram allows large axial deformation, plus the measurement of volumetric compression of the specimen of up to 45.6cc/cm, since this is the volume of oil displaced by the ram entering the cell.

4. There is a large radial margin of 2.2cm between the specimen and the cell on all sides.

5. The top cover (including ram) is easily screwed into and out of the main body of the triaxial cell, allowing quick and easy preparation for testing.

The triaxial cell was wholly constructed within the Department of Mining Engineering's workshops. Uniaxial experiments can be conducted in the cell, using it in a similar manner to Bridgeman's dilatometer, by removing the relief valve and pressure gauge from the system and swapping the air bleed for an 'overflow' pipe.

6.3.3 Safety

Inherent in the electro-hydraulic servo-controlled testing machine is the danger of loss of control through an electronic, or some other, fault. This effectively means that a force of 500 tons could be, instantaneously, unleashed onto whatever lies between the machine platens, without any warning to the operator. The control system is equipped with safety limit trips, but for extra protection, it was decided to include a further safety device in the design of the triaxial cell. This was a safety valve designed to 'blow out' at 10,000 psi (70 MN/m^{-2}) in a direction away from the area of machine operation.

6.4 Summary

In principal, the apparatus described is similar to that used for rocks by Crouch. However, the method used by him to adjust the oil volume, a pressure intensifier has been replaced by a relief valve, allowing the measurement of larger volumetric changes. The apparatus comprises of four basic units:

1. a triaxial cell,
2. a relief valve,
3. a pressure gauge and
4. an inlet valve.

The present design enables experiments to be conducted at confining pressures ranging from 3.5 to 42 MN/m^{-2}. Uniaxial experiments can also be carried out with some minor modifications to the apparatus and testing procedures.

* * *

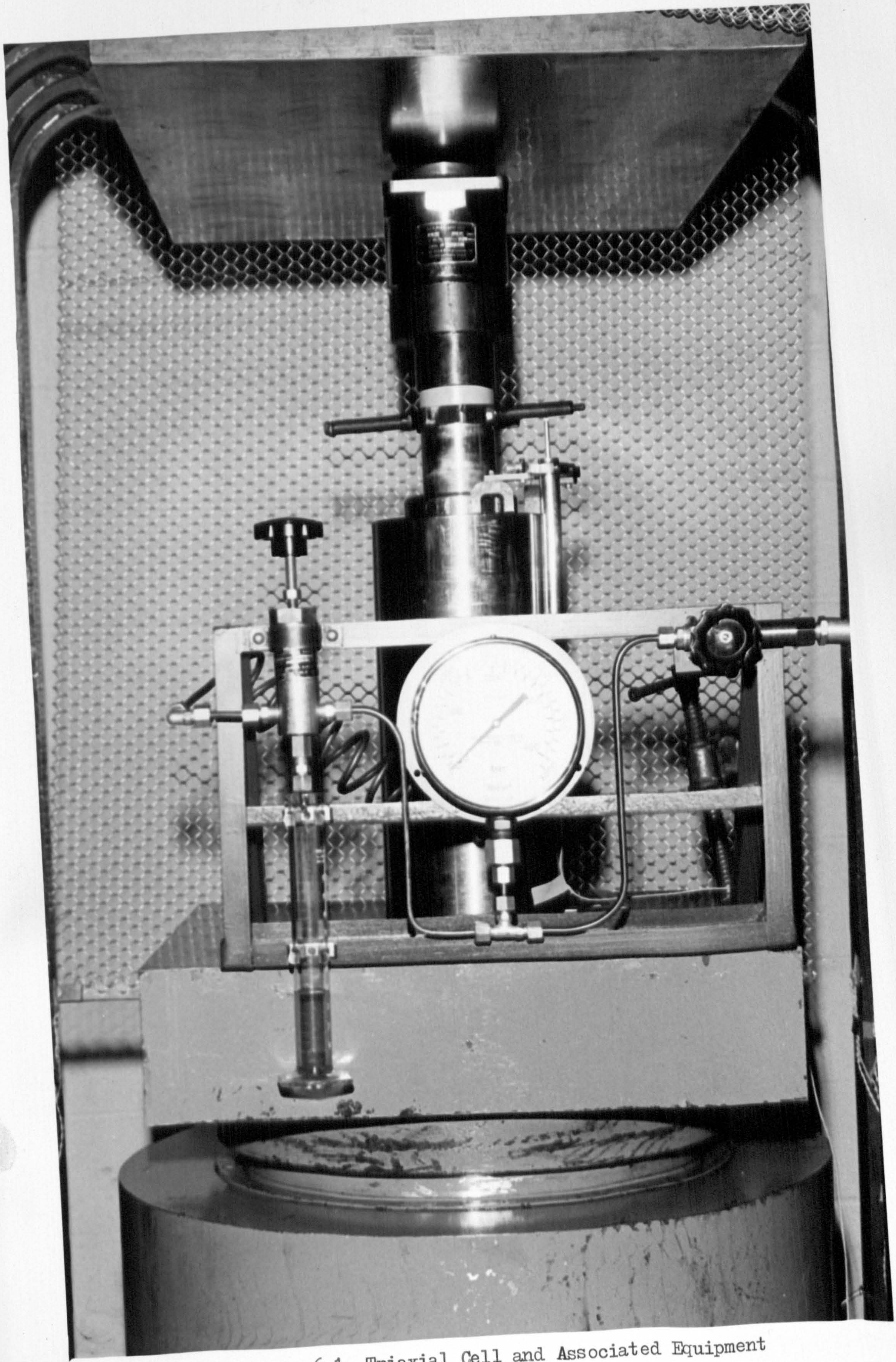

Plate 6.1 Triaxial Cell and Associated Equipment

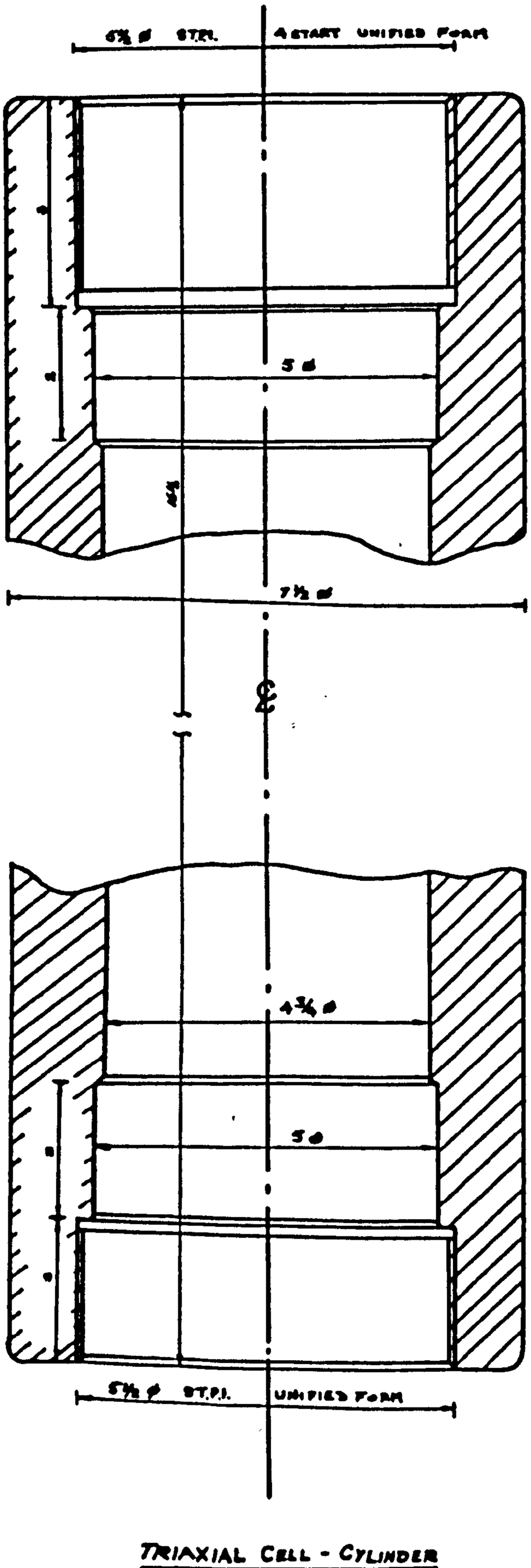

TRIAXIAL CELL - CYLINDER

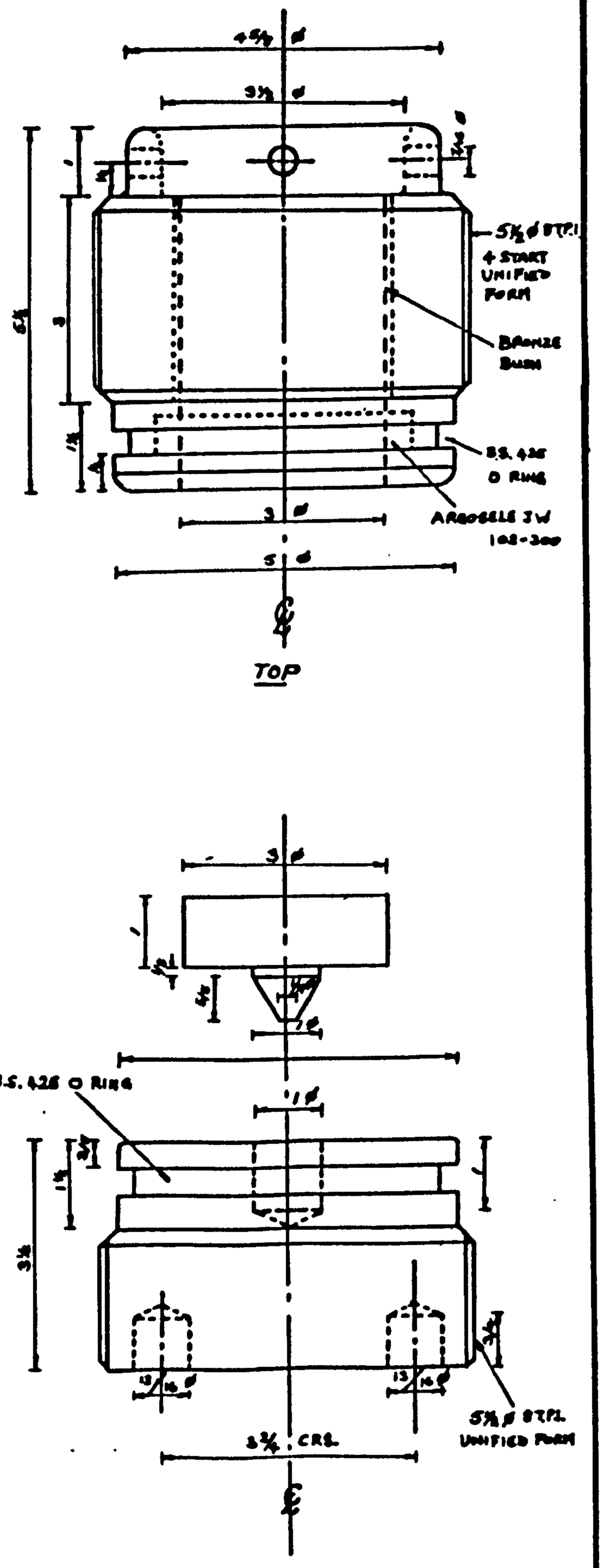

All dimensions are in inches

Fig. 6.1 DESIGN OF TRIAXIAL CELL

(From original drawings by T. Pollock)

CHAPTER SEVEN

DESIGN OF EXPERIMENTS

7.0 Introduction

The preparation for, and design of, an experiment are crucial to the results obtained from it, due to the many interdependent variables involved in the rock's breakdown mechanism. Many of these factors, such as time effects, specimen geometry, stress history, etc. were reviewed in Chapter Two. It is this irregularity of results, due to changes in experimental conditions and specimen structure, which calls for a careful adherence to a predetermined set of conditions and repeated testing, in order to obtain representative results. Unfortunately, difficulties in obtaining host blocks from which to core specimens,severely limited the number of specimens tested under any particular set of conditions. However, the experiments were designed to give qualitative, rather than quantitative results, and in this respect were successful.

7.1 Specimen Preparation

The procedure used for the preparation of specimens was in accordance with the A.S.T.M. standard D2664 (1967). The test specimens were cored to a nominal diameter of 75mm and length of 150mm. They were smooth and free of any abrupt irregularities, with sides parallel to within 0.125mm. The ends were ground parallel to each other (to within 0.01mm) and at right angles to the longitudinal axis. Prior to testing the diameter and length of each specimen were measured, using micrometers, and the average from at least three positions recorded for use in later calculations. Where possible, all specimens of a particular

rock type were taken from the same 'host block'. All specimens were kept at room temperature and were 'room dry' when tested.

For testing the specimens were mounted between two platens, whose faces were flat, clean and dry. A flexible membrane was fitted over the specimen and platens, and trimmed square with the platen ends. Then a second flexible membrane was fitted over the first and folded back over and under two rubber O-rings at each end. The use of two flexible membranes was adopted when initial tests came to abrupt ends after about 4% axial strain, due to rupture of the single membrane. This rupturing resulted from the flexible membrane becoming trapped in shear faults, along which differential sliding took place, tearing the membrane. Experimentation with two flexible membranes showed that, whilst the inner one became torn and punctured, the outer one continued to act as an effective oil seal (Plate 7.1).

7.2 Triaxial Testing Procedure

The initial procedure for applying the hydrostatic confinement is as follows. First, the inlet valve is open (system open) and the system purged of air by means of an air bleed located at the top of the pressure chamber. The air bleed is then closed off and a small axial load is applied to the specimen. The system is then loaded to the required confining pressure, whilst a hydrostatic stress field is maintained manually throughout by 'pacing' the confining pressure acting on the specimen, against the axial stress controlled by the servo-unit. Once the required confining pressure is reached, the relief valve is finely adjusted if needed, and the inlet valve closed

(system closed). It should be noted that the operating level of the relief valve is initially set before the experiment, whilst disconnected from the triaxial cell. As previously shown, once the system is 'closed', any further axial loading of the specimen will cause an increase in the confining pressure and thus operate the relief valve. The oil displaced in this manner is collected and its volume recorded manually to an accuracy of 0.25cc against the axial strain. The axial strain and axial load are continuously monitored by means of a linear voltage displacement transducer (LDVT) and load cell respectively, and recorded on an x-y plotter. Thus, at any moment in the test, knowing the oil displacement and axial strain, the volumetric strain of the specimen can be calculated.

7.3 Uniaxial Testing

The specimens for uniaxial testing are prepared in the same manner as for the triaxial tests. The apparatus is, however, modified by removing the inlet valve, pressure gauge and relief valve, and by connecting the hydraulic pump directly to the triaxial cell. Air is purged from the system in a similar manner to that described for triaxial testing and the air bleed closed. The pump is then disconnected from the triaxial cell to prevent any back flow of oil and the air bleed is replaced by an overflow pipe, from which the displaced oil is collected. The test then continues using the cell as a simple uniaxial dilatometer. In all tests the strain rate adopted was approximately $21 \mu\varepsilon s^{-1}$, chosen by trying to balance the effect of strain rate on the control and behaviour of the specimen and the lack of long term reliability of the testing system.

7.4 Treatment of Data

From the recorded raw data, true volumetric, axial and radial strains, plus instantaneous Poisson's ratio can be calculated. As the oil is released from the triaxial cell, it expands, due to the reduction in pressure. Therefore, the true volume of oil displaced, V_t, is given by the equation:

$$V_t = fV_o \qquad \ldots\ldots (7.1)$$

where V_o is the measured volume of oil displaced, and f is a factor of compressability, taken from technical data supplied by Shell (1967) for 'Tellus 27' oil. The factors used are given in Table 7.1. This true volume of oil displaced is composed of two elements; the oil displaced by the loading ram entering the triaxial cell, and the oil displaced by the volumetric change of the specimen ΔV. The latter is thus defined by the equation:

$$\Delta V = V_t - V_R \qquad \ldots\ldots (7.2)$$

where V_R is the volume of the ram entering the cell, with its measured displacement corrected for elastic deformation of the ram, and is given by the equation:

$$V_R = (\pi r^2 - P/E)l \qquad \ldots\ldots (7.3)$$

where r = the radius of the ram

P = the axial load acting on the ram

E = the Young's modulus of the ram

and l = the measured displacement of the ram.

Substituting equations 7.1 and 7.3 in 7.2 the percentage volumetric change of the specimen is given by:

$$\frac{\Delta V}{V} = \frac{100}{V} \not\leftarrow (f.V_o - (\pi r^2 - P/_E) 1) \quad \text{per cent} \quad \ldots\ldots (7.4)$$

where V = the specimen's original volume.

The average axial strain of the specimen, ε_1, is given by the equation:

$$\varepsilon_1 = \frac{1001}{L} (1 - \frac{P}{\pi r^2 E}) \quad \text{per cent} \quad \ldots\ldots (7.5)$$

where L - the original length of the specimen.

Then using the equation for volumetric strain (Jaeger and Cook, 1971):

$$\frac{\Delta V}{V} = \varepsilon_1 + \varepsilon_2 + \varepsilon_3 \quad \ldots\ldots (7.6)$$

which reduces, in this case, to:

$$\frac{\Delta V}{V} = \varepsilon_1 + 2\varepsilon_2 \quad \ldots\ldots (7.7)$$

the lateral strain, ε_2, is given by:

$$\varepsilon_2 = \tfrac{1}{2} (\Delta V/_V - \varepsilon_1) \quad \text{per cent} \quad \ldots\ldots (7.8)$$

and instantaneous Poisson's ratio, ν, by:

$$\nu = \tfrac{1}{2} (\frac{\Delta V}{V \varepsilon_1} - 1) \quad \ldots\ldots (7.9)$$

* * *

Plate 7.1 Example of Torn Inner Sleeve

CHAPTER EIGHT

EXPERIMENTAL RESULTS

8.0 Introduction

The seven rock types selected for study have been listed in Table 8.1. The sandstone, silty sandstone and mudstone were selected as being representative of Coal Measures rocks, whilst the rock salt and carnallite marl were selected to simulate the breakdown mechanism of the weaker Coal Measures rocks, samples of which could not be easily obtained. Three of the seven rock types exhibited a transition from strain softening to strain hardening behaviour within the range of confining pressures used. Table 8.2 gives a summary of those tests conducted and the deformation mechanism of the individual specimens. Plates 8.1 to 8.8 show the specimens after testing.

8.1 Portland Stone

The Portland Stone, a strong, homogeneous spheroidal limestone, was the first rock type experimented with using this equipment and, of twenty-two tests, nine are regarded as preliminary and eleven as valid. All of the experiments using Portland Stone were duplicated to determine the reproducibility of the data. Experimental plots of axial stress and volumetric strain versus axial strain, demonstrating the degree of reproducability are given in Figs. A1 to A5 (Appendix A).

All the specimens of Portland stone behaved in a strain softening manner, typically dropping to a residual stress level at about one half or two-thirds of its peak stress (Fig. 8.1). The exception is the uniaxial test which dropped to a token residual strength, probably a measure of

the artificial cohesion created by the rubber sleeves. Specimens tested at confining pressures of 14 MN/m^2 and above failed uncontrollably (represented by dashed lines in the figures). All of the specimens failed in a brittle manner and most had conjugate fault planes transecting them.

Fig. A1 ?

The post-failure data obtained from the experiments had straight lines fitted to it using a least squares analysis, and these were then averaged for each confining pressure, and plotted in Figs. 8.2 to 8.4.

The volumetric strain, lateral strain and instantaneous Poisson's ratio versus axial strain plots for different confining pressures are given in Figs. 8.2 to 8.5, and demonstrate the typical results obtained for all the rock types; namely, that increased confining pressure reduces the magnitudes of the volumetric expansion, lateral expansion and the instantaneous value of Poisson's ratio.

8.2 Saccharoidal Limestone

The host block from which the specimens of saccharoidal limestone were cored, was obtained from an outcrop on the shore of the Cow Green Reservoir in Upper Teesdale. This medium to coarse grained, homogeneous, marmitised limestone was selected for testing with a view to obtaining strain hardening behaviour, together with total cataclasis of the specimen, similar to that reported by Scholz (1968a). However, only the uniaxial specimen cataclased, whilst the others failed with either conjugate brittle faulting, or ductile faulting. An example of ductile faulting is given in Plate 8.9. The axial stress-strain curves from these experiments are plotted in Fig. 8.7. These show a slow transition from the strain softening towards

the strain hardening behaviour in which each additional increment of strain requires an additional increment of stress. The volumetric strain plots are given in Fig. 8.8, where the axial strain axes have been separated to aid clarity. Once again, it is apparent from this figure that there is a large reduction in the magnitude of the volumetric expansion, between the uniaxial and triaxial experiments. For this particular rock type, the triaxial volumetric curves converge at about four or five percent axial strain, which is most clearly illustrated in figure 8.10, where the plots of Poisson's ratio are quite distinctly different before four percent axial strain, but are virtually coincident beyond five percent. For simplicity, certain curves have been omitted from Figs. 9.8 and 8.10, and these are presented in Appendix A (Figs. A6 and A7).

8.3 Sandstone

The sandstone, silty sandstone and mudstone samples were obtained from the Woodhorn to Ashington cross-measures drift, Woodhorn Colliery, during some site investigations carried out jointly with J. Armstrong and reported by him elsewhere (Armstrong, 1978).

This medium grained sandstone exhibited strain softening behaviour similar to that of the Portland Stone. The uniaxial specimen fractured in a combination of columnar and shear failure, with end cones formed but split into two or more pieces. At lower and higher range confining pressures, triaxial specimens exhibited spalling and and brittle faulting respectively. Difficulty was experienced in testing this rock over large axial strains, because in several experiments both the inner and outer sleeves split and the experiments were abandoned.

For this reason the 7 and 14 MN/m^{-2} confining pressure experiments were repeated. Both sets of results are presented in Appendix A (Figs. A8 to A11). Plots of volumetric strains, lateral strains and instantaneous Poisson's ratio are presented in Figs. 8.14 to 8.16.

8.4 Silty Sandstone

This medium grained sandstone with silt inclusions was taken from the same site as, and behaved in a similar manner to, the sandstone. It was, however, weaker than the sandstone (Fig. 8.18) and axial deformation resulted in the formation of conjugate fault planes for triaxially tested specimens instead of slabbing. The triaxial test conducted at a confining pressure of 42 MN/m^{-2} resulted in a transition in the mode of deformation from conjugate brittle faulting to ductile faulting. The magnitudes of the volumetric changes for the silty sandstone were also less than those for the sandstone (Fig. 8.19). Data plots for the 29 and 42 MN/m^{-2} confining pressure experiments are presented separately in Appendix A (Figs. A12 to A14).

8.5 Mudstone

The mudstone specimens, although taken from the same host block, differed markedly in their composition. Visual analysis of the specimens identified bands or zones with varying concentrations of silt, ironstone and coal inclusions. The ironstone having a higher strength than the mudstone often caused peculiar failure formations in the specimens (e.g. Plates 8.5 and 8.10) due to the stronger bands acting as platens. These variations are illustrated by Figs. 8.24 to 8.26, in which Schore-Schleroscope rebound numbers are plotted for four traverse lines along each of the three specimens. Fig. 8.23 illustrates well the effects

of confining pressure on the axial stress-strain curve for rock as outlined in section 2.3.

Fig. 8.27 shows the typical result of increasing confining pressure on measured volumetric strain for three of the specimens tested. However, the volumetric strains recorded were influenced by the amount of the specimen which actually deformed. Therefore, a correction for the length of the specimen failed was applied and a least squares analysis performed on the corrected data. The calculated 'best fit' curves are presented in Fig. 8.28, whilst the actual recorded values are plotted in Fig. A15 (Appendix A). Plots of the lateral strains and instantaneous Poisson's ratio are given in Figs. 8.29 and 8.30 and Figs. A16 and A17 (Appendix A).

8.6 Rock Salt

The rock salt and carnallite marl specimens were chosen for this series of experiments in order to model the behaviour of the weaker Coal Measures rocks, such as fireclays, of which samples could not be easily obtained.

The rock salt behaved in a ductile manner and there was a transition from strain softening behaviour in the uniaxial experiment to that of strain hardening in the triaxial experiments (Fig. 8.32). The actual axial stress-strain plots have been smoothed, since it was apparent that fluctuations in the curves were not a property of the rock itself, but rather, of the system. This problem will be discussed more fully later in this thesis.

The volumetric strains measured (Figs. 8.33 and 8.34) are typical of all the other rock types except that, within the range

of confining pressures used here, this rock experiences a transition from expansion to contraction with increasing confining pressure. Even so, the specimen tested at 42 MN/m^{-2} has reached a maximum compression and has started to expand, although still smaller than its original size. An interesting observation was that, after testing, those specimens tested at confining pressures below 14 MN/m^{-2} were dry and had not extruded any marl from inclusions, and those tested above 14 MN/m^{-2} were wet and had extruded marl. This moisture can be attributed to pore brine trapped within the specimen and driven out along grain boundaries during compression.

A series of experiments were also conducted at a constant confining pressure of 14 MN/m^{-2}, but at different strain rates. The axial stress-strain plots are presented in Fig. 8.39, which demonstrates, as might be expected, that the faster strain rates yield higher strengths. The data obtained from these tests for volumetric changes were inconclusive and unreliable, due to machine problems, and have, consequently, not been presented. The chief mode of deformation for all the triaxial tests was that of uniform flow.

8.7 Carnallite Marl

Once again, the smoothed, axial stress-strain plots (Fig.8.40) reveal a slow transition from strain softening to strain hardening behaviour, with increasing confining pressure. This transition occurs somewhere between a confining pressure of 7 and 14 MN/m^{-2}, and is reflected in the volumetric strain plots (Figs. 8.41 and 8.42) by a transition from expansion to contraction with increasing confinement.

This transition was also marked by a change from brittle to ductile faulting as the chief deformation mode. Specimen C22 was a composite sample made from two broken cores, which may explain its slightly uncharacteristic behaviour relative to the other specimens in some plots.

8.8 Discussion

Pressure had a pronounced effect upon the stress-strain properties of the rocks tested. The axial stress-strain curves as presented (Figs. 8.1, 8.7, 8.13, 8.18, 8.23, 8.38 and 8.40) all show that increased confining pressure both strengthens the rock and results in an eventual transition from strain softening to hardening behaviour. These effects seem to diminish as the high confining pressures are reached. There is also an increase in the axial strain to failure and often a shallower post failure curve as confining pressure increases.

The 'waviness', typical of most of the axial stress-strain curves, is not due totally to stick-slip along the failure surface, as one would initially think, but is a property of the testing apparatus. The 'stick-slip' account is suspect, since the confining pressures used here are lower than is normal for this type of behaviour, and also because it occurs with the strain hardening rocks. It was also often noted during experiments that sudden movements or volume changes in the specimen caused the valve to 'over-release' and thus allow the pressure to drop too far. Prime examples of this were the sudden releases of oil and pressure drops, accompanying uncontrolled failure of specimens. Once the release valve had closed again the pressure

would slowly build up to the test pressure, and this course of events might repeat itself. This mechanism seemed more frequent at the higher confining pressures. It is for this reason that, where curves have been smoothed, bars showing the maximum variation of data from the smoothed curve have been included.Since the curves have tended to be smoothed towards the boundary corresponding to the correct confining pressure and, because of occasional large pressure drops, these bars are often uneven and show large variations.

The volumetric strain versus axial strain plots show a systematic change with confining pressure. All the curves show the same general form; a small volume decrease occurring at low strains, the slope of the curve changing rapidly in the yielding region, and a final, near linear, curve after yielding. In all cases, the uniaxially tested specimens gave very large volumetric expansions with increasing axial strain typically of the order of ten to twenty percent, at ten percent axial strain. The effect of confining pressure on the volumetric expansion is very marked, with a large reduction for an increase in confining pressure at low confining pressures, diminishing as confining pressure is increased. If the confining pressure is increased to above a certain threshold value, dependent upon the rock type, no volumetric expansion will occur. These variations in volumetric strain with increasing confining pressure are, perhaps, more clearly demonstrated in the plots of confining pressure against volumetric strain, at an axial strain of ten percent for each rock type (Figs. 8.6a, 8.11, 8.17a, 8.22a, 8.31a, 8.38a and 8.46). In all but one case these curves demonstrate an 'exponential' form of decay of the volumetric expansion with increasing confining

pressure. The exception is the saccharoidal Limestone curve (Fig.8.11) which, at two percent axial strain, gives a curve similar to the others but deformed past about four or five percent, gives similar magnitudes of volumetric strain for all of the triaxial experiments. In the case of the saccharoidal limestone the curves are steeper at yield than at the higher strains past their convergence point. This initial slope becomes shallower as the confining pressure is increased, and thus the change in slope becomes less marked with increasing confining pressure. This observation is also true of the other rock types, although their secondary slopes are neither parallel nor superimposed. The reason for this phenomenon in the saccharoidal limestone experiments is not readily apparent. It seems unlikely that it is the result of the deformation mechanism, but it may be that this behaviour is characteristic of this type of rock structure.

The shape of the volumetric curves is typical of those reported for soils and rocks elsewhere[1], and corresponds to the axial stress-strain behaviour of the rock. At all pressures below the threshold point, axial deformation leads first to elastic compaction of the specimen corresponding to the elastic region of the axial stress-strain curves. The specimen then expands at a rate dependent upon the rate of fracturing, reflected in the rate of unloading in the axial stress-strain curves. Then, once macrofracturing has occurred, the mechanism of deformation is frictional sliding, giving approximately constant residual stress and linear volumetric strain curves.

---

[1] Lambe and Whitman (1969); Atkinson and Bransby (1978); Scholz (1968a, 1967); Rowe (1962); Edmond and Paterson (1972); Handin et al. (1963); Cogan (1976); Jamison and Teufel (1979).

Some distinctions must be made about the relationship of deformation mechanisms to the strain softening to hardening transition. This transition cannot be related to a change in the mechanism of deformation or to the transition from volumetric expansion to contraction. The 'strain hardening' mechanisms of intercrystalline gliding and recrystallisation are not the sole mechanisms associated with the transition, cataclasis or microcracking has been reported above this transition (Scholz, 1968a; Edmond and Paterson, 1972). In the case of saccharoidal limestone, for instance, there is a definite visual change in deformation mechanism which is also reflected in the axial stress-strain relationship, but the ductile faulting still involves cataclasis within concentrated zones. The volume also increases in order to accommodate the relative movement of the grains and their fragments, in agreement with Reynolds' (1885) original observations. It follows from this then that volumetric expansion is an indication of a deformation mechanism involving cataclasis. However, as discussed by Edmond and Paterson (op. cit), this does not mean that no volumentric expansion is indicative of intercrystalline plasticity. This is demonstrated in these experiments by the carnallite marl sample, CM22, tested at a confining pressure of 42 MN/m^{-2}, which reaches and maintains a nearly constant compaction of two percent and yet exhibits clear shear planes. The strain softening-hardening transition must, therefore, be defined as the point above which microcrack propagation is stable and uniform throughout the specimen.

Perhaps more diagnostic of the effect of confining pressure on volumetric strain are the instantaneous Poisson's ratio versus confining pressure plots (Figs. 8.6b, 8.12, 8.17b, 8.22b, 8.31b, 8.38b and 8.45).

The values of Poisson's ratio plotted here are the instantaneous ratio of lateral to axial strains, calculated at an axial strain of ten percent. Curves for the progressive changes in instantaneous Poisson's ratio are also presented in Figs. 8.5, 8.10, 8.16, 8.21, 8.30, 8.36, 8.37 and 8.44.

Poisson's ratio decreases very rapidly as confining pressure is increased and appears to reach a constant value which, for most rock types, is 0.5, corresponding to no volume change in the specimen with deformation. The exceptions to this are the curves for the saccharoidal limestone and carnallite marl which tend towards 0.8 and 0.4 respectively. Fig. 8.44 presents the plots for carnallite marl at 5, 10 and 15 percent, and a change in the shape of the curve due to a reduction in the uniaxial value of Poisson's ratio with strain is readily apparent and is typical of all the rock types. The magnitude of Poisson's ratio approaches a near constant value for each confining pressure once frictional sliding occurs. The shapes of both these types of plot are similar to those reported elsewhere (Scholz, 1967, 1968a; Walsh, 1965; Walsh and Brace, 1966).

It has been observed before that lateral strain increases and accelerates as failure progresses (Brace et al., 1966; Crouch, 1970, 1971; Barnard, 1964). Similar behaviour has been recorded in these experiments (Figs. 8.4, 8.9, 8.15, 8.20, 8.29, 8.35 and 8.45). As would be expected from the previous observations and from the mechanism of dilatancy, lateral strains decrease with increased confining pressure. In all cases the maximum rate of change of lateral straining occurs in the neighbourhood of the peak axial stress and then reduces to a near constant value giving a near linear curve.

* * *

Rock	Density g/cc	Porosity %	Uniaxial Strength MN/m^2	Place of Origin
Portland Stone (Limestone)	2.29	12.6	73	
Saccharoidal Limestone	2.67	-	49	Cow Green Reservoir, Teesside
Sandstone	2.50	7.0	97	Woodhorn Coll. North'land
Silty Sandstone	2.34	10.2	61	Woodhorn Coll. North'land
Mudstone	2.63	-	9	Woodhorn Coll. North'land
Rock Salt	2.17	-	26	Cheshire
Carnallite Marl	2.24	-	10	Boulby Potash Mine, Yorkshire

Table 8.1 Rocks Tested

Rock and Exp. No.	Confining Pressure MN/m^{-2}	Strain Rate $X10^{-6}S^{-1}$	Deformational Mode		Description
Portland Stone					
PT 10	14	21		Brittle Faulting	
PT 11	14	21		Conjugate B.F.	
PT 12	14	21		Conjugate B.F.	
PT 13	7	21	—	-	Sleeve Failed
PT 14	7	21		Conjugate B.F.	
PT 15	7	21		Brittle Faulting	
PT 16	7	21		Conjugate B.F.	
PT 17	28	21		Conjugate B.F.	
PT 18	28	21		Conjugate B.F.	
PT 19	28	21	—	-	Machine Failure
PT 20	21	21		Conjugate B.F.	
PT 21	21	21		Conjugate B.F.	
PT 22	0	21		Slabbing	
Saccharoidal Limestone					
S 1	7	21		Conjugate B.F.	
S 2	14	21		Conjugate B.F.	
S 3	21	21		Ductile Faulting	
S 4	28	21		Ductile Faulting	
S 5	35	21		Ductile Faulting	
S 6	42	16		Ductile Faulting	Error in strain rate setting
S 7	0	21		Cataclasis	

Table 8.2 Summary of Experiments (contd...)

Rock and Exp. No.	Confining Pressure MN/m^{-2}	Strain Rate $X10^{-6}S^{-1}$	Deformational Mode		Description
<u>Sandstone</u>					
WS 1	4	21		Slabbing	
WS 2	21	21		Conjugate B.F.	
WS 3	14	21		Slabbing	Sleeve Failed
WS 4	14	21		Brittle Faulting	Sleeve Failed
WS 5	7	21		Slabbing	Sleeve Failed
WS 6	7	21		Slabbing	Sleeve Failed
WS 7	0	21	-	-	Machine Failure
WS 8	0	21		Columnar	
<u>Silty Sandstone</u>					
SS 1	7	21		Conjugate B.F.	
SS 2	14	21	-	-	System Failure
SS 3	21	21		Conjugate B.F.	
SS 4	29	21		Conjugate B.F.	
SS 5	36	21		Conjugate B.F.	
SS 6	42	21		Ductile Failure	
SS 7	0	21	-	-	System Failure
U 1	4	21		Conjugate B.F.	
U 2	0	21		Slabbing	

<u>Table 8.2</u> (Sheet 2)(contd....)

Rock and Exp. No.	Confining Pressure MN/m^{-2}	Strain Rate $X10^{-6}S^{-1}$	Deformational Mode		Description
<u>Mudstone</u>					
M 1	28	21	-	-	System failure
M 2	0	21		Slabbing	Sleeve Failed
M 3	40	21		Ductile Faulting	Faulting isolated to bottom half
M 4	35	21		Conjugate B.F.	
M 5	28	21		Conjugate B.F.	Faulting isolated to top half
M 6	21	21		Conjugate B.F.	Sleeve failed. Faulting isolated to bottom third
M 7	14	21		Conjugate B.F.	Faulting isolated to bottom half
M 8	7	21		Conjugate B.F.	Faulting isolated to bottom half
<u>Rock Salt</u>					
R 1	7	21		Uniform Flow	Major grain boundary distortion also visible. Dry after test
R 2	14	21		Uniform Flow	Extrusion of marl. Localised straining. Moist after test
R 3	21	21		Uniform Flow	Marl extrusion Some open cracks along grain boundaries. Wet after test
R 4	28	21		Uniform Flow	-do-
R 5	35	21		Uniform Flow	-do-
R 6	42	21		Uniform Flow	Marl extrusion Wet after test No cracks visible
R 7	0	21		Cataclasis	Cataclasis of grains all of which exhibit axial cracking. Dry after test.

Table 8.2 (Sheet 3) (contd...)

Rock and Exp. No.	Confining Pressure MN/m^{-2}	Strain Rate $X10^{-6}S^{-1}$	Deformational Mode		Description
Rock Salt (contd)					
R 8	3.5	21		Ductile Faulting	Major axial cracking visible plus cracks along grain boundaries.Dry after test
R 9	14	8.5		Uniform Flow	Extrusion of marl plus cracking along boundaries.Wet after test.
R 10	14	85		Uniform Flow	-do- but dry after test.
R 11	14	3.4		Uniform Flow	As R9
Carnallite Marl					
CM 16	29	21		Ductile Faulting	Faulting limited to bottom half.
CM 17	42	21	-	-	System Failure
CM 18	14	21		Ductile Faulting	Faulting limited to top half
CM 19	7	21		Conjugate B.F.	Faulting limited to bottom half
CM 20	3.5	21		Brittle Faulting	
CM 21	0	21		Brittle Faulting	
CM 22	42	21		Ductile Faulting	Composite Specimen

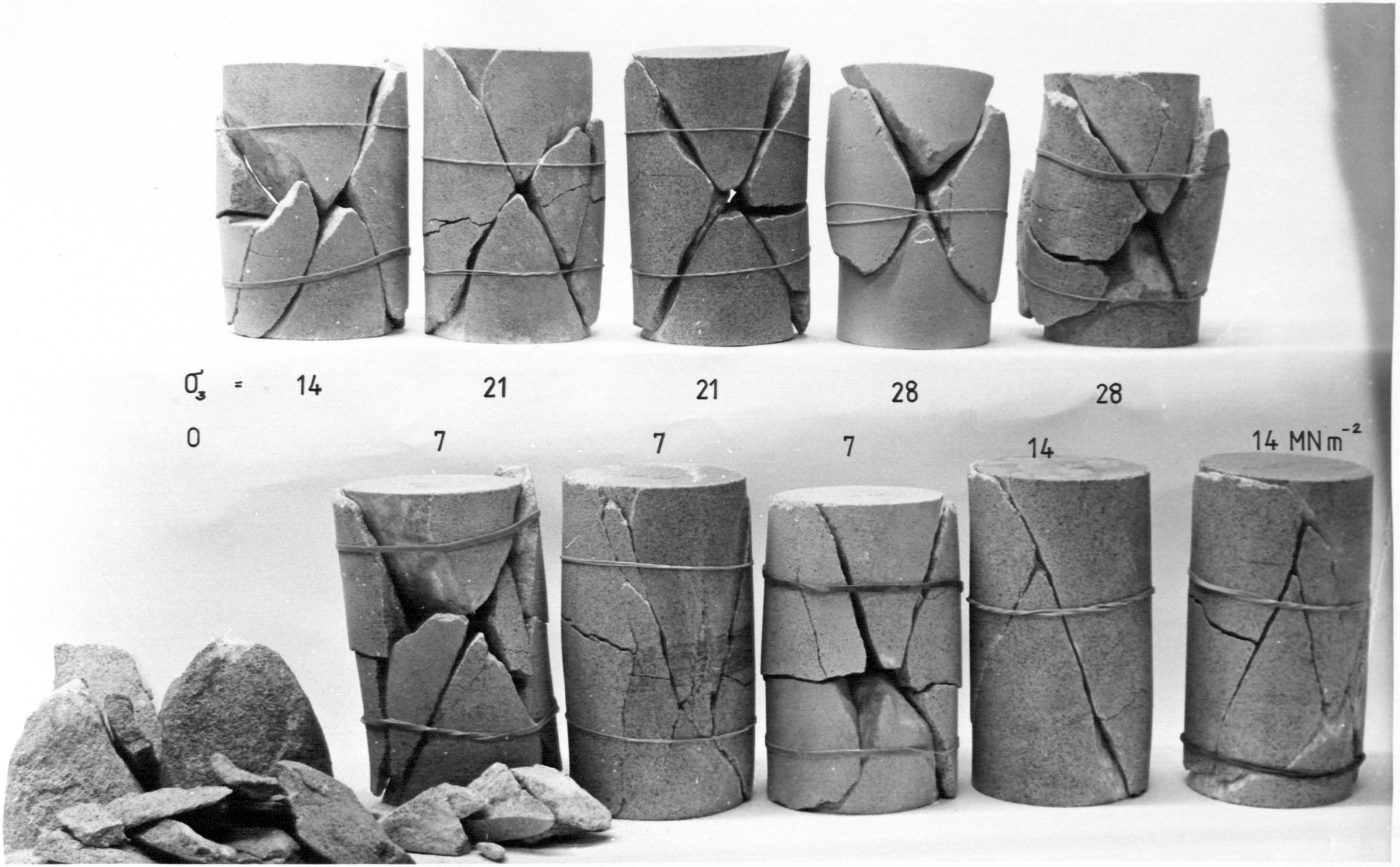

Plate 8.1 Portland Stone Specimens

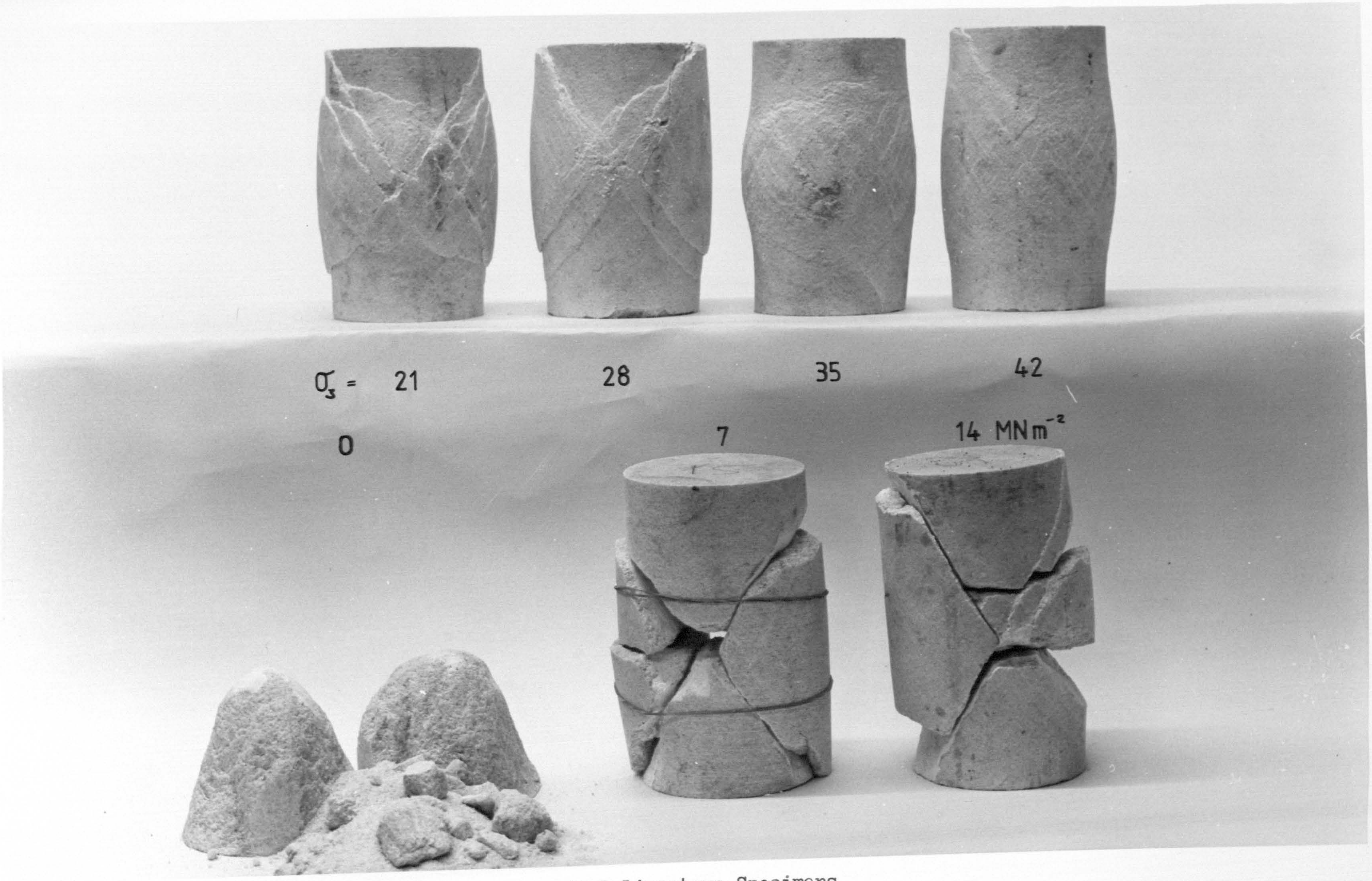

Plate 8.2 Saccharoidal Limestone Specimens

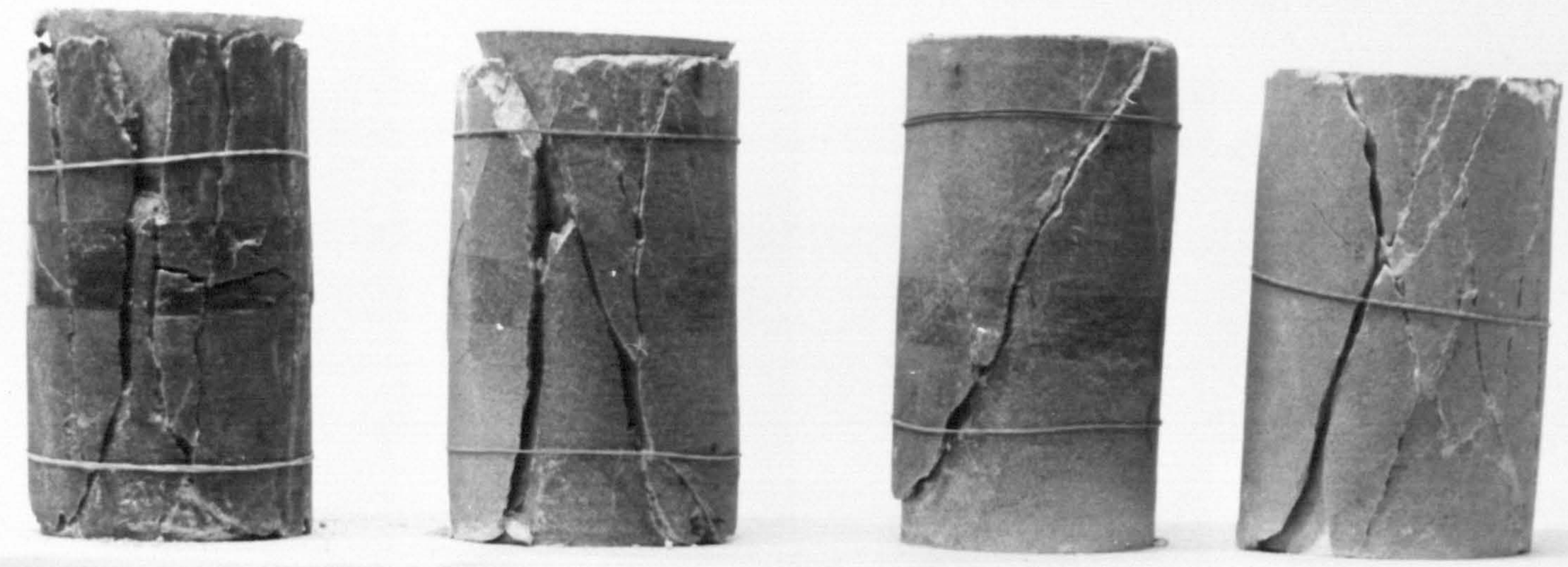

Plate 8.3 Sandstone Specimens

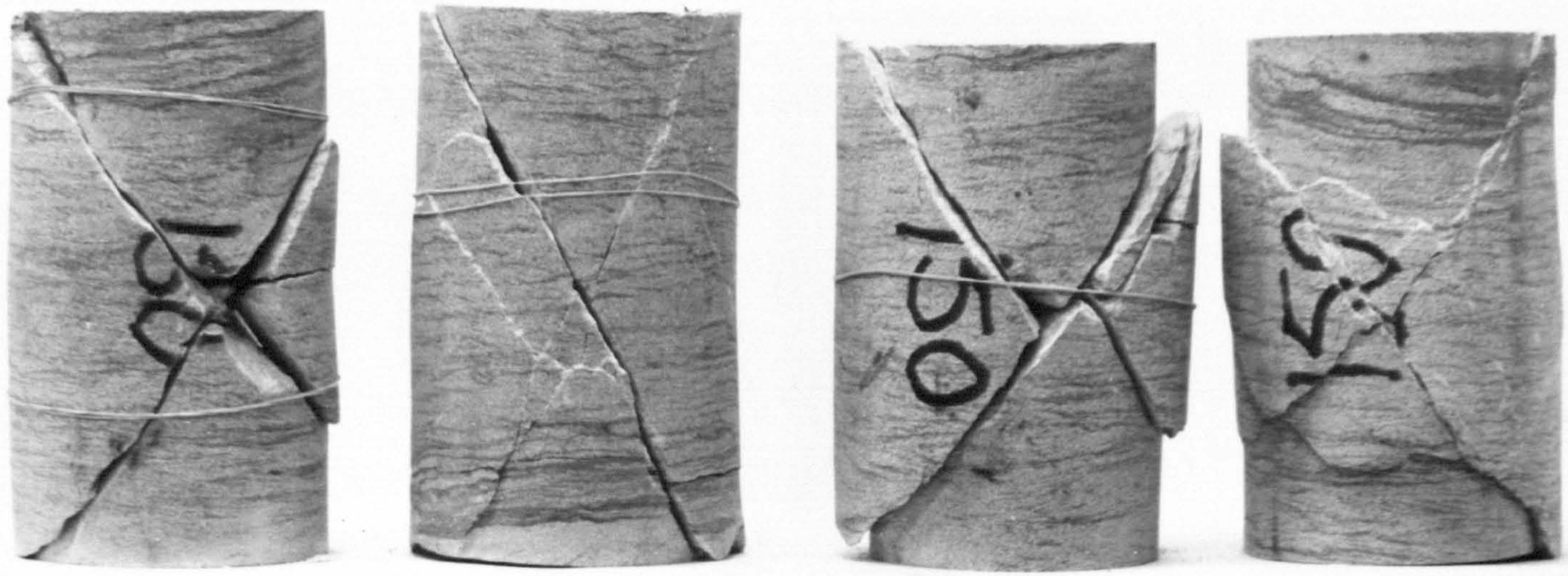

σ_3 = 21 29 36 42

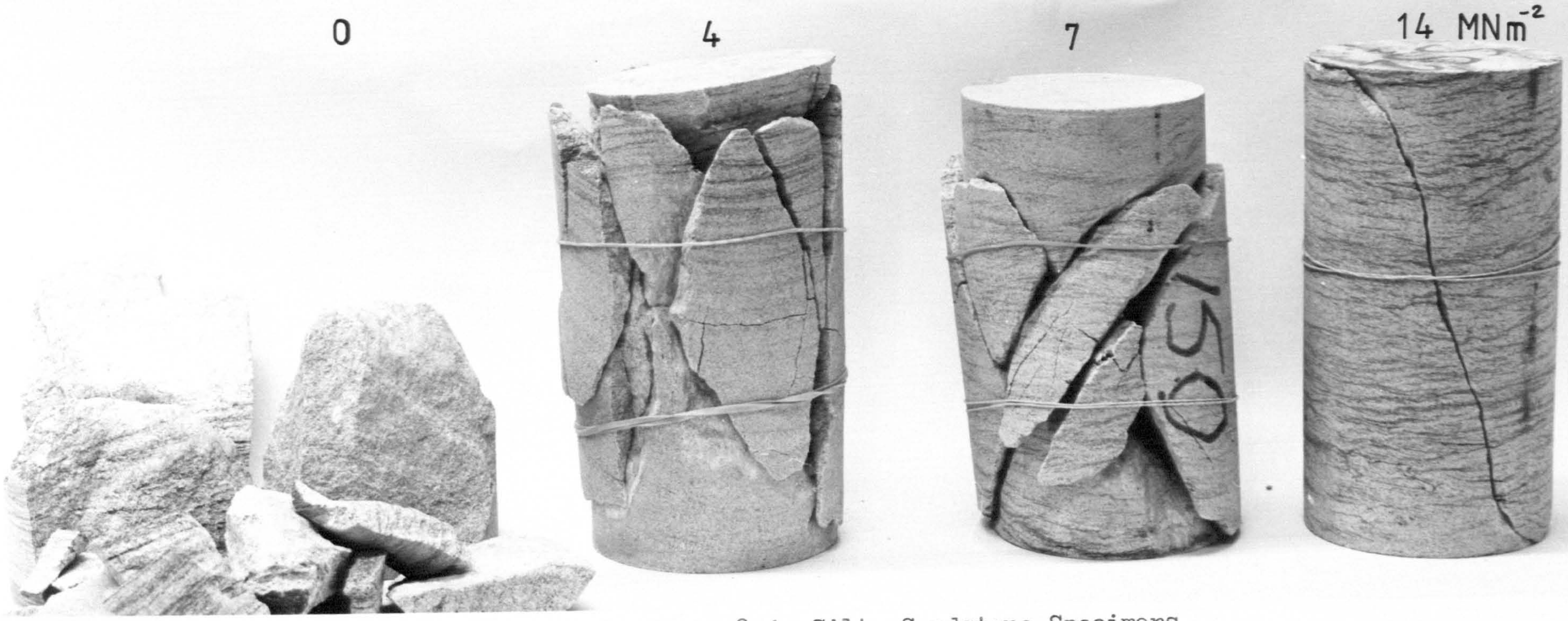

0 4 7 14 MNm^{-2}

Plate 8.4 Silty Sandstone Specimens

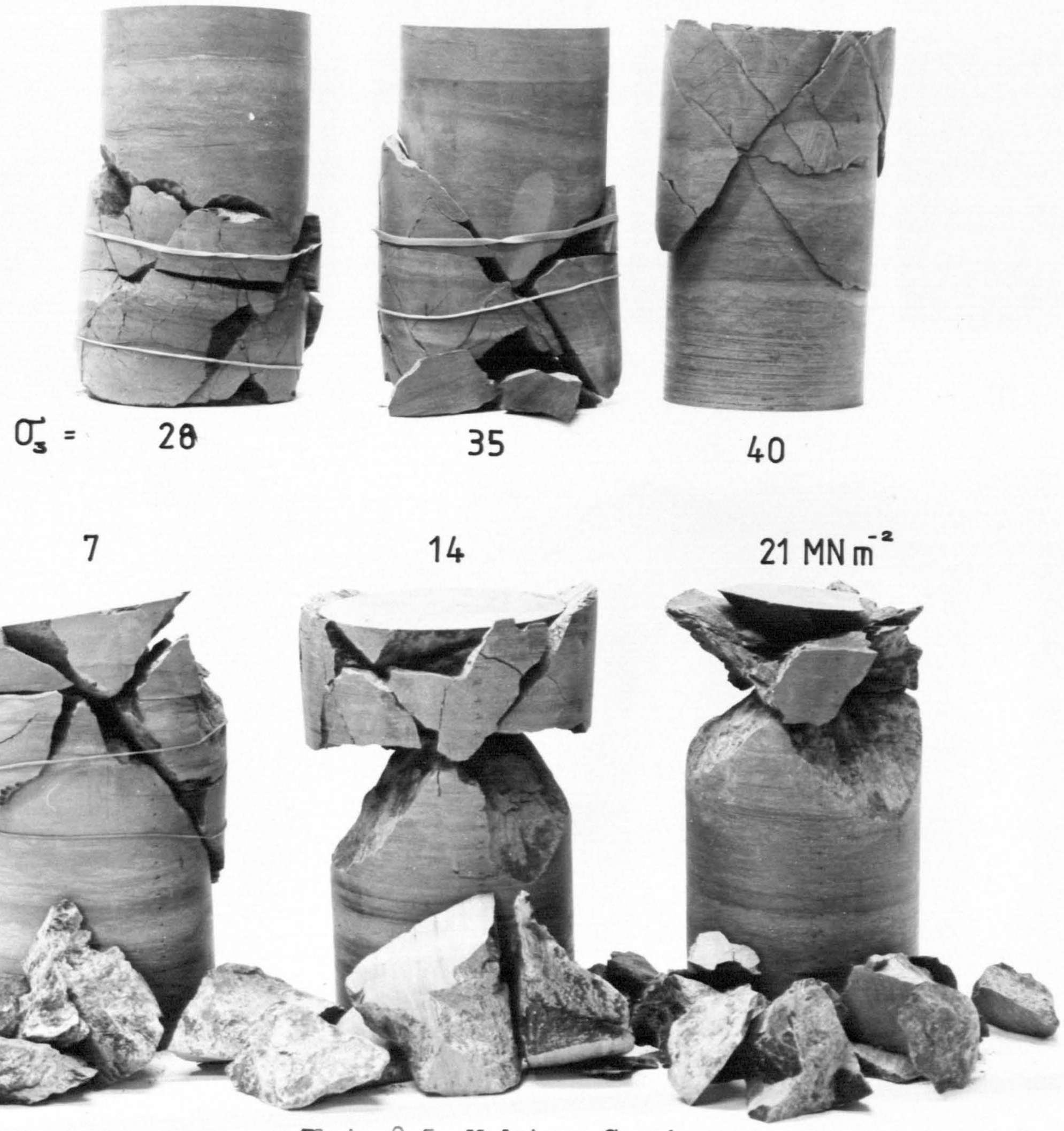

Plate 8.5 Mudstone Specimens

Plate 8.6 Rock Salt Specimens

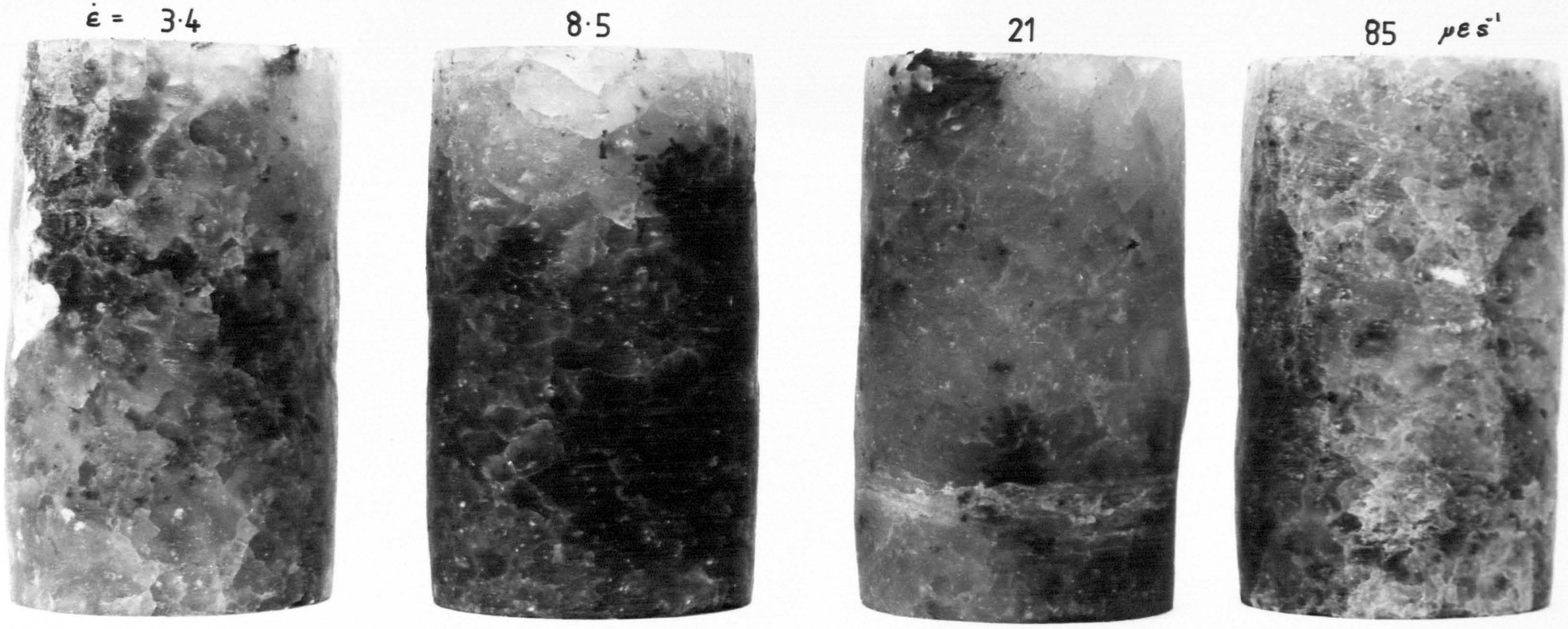

Plate 8.7 Rock Salt Specimens for different strain rates

σ_3 = 14 29 42

0 3·5 7 MN m^{-2}

Plate 8.8 Carnallite Marl Specimens

Plate 8.9 Saccharoidal Limestone showing Ductile Faulting

Plate 8.10 Mudstone : Crater and End Cone

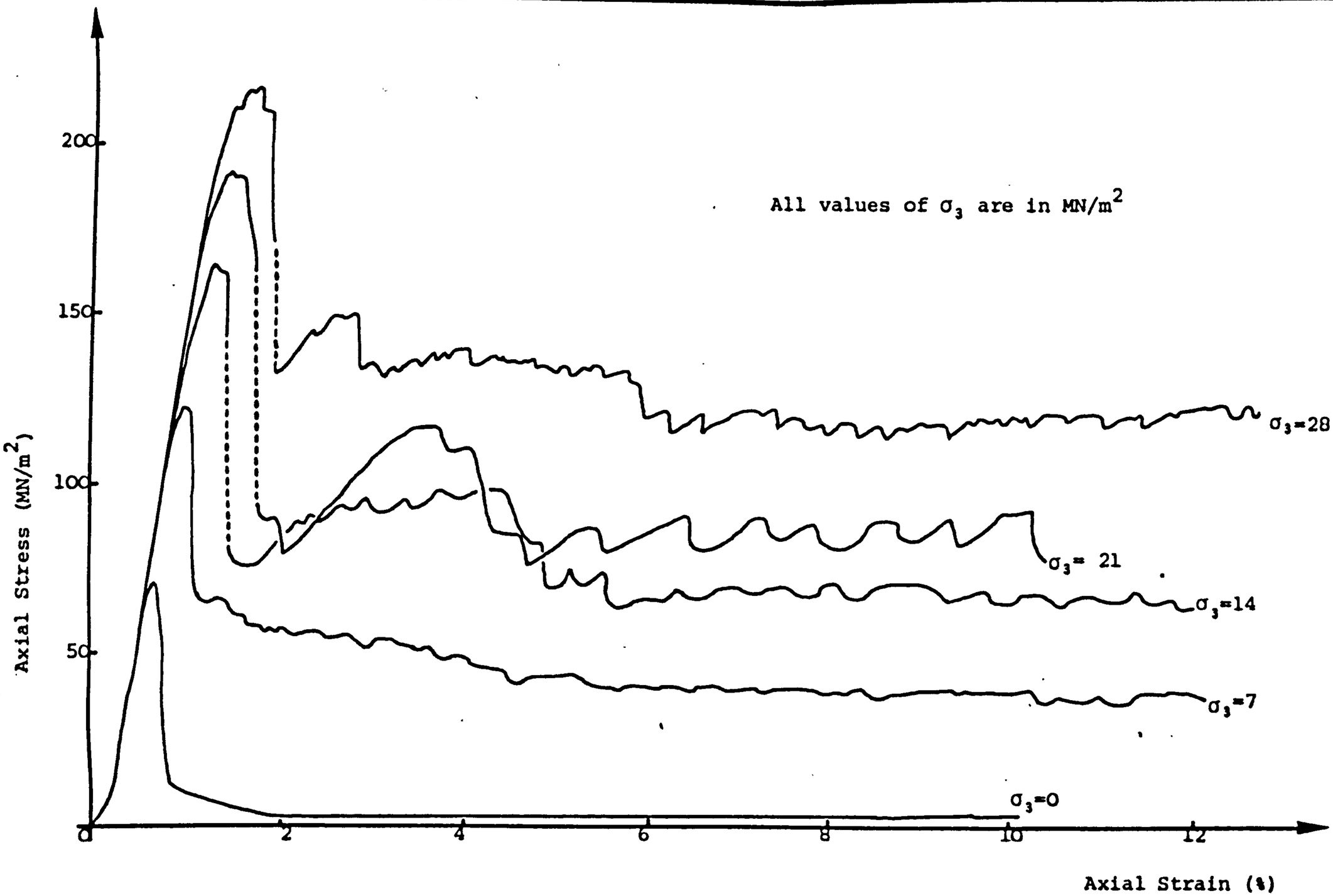

Fig. 8.1 Portland Stone: Typical Axial Stress Strain for different confining pressures

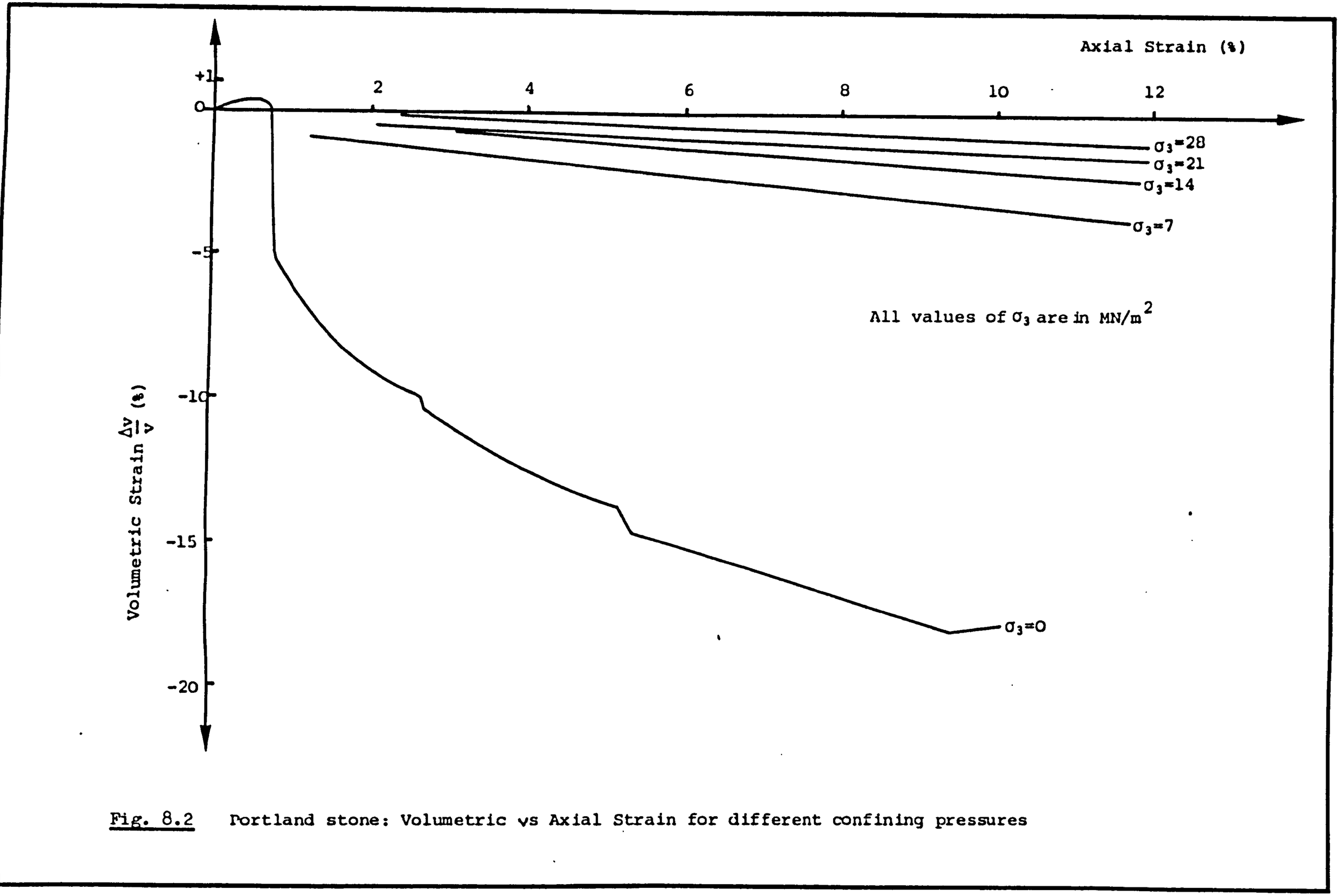

Fig. 8.2 Portland stone: Volumetric vs Axial Strain for different confining pressures

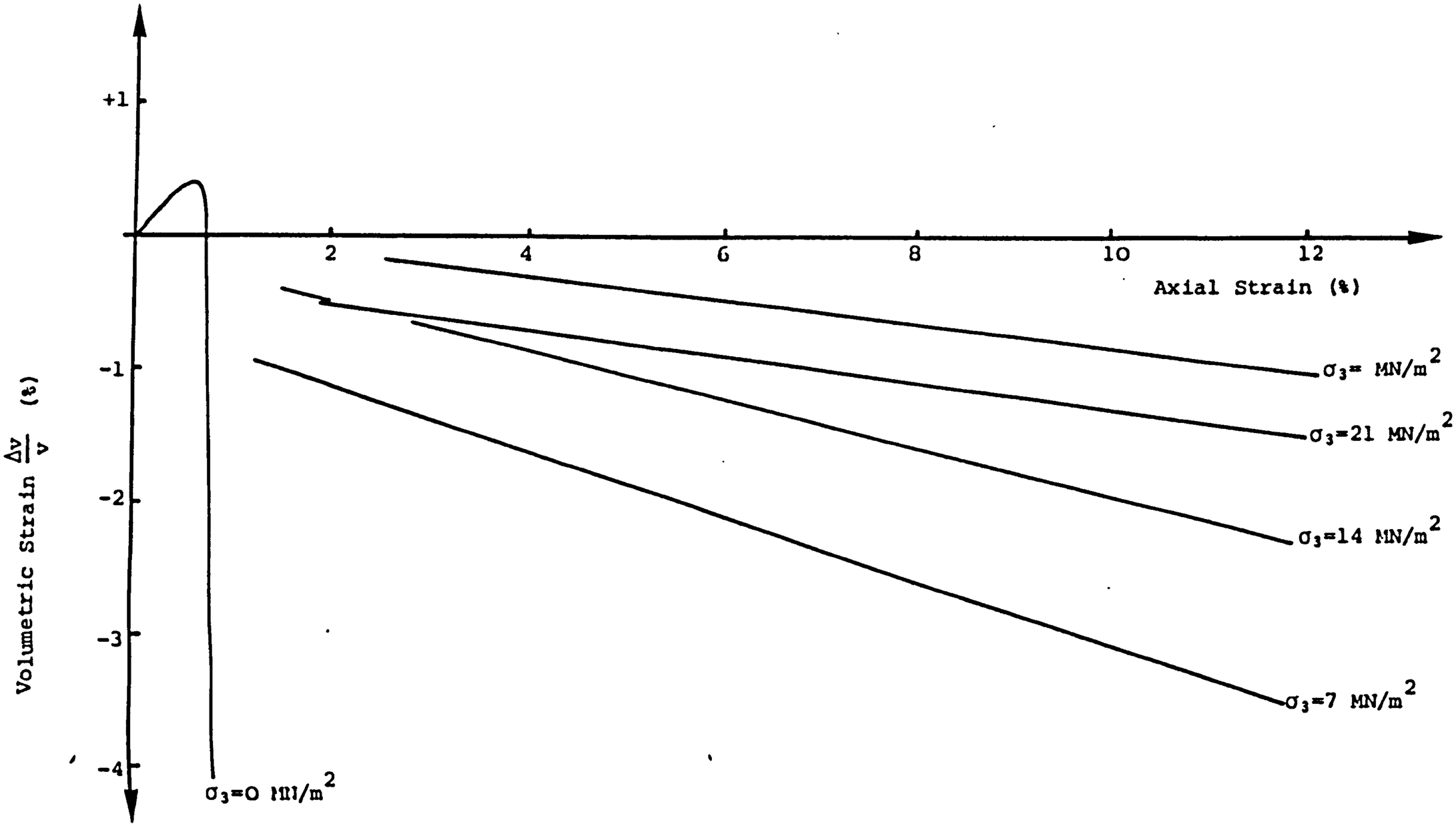

Fig. 8.3 Portland Stone: Volumetric vs Axial Strain for different confining pressures

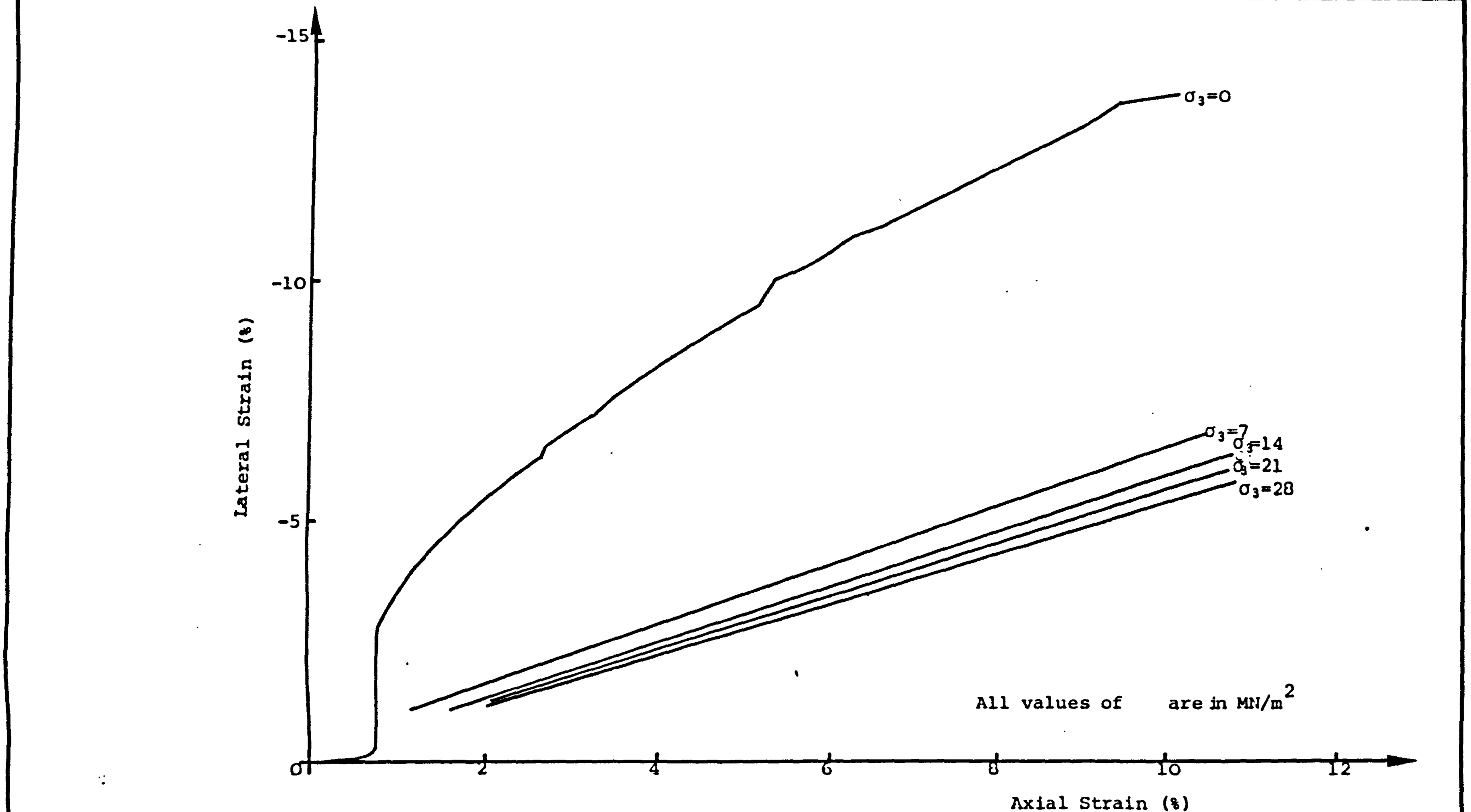

Fig. 8.4 Portland Stone: Lateral vs Axial Strain for different confining pressures

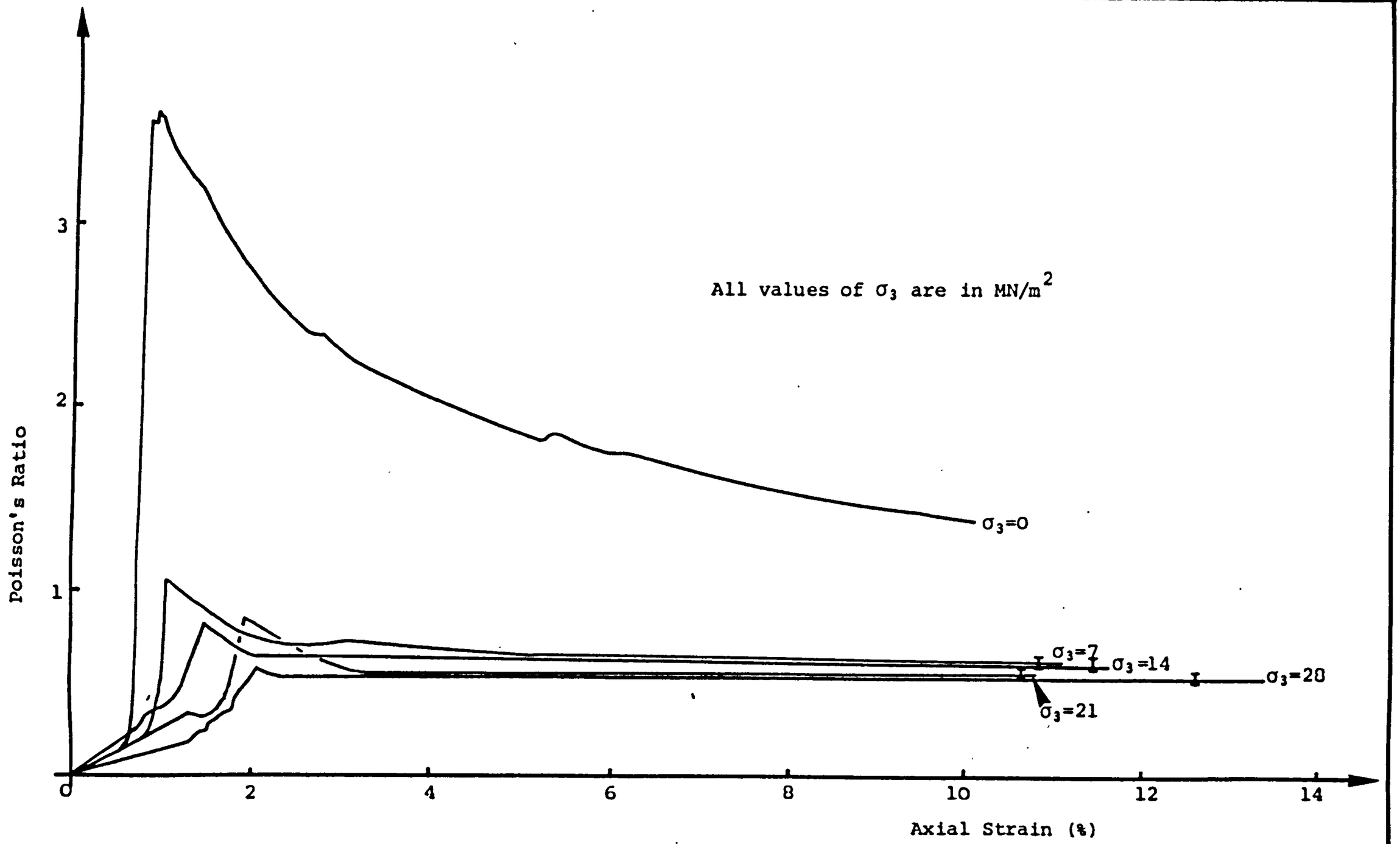

Fig. 8.5 Portland Stone: Typical curves of Poisson's Ratio vs Axial Strain for different confining pressures

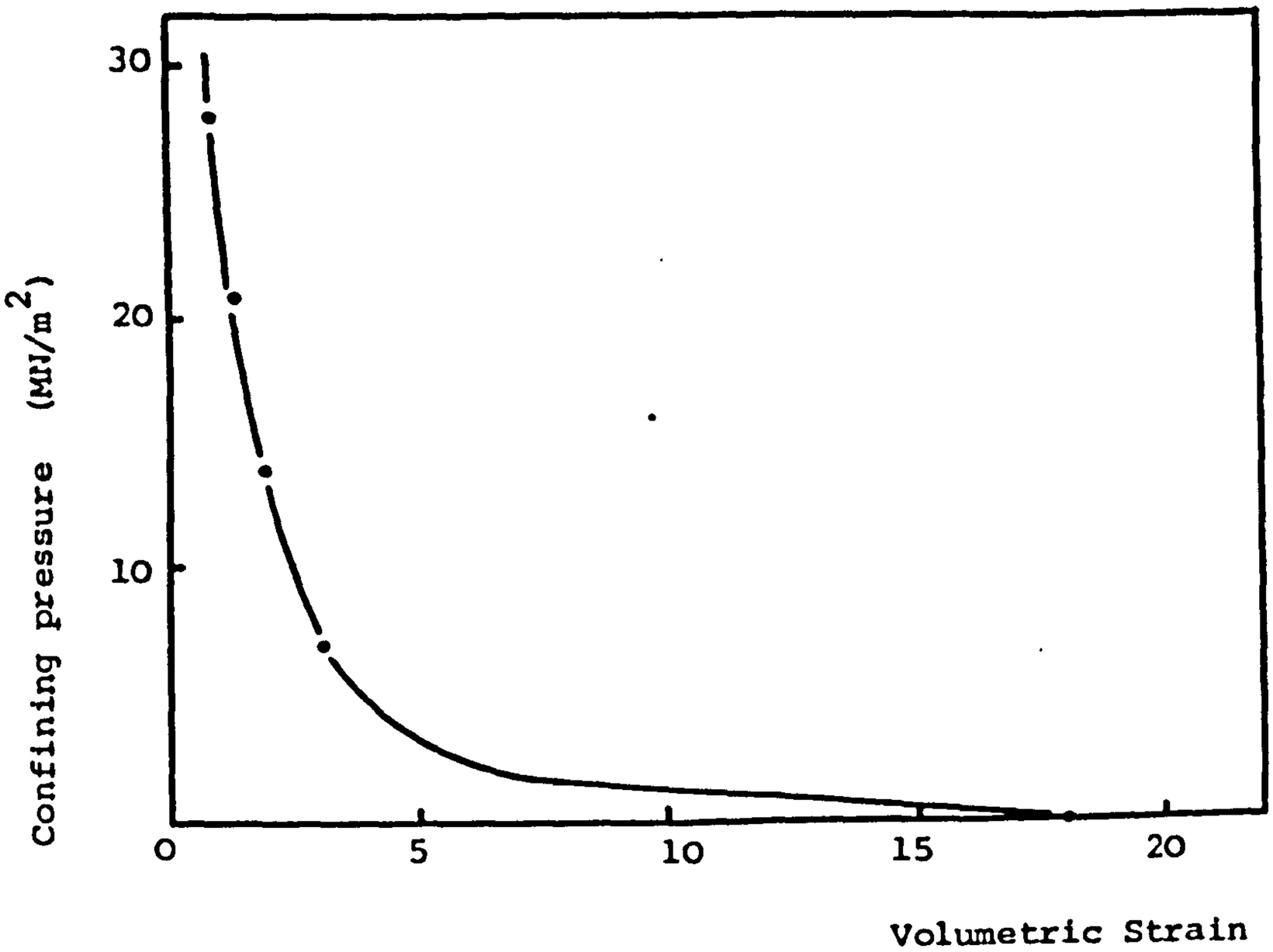

Fig. 8.6a Portland Stone: Confining pressure vs Volumetric Strain at 10% Axial Strain

Fig. 8.6b Portland Stone: Poisson's Ratio vs Confining pressure at 10% Axial Strain

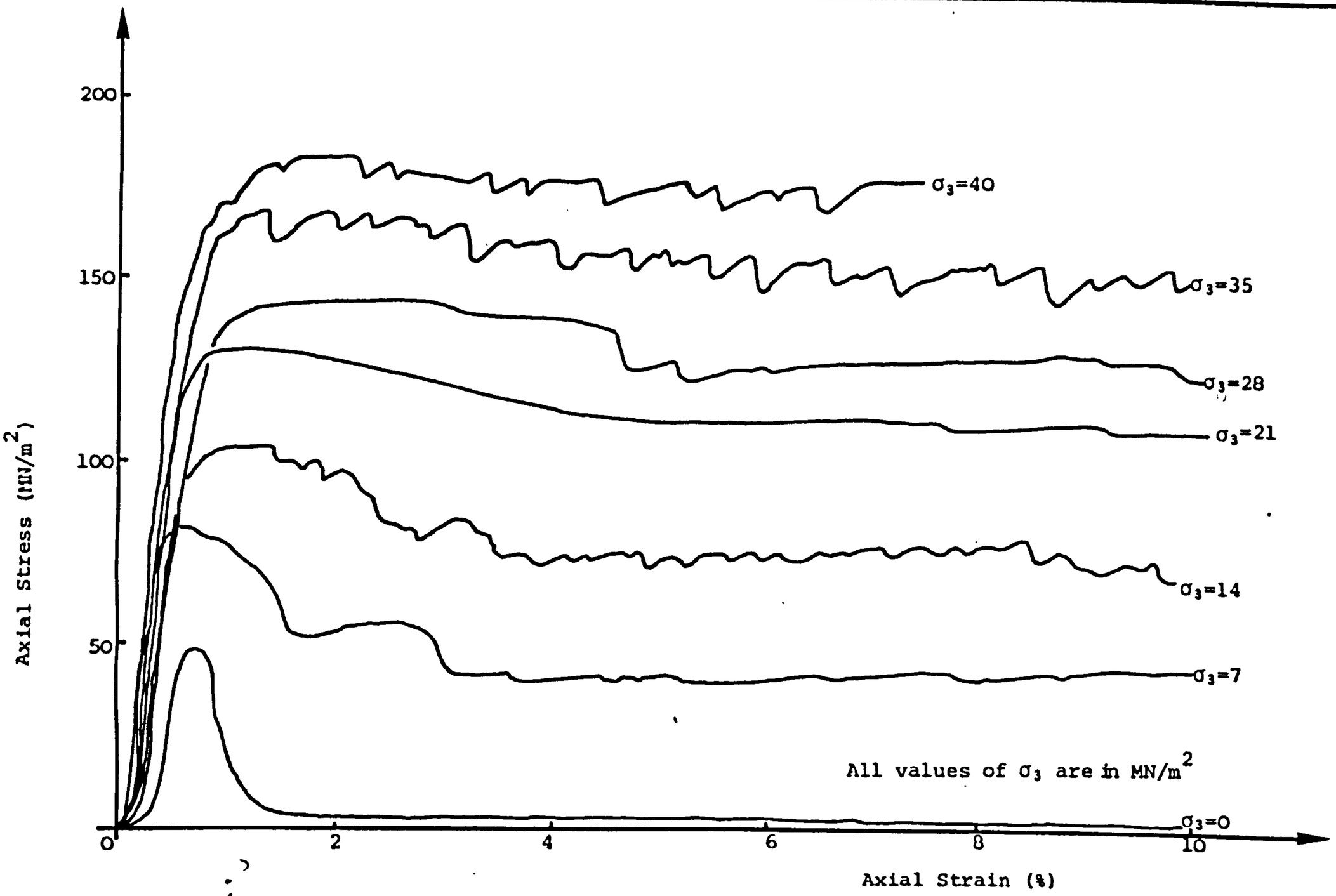

Fig. 8.7 Sacroidal Limestone: Axial Stress vs Strain for different confining pressures

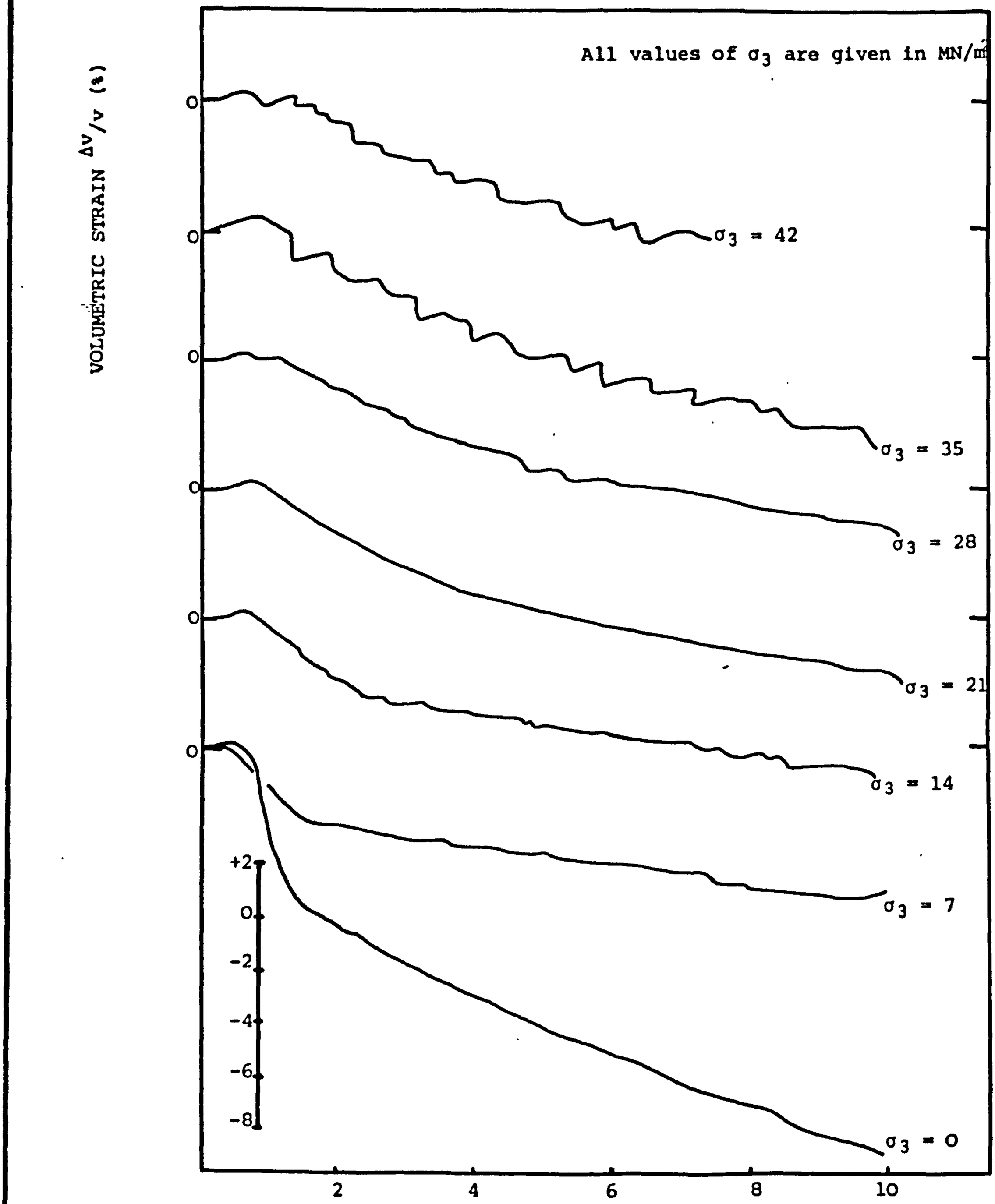

Fig. 8.8 SACROIDAL LIMESTONE: Comparison of volumetric vs Axial Strains at different confining pressures.

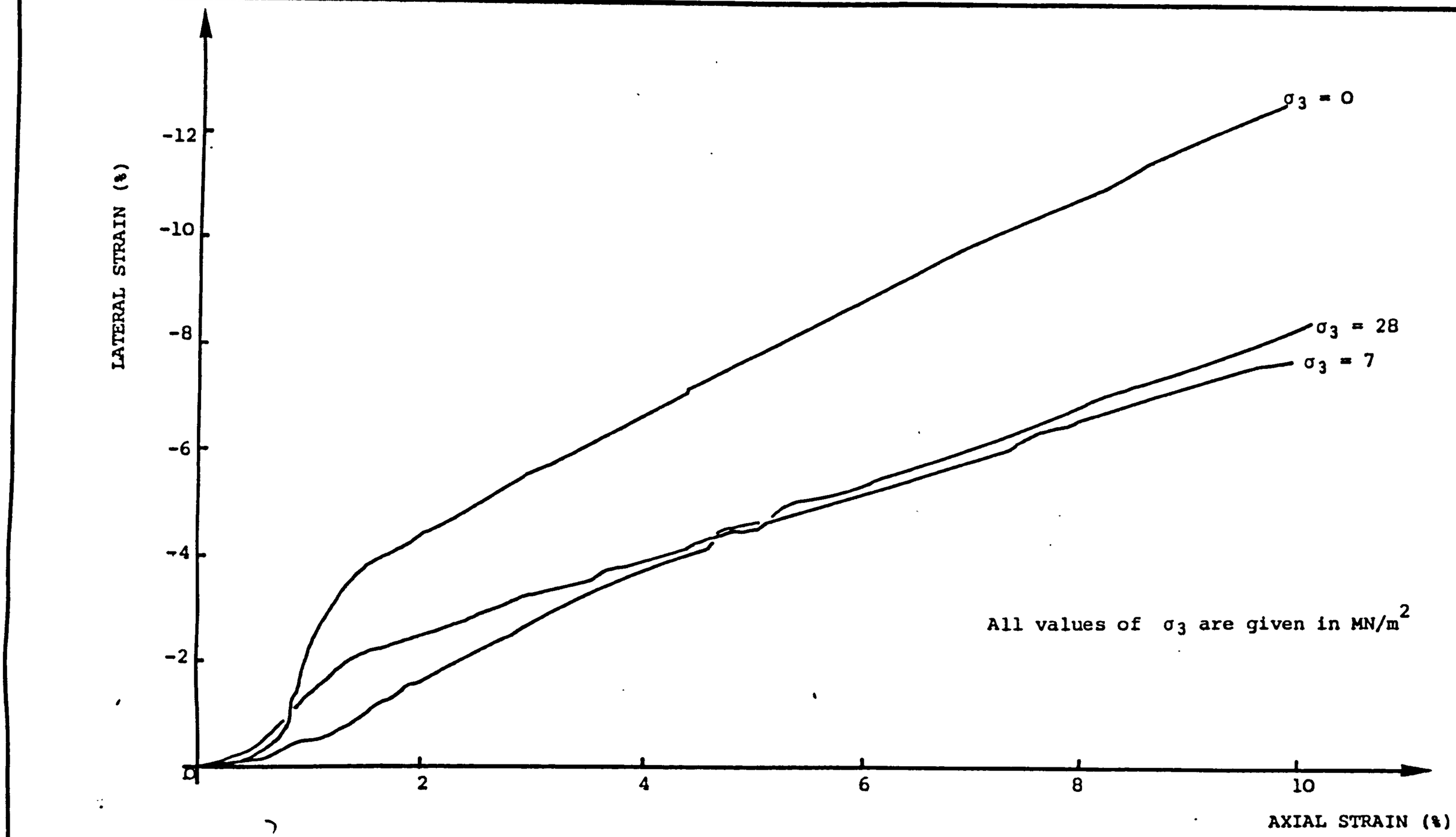

Fig. 8.9 SACROIDAL LIMESTONE: Lateral vs Axial strain for different confining pressures.

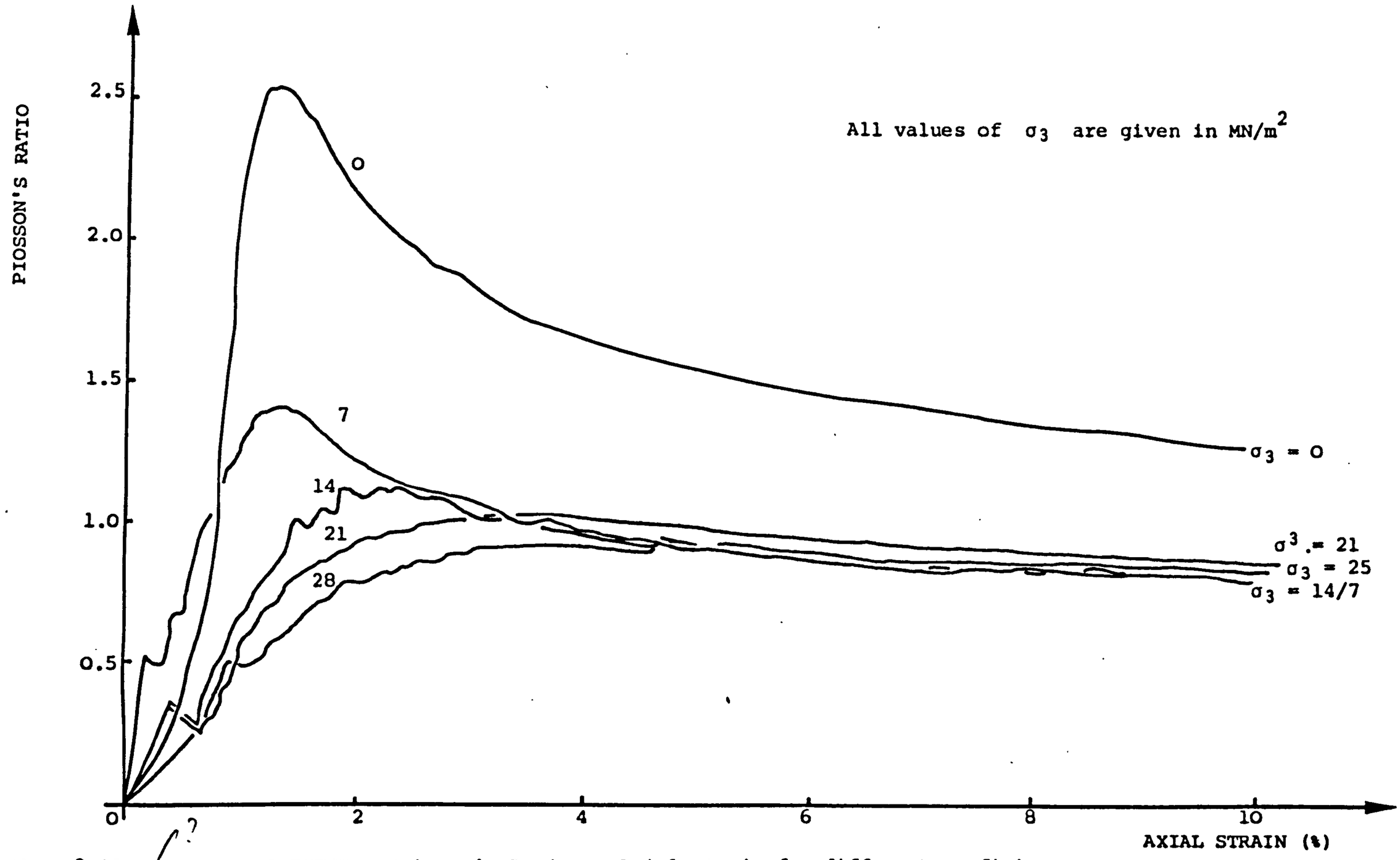

Fig. 8.10 SACROIDAL LIMESTONE: Poisson's Ratio vs Axial strain for different confining pressures.

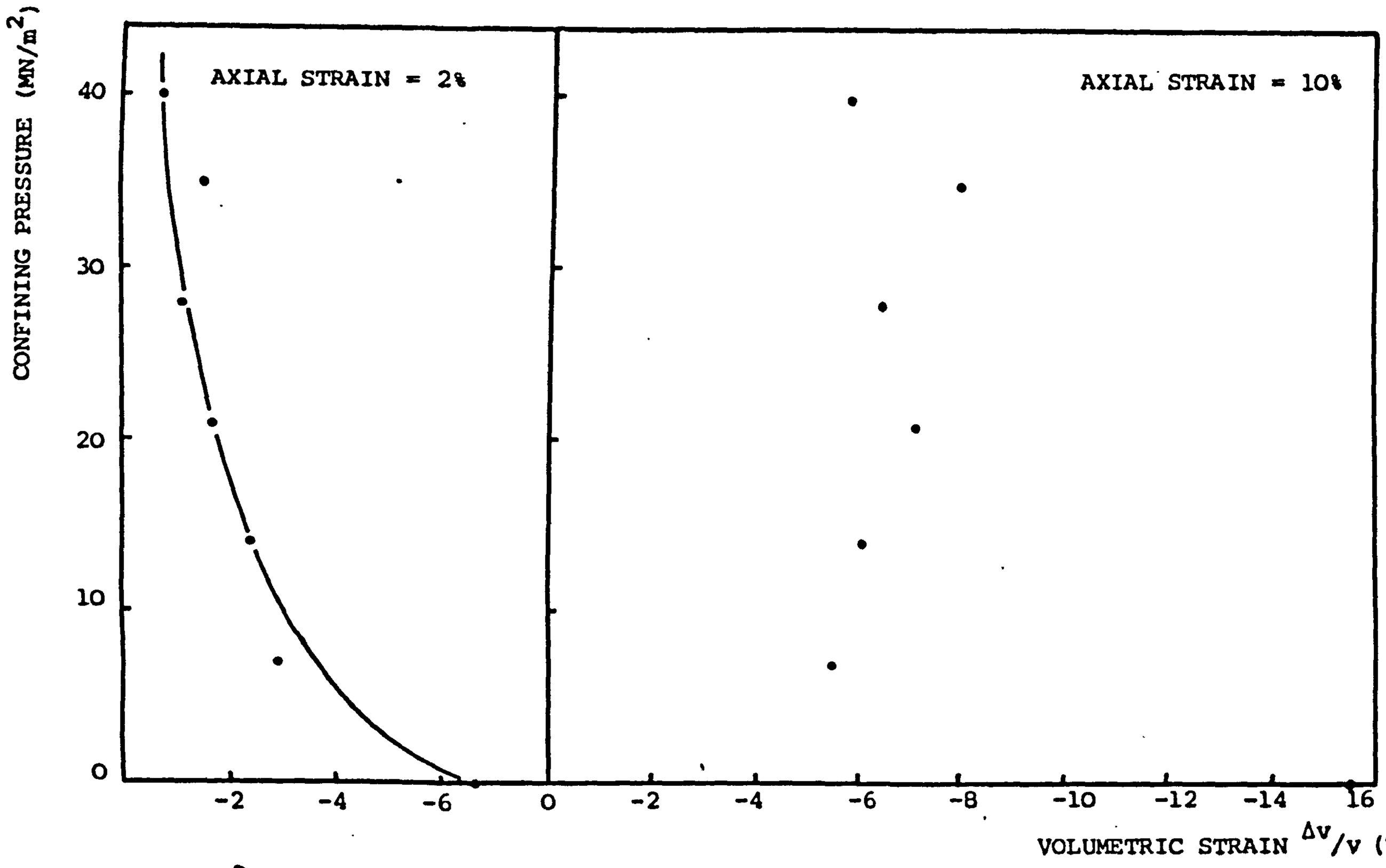

Fig. 8.11 SACROIDAL LIMESTONE: Confining Pressure vs Volumetric strain at 2 and 10% Axial Strain

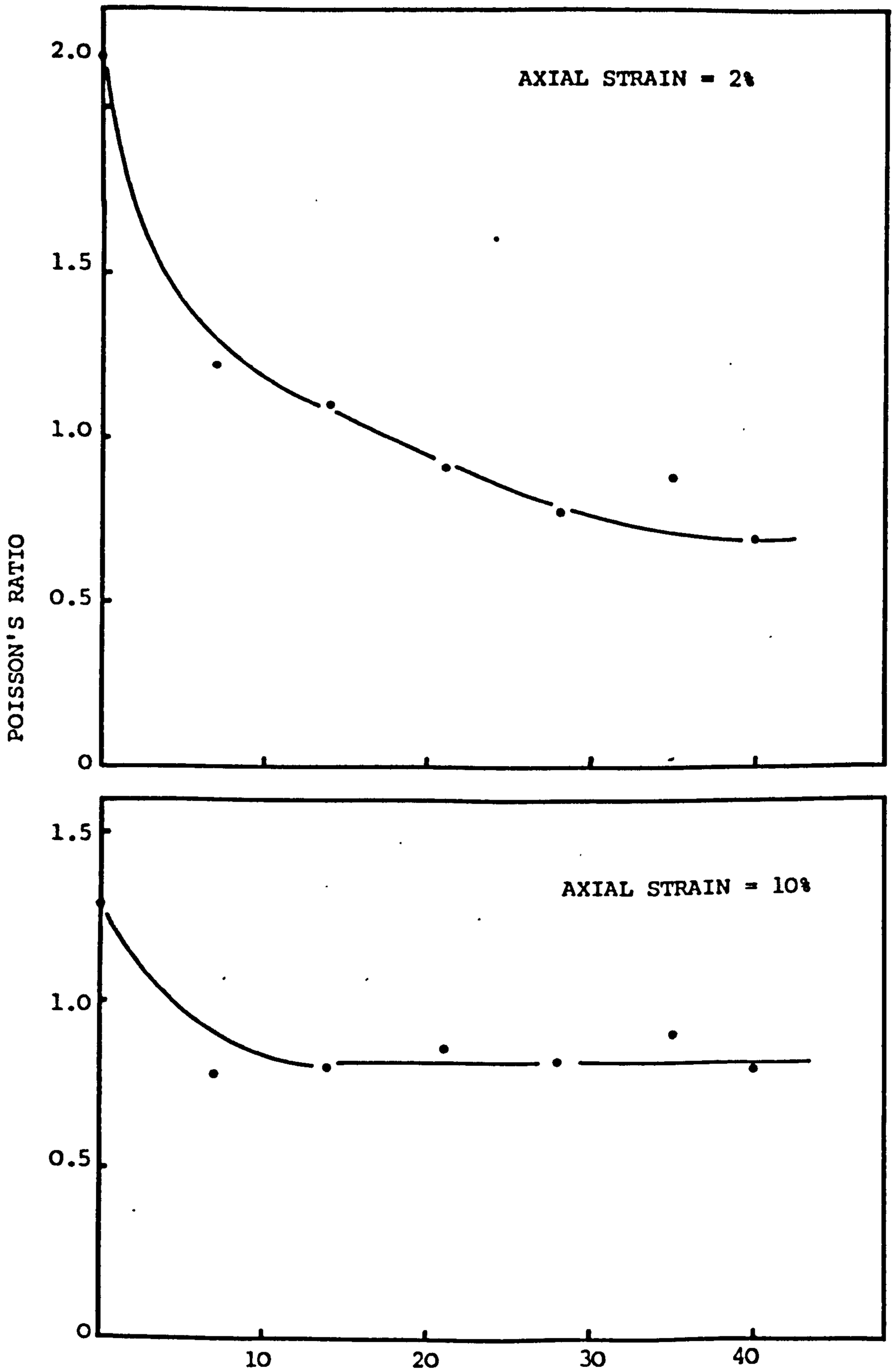

Fig.8.12 SACROIDAL LIMESTONE: Poisson's Ratio vs Confining Pressure at Axial strain of 2 and 10%

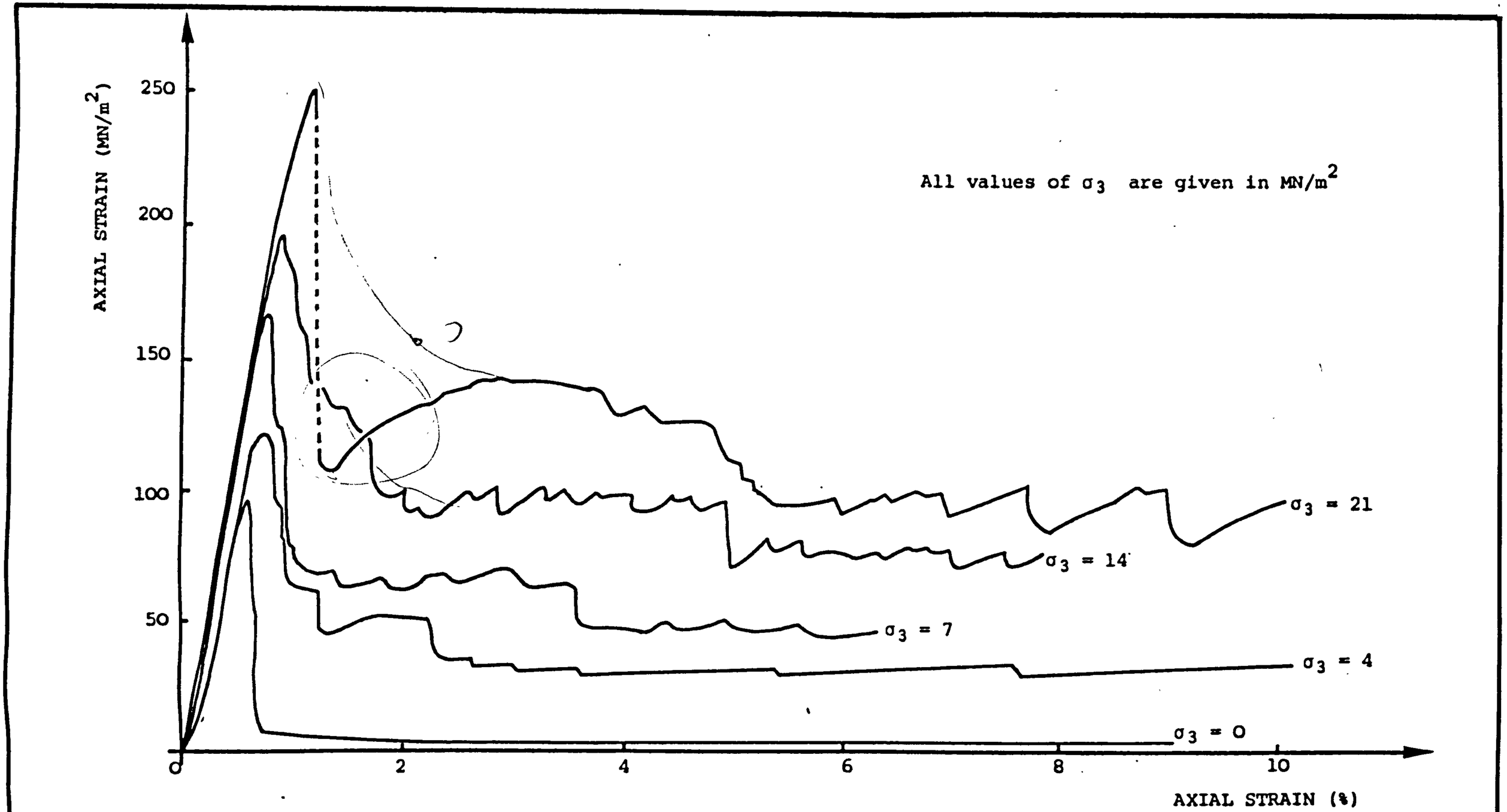

Fig. 8.13 SANDSTONE: Axial stress-strain for different confining pressures

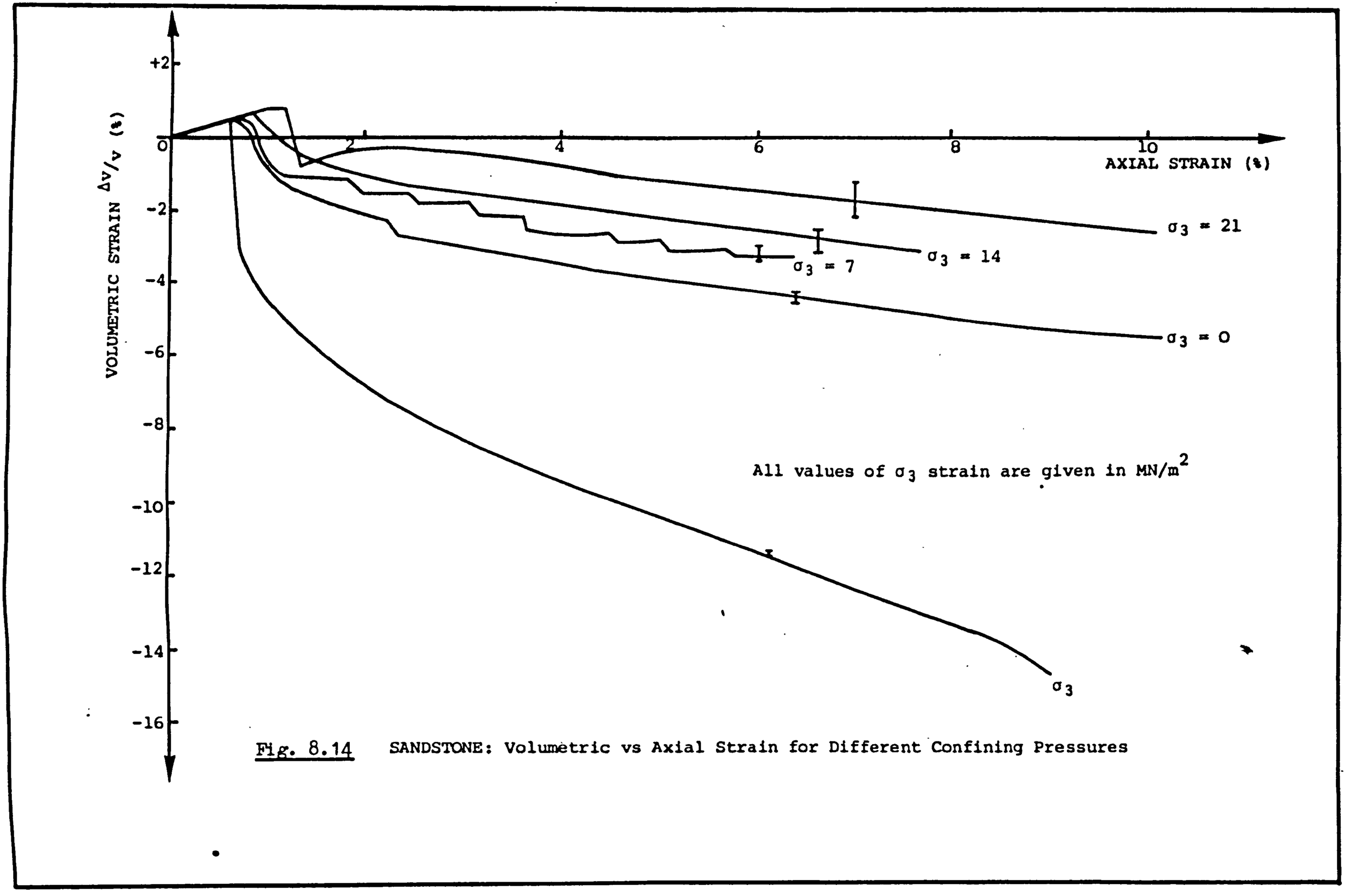

Fig. 8.14 SANDSTONE: Volumetric vs Axial Strain for Different Confining Pressures

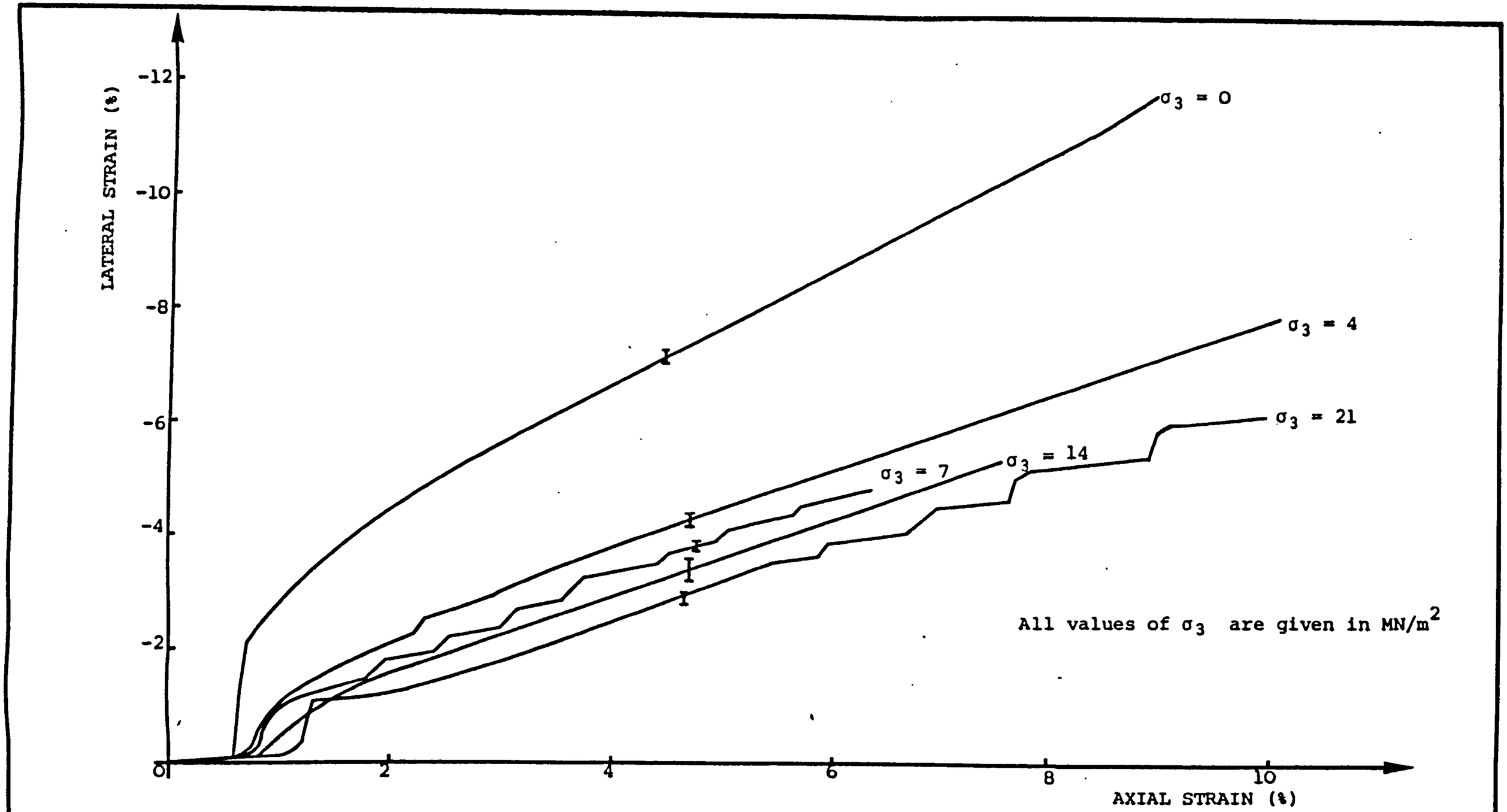

Fig. 8.15 SANDSTONE: Lateral vs Axial Strain for Different Confining Pressures

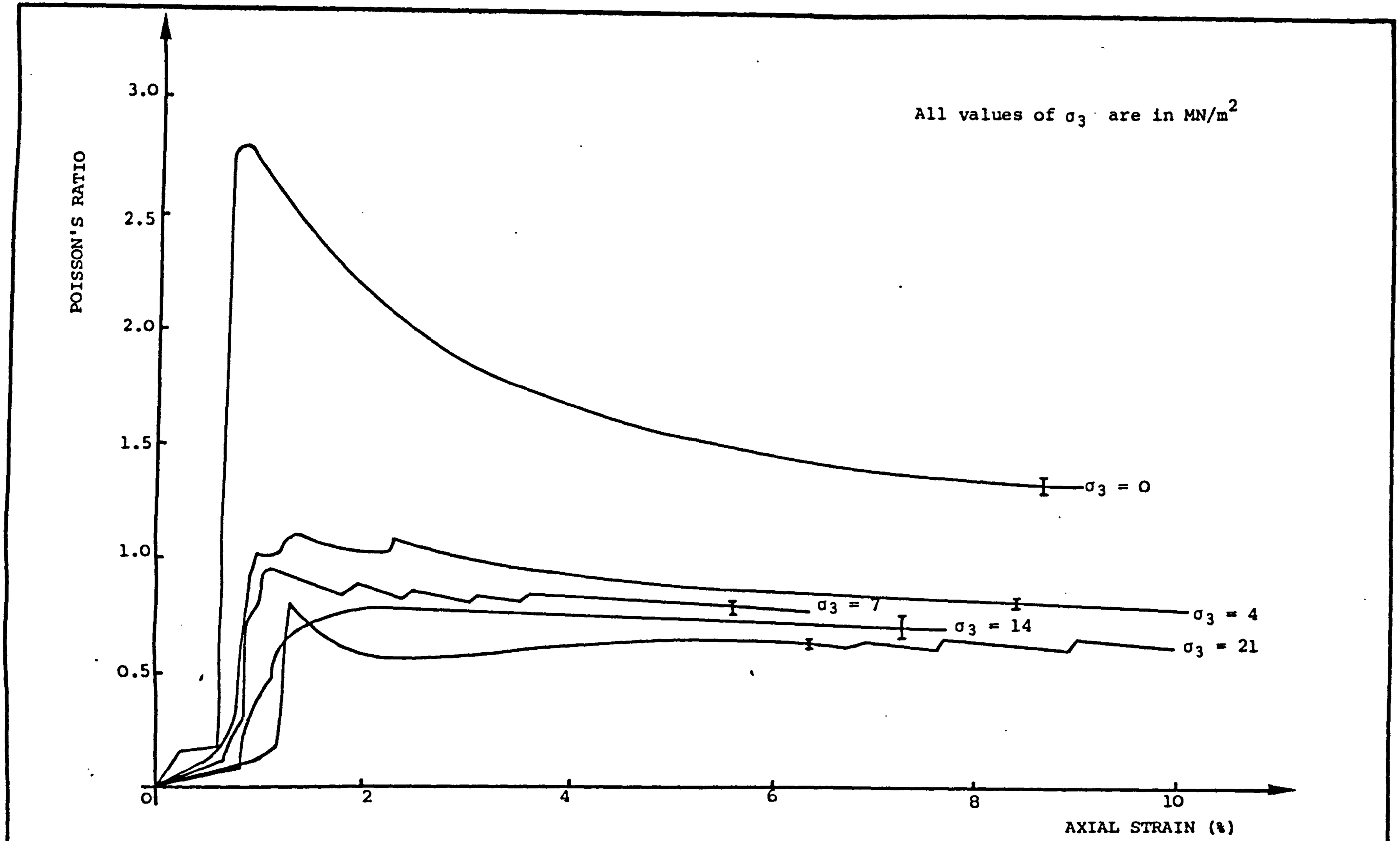

Fig. 8.16 SANDSTONE: Poisson's Ratio vs Axial strain for different confining pressures

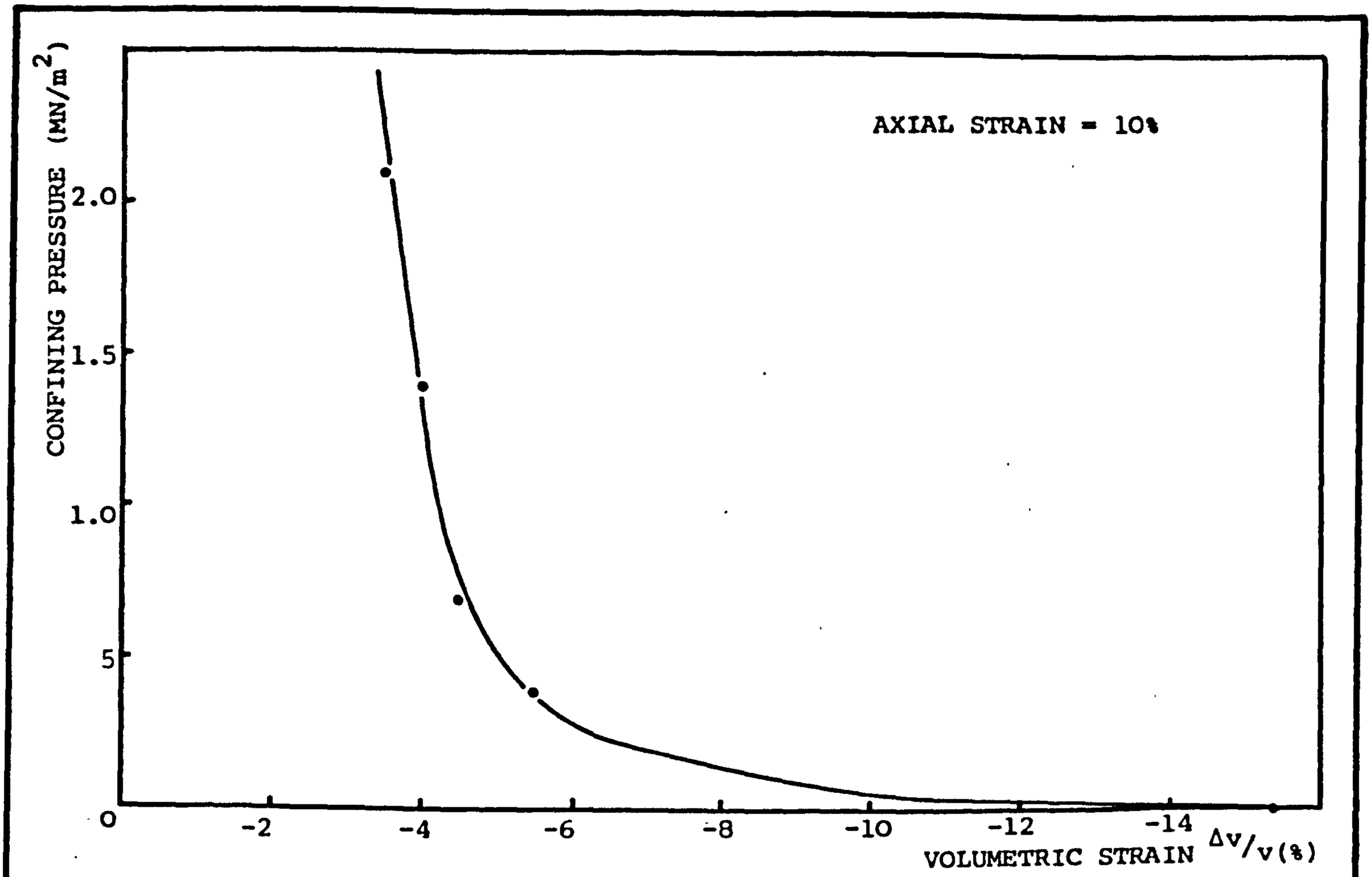

Fig.8.17a SANDSTONE: Confining Pressure vs Volumetric Strain

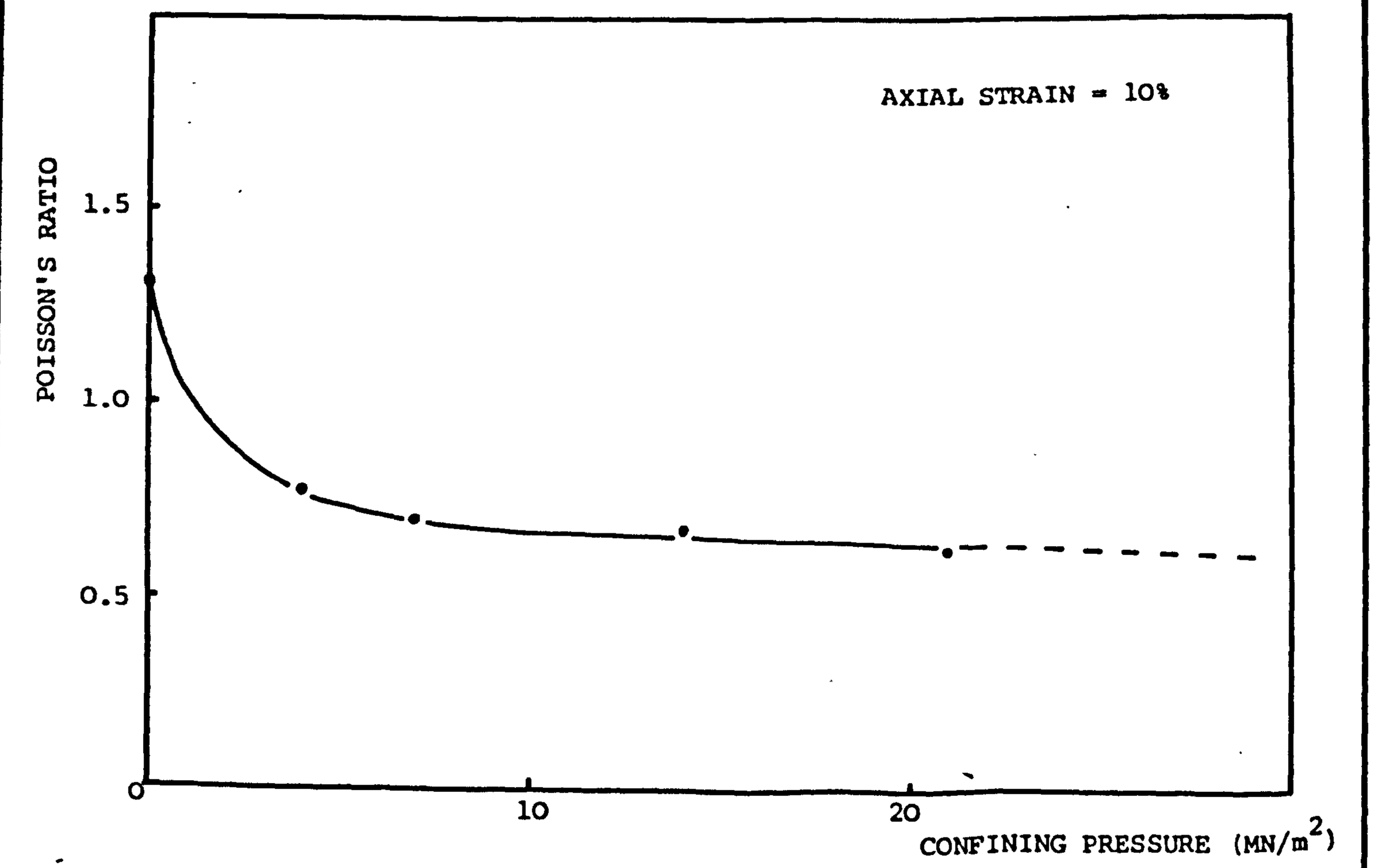

Fig.8.17b SANDSTONE: Poisson's ratio vs Confining Pressure

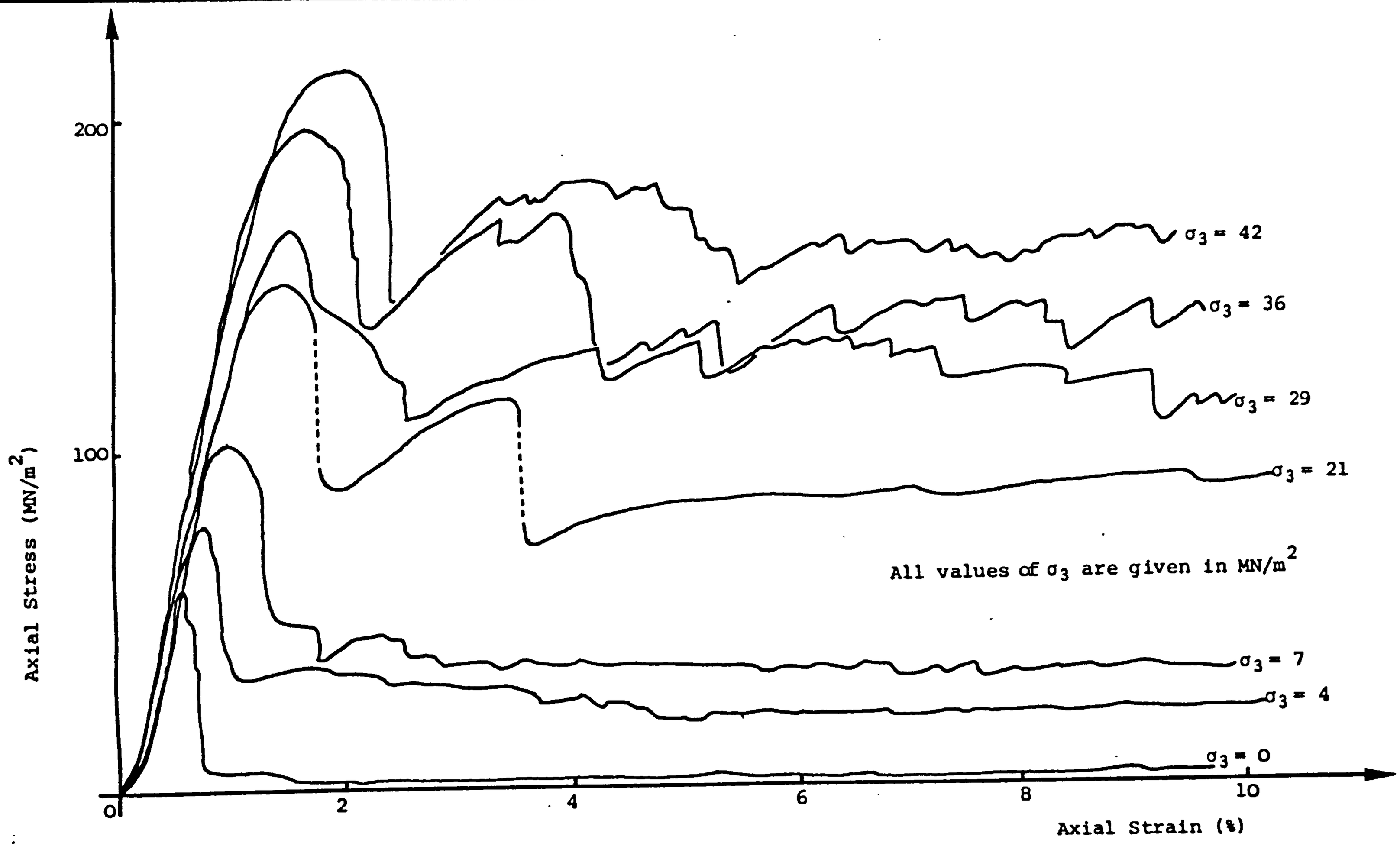

Fig.8.18 Silty Sandstone: Axial stress vs strain for different confining pressures

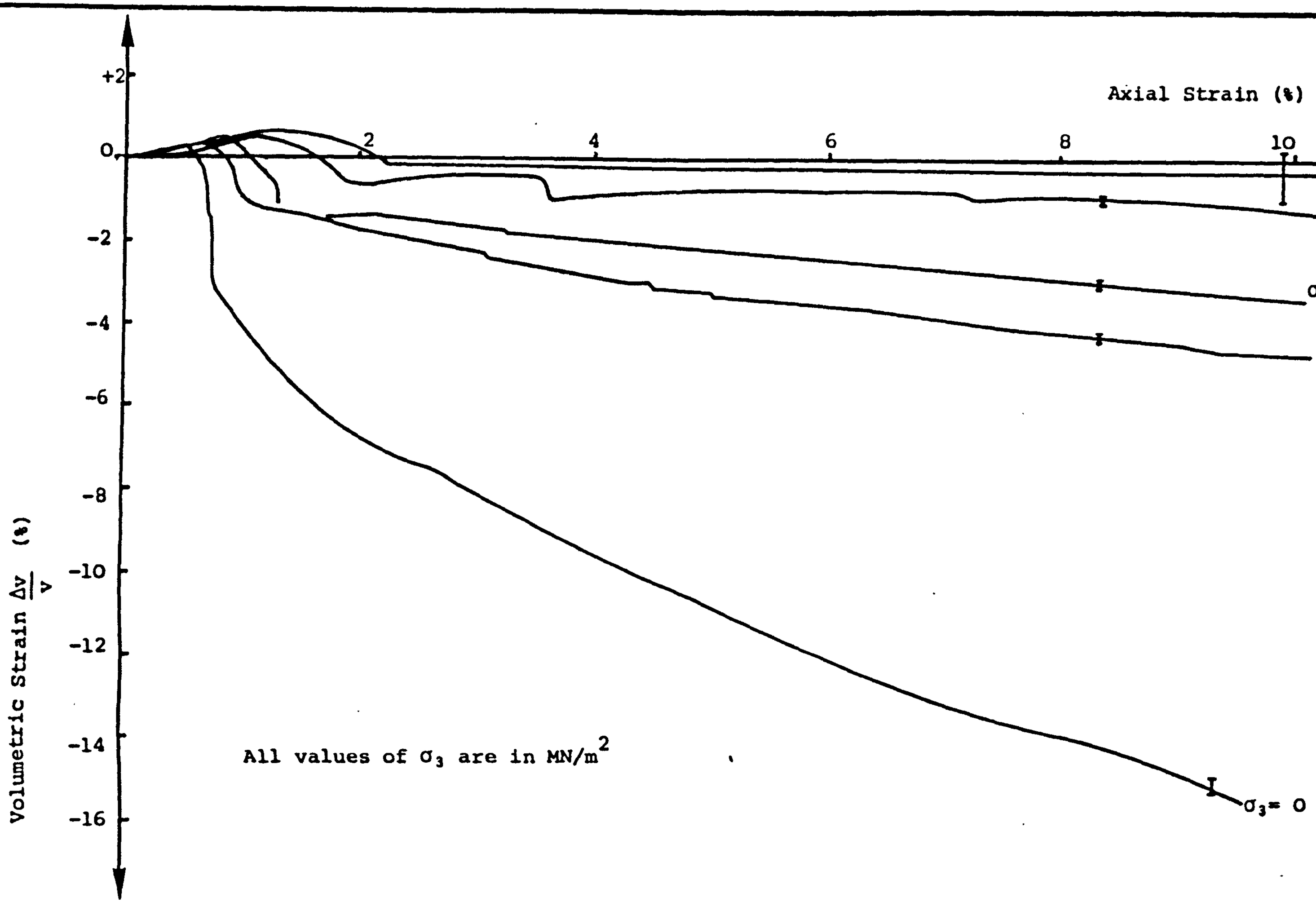

Fig. 8.19 Silty-sandstone: Volumetric vs Axial Strain for different confining pressures

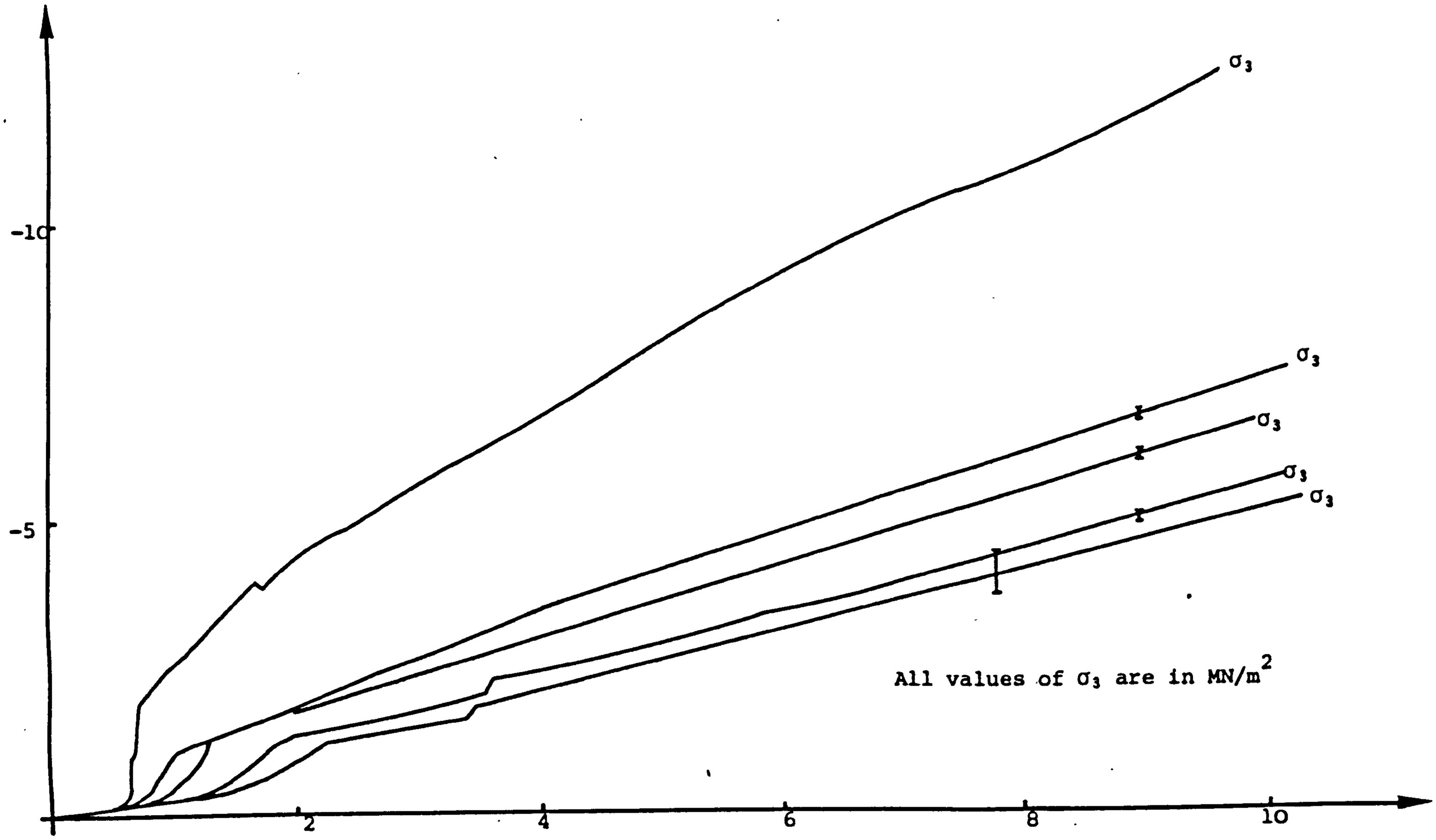

Fig. 8.20 Silty-sandstone: Lateral vs Axial Strain for different confining pressures

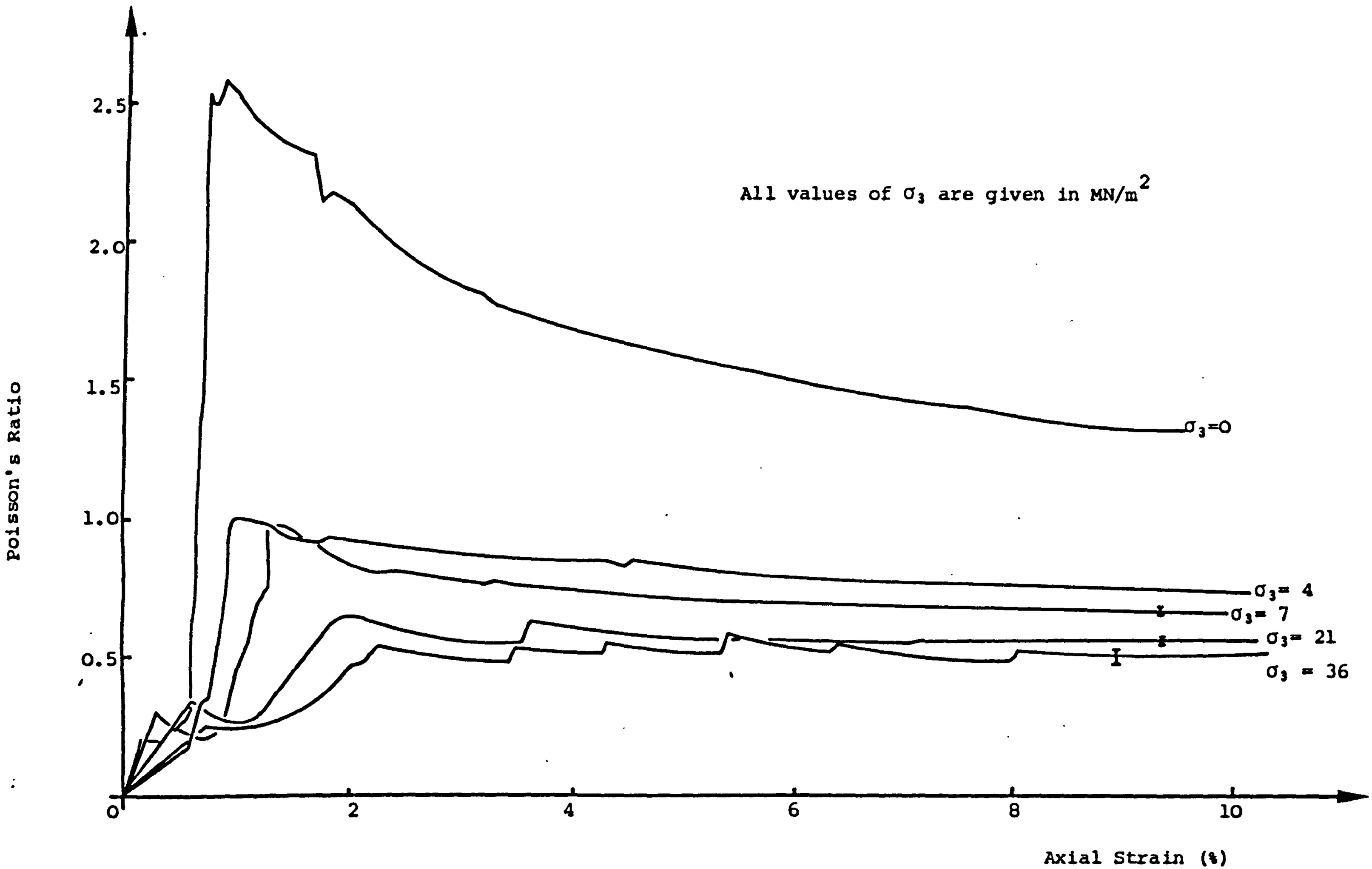

Fig. 8.21 Silty-sandstone: Poisson's Ratio vs Axial Strain for different confining pressures

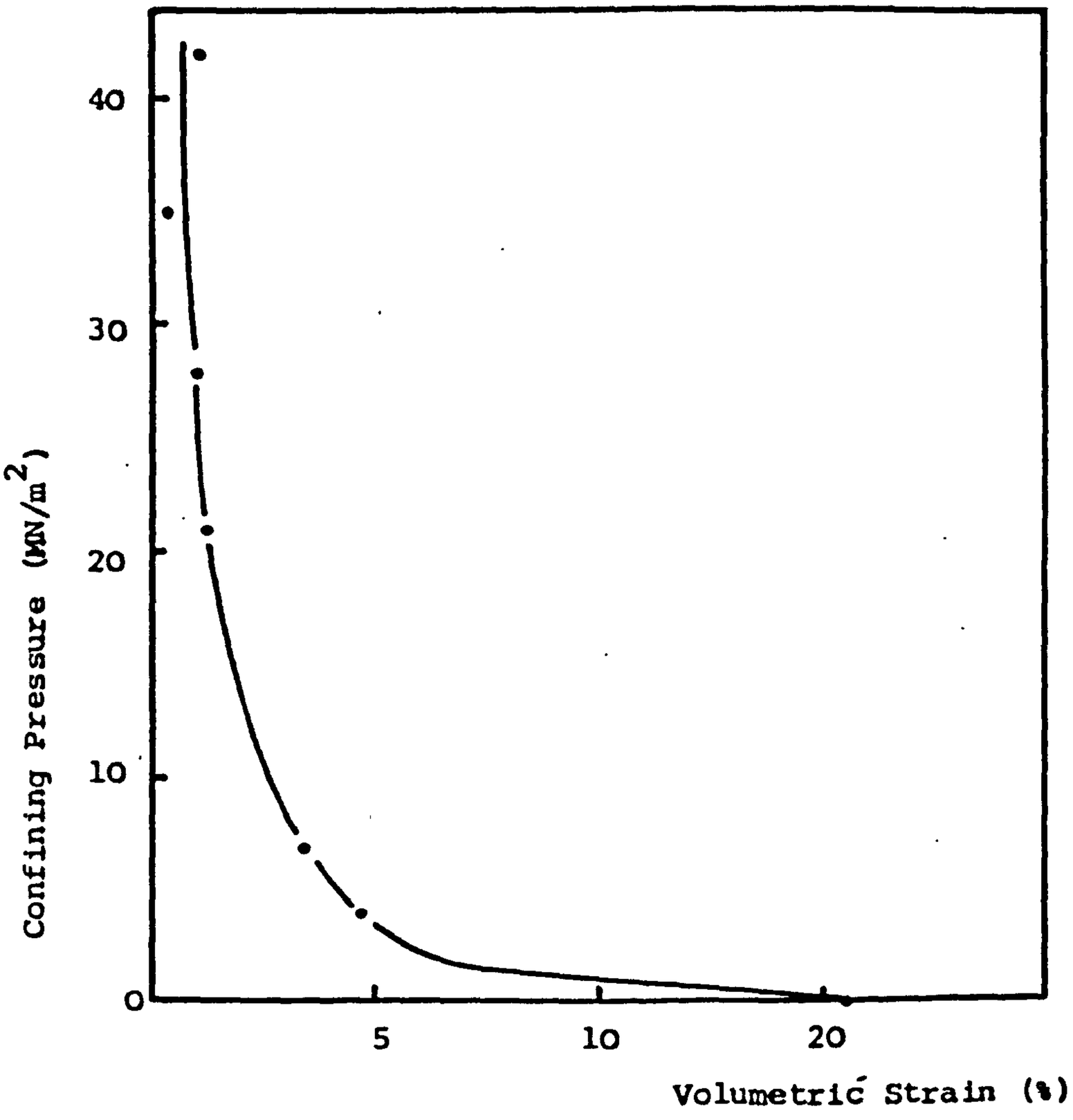

Fig. 8.22a Silty-sandstone: Confining Pressure vs Volumetric Strain at 10%

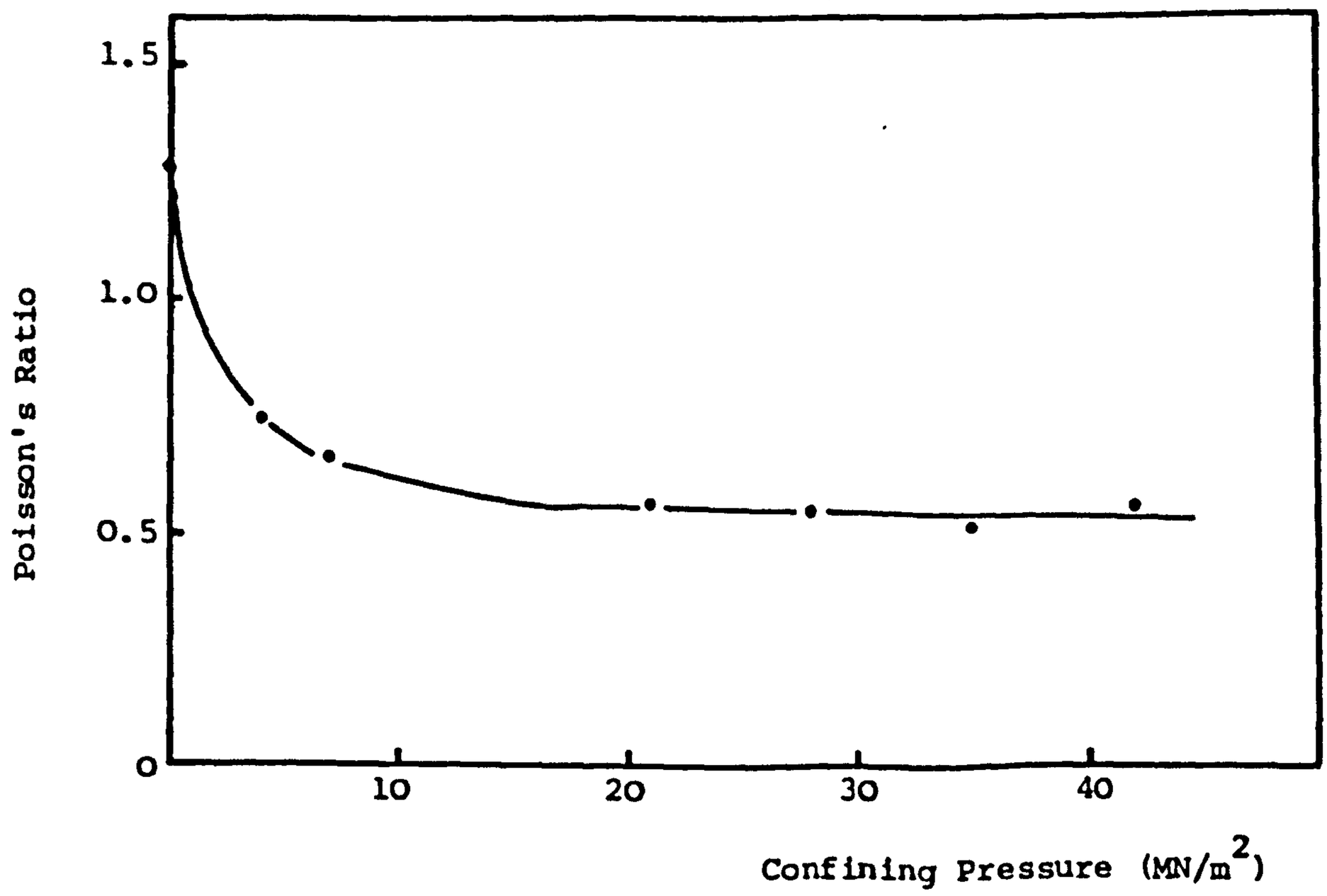

Fig.8.22b Silty-sandstone: Poisson's Ratio vs Confining Pressure at 10% Axial Strain

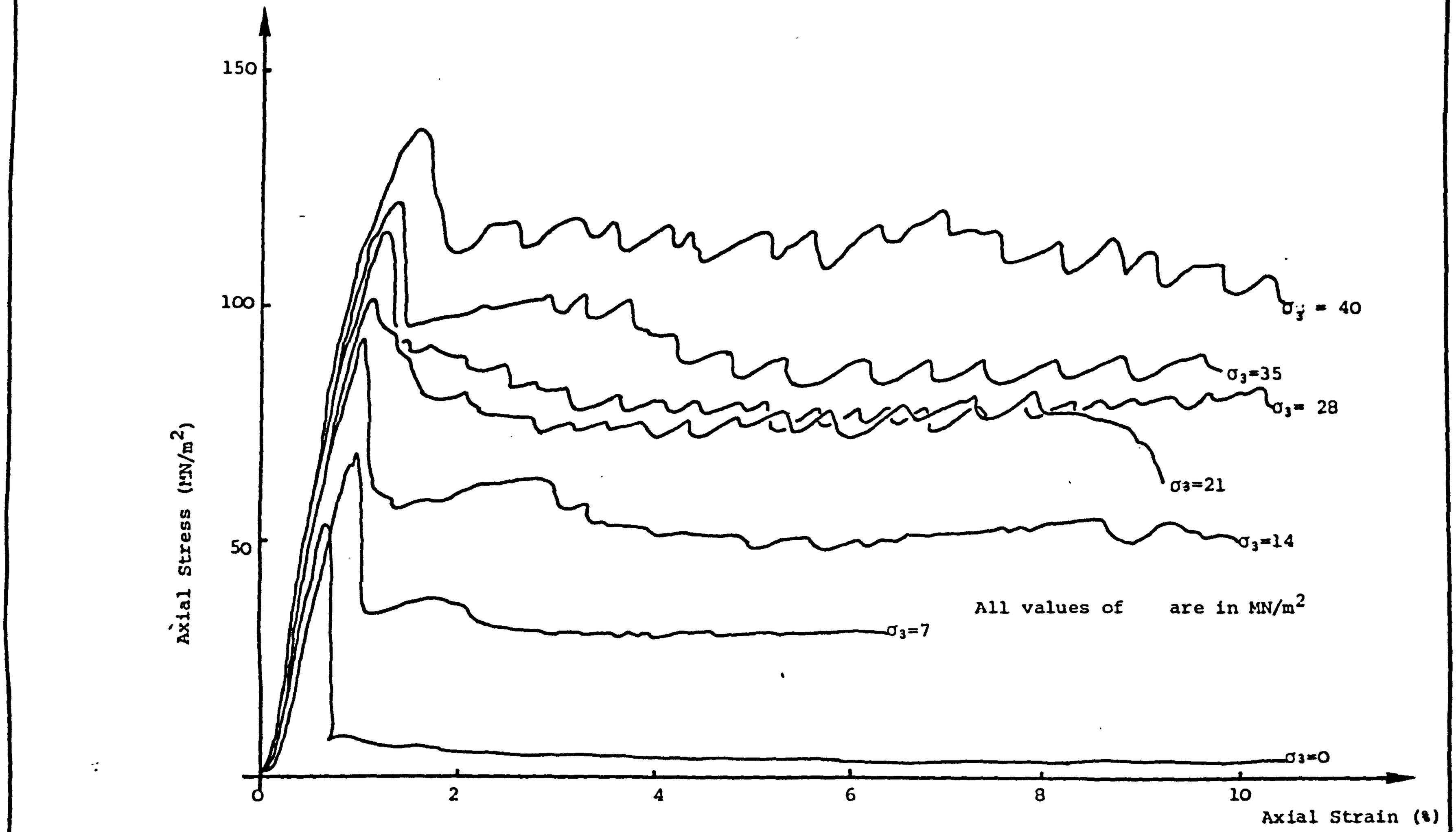

Fig. 8.23 Mudstone: Axial Stress vs Strain for different confining pressures

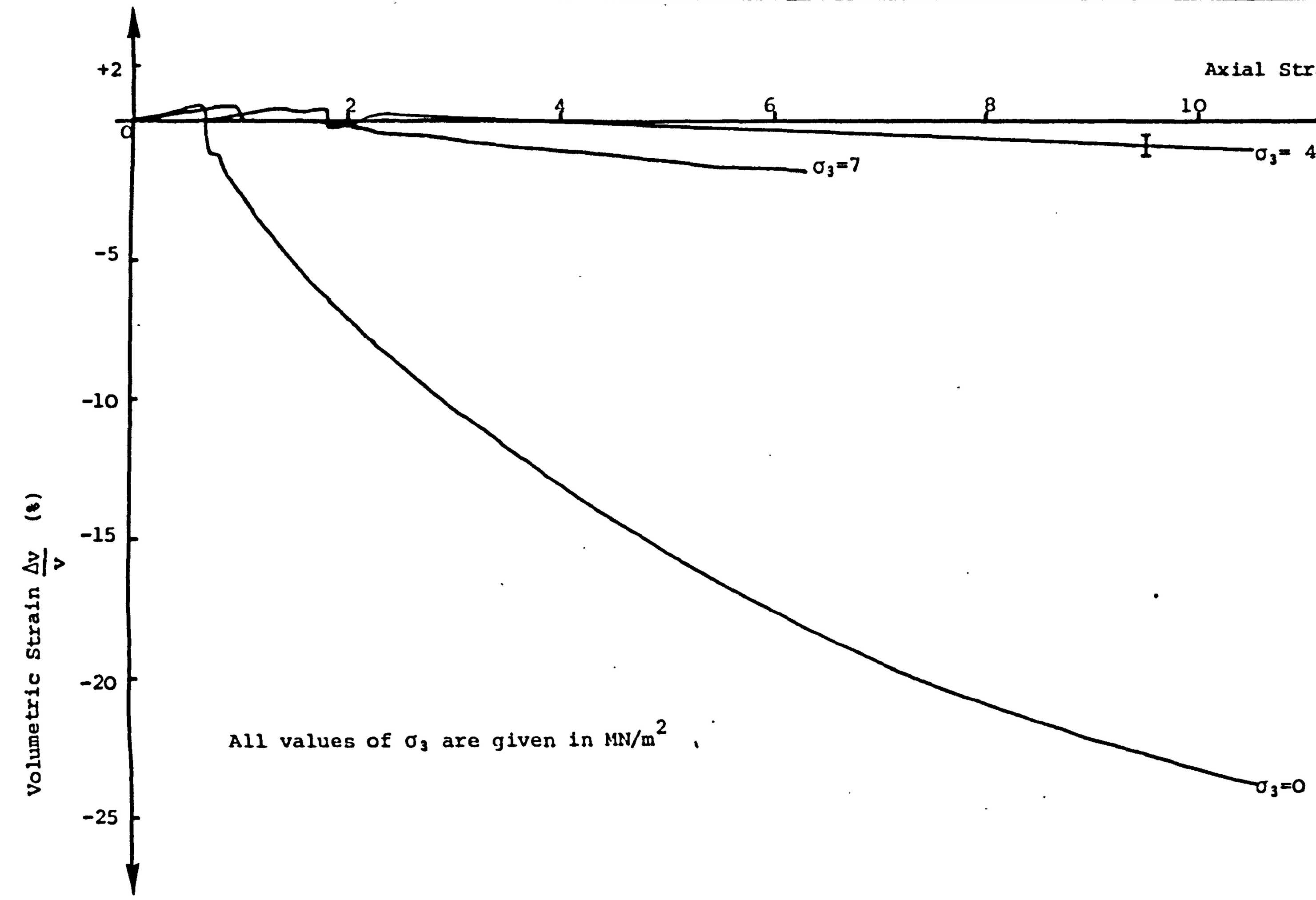

Fig. 8.24 Mudstone: Volumetric vs Axial Strain for different confining pressures

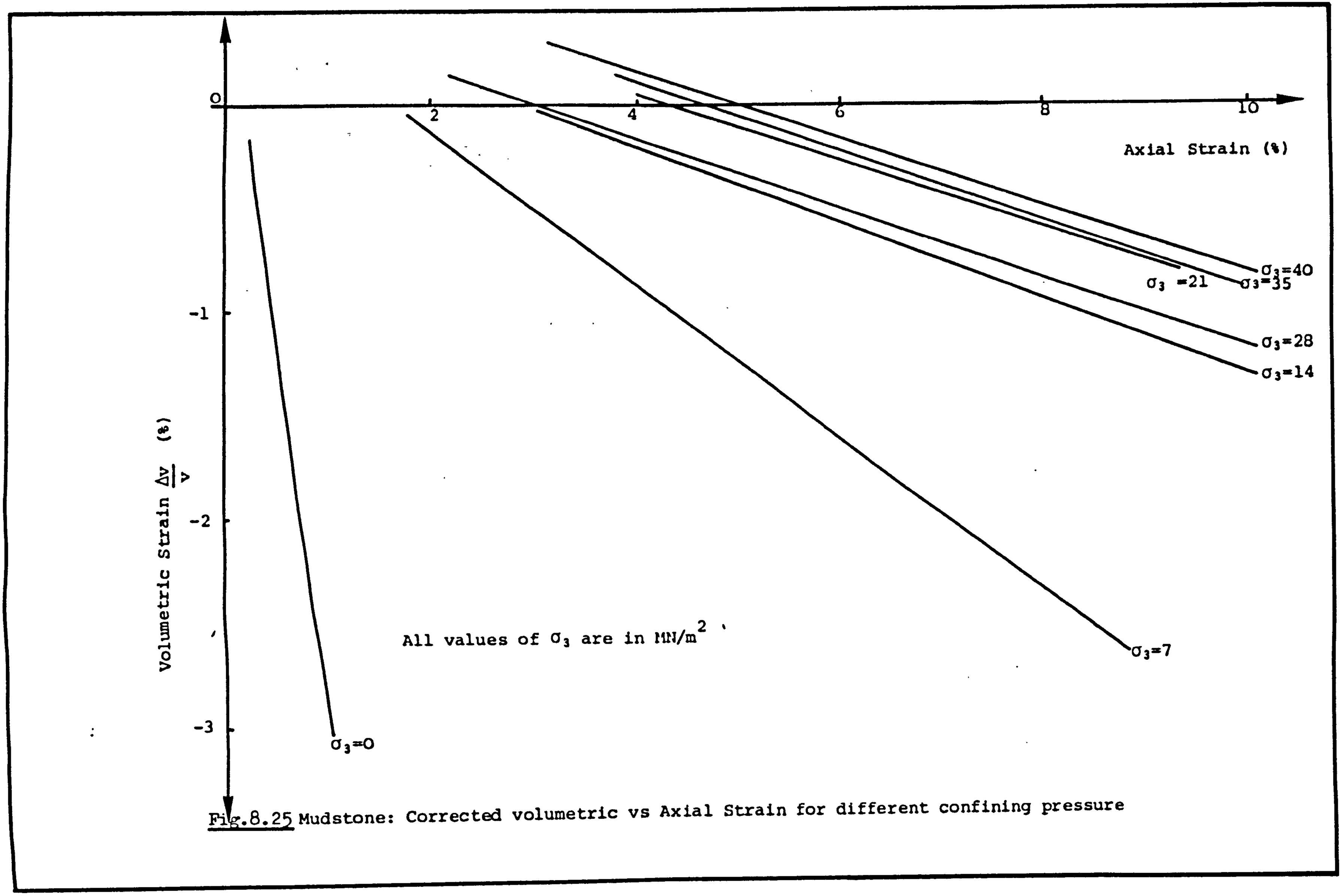

Fig.8.25 Mudstone: Corrected volumetric vs Axial Strain for different confining pressure

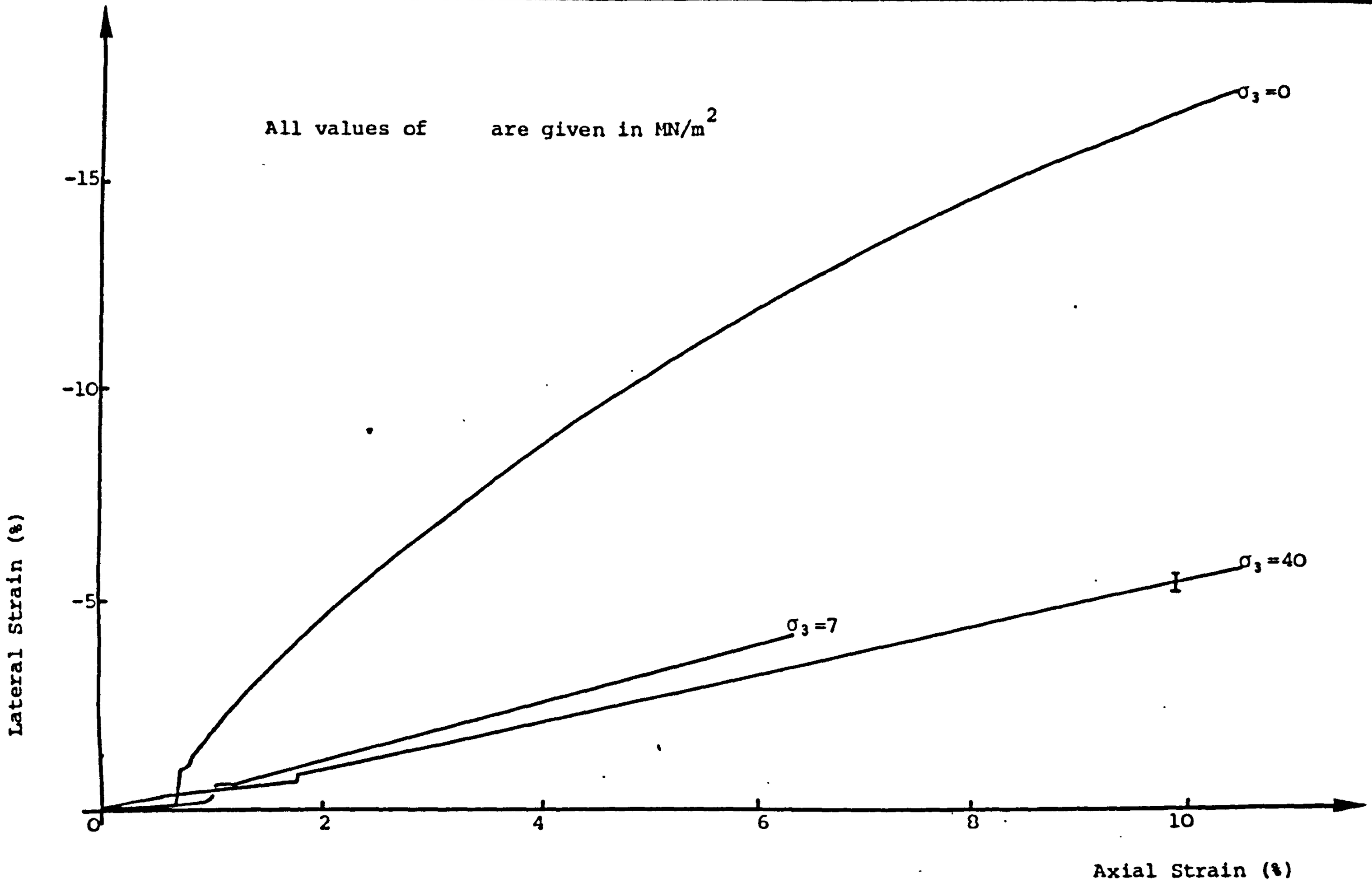

Fig.8.26 Mudstone: Lateral vs Axial Strains for different confining pressures

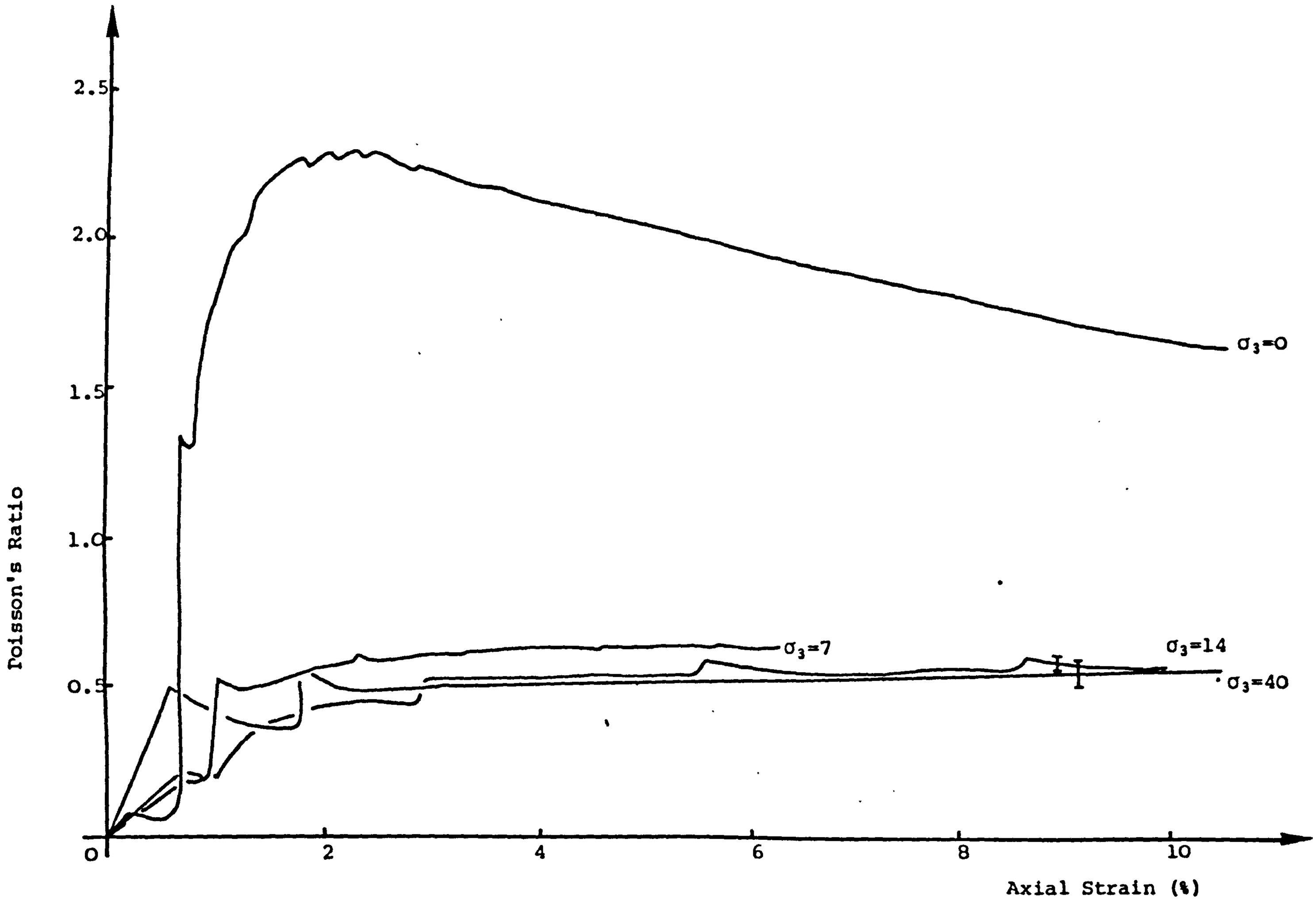

Fig. 8.27 Mudstone: Poisson's Ratio vs Axial Strain for different confining pressures

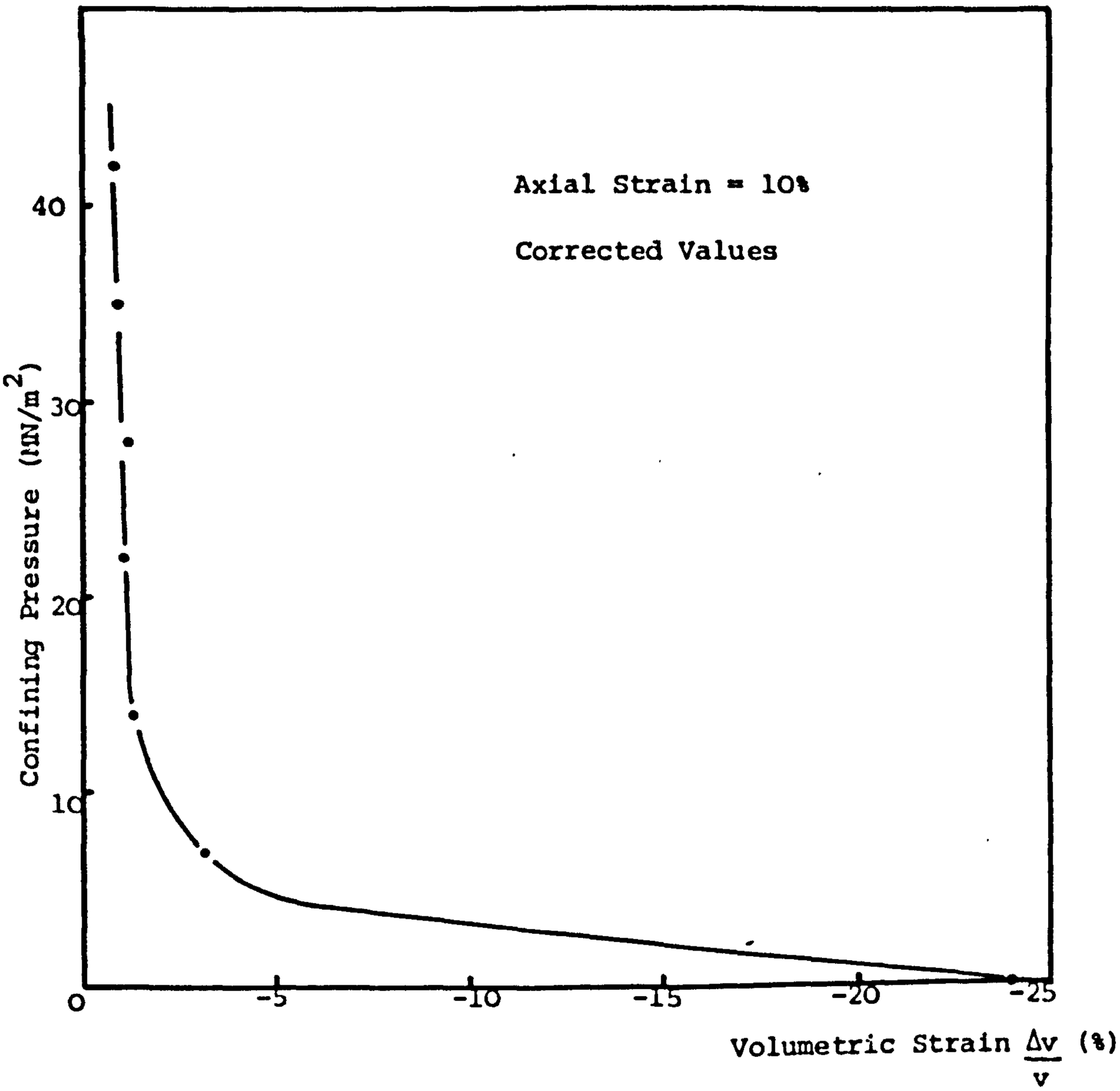

Fig.8.28a Mudstone: Confining pressure vs Volumetric Strain

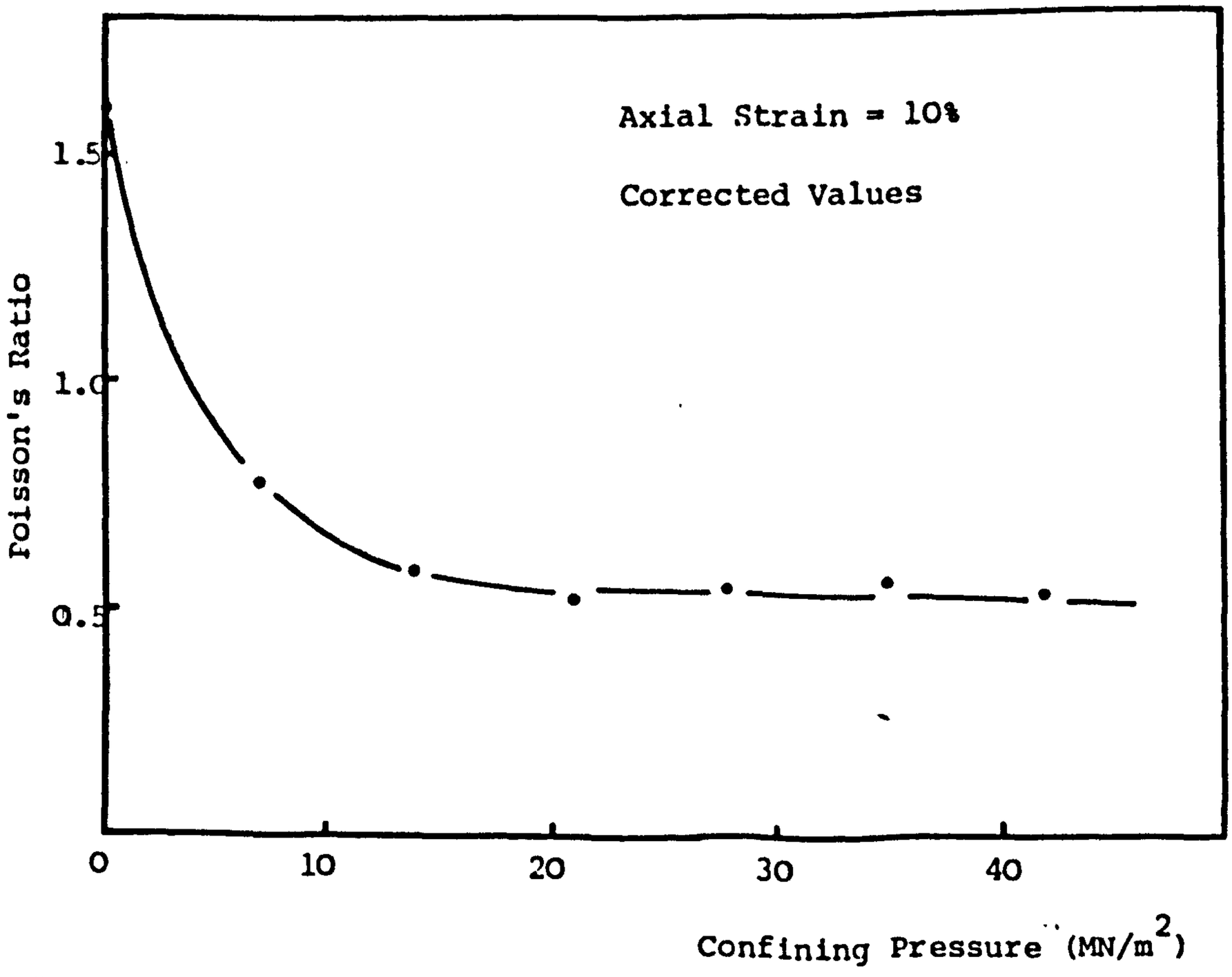

Fig. 8.28b Mudstone: Poisson's Ratio vs Confining Pressure

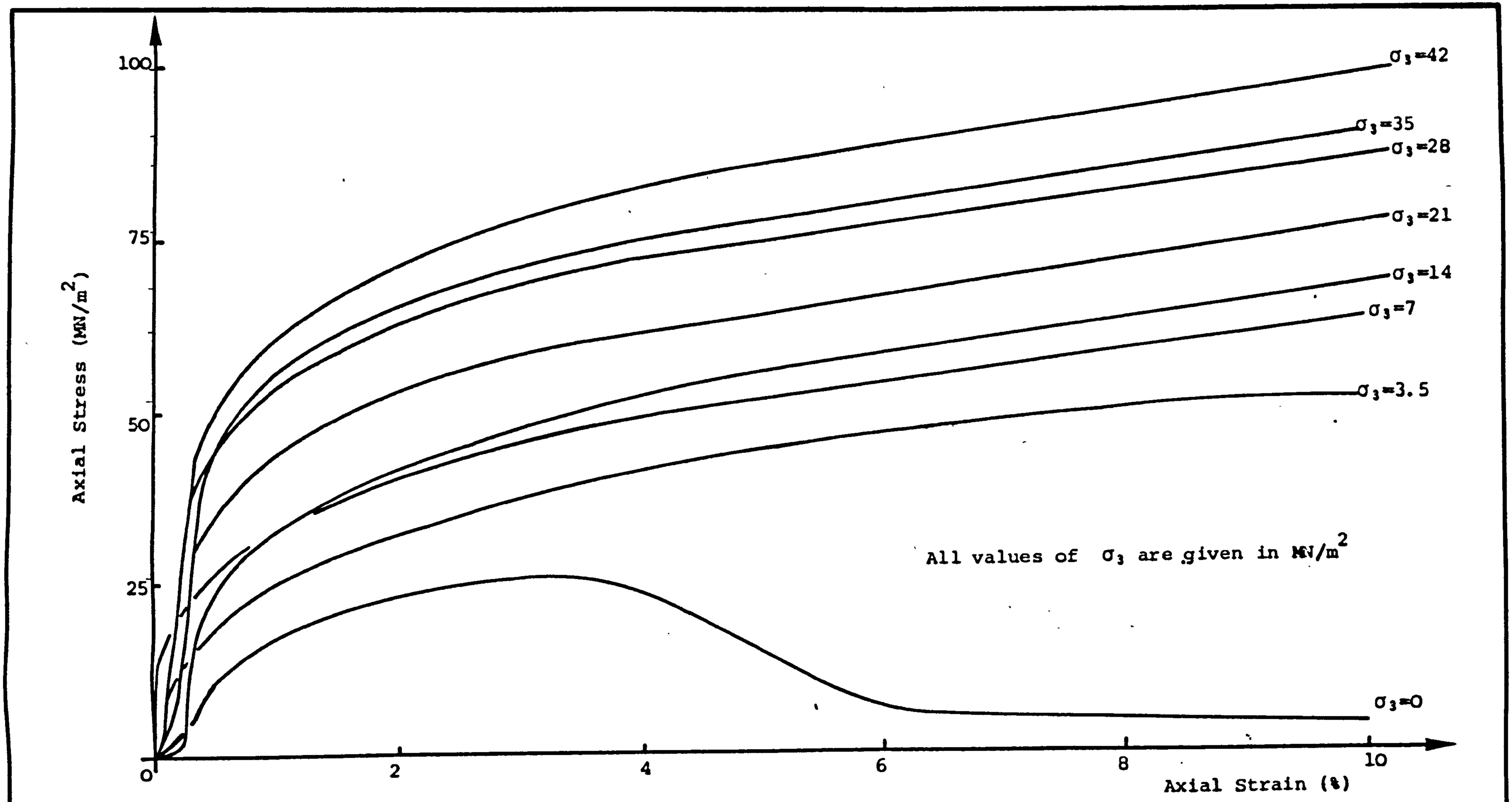

Fig. 8.29 Rock Salt: Axial Stress vs Strain for different confining pressures

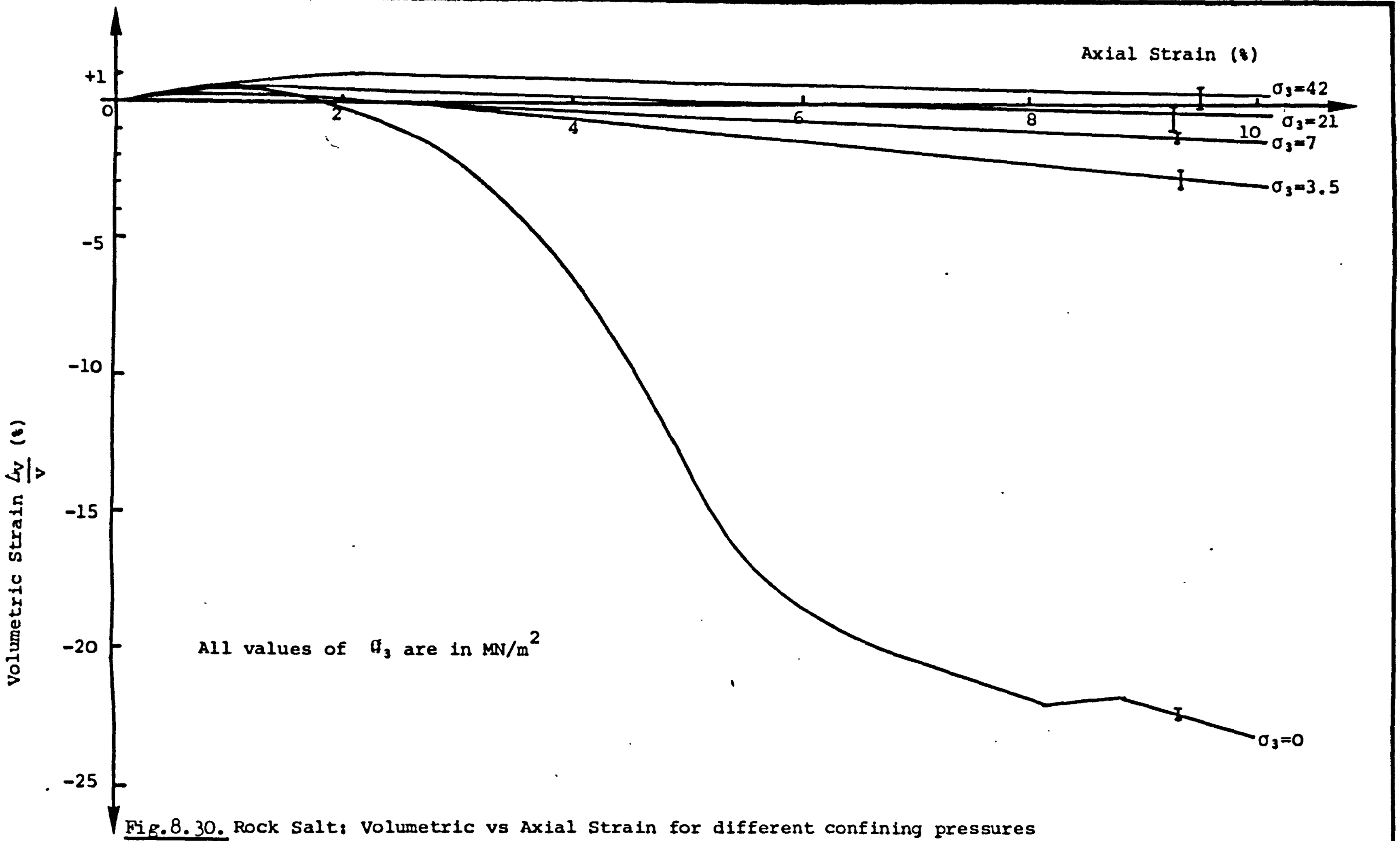

Fig.8.30. Rock Salt: Volumetric vs Axial Strain for different confining pressures

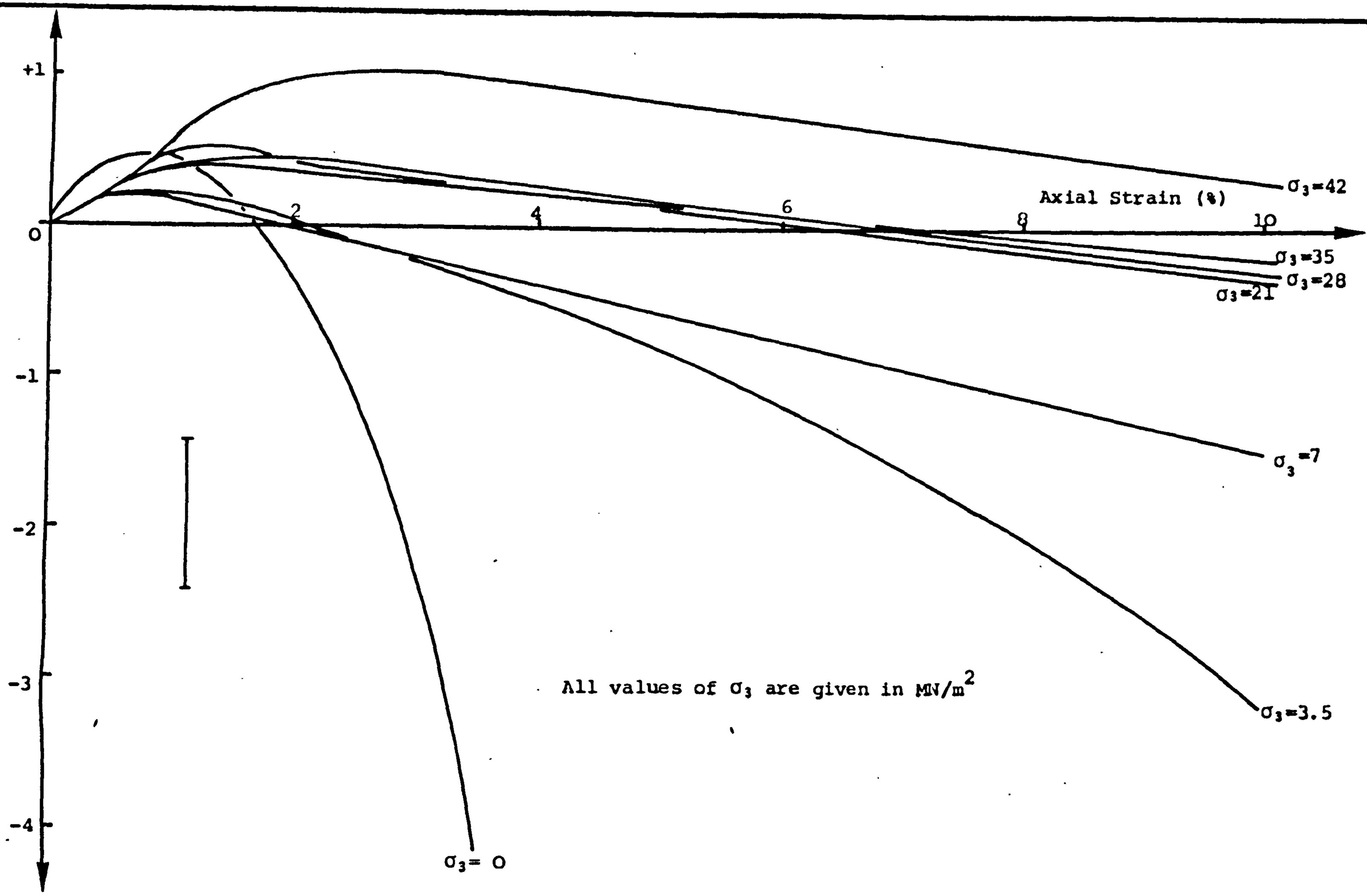

Fig. 8.31 Rock Salt: Volumetric vs Axial Strains for different confining pressures

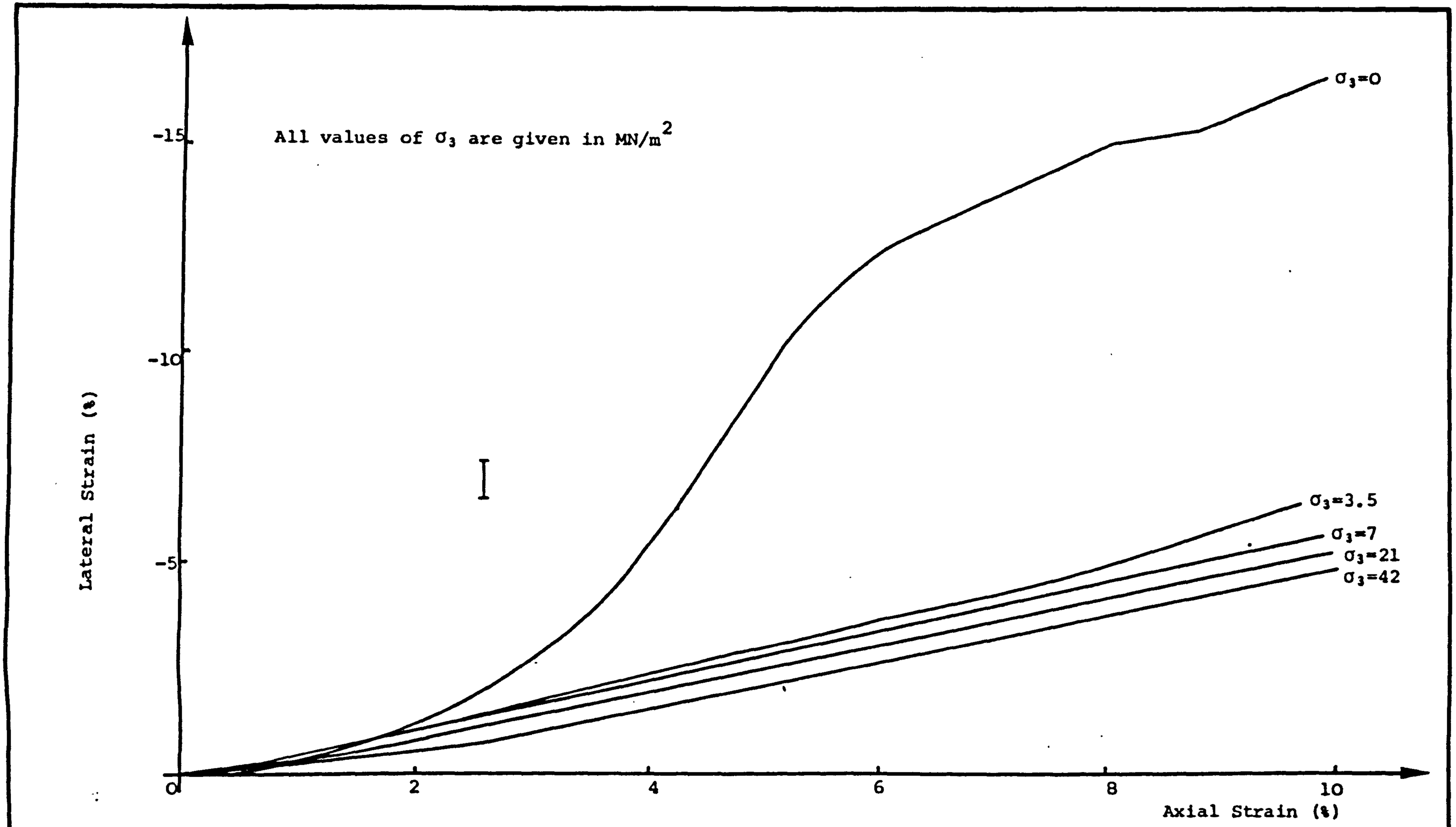

Fig. 8.32 Rock Salt: Lateral vs Axial Strains for different confining pressures

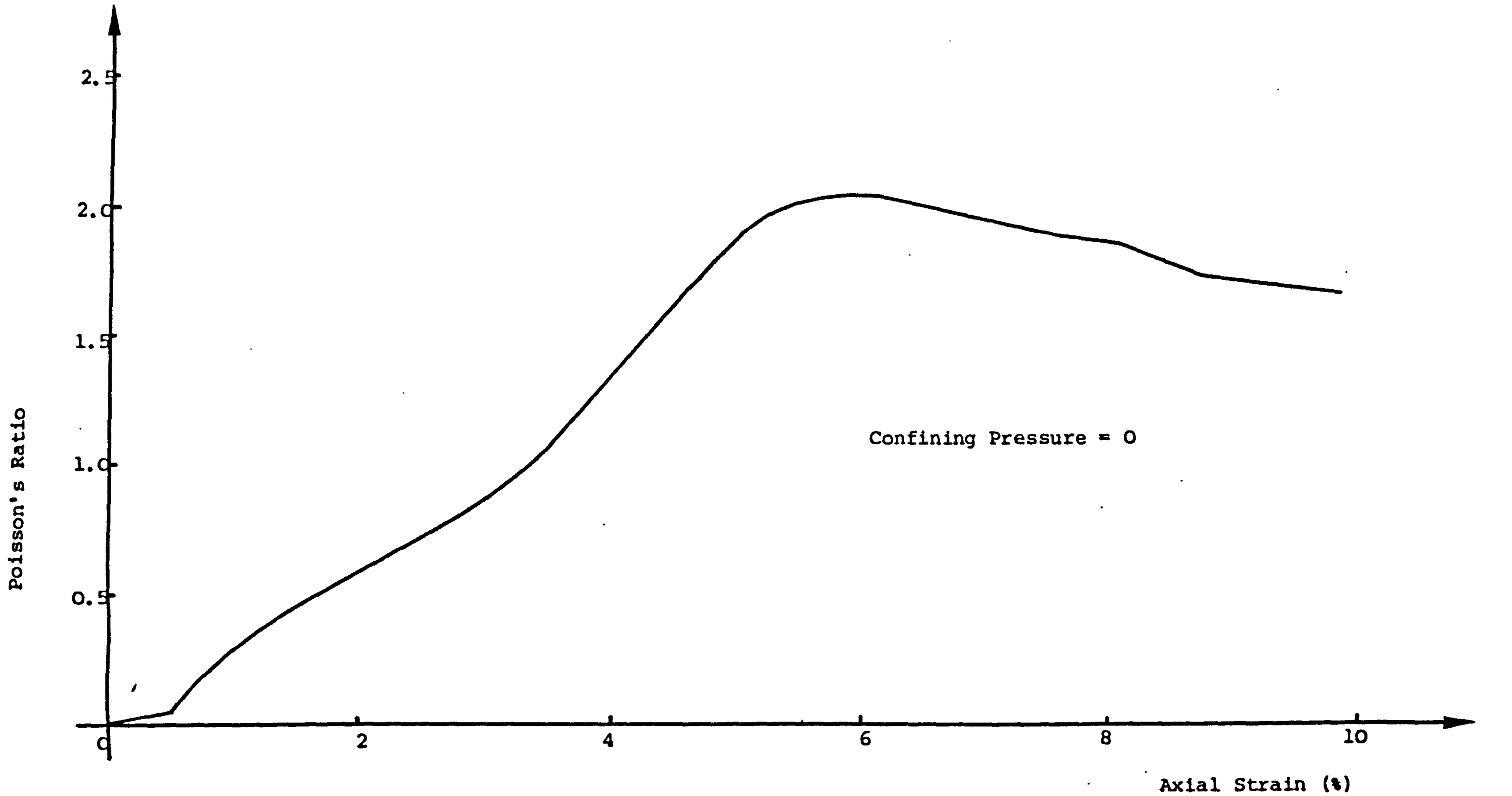

Fig.8.33 Rock Salt: Poisson's Ratio vs Axial Strain for the uniaxial test

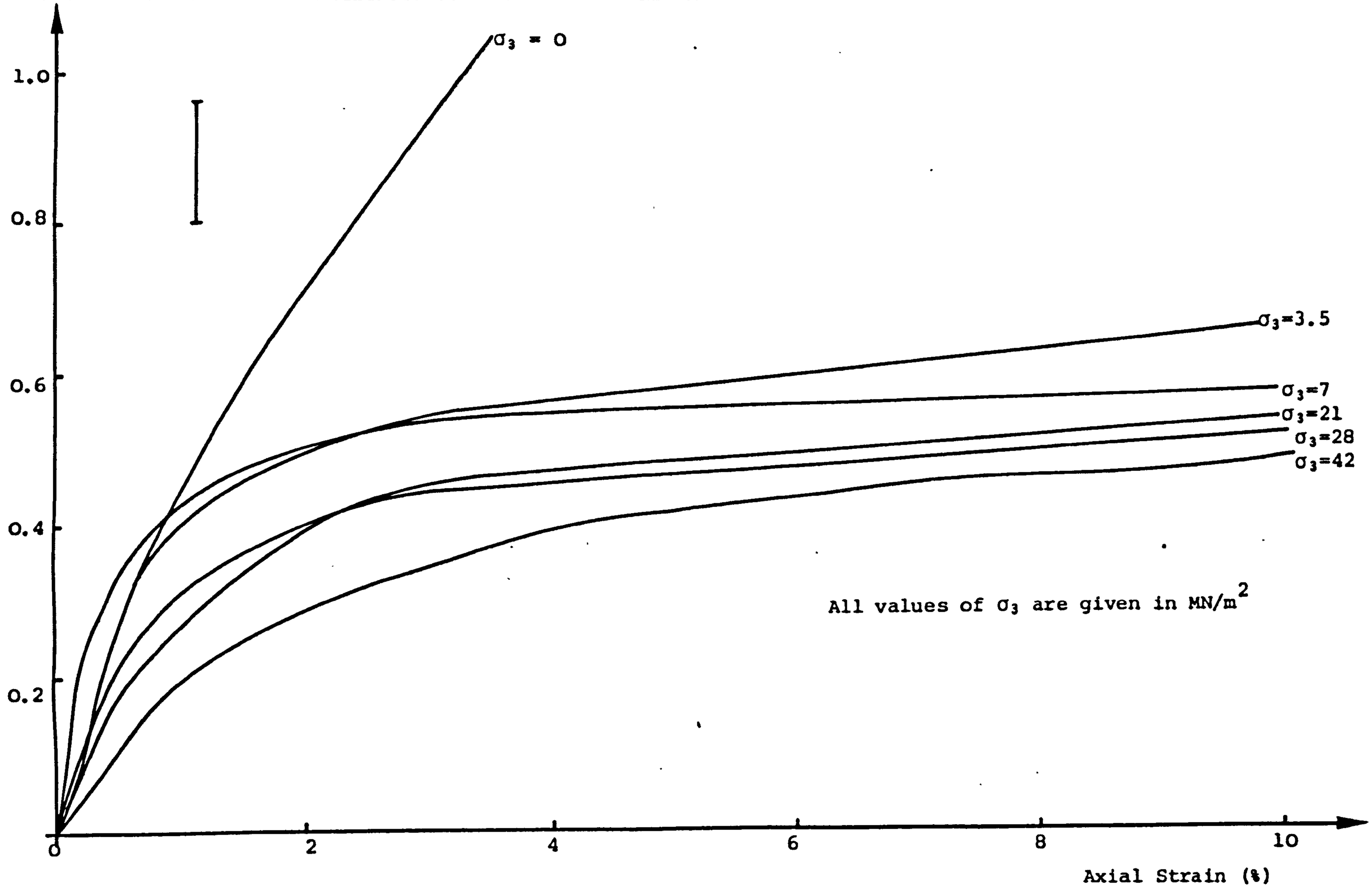

Fig.8.34 Rock Salt: Poisson's Ratio vs Axial Strain for various confining pressures

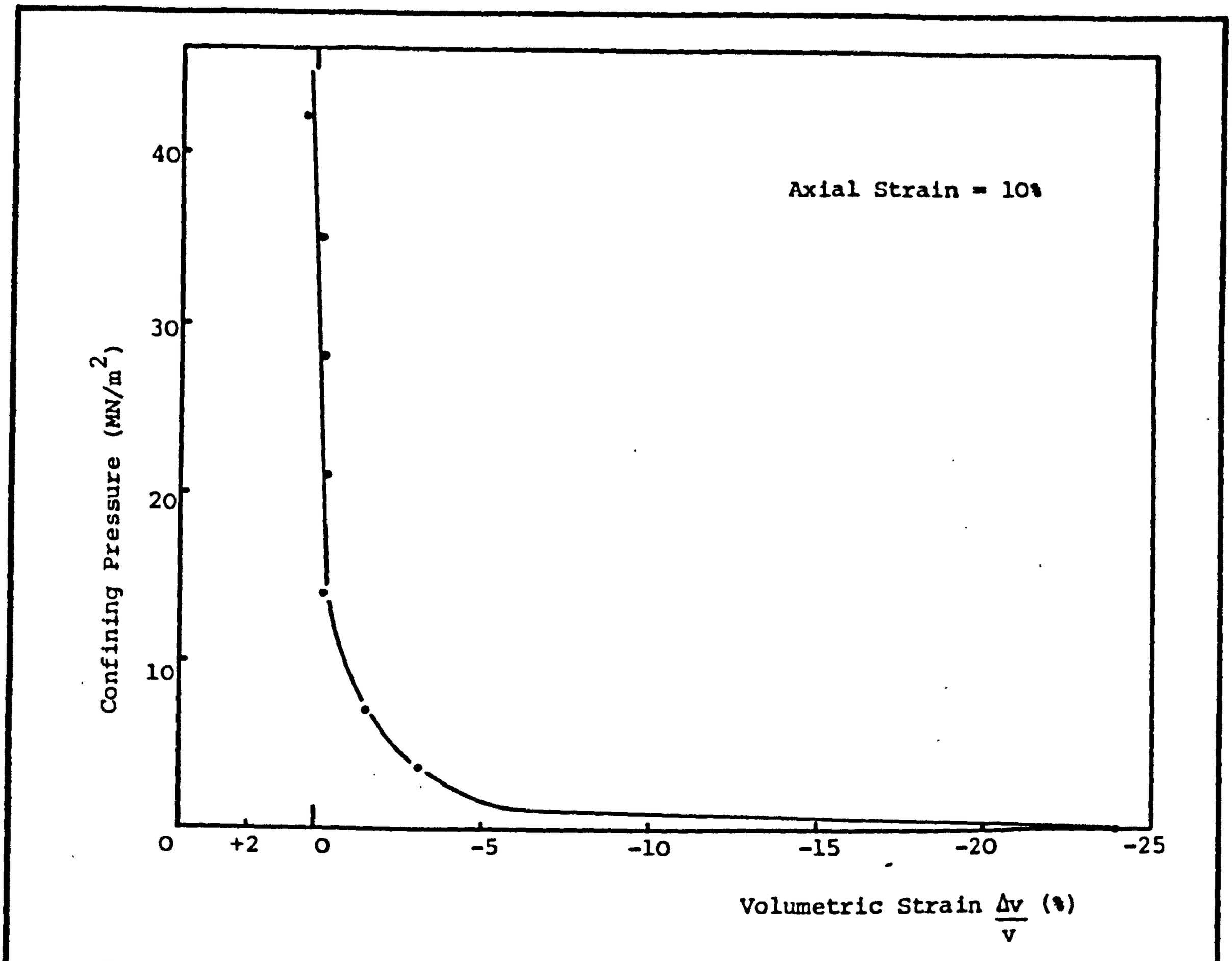

Fig. 8.35a Rock Salt: Confining Pressure vs Volumetric Strain

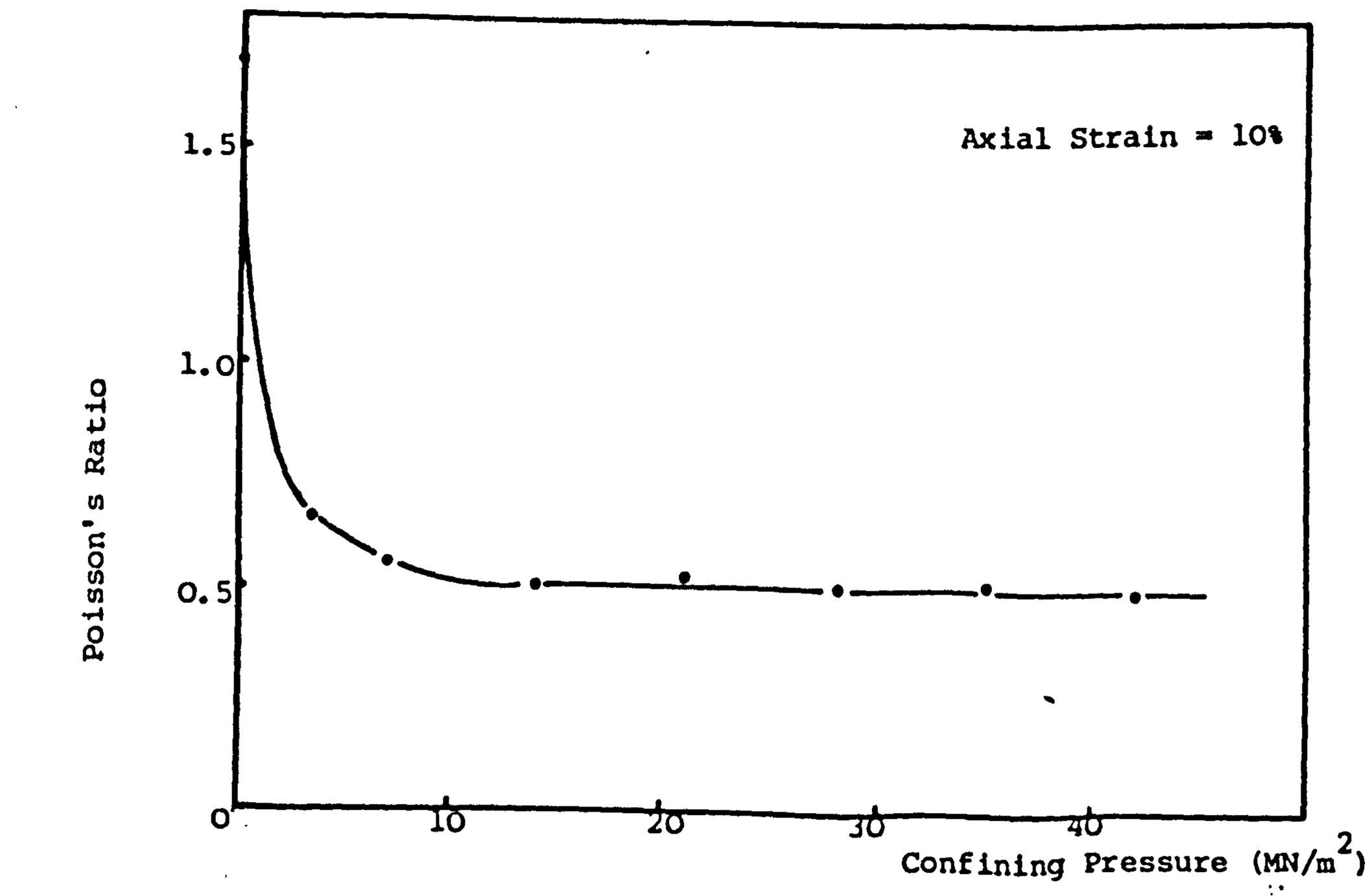

Fig. 8.35b Rock Salt: Poisson's Ratio vs Confining Pressure

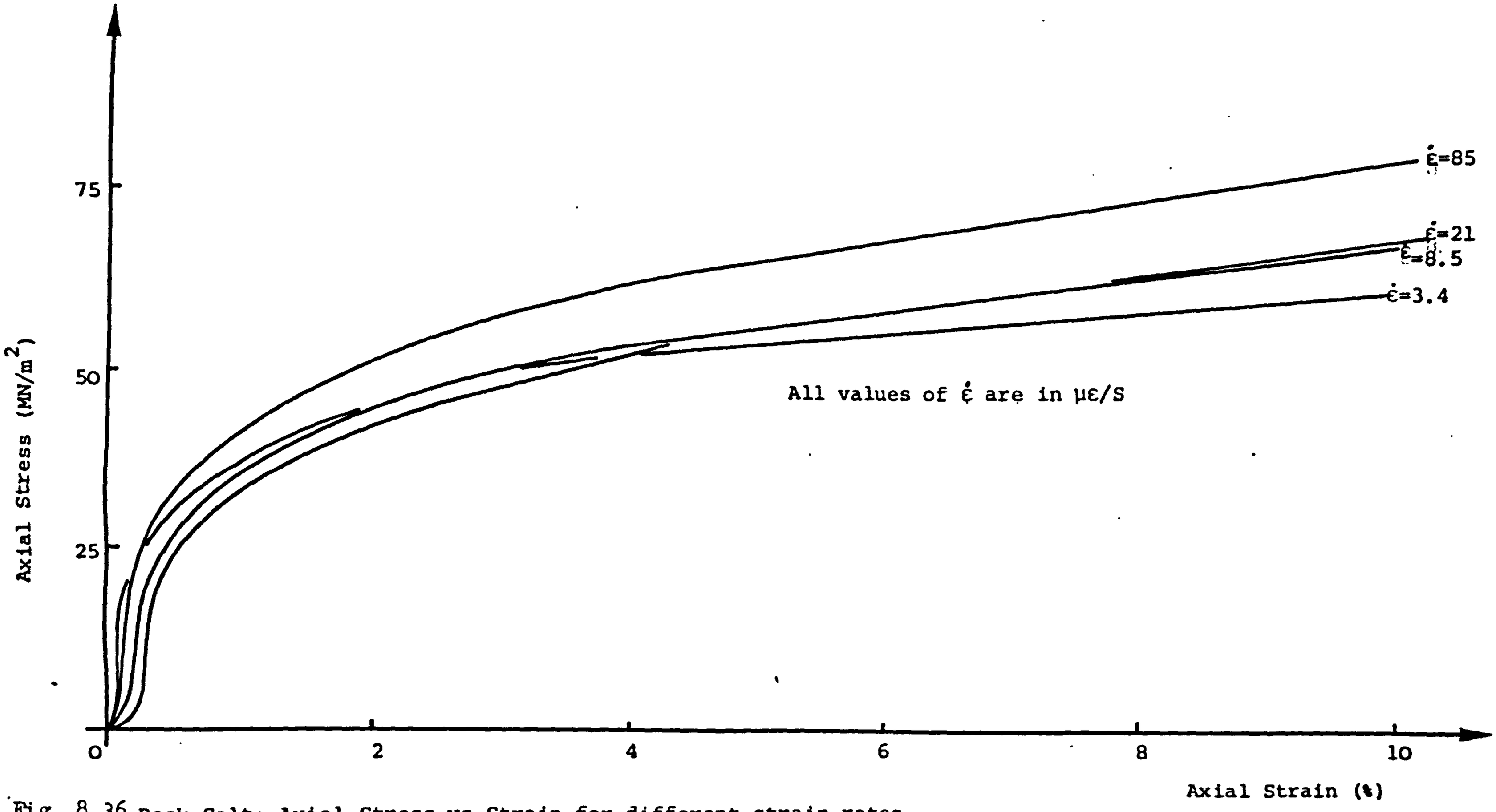

Fig. 8.36 Rock Salt: Axial Stress vs Strain for different strain rates

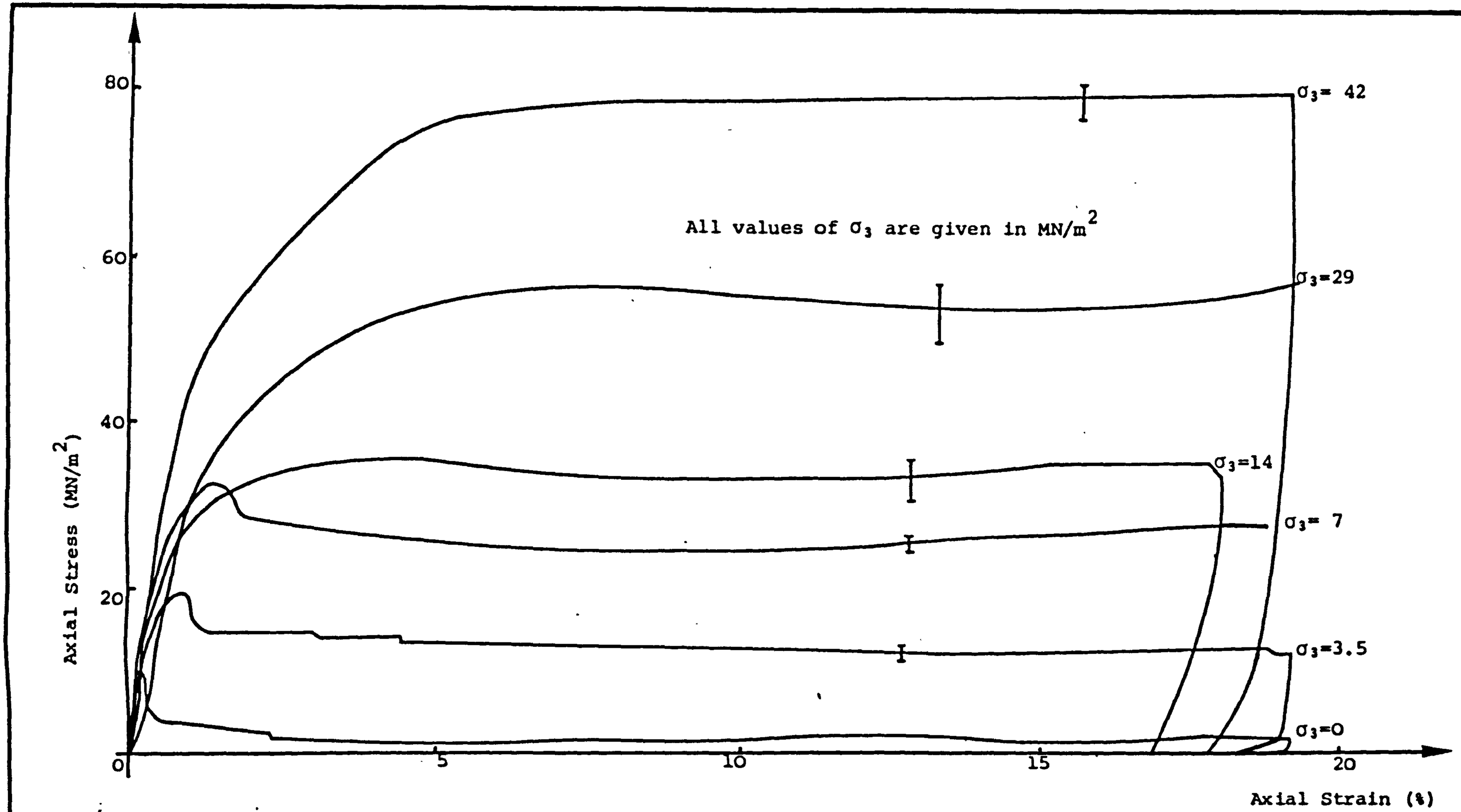

Fig. 8.37 Marl: Axial Stress vs Strain for different confining pressures

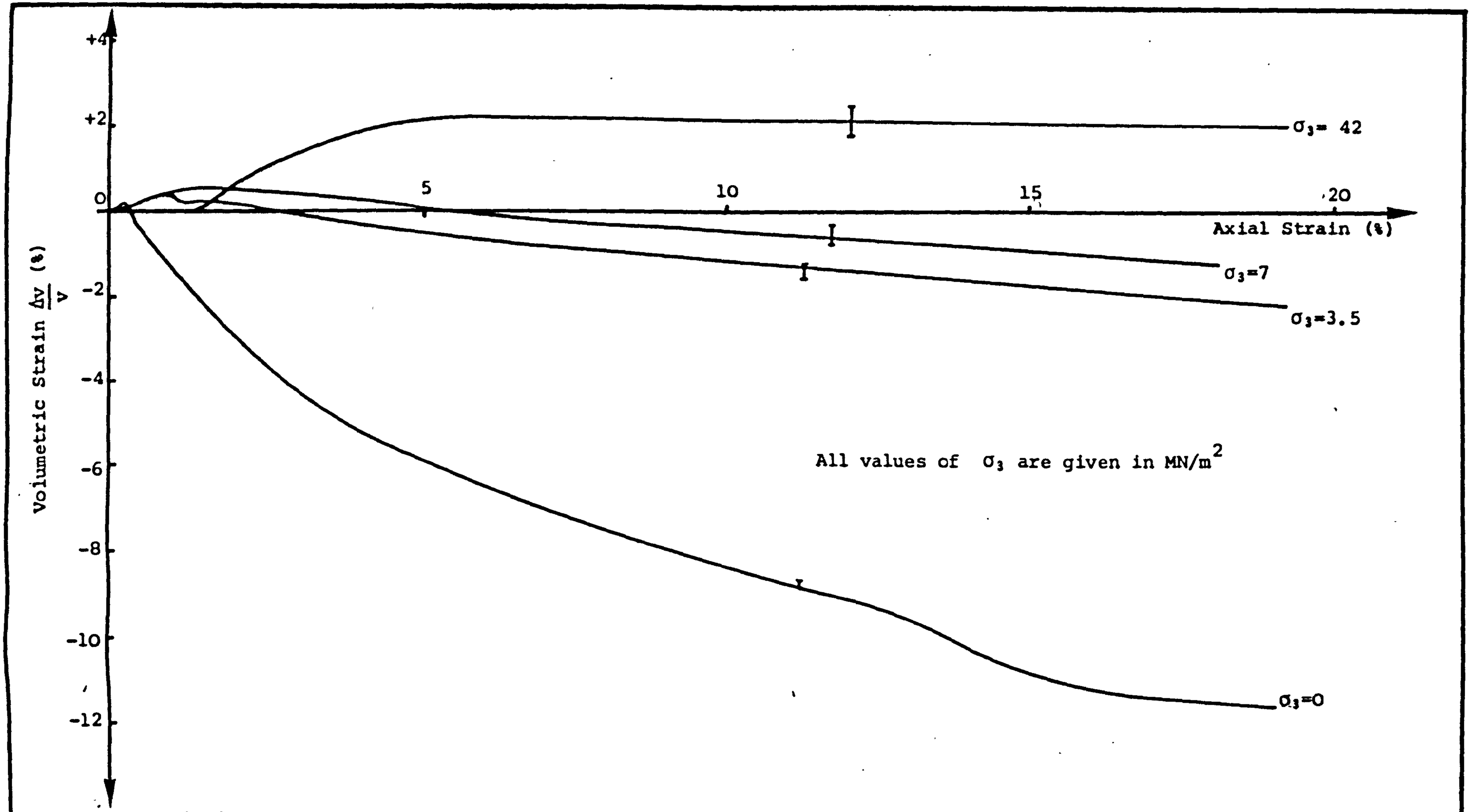

Fig. 8.38 Marl: Volumetric vs Axial Strain for different confining pressures

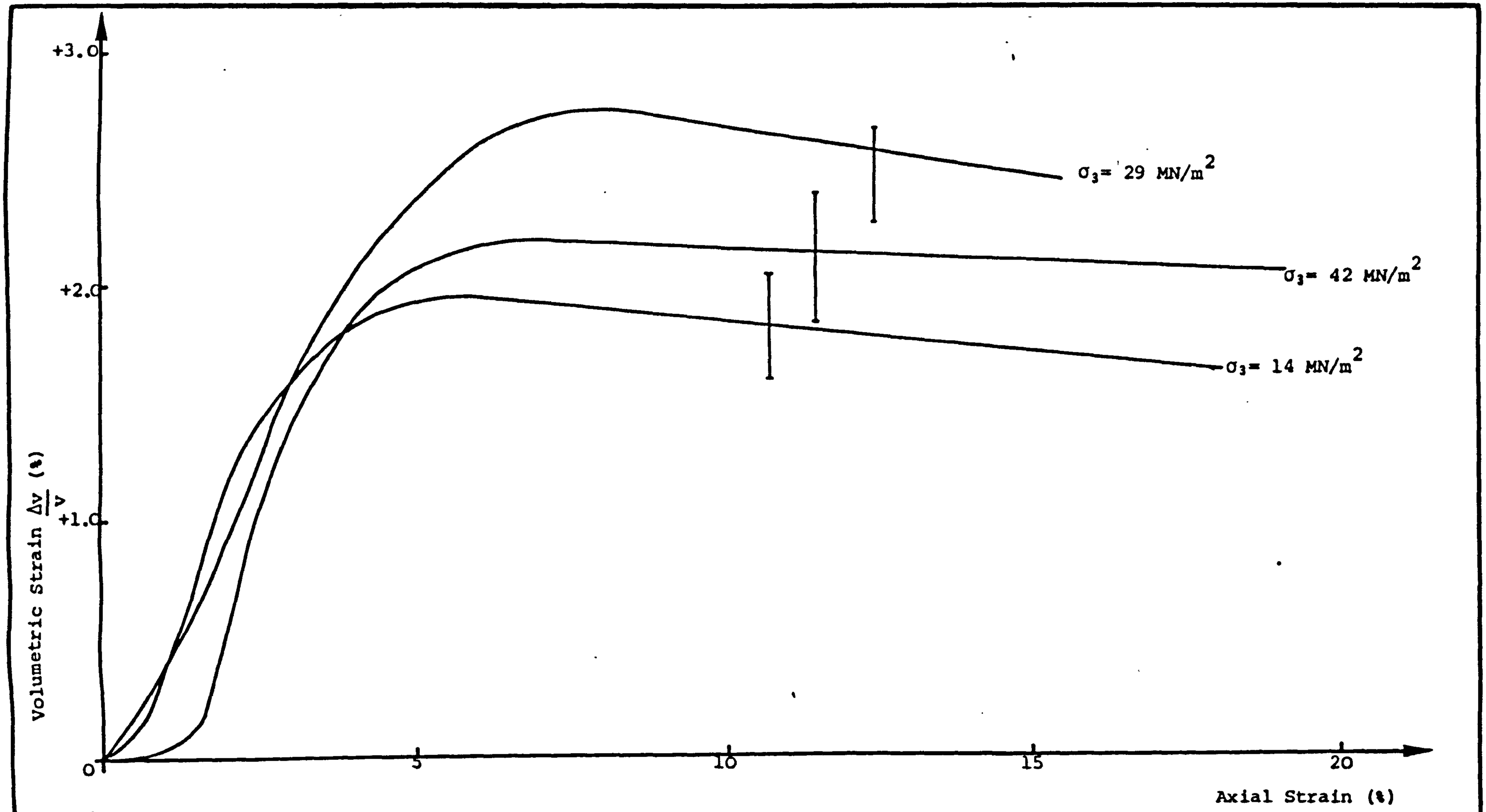

Fig. 8.39 Marl: Volumetric Compression vs Axial Strain for different confining pressures

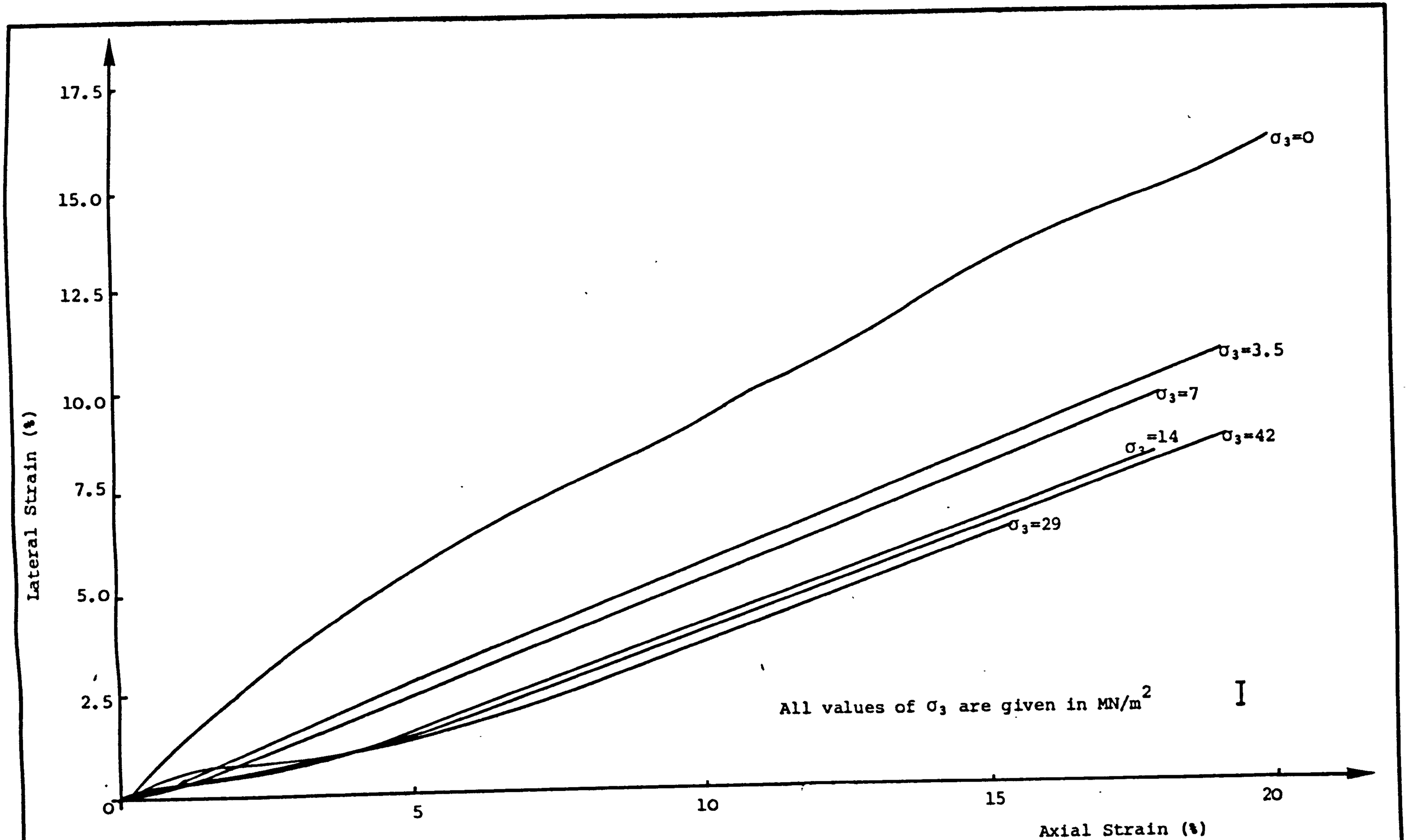

Fig.8.40 Marl : Lateral vs Axial Strain for different confining Pressures

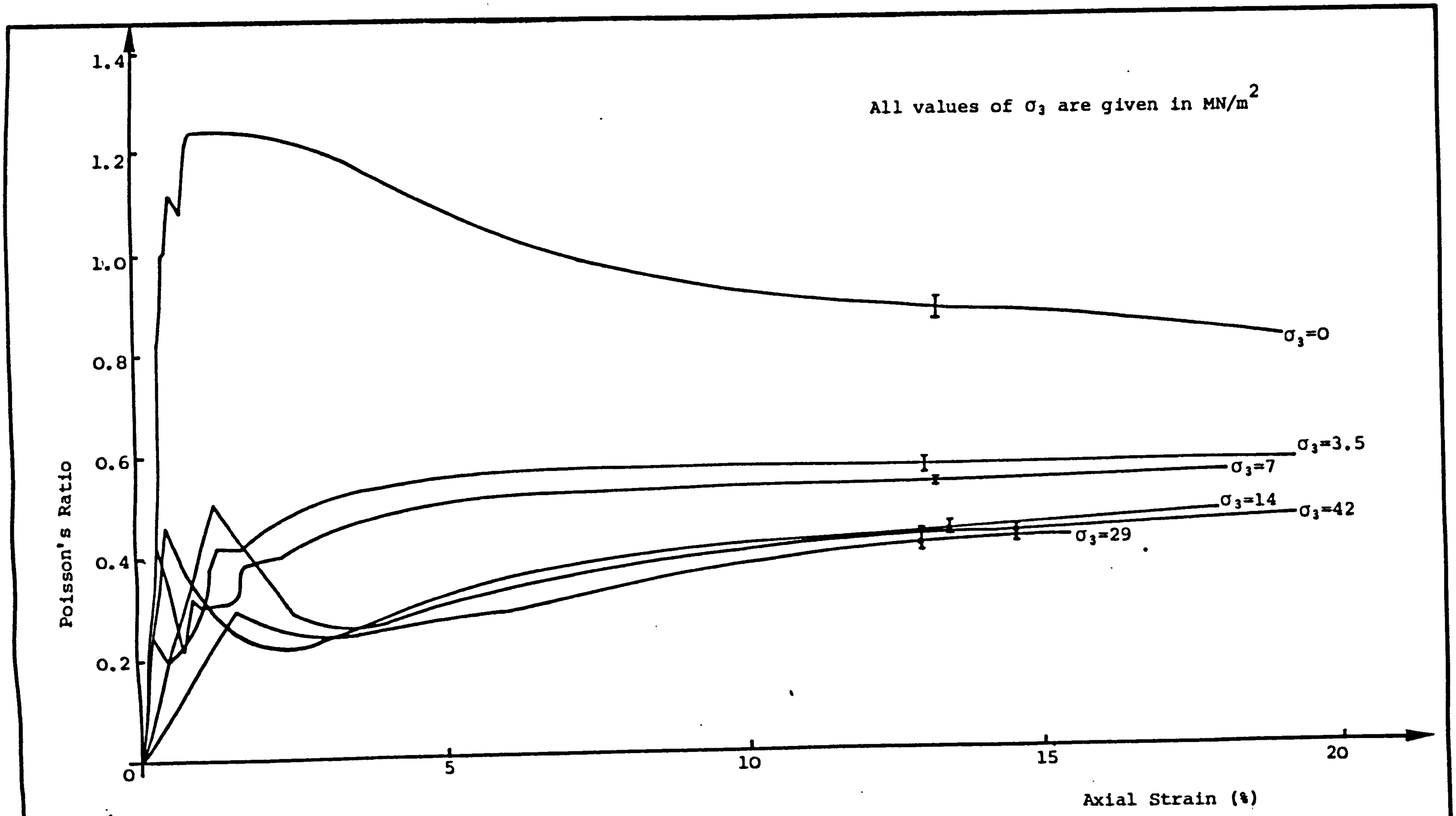

Fig. 8.41 Marl: Poisson's Ratio vs Axial Strain for different confining pressures

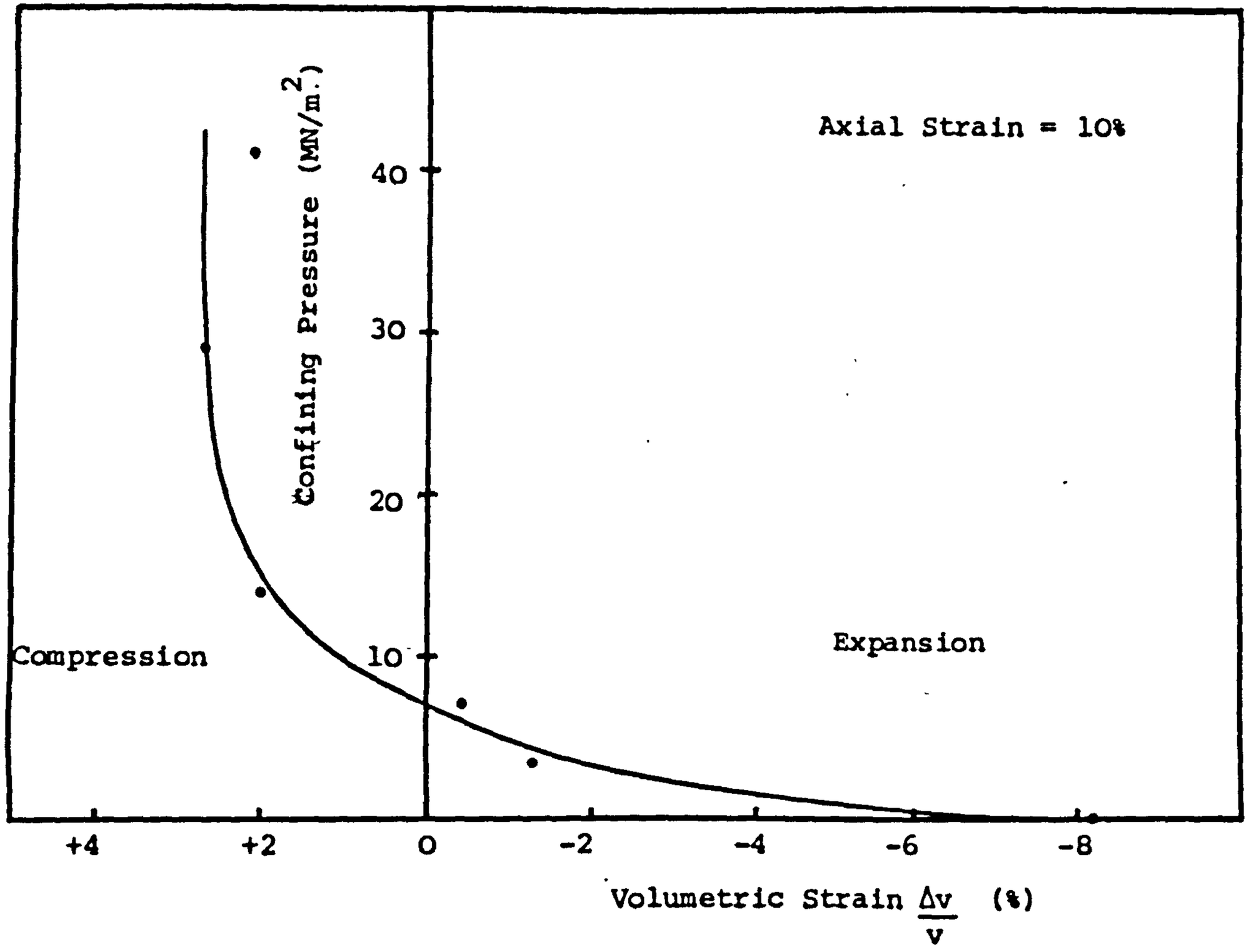

Fig.8.42 Marl: Confining Pressure vs Volumetric Strain

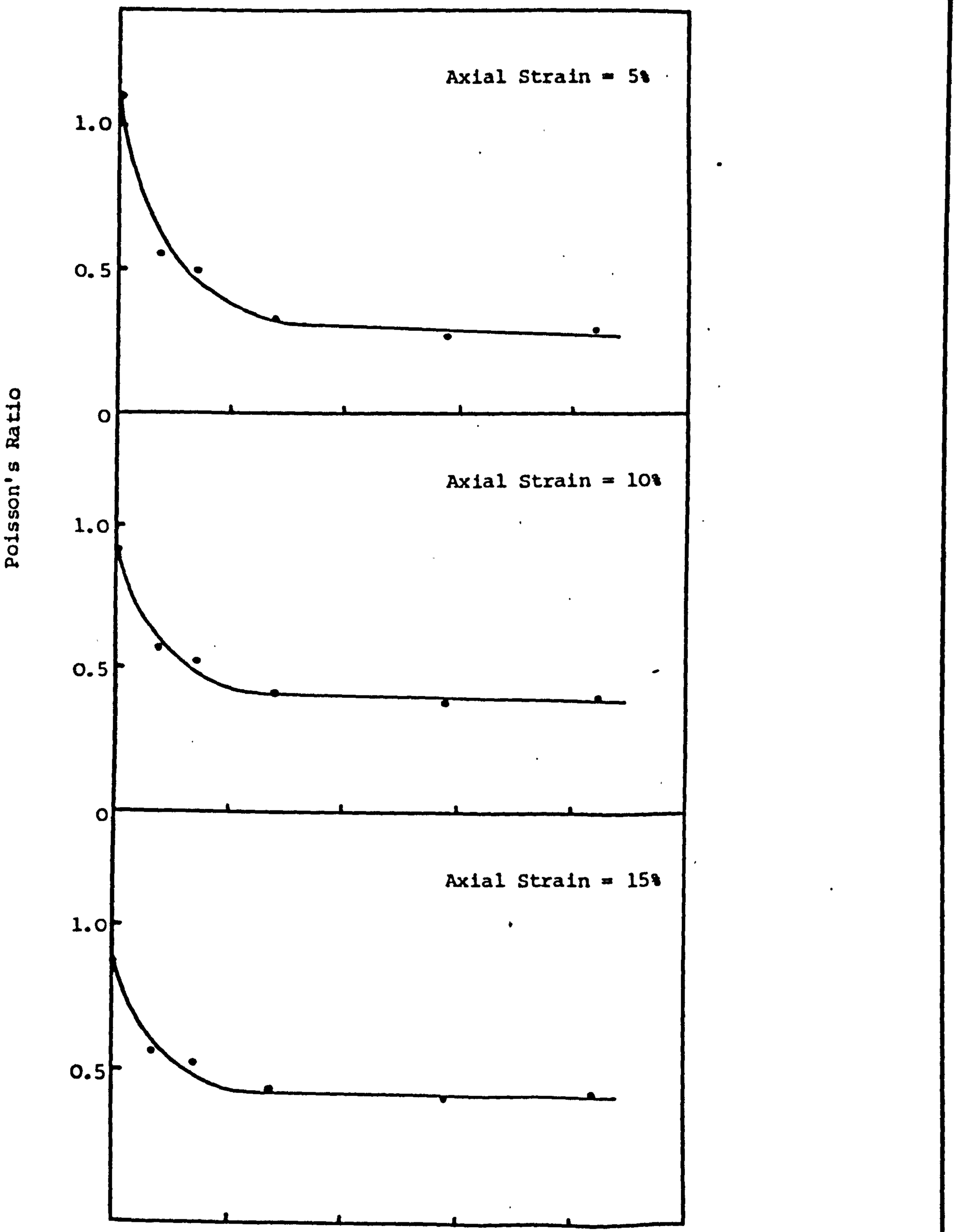

Fig.8.43 Marl: Poisson's Ratio vs Confining Pressure

CHAPTER NINE

THE CRITICAL STATE MODEL

9.0 Introduction

If a specimen of a particulate material - say a drained soil - under triaxial confinement is stressed axially at a controlled rate of strain, there will initially be a small, nearly elastic, compression. As the axial stress increases the specimen will start to yield and this will be accompanied by further compression in the case of a high voids ratio material; or by dilation in the case of a low voids ratio material. The degree of compression or dilation will depend partly on the initial density of the material and partly on the confining stress. There should, however, for all particulate materials, be a unique combination of voids ratio, confining stress and axial stress at which a specimen under test will continue to yield without further change in volume. This idealised plastic state is called the critical state in soil mechanics and has been proposed by Roscoe et al. (1958) and Schofield and Wroth (1958) as a basis of reference for the mechanical description of soils.

9.1 Critical State Concept for Soils

The critical state concept is based on the classical theories of plasticity and Schofield and Wroth (op. cit.) developed two models to describe the yielding of soil as an isotropic rigid-plastic and elastic-plastic material (see also Atkinson and Bransby, 1978). These models describe a series of yield surfaces in principal stress space, which as well as defining 'hardening' and 'softening' of the material as a function of plastic distortion, also define the plastic

volume change as a function of spherical stress. The particular importance of the critical state concept in soil mechanics is that it allows the material to be described mechanically in terms which might be described as fundamental material properties, rather than the results of arbitrary laboratory experiments.

9.2 The Model for Soils

The critical state model proposed by Schofield and Wroth (op. cit.) and Atkinson and Bransby (op. cit.), consists of a family of yield surfaces in q-p space corresponding to different values of specific volume. Fig. 9.1 illustrates the model (after Atkinson and Bransby), in which two main yield surfaces can be identified; the Hvorslev and Roscoe surfaces; separated by the critical state line. These surfaces are also termed state boundaries, since they separate the states which any particular specimen can achieve from those which it can never achieve. Thus, the behaviour of any particulate material tested triaxially can be described or determined using such a model.

9.3 The Critical State Line

The critical state line is defined as the single and unique line of failure points for both drained and undrained tests, where failure is taken to be the state at which large shear distortions occur with no change in stress or in specific volume. The position of the critical state line in q':v:p' space is defined by the equations:

$$q' = Mp'$$

and

$$V = T' - \lambda \ln(P')$$

where q' = effective deviator stress

p' = effective spherical stress

v = specific volume

M & λ are constants

and T' = the specific volume of the soil at the critical state with P' = 1.0 kN m^{-2}.

9.4 The Roscoe Surface

The Roscoe surface is the state boundary described by the idealised curves from drained and undrained triaxial tests on families of specimens, isotropically compressed to different initial values of spherical pressure (Fig. 9.2). Plotted in q-P space the Roscoe surface is curved in shape.

The Roscoe surface is also the state boundary surface for lightly overconsolidated samples. The idealised stress paths in q-P space for these specimens rise to the state boundary and then follow the boundary to the critical state line and failure (Fig.9.3a).

9.5 The Hvorslev Surface

When heavily overconsolidated samples are compressed the specimen's stress-strain curve rises to a peak and subsequently reduces to a residual value with continued straining. The idealised stress paths in q-P space for such samples are presented in Fig. 9.3b, where their paths increase up to a linear state boundary, above the projection of the critical state line and then follow this boundary to the critical state line and failure. This boundary is termed the Hvorslev surface and is bounded at one end by the critical state line and at the other by the tension cut-off line, where the specimen will fail in tension.

In practice, however, heavily overconsolidated samples are more likely to fail prematurely, due to inhomogeneties in the specimen under test. Therefore, two particular states of these specimens must be distinguished. The first is the 'failure state' which occurs at the point of maximum deviator stress, whilst the second is the 'ultimate state' where the conditions for the critical state line are met; that is, the state at which large shear distortions can occur with no change in stress or volume. Consequently, although a particular specimen may have only attained its failure state, elements within it may have attained their ultimate state and thus their critical state.

Atkinson and Bransby (1978, p.215) give the equation for the Hvorslev surface as:

$$q' = (M-h) \exp\left(\frac{\Gamma-v}{\lambda}\right) + h\, p'$$

where h is another constant.

From this equation it is clear that the deviator stress at the point of failure of an overconsolidated specimen is proportional to the effective spherical stress, $p' = \frac{1}{3}(\sigma_1' + \sigma_2' + \sigma_3')$, specific volume, and certain soil constants.

9.6 Critical State Concept for Rocks

Recently, Barton (1976), Gerogiannopoulos (1976), Gerogiannopoulos and Brown (1978) and Brown and Michelis (1978) have applied the critical state concept to rock materials.

Barton (1976) defined the critical state for initially intact rocks as "the stress conditions under which the Mohr envelope of peak

shear strength reaches a point of zero gradient" and proposed a critical state line having the equation:

$$\sigma_1 = 3\sigma_3 \quad \text{for drained specimens}$$

$$\text{and} \quad \sigma_1 = 2\sigma_3 \quad \text{for undrained specimens.}$$

These equations should describe the points at which differential stress reaches a maximum with increasing confining pressure for any particular rock type. The plots of differential stress against confining pressure for the rock types tested here are presented in Fig. 9.4. Of these, only two, rock salt and marl, were tested through Barton's critical state lines. As proposed by Barton, there is evidence of peaks in these curves corresponding to his definition of the critical state. However, from examining the plots of the measured volumetric strains of these rocks (Figs.8.33, 8.34, 8.41 and 8.42), it would seem that, whilst the marl has probably attained its critical state, the rock salt appears not to have. The reason for the discrepancy may be that the data for rock salt plotted in Fig. 9.4 were calculated at two percent axial strain and not at peak axial stresses. Curve 3 for the mudstone (Fig.9.4) is the only other curve which is approaching Barton's critical state lines, but again, on examination of the volumetric plots (Figs. 8.27 and 8.28), there seems little evidence of a true critical state being approached.

The approach of Gerogiannopoulos (1976) and others (Gerogiannopoulos and Brown,1978; Brown and Michelis, 1978) was to modify Schofield and Wroth's original "Granta-gravel", rigid-plastic model, to allow for the energy required to satisfy the creation of new fracture surfaces during yield. They examined experimental data obtained from triaxial compression tests on different rock types and

have shown that their modified model can be used to simulate accurately the mechanical behaviour of intact rock specimens up to peak stress. Their ultimate aim, however, was to apply the critical state concept to model the behaviour of discontinuous or fractured rock masses and to describe the post-peak stress behaviour of rock materials - an important practical problem in the vicinity of deep underground excavations.

Inherent in the critical state approach is the requirement that the energy input to the test specimen from the test system for any given strain increment can be controlled, so that there will never be a negative energy input into the specimen. This condition is known as stable deformation. In triaxial testing this requirement can be met in soils looser than the critical state, but in rocks and soils denser than the critical state only at axial stresses less than the peak-stress or at high confining pressures.

CSSM Eqn. 5.1.

It is nevertheless possible to find in the literature test data on rocks which fit the critical state model. Scholtz (1967) carried out a series of triaxial tests at confining pressures of between 25 and 400 MN/m^{-2} on weak marble specimens (50mm long by 16mm diameter) with an average unconfined compressive strength of 40 MN/m^{-2} and grain diameter of 0.20mm at a strain rate of 10^{-5} s^{-1} in a machine of high stiffness (10^5 MN/m^{-2}). These deformed cataclastically, breaking down through gradual loosening of grains into individual grain particles during the test. The ultimate form of the marble was like a granular material. Except in the case of the unconfined test deformation was stable.

units?

In Fig. 9.5 Scholz's results are presented and also replotted using Schofield and Wroth's terminology as $q = \sigma_1 - \sigma_3$ against $P = \frac{1}{3}(\sigma_1 + 2\sigma_3)$ for constant volumetric expansions. The initial void ratio was 0.013 and the specific volume 1.013. The maximum axial strain to which the tests were carried out was 1.5%. Although neither the curves nor Scholz's results are complete, they appear to form a series of yield curves which make up the three-dimensional state boundary surface discussed earlier and plots data appear to approach the critical state. For comparison, Barton's critical state lines have also been included in Fig. 9.5, and in a plot of differential stress against confining pressure (Fig.9.6).

In the present series of tests, similar curves to those produced from Scholz's results were obtained for the experiments carried out on rock salt. Apart from the uniaxial test, all the specimens deformed stably, and remained intact throughout. The final shape for all of the latter specimens was that of an uneven barrel. These curves are presented in Fig. 9.7. In both Scholz and this case the q-p curves for the different magnitudes of volumetric expansion converge at the lower q-p values; this phenomenon can be explained in terms of stability and the nature of the breakdown of the material.

The more typical series of curves obtained from the rock types tested here are given in Figs. 9.8 and 9.9. Here, the q-p data for different magnitudes of volumetric expansion for each rock type are scattered about single curves, representing their residual strength envelopes. This scatter is largely the result of the

fluctuations in the post-failure stress levels. The Portland stone, sandstone, silty sandstone and saccharoidal limestone all deformed unstably, along shear planes, with the exception of the saccharoidal limestone, which, at the higher confining pressures, deformed along ductile faults.

The mudstone and marl results have not been included here because of the unrepresentative results of the first and the limited data available from the second.

9.7 A Description of Yielding Rock

These different types of deformation illustrate the breakdown mechanisms in rock and show a distinct analogy with the behaviour of loose and dense soils (Atkinson and Bransby, 1978). For instance, in the case of the strain hardening deformations of Scholz's marble and the rock salt, the specimens get stronger as they deform. Consequently, strain will tend towards homogeneity throughout the confined specimen, since those elements of the rock which have strained most will be stronger than those which have strained less. Then, at failure, defined as the point of maximum deviator stress, or at the end of the test, we would expect a uniformly deformed specimen which, in the case of Scholz's marble, occurred as the complete disintegration of the rock structure and, in the case of the rock salt, as a uniform distribution of cracks or flow of crystals.

On the other hand, in the strain softening case, following peak stress in the other specimens, the specimens will become weaker with increasing strain. Thus strain will tend to be inhomogeneous

and further strain will be concentrated in the weaker elements of the rock, which have already been subjected to the most strain. Thus following peak stress, thin zones of concentrated strain - or shear planes - would be expected to develop. In the case of a cylindrically confined rock specimen these usually take the form of twin inclined fault planes of the type described earlier and by Rummel and Fairhurst (1970), Scholz (1967) and others, and associated by them with the post-peak stresses.

9.8 The Model for Rocks

The p:q(v) curves presented here for those specimens which deformed unstably represent the residual strength envelope of the rock, which is independent of specific volume or volumetric expansion. As the brittle/ductile transition is approached and the material begins to deform stably, this single curve reaches a transition point where specific volume does become important and separate curves for different volumetric strains can be plotted, as for Scholz's marble and the rock salt. These curves form the Hvorslev surface for this particular material. As in the case of the model for soils, this surface is bounded by the critical state line.

Provided, therefore, that a specimen deforms homogeneously, we would expect, with continuing increase in deviator stress, ultimately to reach a critical state at which large distortions would occur without change in volume. But this can only happen where strains throughout the specimen remain essentially homogeneous. If the specimen divides into distinct blocks which slide past each other across relatively narrow zones, then the strength of the specimen will reduce from a postulated critical state to a residual strength.

Evidence?

The evidence for the existence of a "Roscoe Surface" for specimens tested which have been hydrostatically ($q=0$, $\sigma_2 = \sigma_3$) stressed to some value of P greater than that of the critical state is extremely limited. Data from the tests on marl and from Edmond and Paterson's (1972) experiments suggest that such a state boundary does exist for rocks, as would be expected intuitively, but is inconclusive, and much more work is needed in this area.

9.9 Summary

A model has been proposed which consists of a "Hvorslev Surface" for specimens deforming stably, and a residual strength surface for those failing unstably. This proposed model is illustrated in q-p space in Fig. 9.10. A curve corresponding to the peak differential stresses is also included: this surface may be considered as traversing a hypothetical "Hvorslev Surface" but which is so unstable as to be non-existent.

* * *

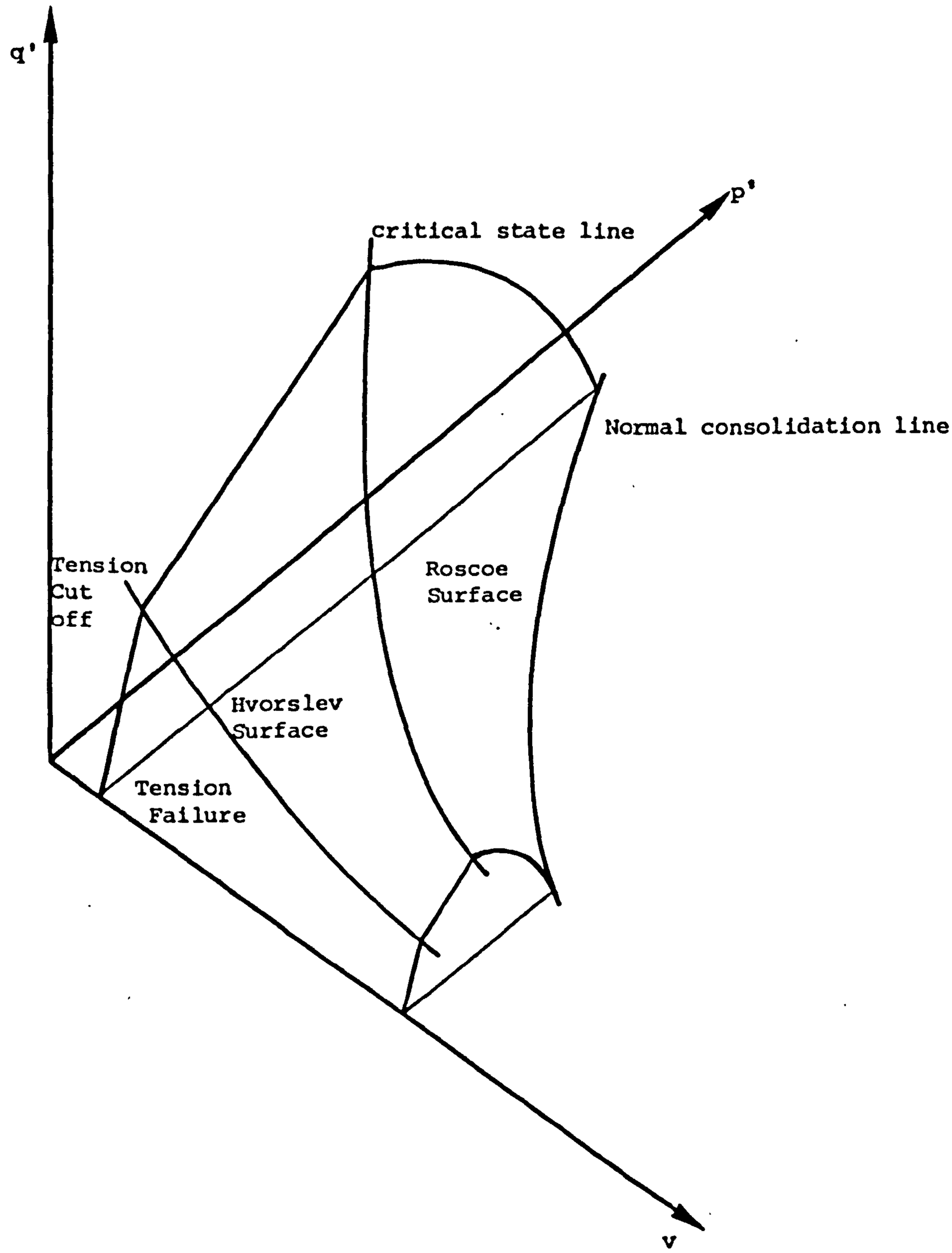

Fig. 9.1 A Critical State Model for Soils
(after Atkinson and Bransby, 1978)

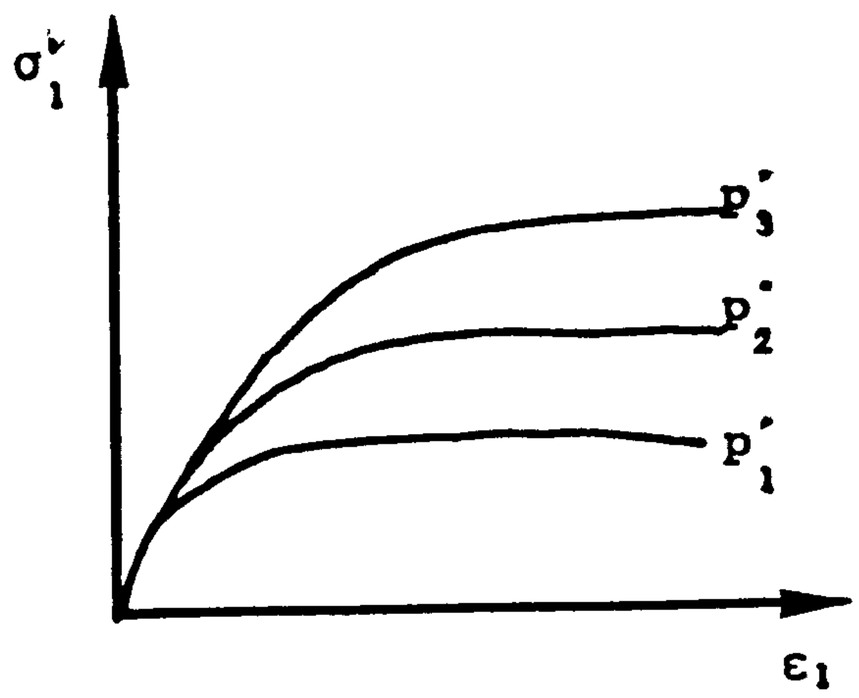

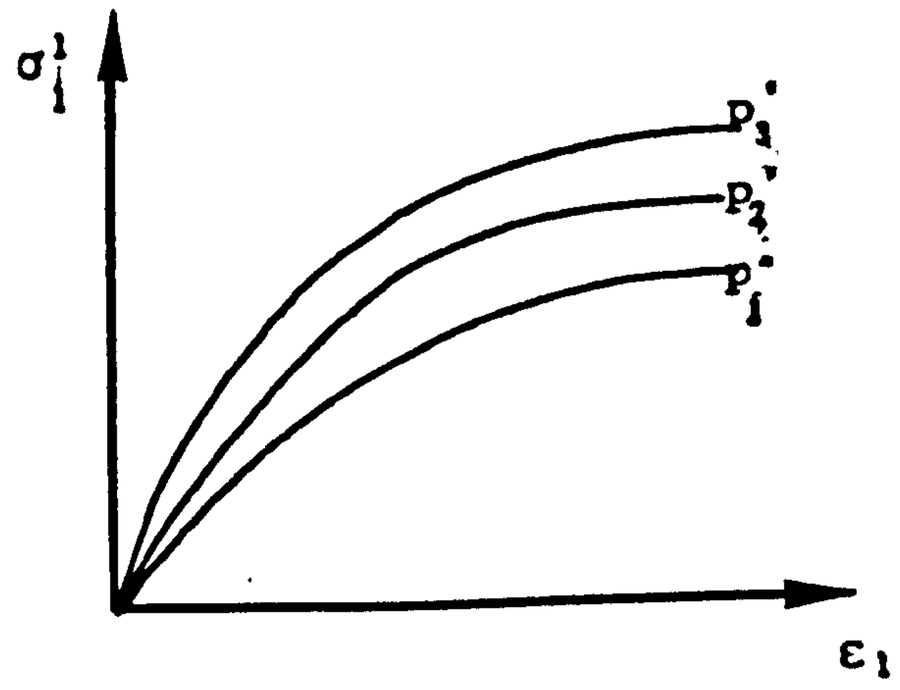

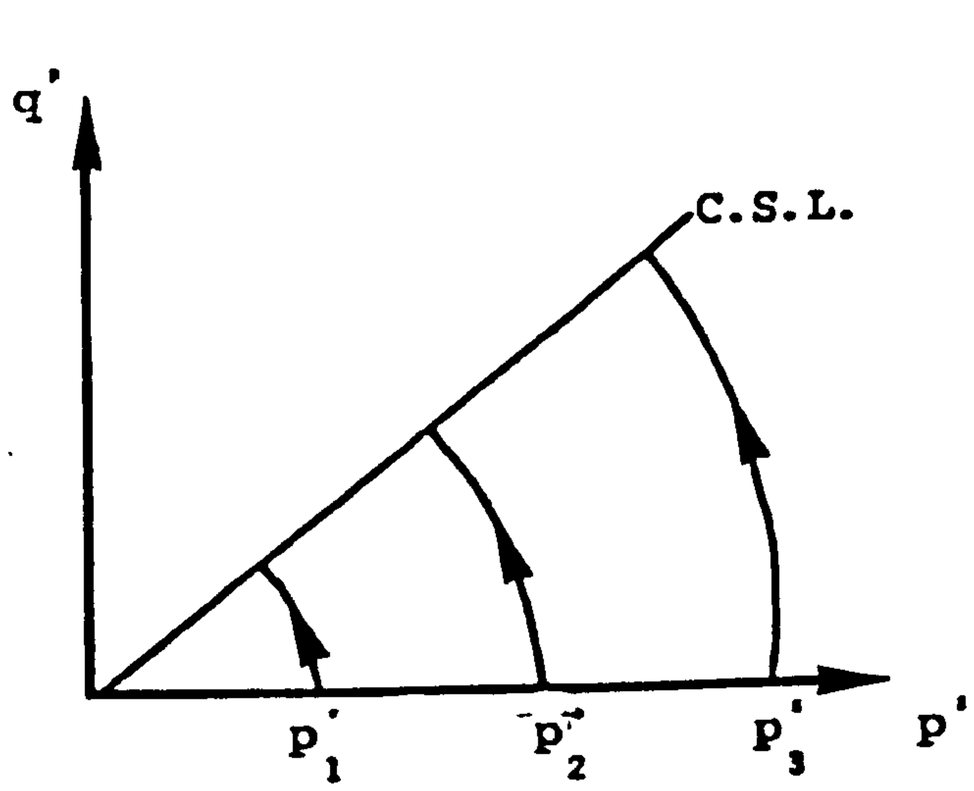

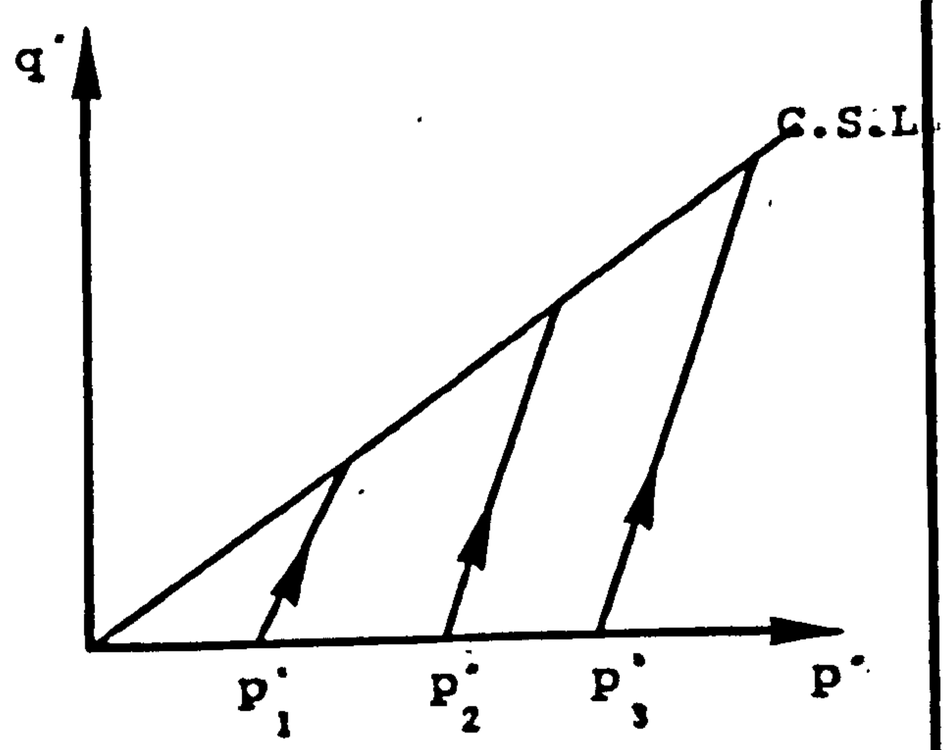

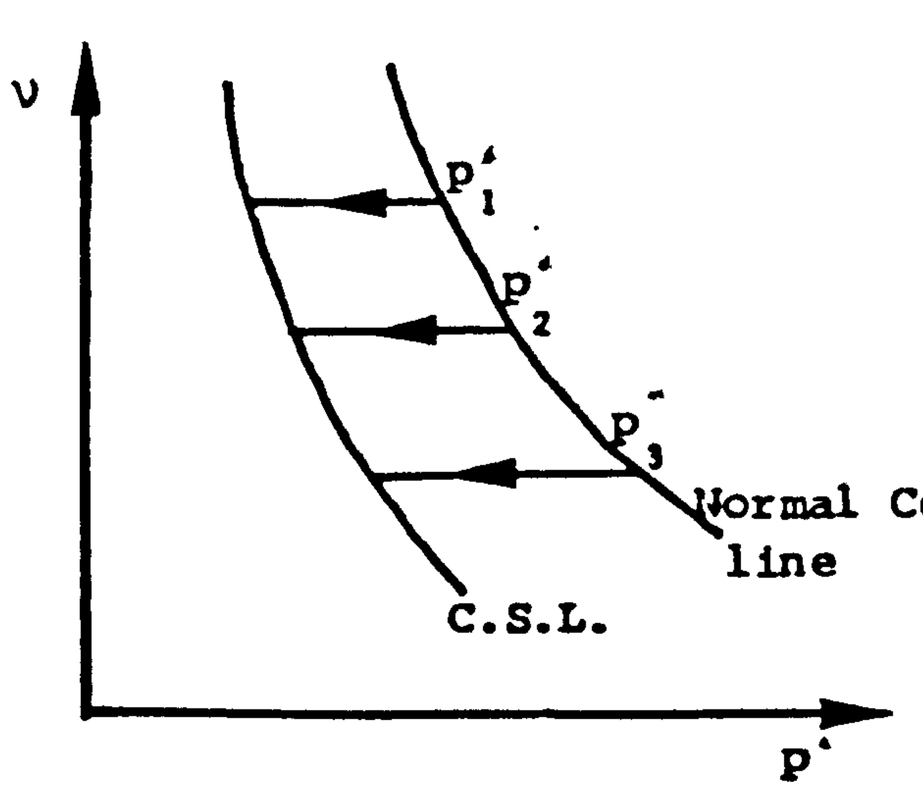

Undrained

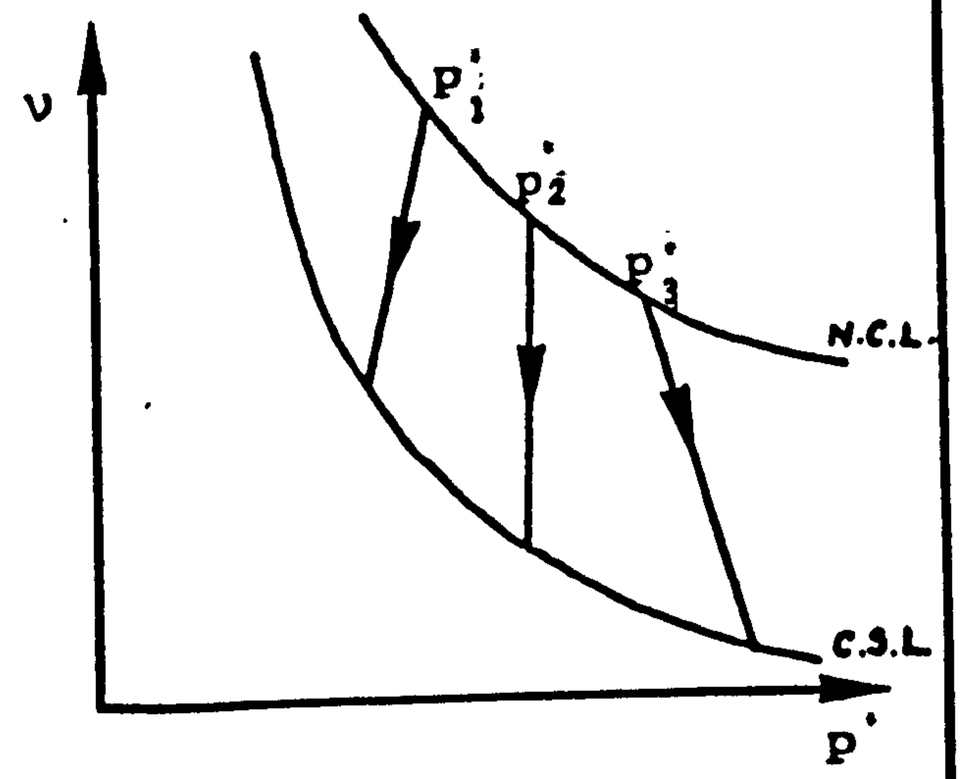

Drained

Fig. 9.2 The Roscoe surface for soils

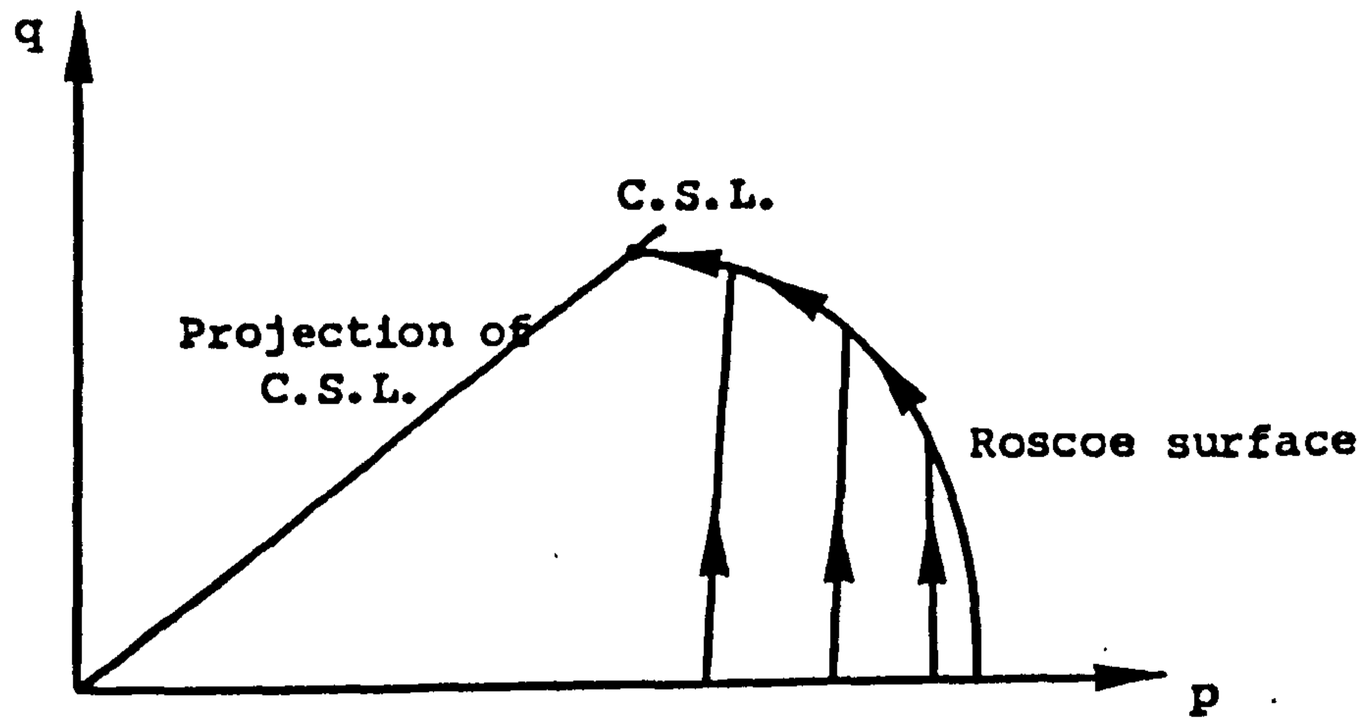

3a. Stress paths for lightly overconsolidated soils

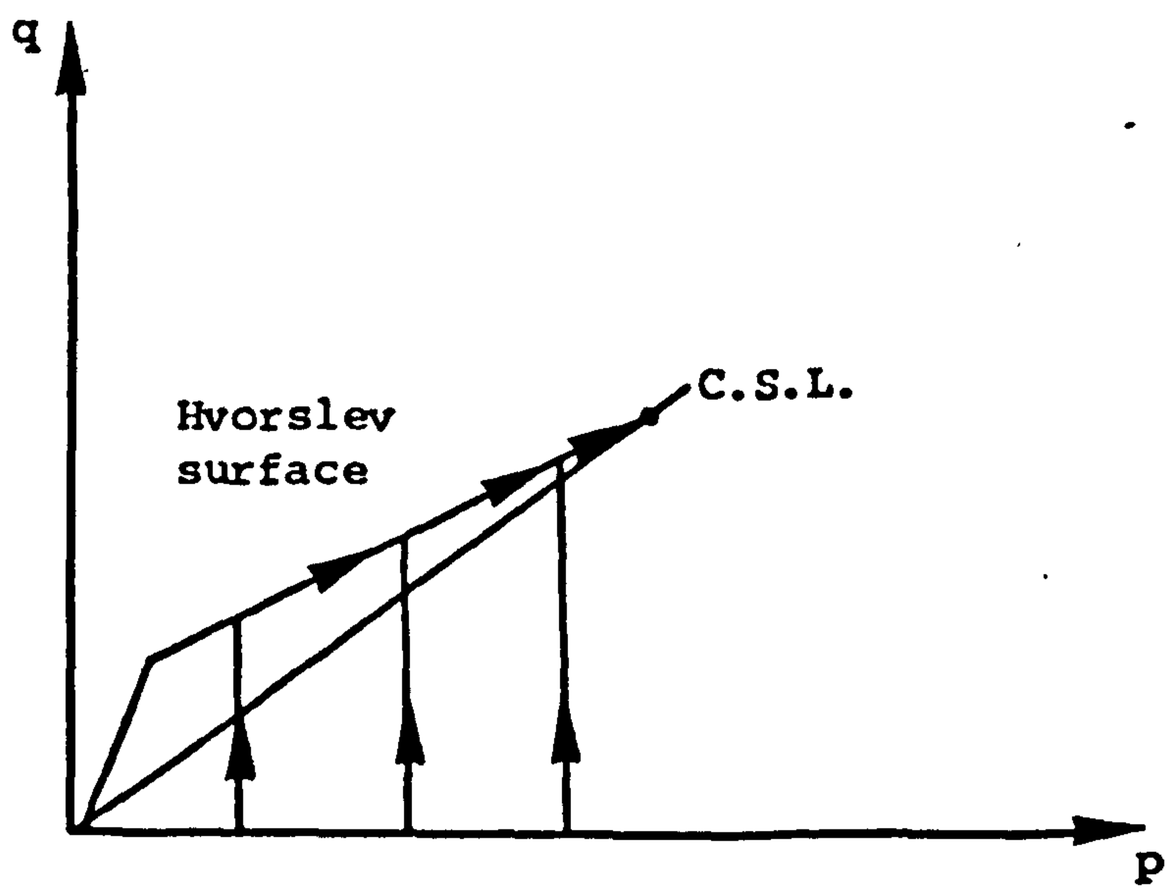

3b. Stress paths for heavily overconsolidated soils

Fig.9.3 Stress Paths for Overconsolidated Soils showing Roscoe and Hvorslev Surfaces

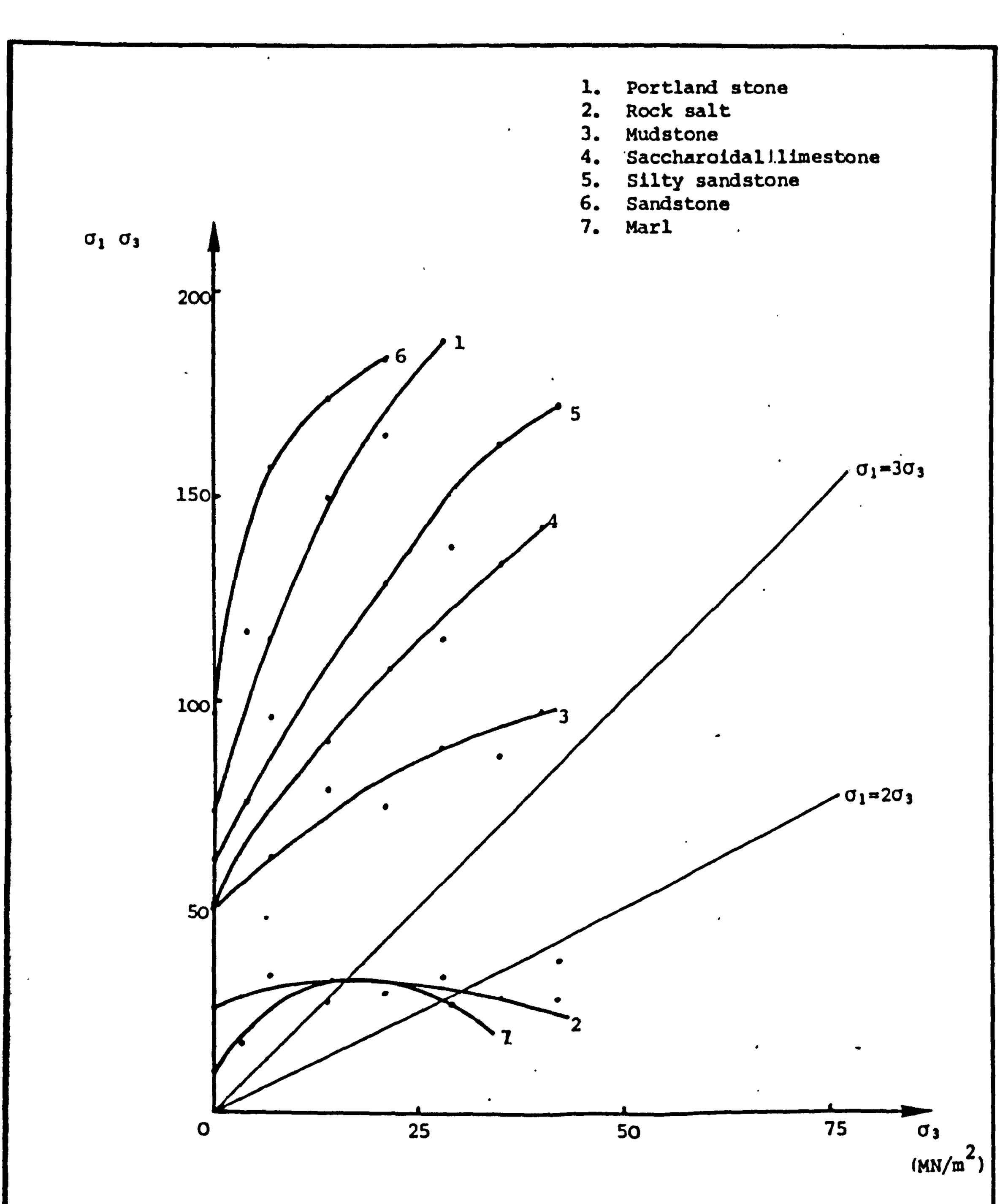

Fig. 9.4 Differential stress versus confining pressure for all the rock types tested

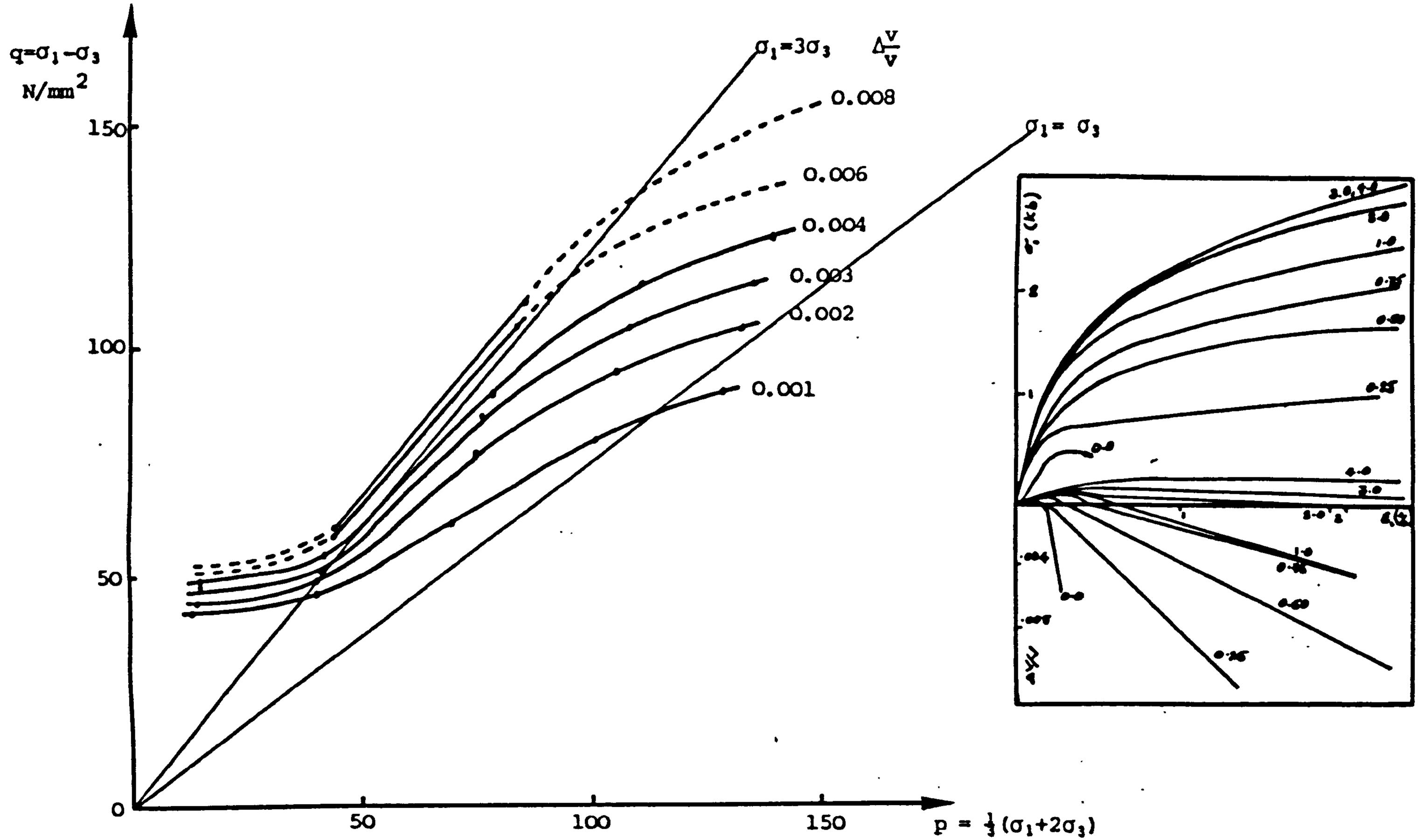

Fig. 9.5 Constant volumetric strain yield paths for marble tested in triaxial compression by Scholz (1967) and original data

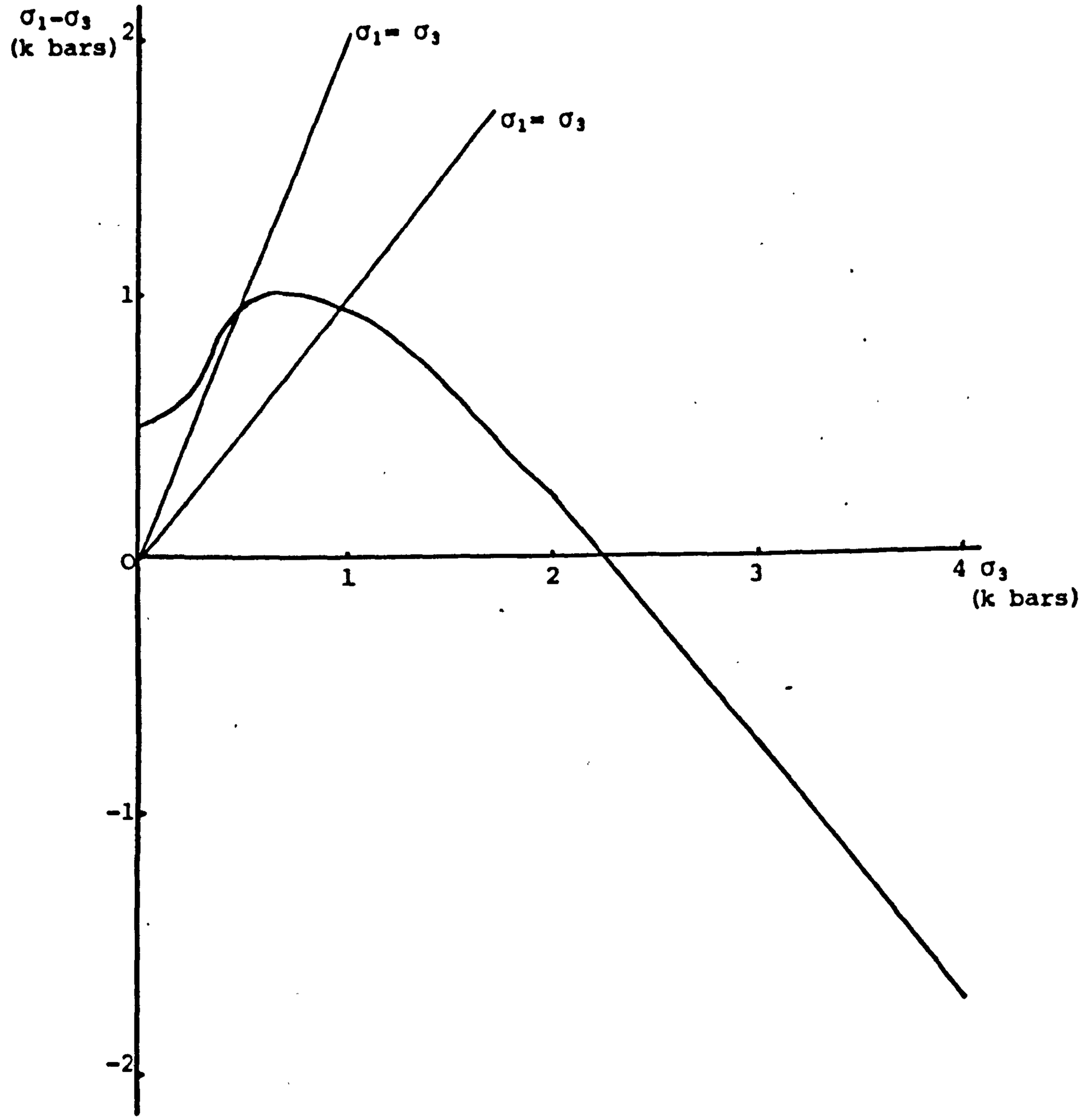

Fig.9.6 Differential stress versus confining pressure for marble measured by Scholz (1967)

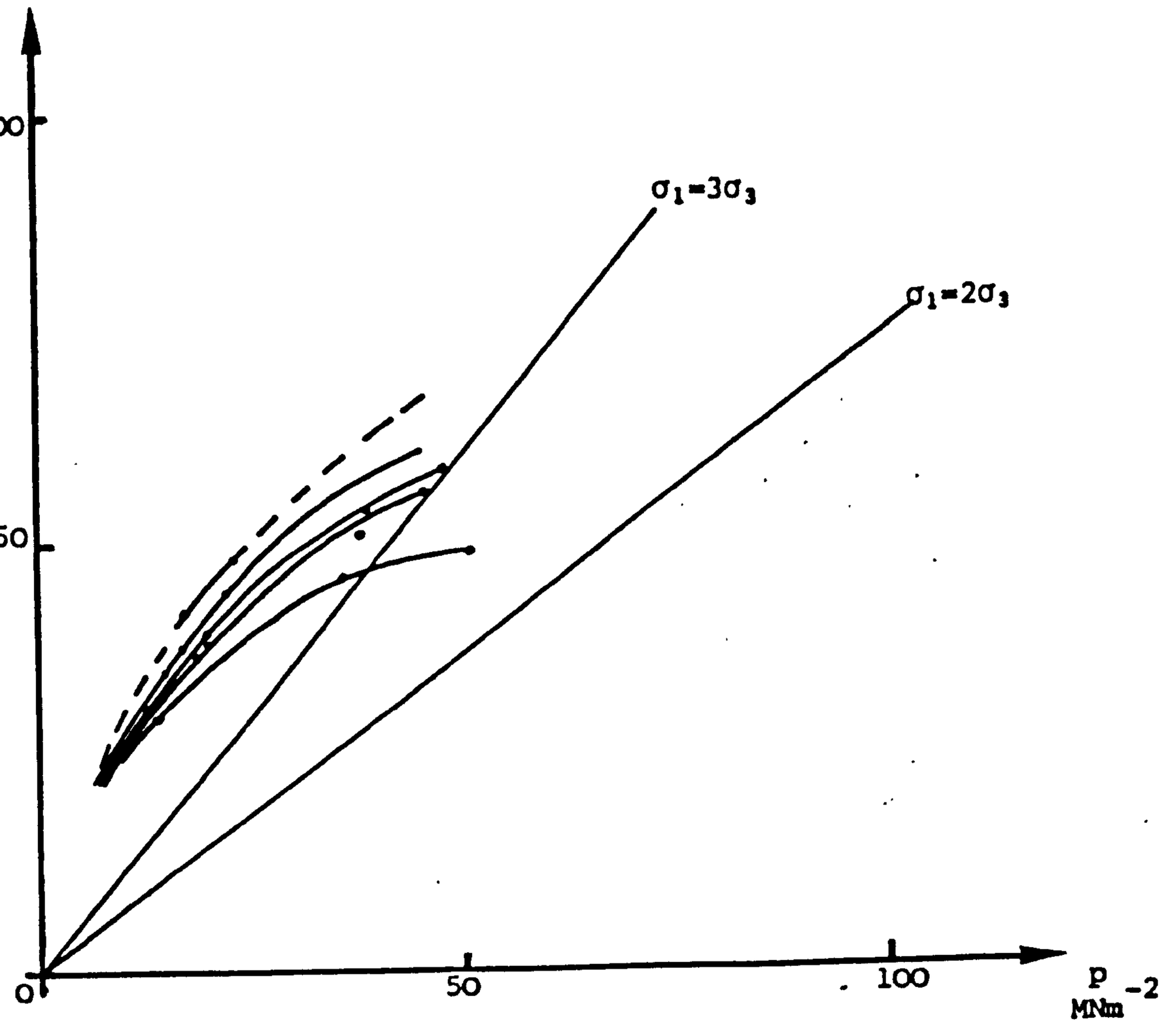

Fig.9.7 Constant Volumetric Yield paths for Rocksalt

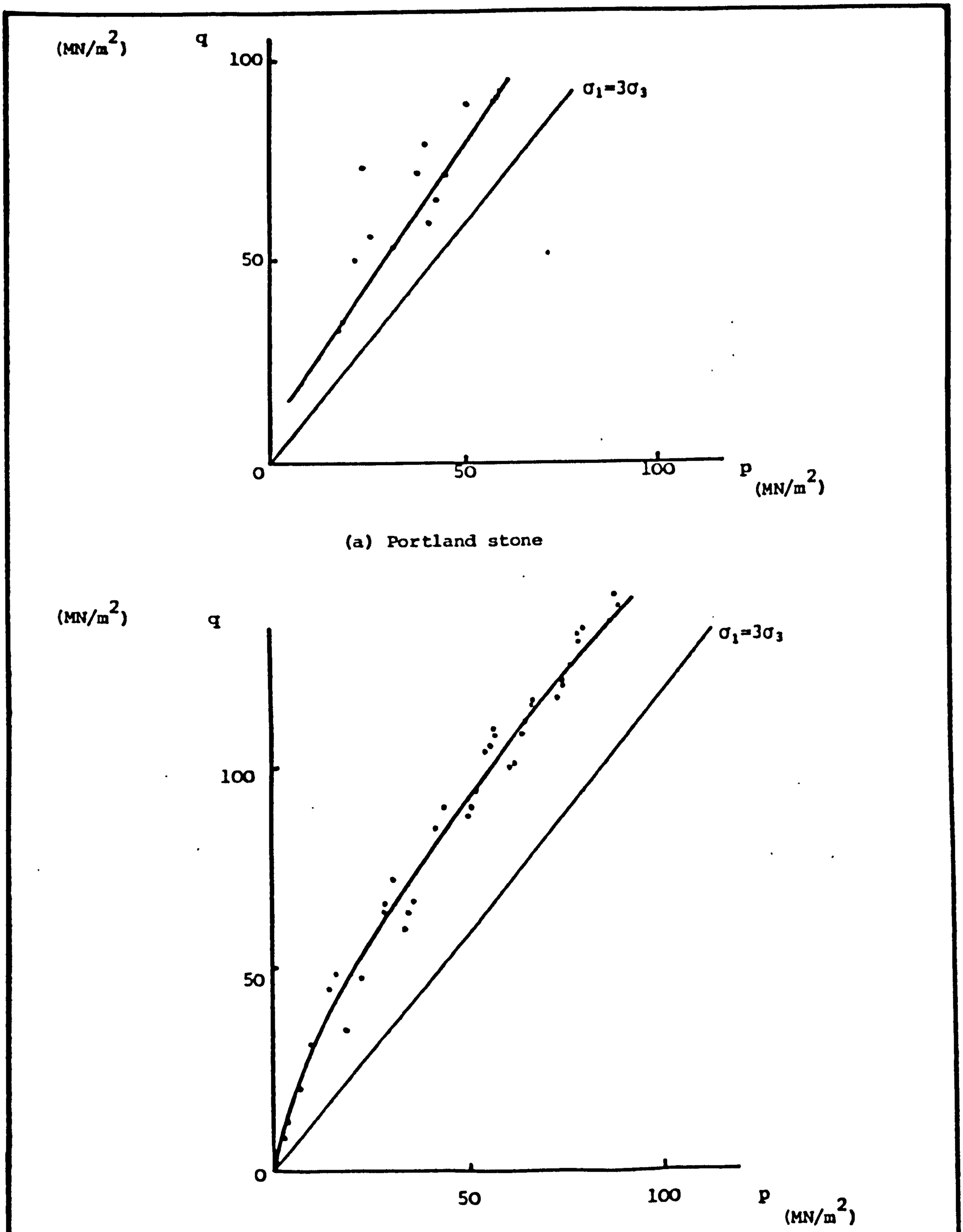

(a) Portland stone

(b) Saccharoidal
Limestone

Fig.9.8 Constant volumetric yield paths for Portland stone and saccharoidal limestone

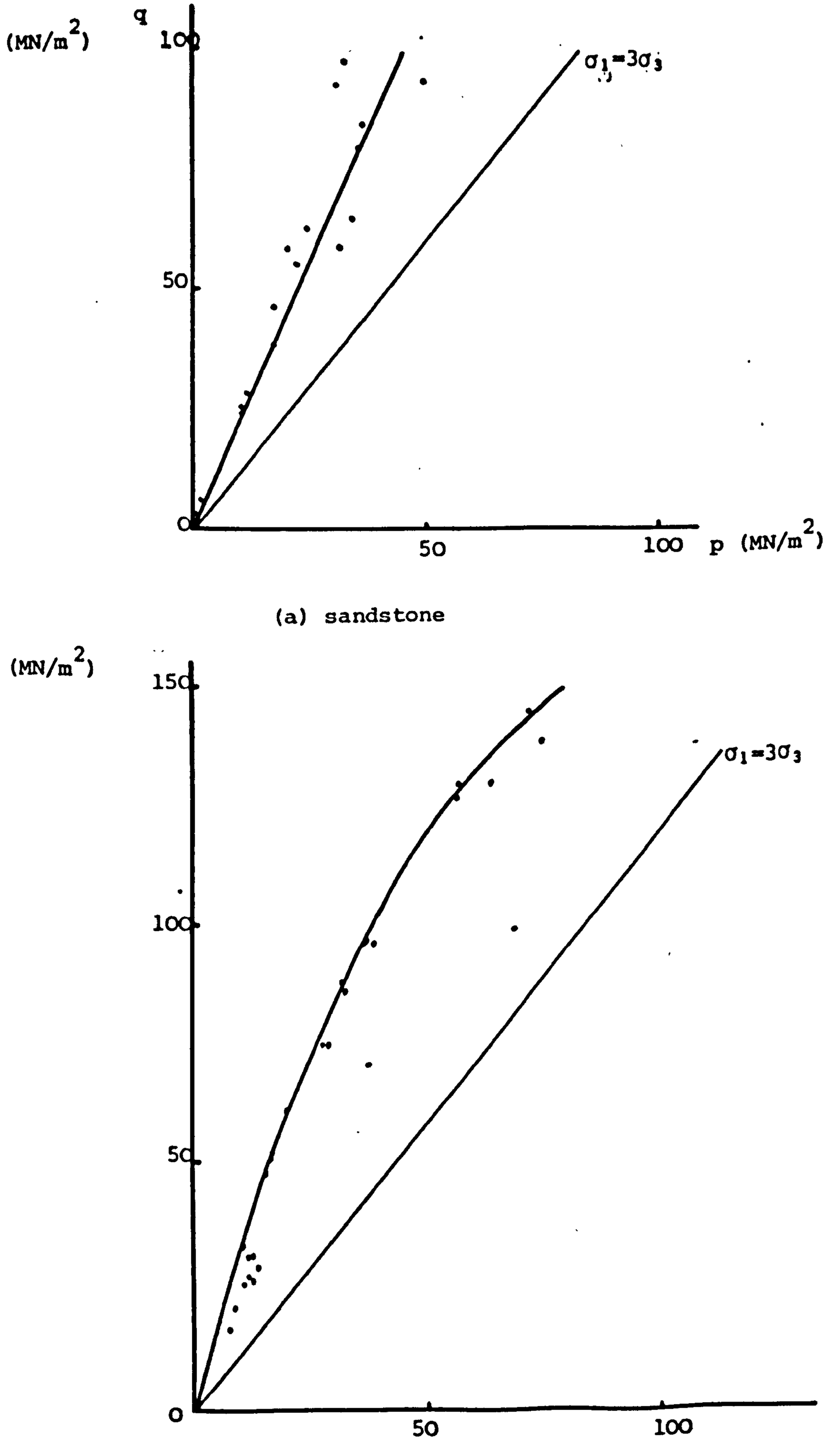

(a) sandstone

(b) silty sandstone

Fig.9.9 Constant volumetric yield paths for sandstone and silty sandstone

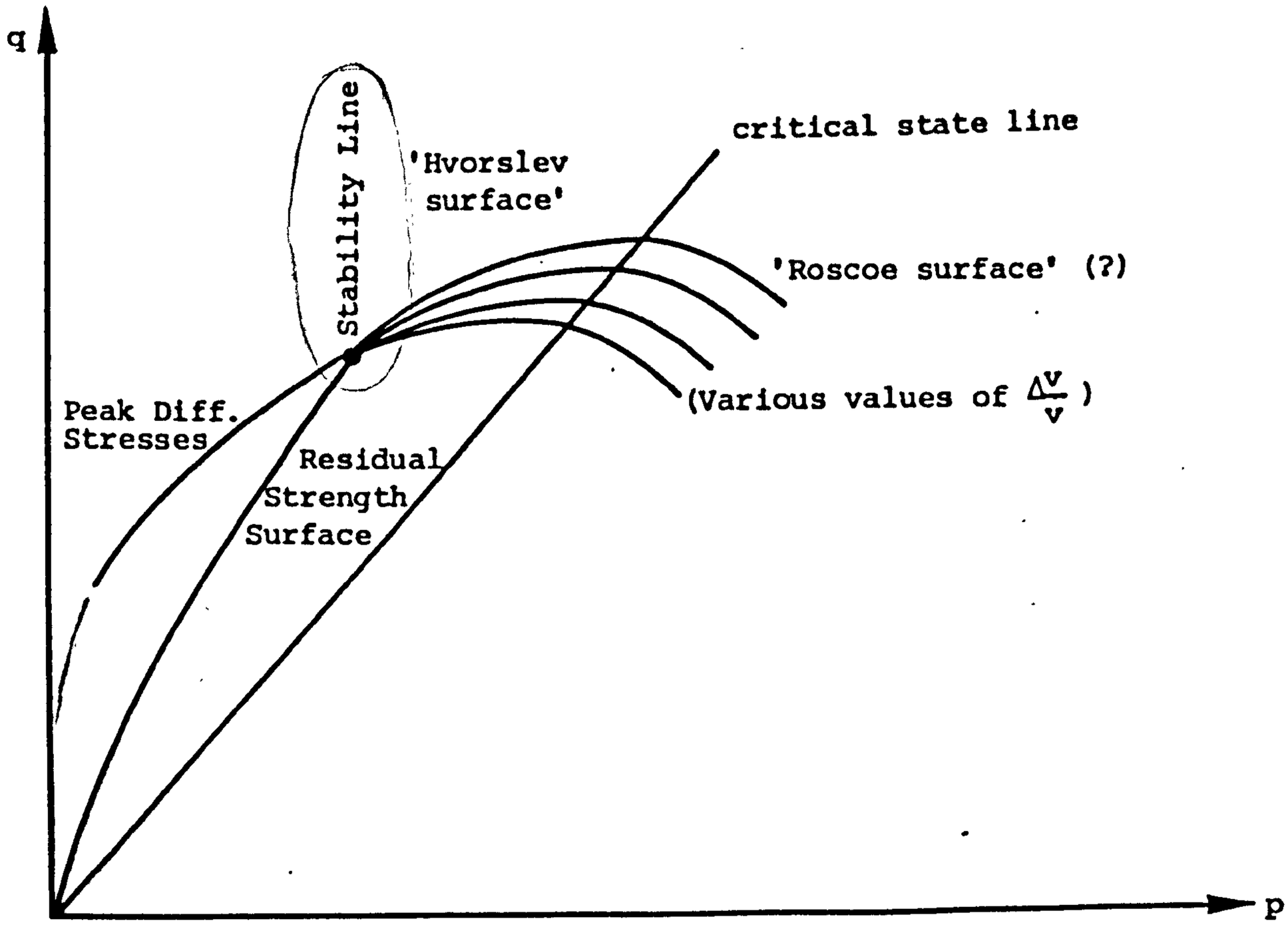

Fig.9.10 Proposed Critical State Model for Rocks

CHAPTER TEN

YIELD ZONE ANALYSIS AND ROADWAY CLOSURE

10.0 Introduction

When any excavation is made underground in virgin rock, the equilibrium of forces in that rock mass, achieved over many years, becomes disrupted and a new configuration of forces results, setting up new stress and strain patterns in the rock. If these exceed the capacity of the rock mass, failure will occur as it attempts to reach a new state of equilibrium, and 'yielded zones' will form in the vicinity of the excavation. These zones will take several forms, depending upon the nature of the excavation and its surroundings. There has been increasing recognition in recent years of the importance of defining and quantifying those factors which contribute to the formation of a new state of equilibrium or stability of the strata about an excavation. The 1972 National Coal Board Working Party Report, "Design of Mine Layouts", stated:

> "... a complex relationship has been established between the stability of mine openings and the effects of strata conditions, the shape of an excavation and its position relative to previous workings. Every encouragement should be given ... in devising a means of relating these factors in a simple way which will facilitiate their more widespread use."

Many different approaches have been used by various workers attempting to relate such factors. These approaches include in-situ observation and quantification, laboratory modelling and testing, and analytical and numerical modelling. This chapter examines the contribution that volumetric measurements, taken on a laboratory scale,

can make, in conjunction with yield zone analysis, to a deeper understanding and quantifying of excavation closure due to rock failure accompanied by dilation.

10.1 Yield Zone Formation

The reason for the formation of the yield zone is demonstrated by considering the peak and residual principal stress curves and stress paths presented in Fig. 10.1, for a hypothetical rock mass surrounding an excavation. Assuming the in-situ virgin rock stress to be hydrostatic and to have a magnitude q, the initial stress conditions can be represented in Fig. 10.1 by point A having the coordinates (q:q). Assuming elastic behaviour of the rock as the excavation is made, the stress path for the surrounding rock will have the equation (Hobbs, 1966; Muir Wood, 1979):

$$\sigma_1 + \sigma_3 = 2P \qquad \ldots\ldots (10.1)$$

and will follow the path A→B marked on Fig.10.1.

If and when this stress path intersects with the peak strength curve at B, the rock will fail and a yield zone will form having zero confinement at the excavation boundary, Point O. The confining stress will increase into the rock mass until it reaches a magnitude C, the confining stress needed to suppress the further failure of the rock mass, and which, therefore, marks the yield zone boundary. Thus, O–C corresponds to the width of the yield zone which is dependent upon the stress gradient across the yield zone. From Fig. 10.1a, the yield zone can be seen to be independent of the residual curve, but dependent upon the slope of the peak curve, and the uniaxial compressive strength, σ_c. If the excavation is supported by supports offering a pressure, P,

to the rock mass, Fig.10.1a would look like Fig. 10.1b, and the yield zone would be reduced in proportion to the pressure. The dependence of the yield zone width on these factors has been expressed mathematically in various yield zone theories.

10.2 Yield Zone Theories

This type of analysis has been widely reported[1], covering many different failure criteria, providing varied quantitative results for the volume of rock which will fail around, and the total volumetric closure of, an excavation. Yield zone analysis normally assumes an excavation of circular cross-section, in a homogeneous, isotropic rock mass and hydrostatic virgin rock stress field. The analyses assume that the rock surrounding an excavation is of two types: unfailed, elastic and failed, plastic. The latter forms a barrier of constant thickness between the roadway and the elastic zone, and is termed the yield zone.

For the present study, five of the analyses have been selected and the yield zone widths predicted by each compared. These were:

(a) Terzaghi's Analysis Ref ?

This analysis assumes the rock to be an elastic-plastic Coulomb material, with the ultimate strength of the rock mass controlled by the Coulomb criterion. If the material is loaded beyond this criterion it maintains its ultimate strength values, so that the failure criteria of the solid and failed rock are identical. The

---

[1] Muir Wood (1979); Hobbs (1966); Jaeger (1961); Ladanyi (1974); Youdan (1978); Abel, Dowis, Richards (1979); Szechy (1973); Terzaghi (taken from Coates, 1970); Wilson (1977a, b, 1976a, b, 1979a, b). See also Ward (1978) for an extensive review.

equations for the stresses within the yield zone and for the radius of the yield zone are developed from the equilibrium equation:

$$\frac{d\sigma_r}{dr} + \frac{\sigma_r - \sigma_\theta}{r} = 0 \qquad \ldots\ldots (10.2)$$

assuming that there are no shear stresses (see Jaeger, 1969). These criteria and equations are written thus:

Failure Criteria:

Yield zone: $$\sigma_1 = \sigma_c + k\sigma_3 \qquad \ldots\ldots (10.3)$$

Solid rock: $$\sigma_1 = \sigma_c + k\sigma_3 \qquad \ldots\ldots (10.4)$$

Stresses in the Yield zone:

tangential: $$\sigma_\theta = \left(\frac{r}{a}\right)^{k-1}\left(\frac{P(1-k) - \sigma_c}{1-k}\right) + \frac{\sigma_c}{1-k} \qquad \ldots\ldots (10.5)$$

radial $$\sigma_r = \left(\frac{r}{a}\right)^{k-1}\left(\frac{P(1-k) - \sigma_c}{1-k}\right) + \frac{\sigma_c}{1-k} \qquad \ldots\ldots (10.6)$$

Radius of the yield zone:

$$R = a\left[\frac{2(q(k-1) + \sigma_c}{(P(k-1) + \sigma_c)(1+k)}\right]^{\frac{1}{k-1}} \qquad \ldots\ldots (10.7)$$

where: a = the radius of the tunnel

q = the virgin rock stress

k = the triaxial stress factor

σ_c = the uniaxial compressive strength

P = the internal support pressure

r = the distance from the tunnel centre.

(b) Wilson's Analysis No.1

In his early analysis Wilson assumed the yielded rock to be like a granular material and to have no cohesion. He also assumed different values of k for the different failure criteria, but in practice

these are taken as approximately the same, giving the following equations:

Failure criteria:

Yield zone: $\sigma_1 = k'\sigma_3$ ..... (10.8)

Solid rock: $\sigma_1 = k'\sigma_3 + \sigma_c$ ..... (10.9)

where $k' \simeq k$

Stresses in the (Y)ield zone: why capital Y?

tangential: $\sigma_\theta = kP\left(\frac{r}{a}\right)^{k-1}$ ..... (10.10)

radial: $\sigma_r = P\left(\frac{r}{a}\right)^{k-1}$ ..... (10.11)

Radius of the (Y)ield zone:

$$R = a\left[\left(\frac{2q-\sigma_c}{P(k+1)}\right)^{\frac{1}{k-1}}\right] \quad \text{..... (10.12)}$$

(c) Wilson's Analysis No.2 Ref?

In his recent analysis Wilson adjusts his failure criteria for the yield zone to include a value for cohesion, corresponding to the stress required to cause movement in the broken material with no confinement. This gives equations of a form similar to Terzaghi's:

Failure Criteria:

Yield zone: $\sigma_1 = \sigma_c' + k\sigma_3$ ..... (10.13)

Solid rock: $\sigma_1 = \sigma_c + k\sigma_3$ ..... (10.14)

Stresses in the Yield zone:

tangential: $\sigma_\theta = \left(\frac{r}{a}\right)^{k-1}\left(\frac{P(k-1)+\sigma_c'}{k-1}\right) - \frac{\sigma_c'}{k-1}$ ..... (10.15)

radial: $\sigma_r = \left(\frac{r}{a}\right)^{k-1}\left(\frac{P(k-1)+\sigma_c'}{k-1}\right) - \frac{\sigma_c'}{k-1}$ ..... (10.16)

Radius of the Yield zone:

$$R = a\left[\frac{2q - \sigma_c + p'(k+1)}{(p+p')(k+1)}\right]^{\frac{1}{k-1}} \qquad \ldots\ldots (10.17)$$

where $$p' = \frac{\sigma_c'}{k-1} \qquad \ldots\ldots (10.18)$$

(taken as 0.1 MN/m^{-2})

(d) Hobbs' Analysis

Hobbs carried out a series of triaxial experiments on samples of broken rock, in which the samples were considered to fail when sliding occurred along any of the existing fracture planes. Hobbs found that his specimens obeyed a failure criteria somewhere between that for an ideal Coulomb granular and an ideal Coulomb solid material. Hobbs analysis using this new failure criteria yields the following equations:

Failure criteria:

Yield zone: $$\sigma_1 = B\sigma_3^{\,b} + \sigma_3 \qquad \ldots\ldots (10.19)$$

Solid rock: $$\sigma_1 = k\sigma_3 + \sigma_c \qquad \ldots\ldots (10.20)$$

Stresses in the Yield zone:

tangential:

$$\sigma_\theta = B^{\frac{1}{1-b}}\left\{(1-b)\left[\ln\frac{r}{a} + \frac{p^{(1-b)}}{(1-b)B}\right]\right\}^{\frac{b}{1-b}}\left\{(1-b)B\left[\ln\frac{r}{a} + \frac{p^{(1-b)}}{(1-b)B}\right]\right\}^{\frac{1}{1-b}} \qquad \ldots\ldots (10.21)$$

radial:

$$\sigma_r = \left\{(1-b)B\left[\ln\frac{r}{a} + \frac{p^{(1-b)}}{(1-b)B}\right]\right\}^{\frac{1}{1-b}} \qquad \ldots\ldots (10.22)$$

Radius of the Yield zone: $$R = ae^c \qquad \ldots\ldots (10.23)$$

where $$c = \frac{\left[\frac{2q - \sigma_c}{1+k}\right]^{(1-b)} - p^{(1-b)}}{B(1-b)} \qquad \ldots\ldots (10.24)$$

where B and b are constants determined by the rock type.

(e) Ladanyi's Analysis

In this analysis the yielded rock is assumed to fail according to the Coulomb criterion and Ladanyi considered both the Coulomb failure envelope and the Fairhurst parabolic failure envelope for the solid rock. Only the latter is considered here, since the former is similar to the other analyses considered. The latter takes into account the uniaxial tensile strength of the intact rock, and yields the following equations:

Failure criteria:

Yield zone: $$\sigma_1 = \sigma_c + k\sigma_3 \qquad \ldots\ldots (10.25)$$

Solid rock: $$\sigma_1 = \sigma_3 + \frac{\sigma_c}{m+1}\left[2\left(1+\frac{n\sigma_3}{\sigma_c}\right)^{\frac{1}{2}} + m - 1\right] \qquad \ldots\ldots (10.26)$$

where, $$n = \frac{\sigma_c}{-\sigma_t} \qquad \ldots\ldots (10.27)$$

and, $$m = (n+1)^{\frac{1}{2}} \qquad \ldots\ldots (10.28)$$

where σ_t = the uniaxial tensile strength.

Stresses in the Yield zone - as Terzaghi's.

Radius of the Yield zone

$$R = a\left[\frac{(q + H - M\sigma_c)}{P + H}\right]^{\frac{1}{k-1}} \qquad \ldots\ldots (10.29)$$

where, $$H = \frac{\sigma_\theta - k\sigma_r}{k-1} = \frac{\sigma_c}{k-1} \qquad \ldots\ldots (10.30)$$

and $$M = \frac{\left[1 + \frac{nq}{\sigma_c} - \frac{1}{4}(m-1)^2\right]^{\frac{1}{2}}}{m+1} \qquad \ldots\ldots (10.31)$$

10.3 Comparison of Calculated Yield Zone Widths

Each of the above analyses is used to calculate the expected yield zone widths for a variety of conditions. The calculations assume

a four metre diameter roadway excavated in two material types with different internal support pressures and at different depths. The parameters used were:

<u>Rock Type A:</u> Uniaxial Compressive Strength, $\sigma_c = 30\ MN/m^{-2}$

Triaxial stress factor, $k = 4$

Uniaxial Tensile strength, $\sigma_t = 10\ MN/m^{-2}$

Constants,[1] $B = 4.82.\ b = 0.709$

Internal Support Pressures, $0.01, 0.2\ MN/m^{-2}$

<u>Rock Type B:</u> Uniaxial Compressive strength, $\sigma_c = 10\ MN/m^{-2}$

Triaxial stress factor, $k = 2.5$

Uniaxial Tensile strength, $\sigma_t = 1\ MN/m^{-2}$

Constants[2], $B = 4.82.\ b = 0.709$

Internal Support Pressures $0.01, 0.2\ MN/m^{-2}$.

The calculated yield zone widths have been plotted in Figs.10.2 to 10.5. These figures clearly demonstrate that the failure criterion chosen for the material in the yield zone is fundamental to its resultant size. It is interesting to note the similarities between the Terzaghi and Ladanyi analyses, and also the much larger yield zones predicted by Wilson's analyses, especially his earlier one. As expected, the constants used in Hobbs' analysis for the rock type B seem to give unrepresentative results, but for the rock type A, his analysis compares well with the others, giving a median value, which seems more reasonable than the <u>conservative values</u> of Terzaghi and Ladanyi, or the exaggerated values of Wilson's early approach. These figures also clearly demonstrate

---

[1] Calculated from Hobbs' (1966) original data by Youdan (1976) for stresses in MN/m^{-2}.

[2] No data was available for this rock type so the same constants were used as for type A, but these will probably be unrepresentative.

the effect of confinement, in the form of internal support pressures, on the extent of the yield zone, and of the effect of the rock strength on the formation of the yield zone. From equations 10.7, 10.12, 10.17, 10.23 and 10.29, the critical rock strengths for the formation of the yield zone under particular conditions can be obtained. These are:

For Terzaghi's, Hobbs' and Wilson's analyses:

$$\sigma_{crit} = 2q - (1 + k) \quad P \qquad \ldots\ldots (10.32)$$

and for Ladanyi's $\sigma_{crit} = (q - p)\gamma_M$ $\ldots\ldots (10.33)$.

Therefore, in the case of excavations in rock masses composed of the rock types tested, with a hydrostatic virgin stress field of 25 MN/m^{-2}, equivalent to 1000 m depth (Wilson, 1977 ; Brown and Hoek, 1978; Jaeger and Cook, 1971), and internal support pressures of the magnitude used above, the Portland stone, silty sandstone and sandstone would remain intact and stable, whilst the others would yield. However, Wilson (1976b) advocates taking a ratio for the uniaxial strength of rock in-situ to its uniaxial strength in the laboratory of 1:5, in which case, all of the rock types tested would yield under the assumed conditions.

The calculated yield zones for these rock types, using Wilson's No.2 analysis, under these conditions, are given in Table 10.1. This analysis was used in preference to Hobbs' as the median one, because the constants B and b in equation 10.24 are not available for the rock types used.

10.4 Roadway Closure

Two of the above analyses have been extended to predict roadway closure due to the volumetric increase of the yield zone through failure.

(a) Ladanyi's Analysis

Ladanyi's approach takes account of the dilation of the yield zone due to the fracturing of the rock and the opening of discontinuities by means of an average plastic dilation using the associated flow rule of the theory of plasticity applied to a limited portion of the post-failure strains. He developed the following equations for the average plastic dilation, e_{av}:

for $1 < \frac{R}{a} < \sqrt{3}$:

$$e_{av} \simeq \frac{2(u_e/r_e)(r_e/r_i)^2}{[(r_e/r_i)^2-1][1+\frac{1}{2}D\ln(r_e/r_i)]} \quad \ldots\ldots (10.34)$$

and for $\frac{R}{a} > \sqrt{3}$: $e_{av} \simeq \frac{2(u_e/r_e)(r_e/r_i)^2}{[(r_e/r_i)^2-1][1+1/1.1\,D]}$ $\ldots\ldots (10.35)$

where $(u_e/r_e) = \frac{\sigma_c M(1+\nu)}{E}$ $\ldots\ldots (10.36)$

$$(r_e/r_i) = \left[\frac{(q+H-M\sigma_3)}{P+H}\right]^{\frac{1}{K-1}} \quad \ldots\ldots (10.37)$$

and $$D = \frac{(m-1)}{2(1+\frac{n\sigma_3}{\sigma_c})^{\frac{1}{2}}+m-1} \quad \ldots\ldots (10.38)$$

where ν = Poisson's ratio

and E = Young's modulus.

This value of the average plastic dilation is then substituted into equation 10.39 to obtain a value for the roadway closure, U_t :

$$U_i = a\left(1-\left((1-e_{av})/(1+A)\right)^{1/2}\right) \qquad \ldots\ldots (10.39)$$

where

$$A = \left(2M\alpha\varepsilon\left(\frac{1+\nu}{E}\right)-e_{av}\right)\left[\frac{q+H-M\alpha\varepsilon}{P+H}\right]^{\frac{2}{k-1}} \qquad \ldots\ldots (10.40)$$

(b) Wilson's Analysis

Wilson's second analysis is developed to take into account the bulking of elements within the yield zone, producing voids and thus closure. The final form of his equation for the closure, U_i, is:

$$U_i = 2a\left(\frac{1+\nu}{E}\right)\left[\frac{(k-1)q+\sigma/f}{(k+1)}\right]\left[\frac{2q-\sigma/f}{(P+P')(k+1)}\right]^{\frac{2+\varepsilon}{k-1}} \qquad \ldots\ldots (10.41)$$

where f is his factor relating laboratory strength to in-situ strength and takes into account the degree of jointing or fracturing and is taken as 5:1. From equation 10.41 the limiting value of f, allowing roadway closure, is given by:

$$\frac{\sigma_c}{(1-k)q} \geqslant f \geqslant \frac{\sigma_c}{2q} \qquad \ldots\ldots (10.42)$$

since the first term will always be negative, the actual limiting value of f is given by:

$$f \geqslant \frac{\sigma_c}{2q} \qquad \ldots\ldots (10.43)$$

which is equivalent to equation 10.32. ε is an expansion factor which he gives a nominal value of 0.2, and is defined by the equation:

$$\varepsilon = \frac{100(B-1)}{s} \qquad \ldots\ldots (10.44)$$

where s is strain in percent and B is the bulking factor.

Another indication of the expected roadway closure can be obtained from considering the measured volumetric expansion of the laboratory specimens. Consider the 4 metre diameter tunnel used in the analyses so far. The average tensile strain, ϵ_{av}, across a yield zone of width, W, due to a radial closure, u_i, of the tunnel, is given by:

$$\epsilon_{av} = \frac{100\, u_i}{W} \qquad \ldots\ldots (10.45)$$

so that closures of say 0.5m and 0.3m from a yield zone of width 4m would give average strains of 12.5% and 7.5% respectively. The strain of an element within the yield zone will vary from a maximum at the tunnel boundary to a minimum at the yield zone periphery, in relation to the square of the radius. Since the strain at the yield zone periphery will be in the region of 1.5%, the strains at the tunnel boundary for the above closures will be approximately 36% and 16% respectively. Tending towards the latter case, which gives a percentage volume closure of the tunnel consistent with measurements made by Clook (1973), the average strain within the yield zone is taken to be 10%, which corresponds approximately to a compressive strain also of 10% (see earlier lateral versus axial strain figures). Then, if the average confining stress within the yield zone is taken as one quarter of the virgin stress (see the plots of stress in the yield zone reported by Hobbs, 1966), a value for the bulking factor, B, for the rocks tested can be obtained from Figs.8.6a, 8.11, 8.17a,8.22a, 8.31a, 8.38a and 8.46. Knowing the bulking factor, and having calculated the yield zone radius, R,using one of the earlier equations, the roadway closure, u_i, can be calculated using the equation:

$$u_i = a - ((1-B)R^2 + Ba^2)^{1/2} \qquad \ldots\ldots (10.46)$$

10.5 Comparison of Calculated Roadway Closures

All three analyses were used to calculate the roadway closure for each rock type tested, under the conditions described for them in section 10.3, and the results presented in Table 10.1. In each case values of 1:1 and 5:1 for the ratio of laboratory to in-situ uniaxial compressive strength were used. In Ladanyi's analysis the values of Young's modulus and the uniaxial compressive strength were taken as 0.5 and 0.7 of those measured respectively, in order to obtain a value for the long term closure. As might be expected from the conservative magnitudes of the yield zone widths calculated with Ladanyi's analysis, the magnitudes of roadway closure are also much smaller than the values obtained from the other analyses.

The other two analyses were based on Wilson's analysis of the expected yield zone widths, also presented in Table 10.1. It is immediately apparent from the table that such analyses are inadequate when dealing with the rock types such as the rock salt and carnallite marl, giving impossible yield zone widths. Therefore, such analyses can not be used to describe the behaviour of ductile rocks which, under the conditions set here, will fracture at the excavation periphery, but will tend to flow rather than fracture given a small amount of confinement. This is clearly demonstrated by the experimental results reported earlier. It is also true that these analyses take no account of time effects, offering absolute values of closure only.

Where possible, the values substituted into the equations for calculating the roadway closure were taken from the measured data, hence the large post-failure values of Poisson's ratio used. For each

rock type the closure calculated using the analysis presented in the form of equation 10.46 is larger than that using Wilson's analysis (equation 10.41), although the same yield zone widths were used.

The closures calculated for the coal measures, using equation 10.46 especially, compare well with those measured in-situ, jointly by the author and J. Armstrong, and reported elsewhere by the latter (Armstrong, 1978). They also compare well with measurements in Coal Measures rocks by other workers (Clook, 1973; Stace, 1973; Hodkin, 1978). In the case of the Coal Measures, the laboratory U.C.S., in-situ U.C.S. ratio has a small effect upon the magnitudes of the calculated closures. The use of this factor will be discussed further in the next chapter.

* * *

Rock Type	Bulking Factor B	Expansion Factor,	Young's Modulus $GN\ m^{-2}$	Poisson's Ratio	U.C.S. MN/m^{-2}	k	Yield Zone Width from Eqn. 10.17		Hio Roadway Closure from Eqn. 10.46 (m)		Ladanyi Roadway Closure from Eqn. 10.39 E=0.5 =0.75 (m)		Wilson Roadway Closure from Eqn. 10.41 (m)	
							$\sigma_{lab}/\sigma_{insitu}$ = 1	5	1	5	1	5	1	5
Portland Stone	1.035	0.35	13	0.64	73	6	Nil	2.32	Nil	0.133	Nil	0.008	Nil	0.061
Silty Sandstone	1.038	0.38	13	0.66	61	4.3	Nil	5.11	Nil	0.222	Nil	0.011	Nil	0.185
Sandstone	1.049	0.49	13	0.72	97	6.2	Nil	2.06	Nil	0.159	Nil	0.009	Nil	0.063
Saccharoidal Limestone	1.060	0.60	13	0.94	49	3.5	1.07	9.66	0.083	*comp	0.011	0.016	0.031	0.929
Rock Salt	1.020	0.20	22	0.58	26	1.3	$8x10^6$	$63x10^6$	*comp	*comp	0.008	0.518	*comp	*comp
Carnallite Marl	1.005	0.05	8	0.54	10	2.2	101.90	199	*comp	*comp	0.050	0.243	*comp	*comp
Mudstone	1.038	0.38	10	0.84	9	4.8	4	4.26	0.331	0.368	0.018	0.016	0.179	0.184

Note: *comp = complete

Table 10.1 Comparison of Calculated Roadway Closures

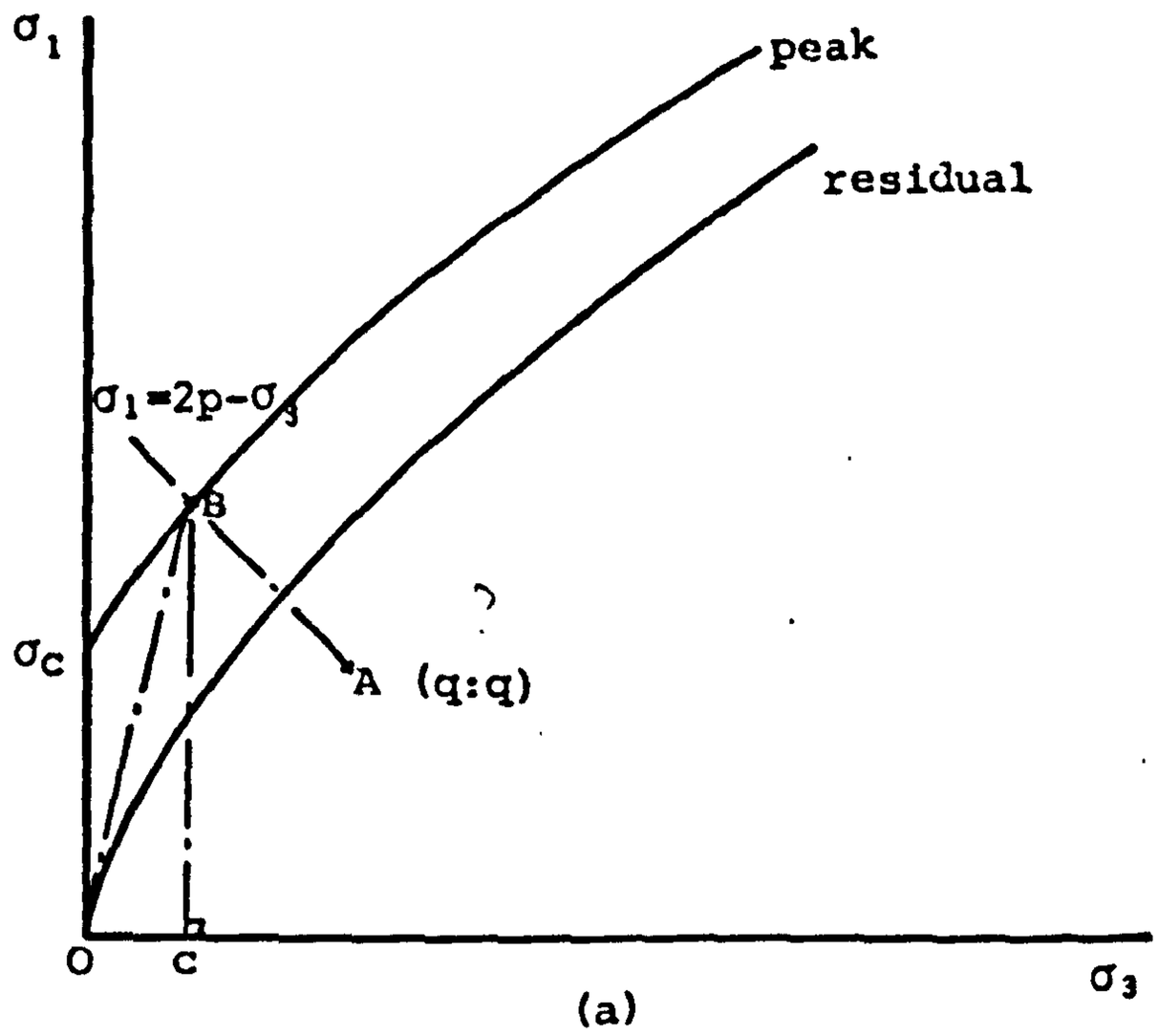

(a)

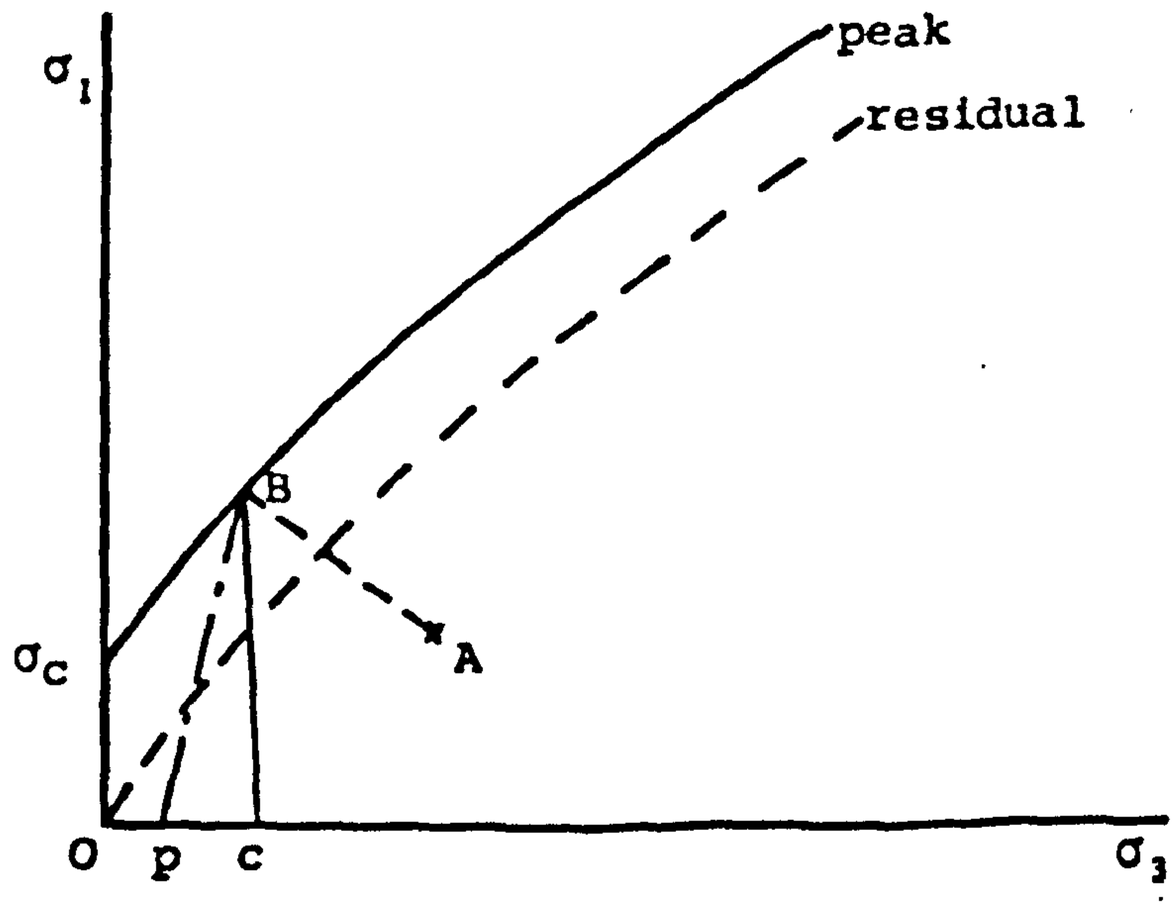

(b)

Fig.10.1 Stress Paths for a Hypothetical Rock Mass Surrounding An Excavation

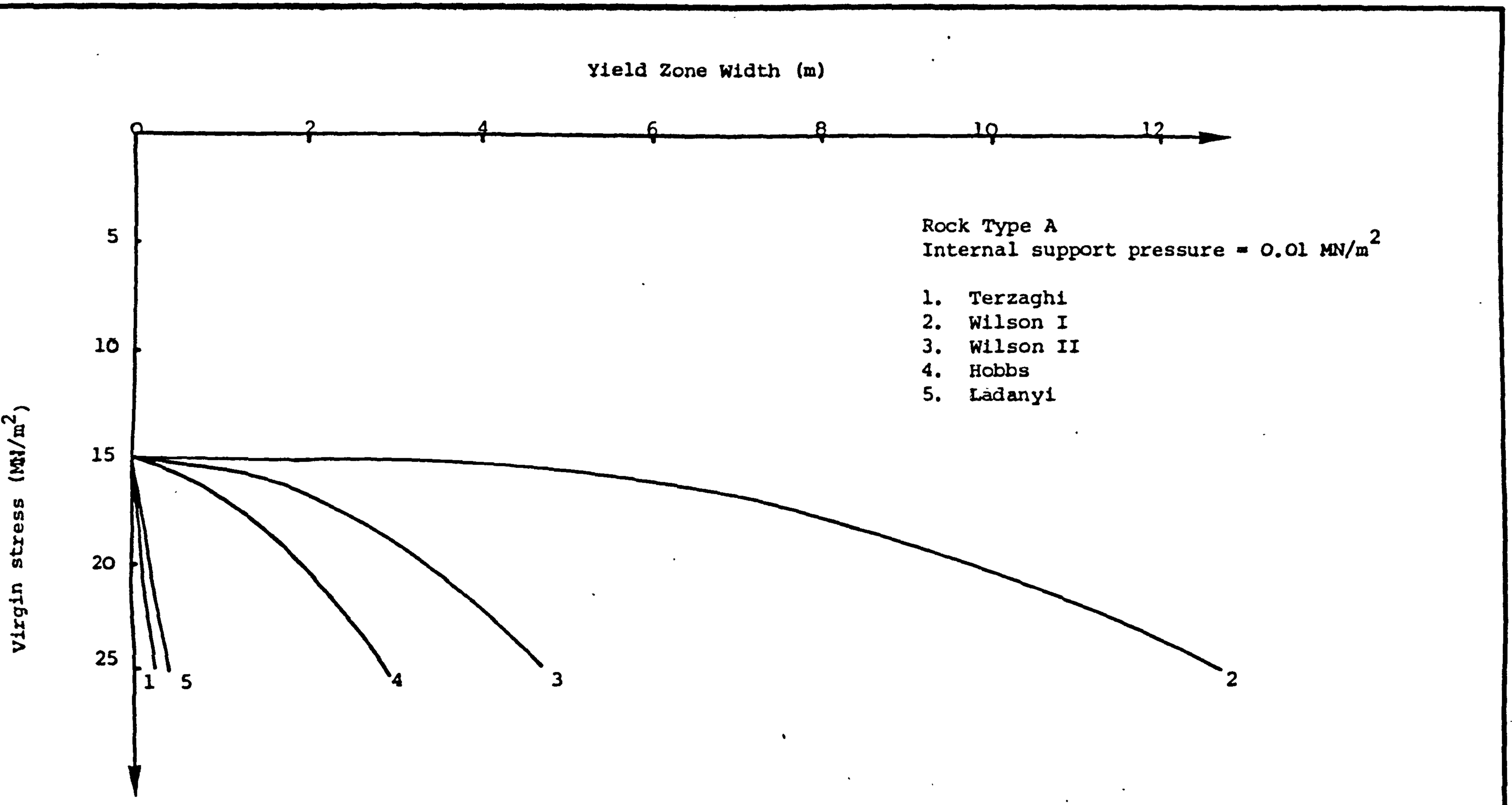

Fig.10.2 Comparison of yield zone widths for Rock Type A

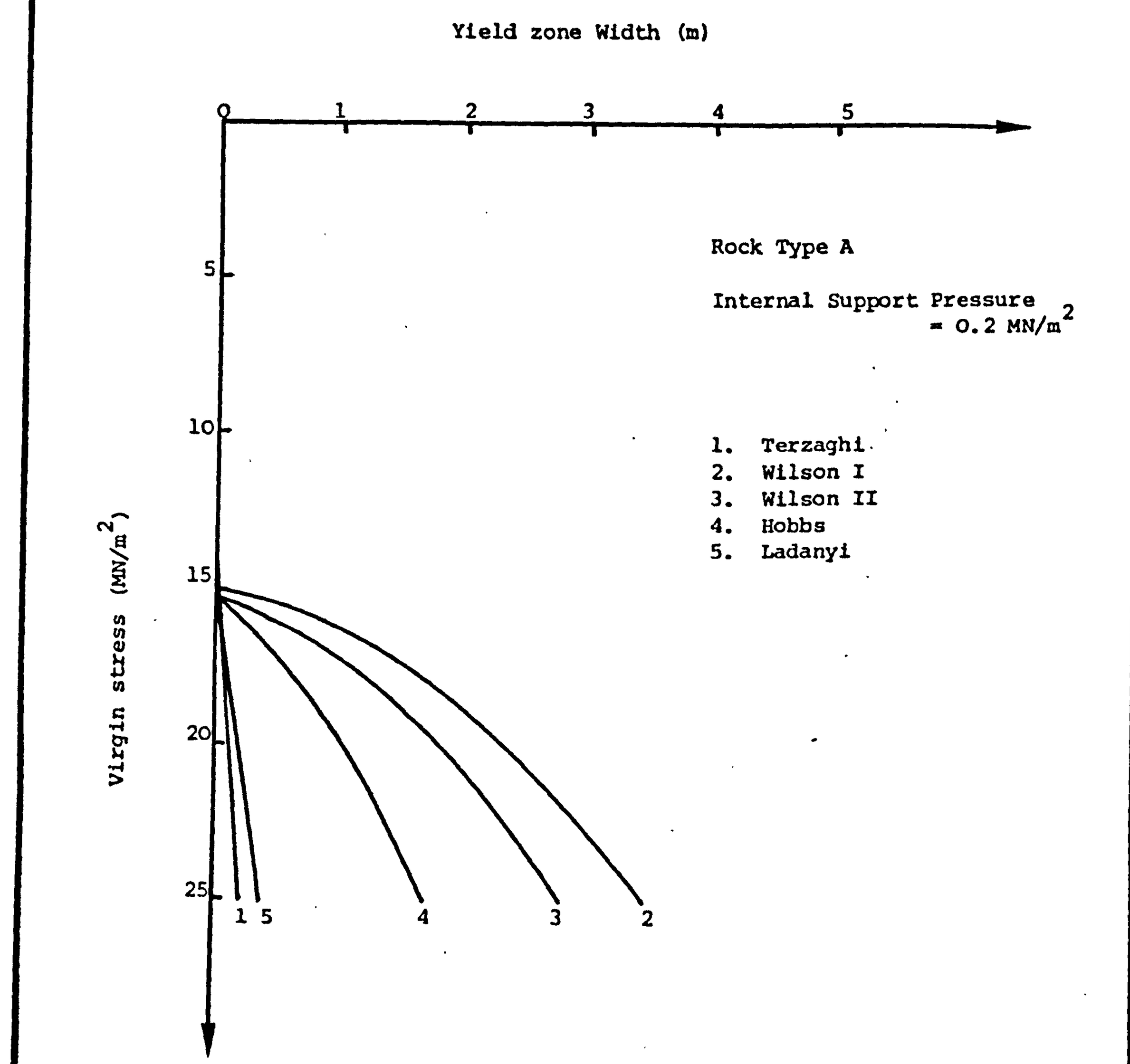

Fig.10.3 Comparison of calculated yield zone widths for Rock Type A

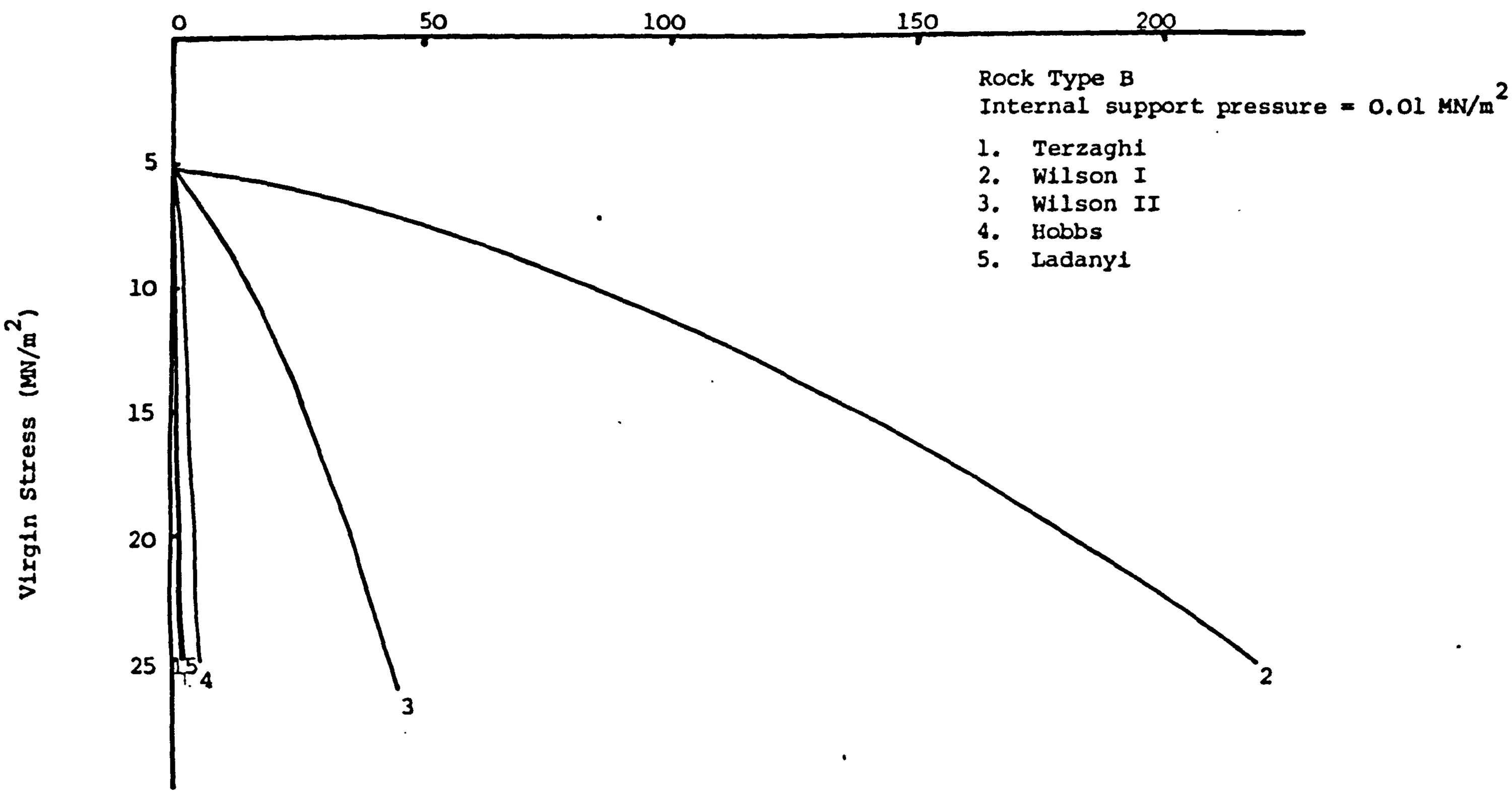

Fig.10.4 Comparison of yield zone widths for Rock Type B

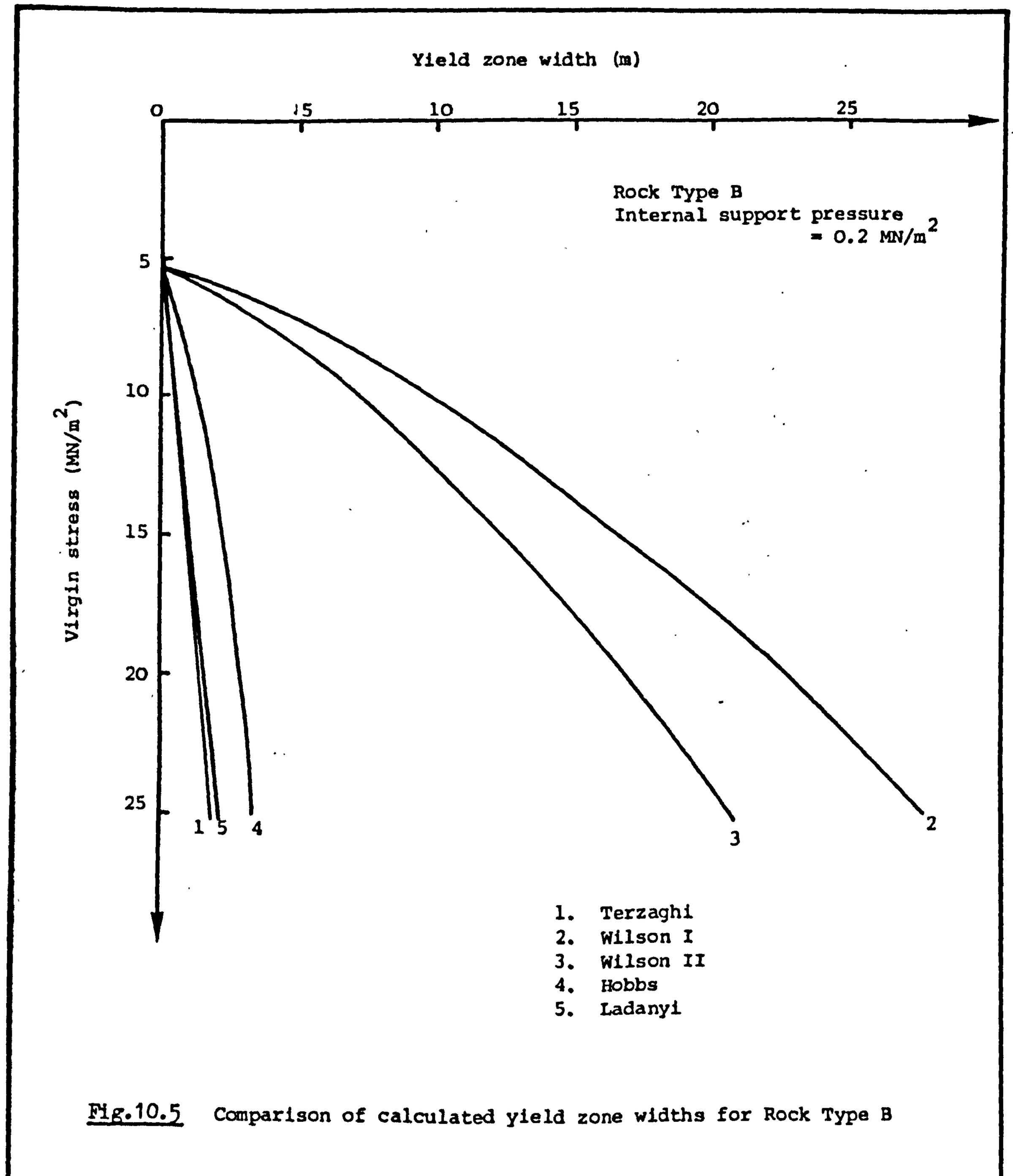

Fig.10.5 Comparison of calculated yield zone widths for Rock Type B

CHAPTER ELEVEN

YIELD IN STRATIFIED DEPOSITS

11.0 Introduction

The previous chapter discussed the development of stresses and yield zones in the rock mass surrounding an excavation. The rock mass was considered to be homogeneous and isotropic, and the excavation circular in cross-section. However, the majority of mine roadways in this country are located in the Coal Measures rocks, with widely varying uniaxial compressive strengths and deformational behaviour, and often large variations over small areas. Further, the analyses took no account of structural discontinuities in the rock mass, except in Wilson's analysis, where he used a factor to relate laboratory U.C.S. to in-situ U.C.S., usually taken as 5:1. He justifies this factor by taking into account the selective process by which test specimens are obtained. However, the use of such a factor is open to some question, concerning the nature of the analysis and its application. Since the analyses are concerned with the failure of the rock mass and consequent expansion, the rock mass being analysed should be competent and intact with few discontinuities. If, however, discontinuities play a major role in the mechanism of deformation, the laboratory testing should take this into account. It is, however, interesting that Whittaker and Singh (1979) have indicated the abutment pressure to be approximately five times the cover load, which may well have a similar effect in the yield zone analysis to that of Wilson's factor. The limitations of such analyses require that they be used as no more than a first approximation in strata stability problems. In their recent paper, Whittaker and

Singh (op. cit.) summarised their research into factors affecting the stability of ribside roadways. These included: the strength of the surrounding rock types; faulting and washouts; cleats; quantity of water present; dimensions and shape of roadway; excavation method; support type, strength, density, setting and degree of lagging; profile finish; pack; extraction and reinforcement. Although ribside roadways are, perhaps, a more complicated case, this list of factors underlines the complexity of the problem of analysis. There is a need for a much more mechanistic approach to the problem of stability and closure, which takes into account the stratigraphy, rock type and strength, behaviour under confinement, yielding mechanism, and the response of the rock as a mass and as a material, including the problem of discontinuities.

11.1 Stratigraphy

Roadways in Coal Measures rocks are, by and large, excavated in or across stratified deposits, varying widely in their properties, especially in the immediate localities of coal seams. This stratification allows yielding to occur preferentially in the weaker strata, such as mudstones, causing localised instability and closure. Roadways in strata composed of competent rock types will sometimes show dilatancy due to the differential settlement of the different rock types causing bed separation, as was observed at Woodhorn Colliery (Armstrong, 1978), between the mudstones and overlying sandstone layers.

Some examples of the effects of stratigraphy on deformation have been taken from the literature (Malone and Gardner, 1963; Leigh, 1962; and the University of Newcastle upon Tyne, 1979) and reproduced in

Figs. 11.1 to 11.3, which illustrate the vertical strain contours above longwall faces, with the geological sections superimposed. Fig. 11.4 gives the theoretical vertical strain pattern based on stochastic and finite element analysis and assuming zero volume change, taken from the University of Newcastle upon Tyne Report (1979). By comparing these plots the dependency of the deformation upon the stratigraphy is readily apparent, especially in Fig. 11.3, where the greater strain concentrations (and, therefore, dilation) are measured in the strong sandstone layer with partings, implying that the lower sandstone beds have collapsed as a unit.

11.2 Rock Type and Strength

As mine workings increase in depth, the dilatancy of strata around excavations is bound to increase, as it becomes impossible to avoid stress levels sufficient to cause rock failure. Fortunately, coal measures strata usually fail gently, and even in their failed state are capable of sustaining quite high stress levels, if confined. This is clearly demonstrated by the results of the experiments described earlier, which also illustrated the different responses from each rock type under any given set of conditions. The most critical factor concerned with excavation stability is the strength of the surrounding rock - a fact reflected in equations 10.32 and 10.33 in Chapter Ten. This is illustrated by the fact that weak rock at shallow depth is capable of greater displacement into the excavation than is strong rock at great depth. Whilst weak rocks at great depth offer serious problems to strata stability, as reported by Hebblewhite (1977) for marl and shale at a depth of over 1000 metres, and by Vaughan-Thomas (1962) for weak, disturbed mudstones and siltstones at a depth of over

720 metres. The latter reported closures of up to 5'4" in a roadway of an original height of 18'0", which he attributed to large in-situ stresses complicated by major fault zones.

11.3 Behaviour under Confinement

The very marked effect of confining pressure upon the volumetric expansion of rock, its stability and the formation and extent of the yield zone has been discussed in earlier chapters. Increased confinement has the effect of restricting the extent of a yield zone and the resultant dilation. Confinement underground, usually applied in the form of some type of support, although sometimes confinement is afforded by supporting a weaker strata by a stronger, more competent one. An example of the latter was described by Hebblewhite (op. cit.) in dealing with the stability problem posed by the weak shales and marl, described earlier. He found that, in order to maintain overall roadway stability, there had to be at least 2 to 3 metres of a competent material, such as Potash, in the roof between the excavation and the weaker rocks.

When using supports the amount of confinement is governed by the support type and density, the amount of lagging, and the effectiveness of its installation. The effectiveness of different support types, offering different degrees of confinment on the closure of a tunnel in mudstone at a depth of 100 metres, has been reported by Ward, Coats and Tedd (1976) and their findings are reproduced in Fig. 11.5. Ward's (1978) illustration of the comparable supporting pressure against deformation, is given in Fig. 11.6. These two figures illustrate well

the differences in confinements applied to the rock mass and the resulting closures.

11.4 Yielding Mechanism

Two types of yielding mechanism were described earlier in this thesis - those of strain softening and strain hardening. All rock types experience a transition from strain softening to strain hardening with increasing confining pressure. However, this transition occurs at a confining pressure dependent upon the rock type, and will, therefore, be at a lower confining pressure for some rock types in the strata than for others. Consequently, under the same stress conditions the rock salt, for instance, would yield in a strain hardening manner, whereas the sandstone would deform in a strain softening manner. From the results of the experiments described earlier, it can be seen that all rocks will behave in a strain softening manner under zero confinement, corresponding to the periphery of an excavation. But, as the confinement increases into the rock mass, the transition to strain hardening behaviour will be reached. In the case of the brittle rocks, a transition to elastic behaviour - marking the yield zone boundary, will occur first.

An example of the transition to strain hardening is given in Plate 11.1 which shows the bottom corner of a potash pillar, Boulby Potash Mine (courtesy of N. Wise). The plate shows the pillar at an age of approximately 255 days, shortly after being trimmed with a roadheader, and, therefore, gives a view of the internal yielding of the pillar. In order to give an appreciation of the magnitude of yield, Fig. 11.7 gives the measured lateral deformation of a similar pillar in the same panel, up to an age of 80 days (Wise, 1978). There is a

transition in the pillar from strain softening behaviour, manifested as spalling, to strain hardening behaviour, characterised by large deformations of the rock without failure. A similar type of behaviour will occur in the weaker, plastic coal measures rocks, such as the seatearths, which tend to experience large deformations without failure.

Strain hardening rocks will tend to deform indefinitely whilst there is a high enough driving stress and low enough confining stress, whereas strain softening rocks will tend to deform until a new state of equilibrium, in the form of some sort of yield zone, is reached, preventing further dilation. Examples of the former case are given in Figs. 11.8 and 11.9 (Hebblewhite, 1977 and Hebblewhite, Miller and Potts, 1977), for roof closure and shaft radial closure respectively. The curves reveal an initial rapid rate of deformation which reduces to a near constant rate of increase, so that even after 500 and 1200 days the rock is continuing to deform. The latter case of strain softening behaviour is illustrated by Fig. 11.10, showing measurements in coal measures rock by Kirmani (1972), and by Fig. 11.11, giving some measurements taken at Woodhorn Colliery. These curves show an initial rapid rate of increase of deformation which tails off with time to zero, as the rock attains a new state of equilibrium. The Woodhorn curves are complicated by the differing behaviour of the strata involved. These measurements were taken in strata varying from sheared fireclay to sandstone (see the geological section given in Fig.11.11). The mechanism of deformation proposed in this example is one in which most of the deformation is restricted to the first three metres of the roof, whilst the strong sandstone-mudstone beam retains its competence. At the top of the borehole the weak shaly-mudstones fail and are squeezed, resulting in the negative bay strains (Fig. 11.11).

11.5 Discontinuities

If a rock mass contains a high density of discontinuities, its stability will be governed by their geometry and spacing, rather than by its intact properties. The importance of discontinuities on strata stability has been well described with the aid of block models by Ward (1978). He illustrated that collapses in tunnels with discontinuities are distinctly three-dimensional and governed by their locations and orientations (see also Shepherd and Fisher , 1978). The discontinuities isolate blocks in the roof and especially shoulders of the excavation, which will drop out unless suitably supported. Whittaker, Daws and Szwilski (1974) also draw attention to the instability between blocks and slabs as frictional restraint is lost due to relaxation of stresses above the excavations.

11.6 Use of the Critical State Model

In Chapter Nine a critical state model for rocks was proposed, based upon the results of the experiments described earlier and on Schofield and Wroth's original model for soils. It should be possible to use such a model to describe the conditions for stability, given the geological environment. A series of such models could be prepared for each rock type in the strata to describe the effects of the conditions described above on stability.

The model proposed in Chapter Nine has been modified and is presented in Fig. 11.12. The model describes the response of the material to increasing confinement and can be used to predict the expected yielding mechanism. For instance, if the rock mass follows

the stress path (1) to C, it will yield in a strain hardening manner, and will continue to deform until the stresses reach a new state of equilibrium; whereas, if it follows the stress path (2) to A or B, it will yield in a strain softening manner, resulting in the formation of a yield zone. In the model the peak differential stress curve defines the point of instability (at A, for example) for a rock mass with a low density of discontinuities. The residual strength surface defines the point of instability (B) for a rock mass with a high density of discontinuities, around the periphery of the excavation. However, this curve would be modified if the discontinuties were filled to that of the fill material.

11.7 Summary

Some of the many complex factors involved in estimating the behaviour of a rock mass surrounding an excavation have been outlined, which highlight the limitations of idealised analyses applied to strata control. Whilst analyses such as those discussed in the previous chapter offer useful first approximations, they cannot be relied upon as a means of predicting excavation behaviour and support requirements. This chapter has discussed the critical importance of geological conditions in determining the response of the strata to excavation, and has proposed the use of the critical state model in determining rock stability. However, there is a need for a greater understanding of the influence of geological conditions, amongst other factors, on the stability and dilatancy of the rock mass surrounding and excavation, and thus on the support design. Since the prediction of geological conditions is notoriously uncertain, an approach similar to that of Vick and Einstein (1974), using a complex decision tree, leading to a description of the

conditions and support requirements, should be used. Farmer and Shelton (1979) have proposed a design approach for rock reinforcement in underground excavations, which takes into account the required life span, discontinuities, depth and rock strength, of a simpler, but similar type to Vick and Einstein's in structure.

* * *

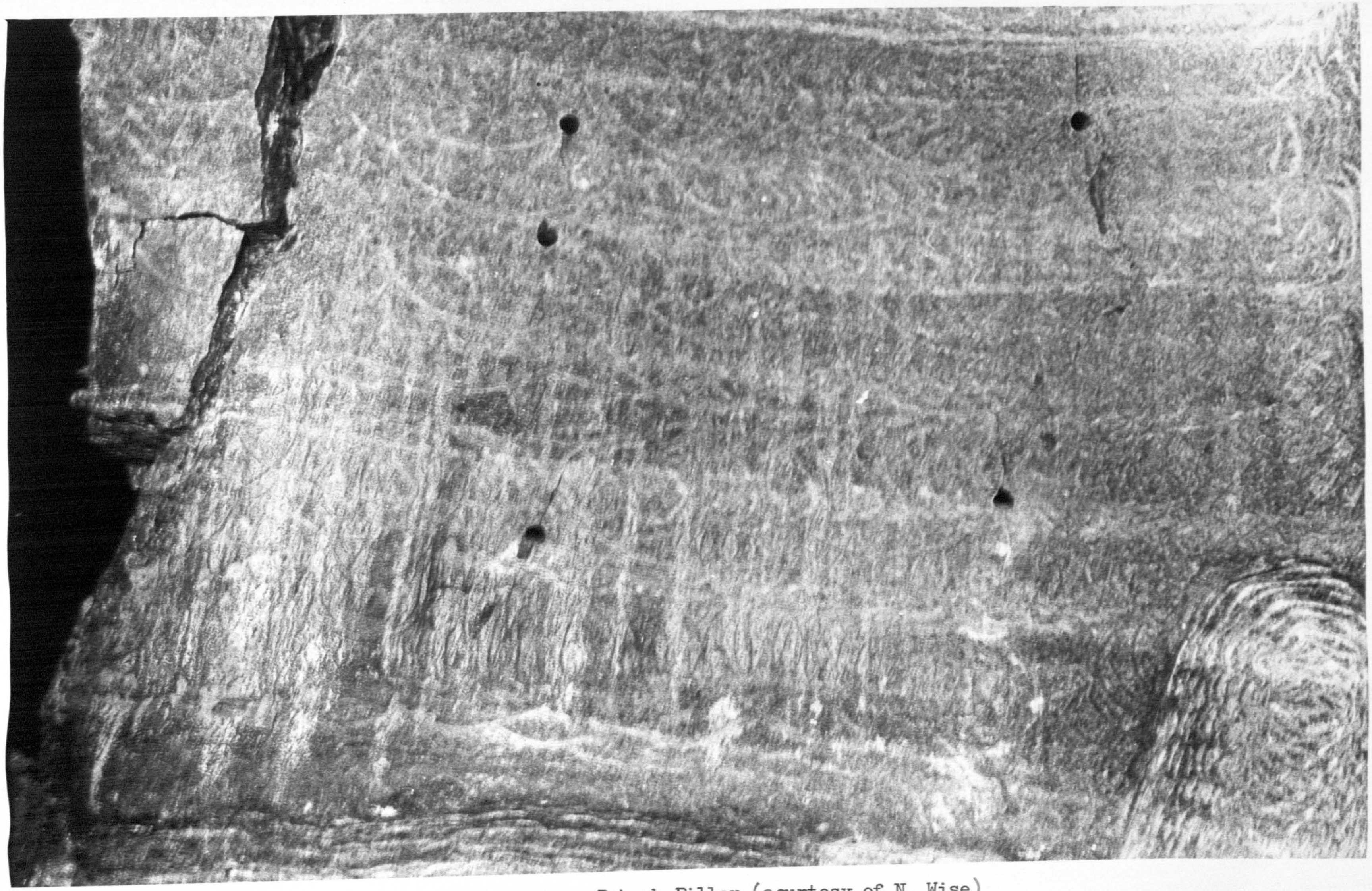

Plate 11.1 Flow and Fracture in a Potash Pillar (courtesy of N. Wise)

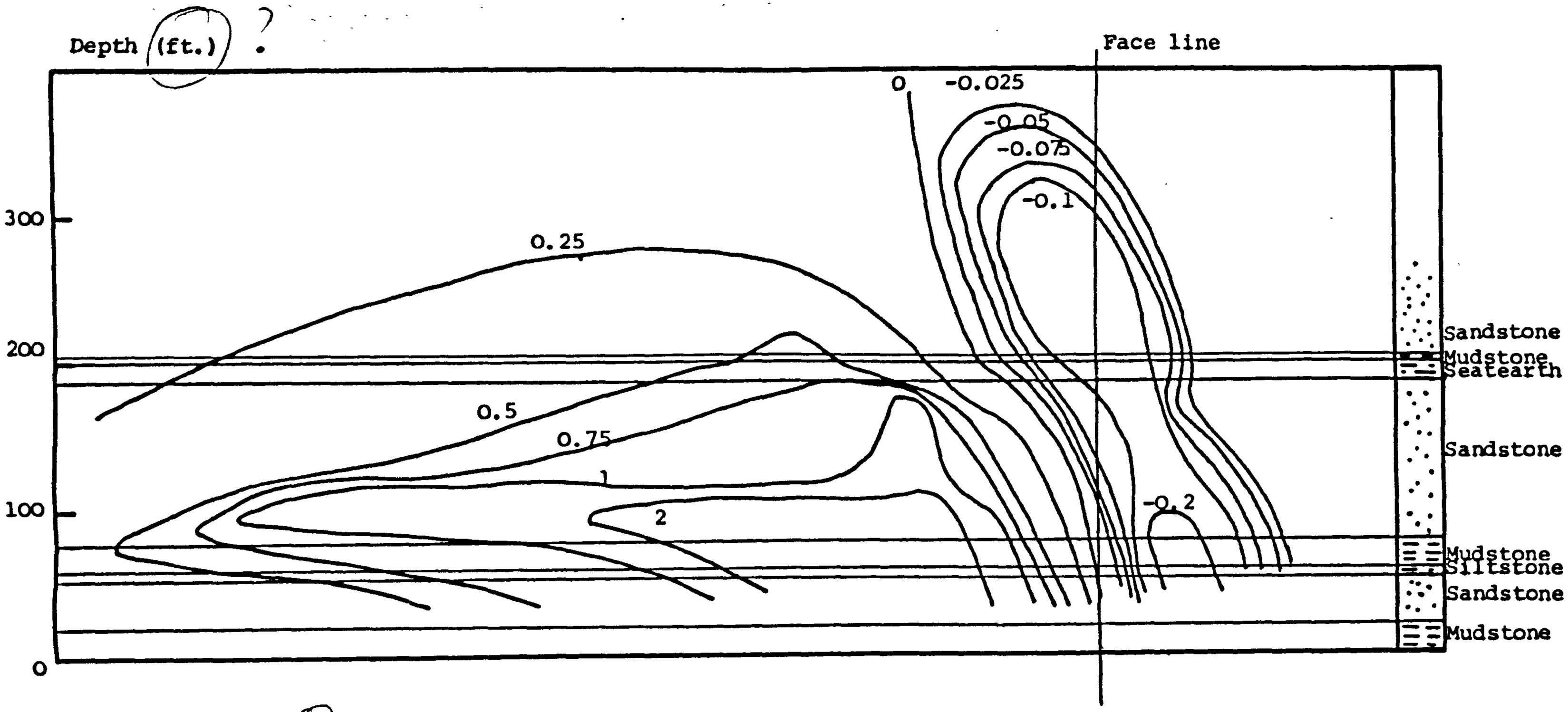

Fig.11.1 Example of the effects of stratigraphy on the vertical strain contours (%) above a face (after Malone and Gardener, 1963)

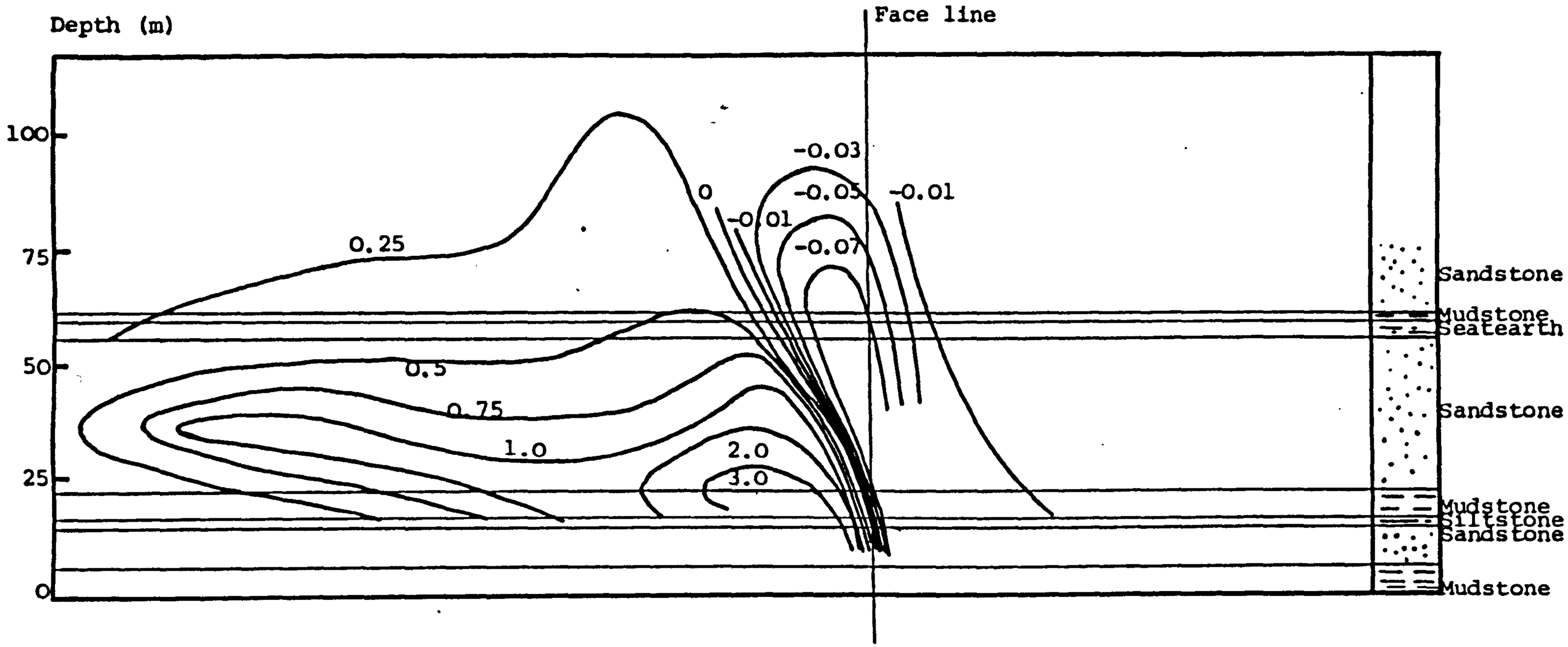

Fig.11.2 Example of the Effects of Stratigraphy on the Vertical Strain contours (%) above a face (After Leigh, 1962)

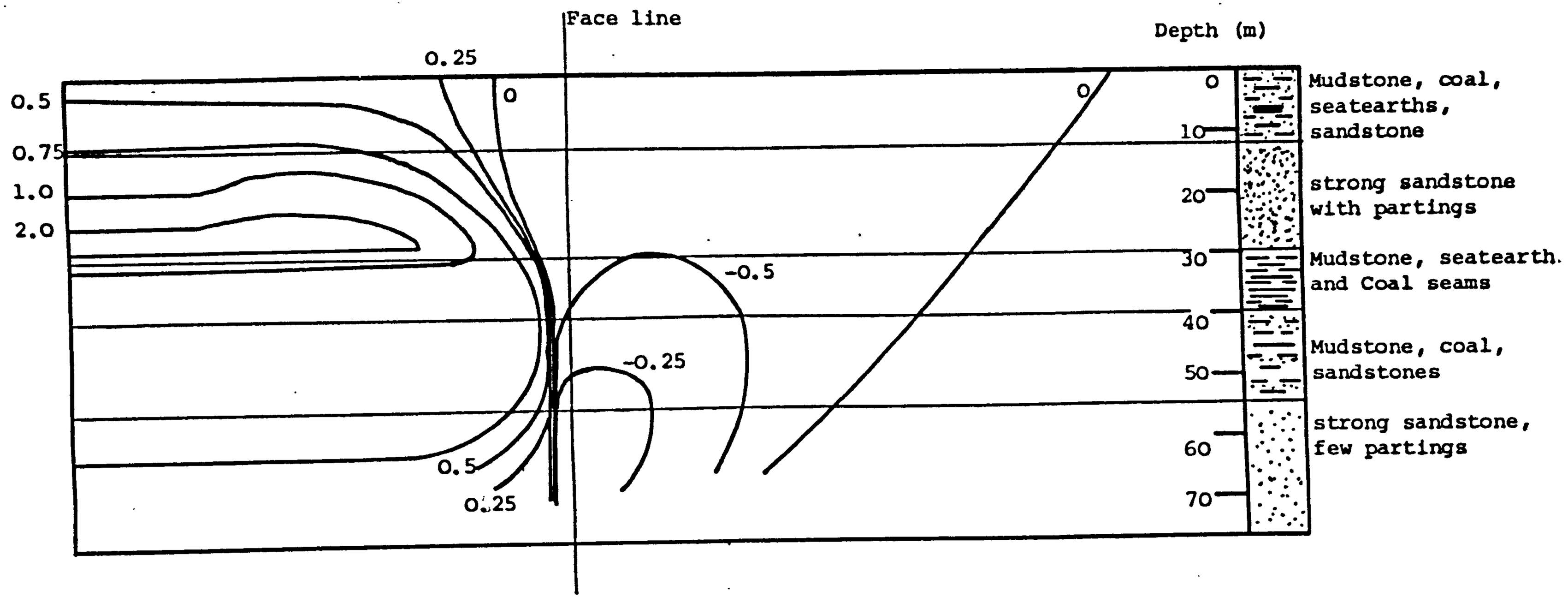

Fig. 11.3 Effects of stratigraphy on vertical strain contrours (%) above a face (After University of Newcastle upon Tyne, 1979)

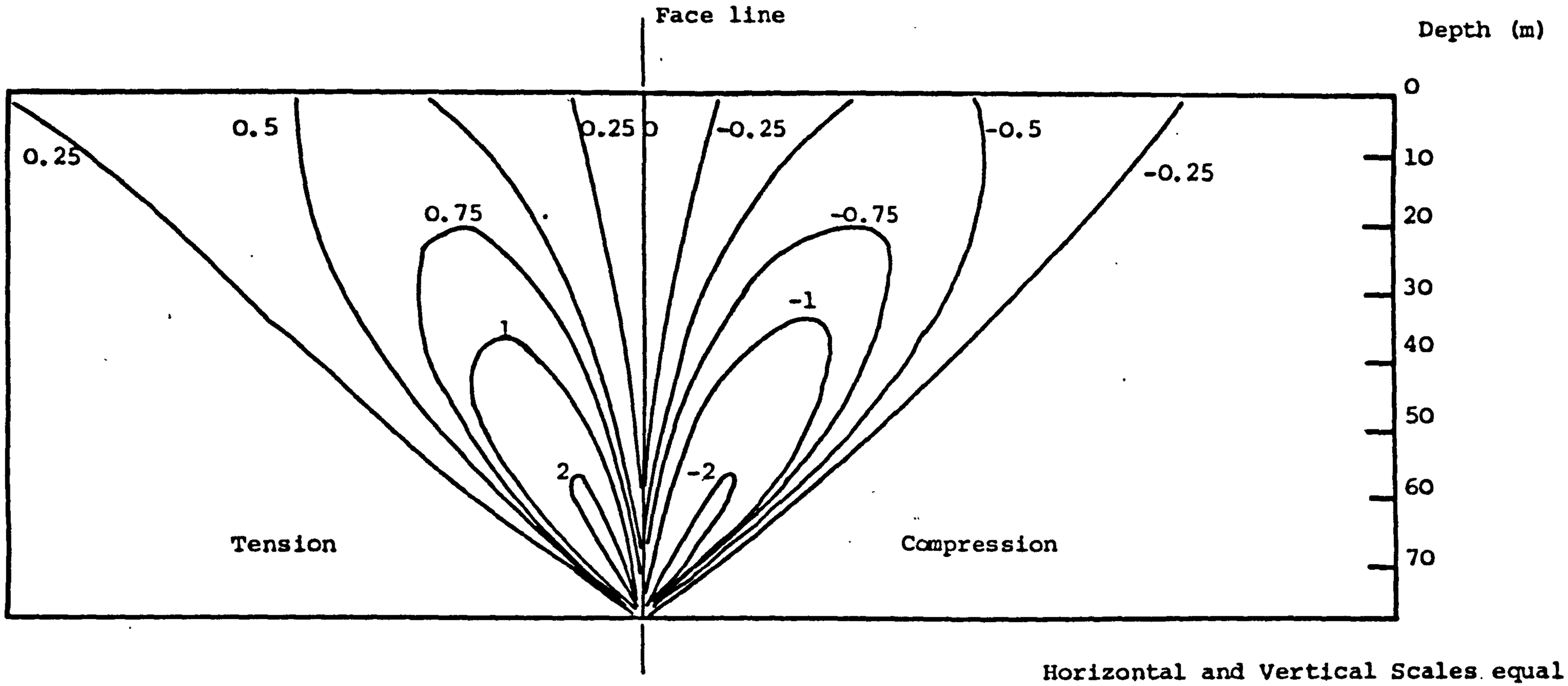

Horizontal and Vertical Scales equal

Fig. 11.4 THEORETICAL CONTOURS OF VERTICAL STRAIN (%) ABOVE A FACE

(after University of Newcastle upon Tyne, 1979)

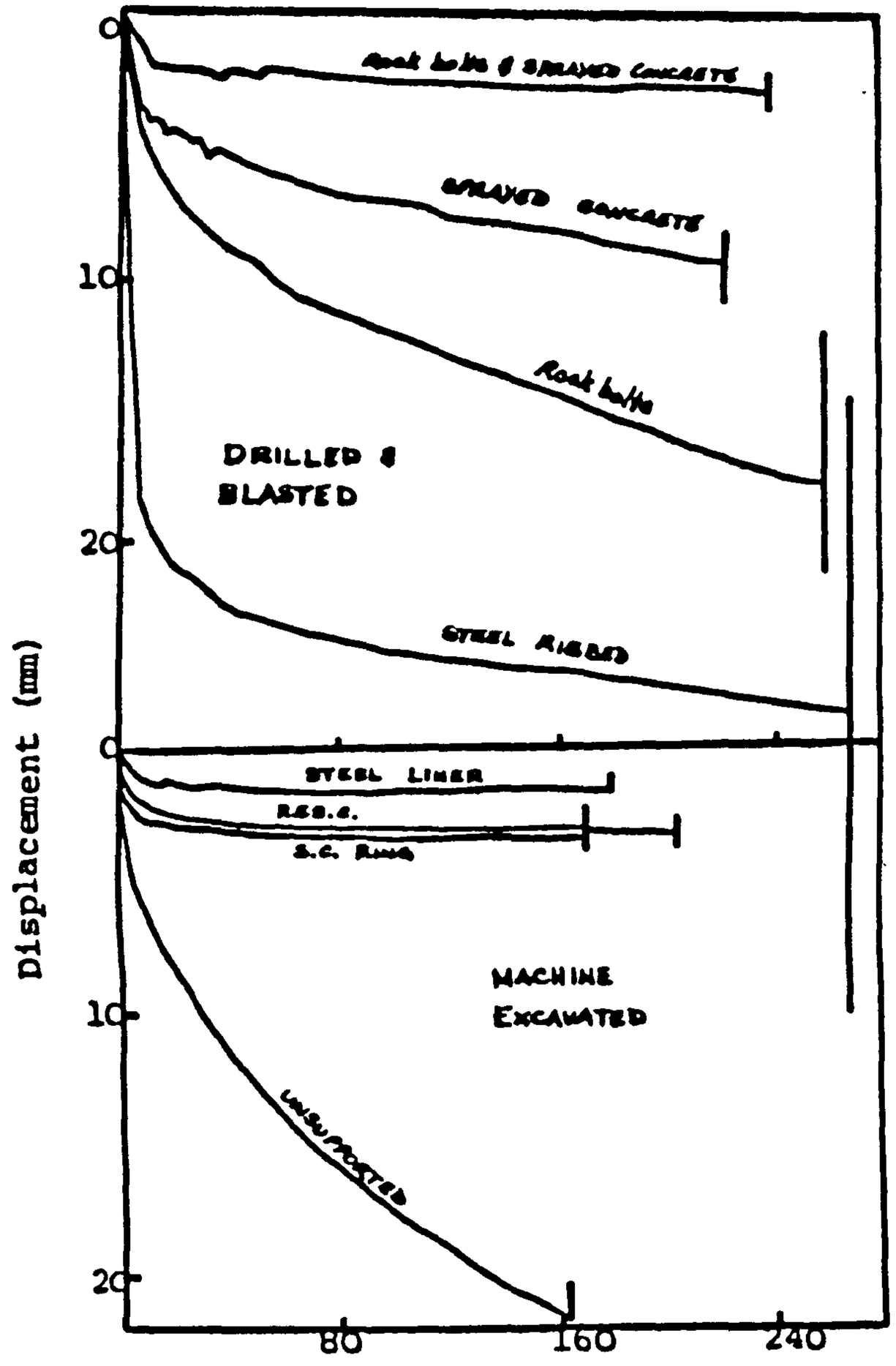

(after Ward et al, 1966)

Fig.11.5 Support Resistance and deformation

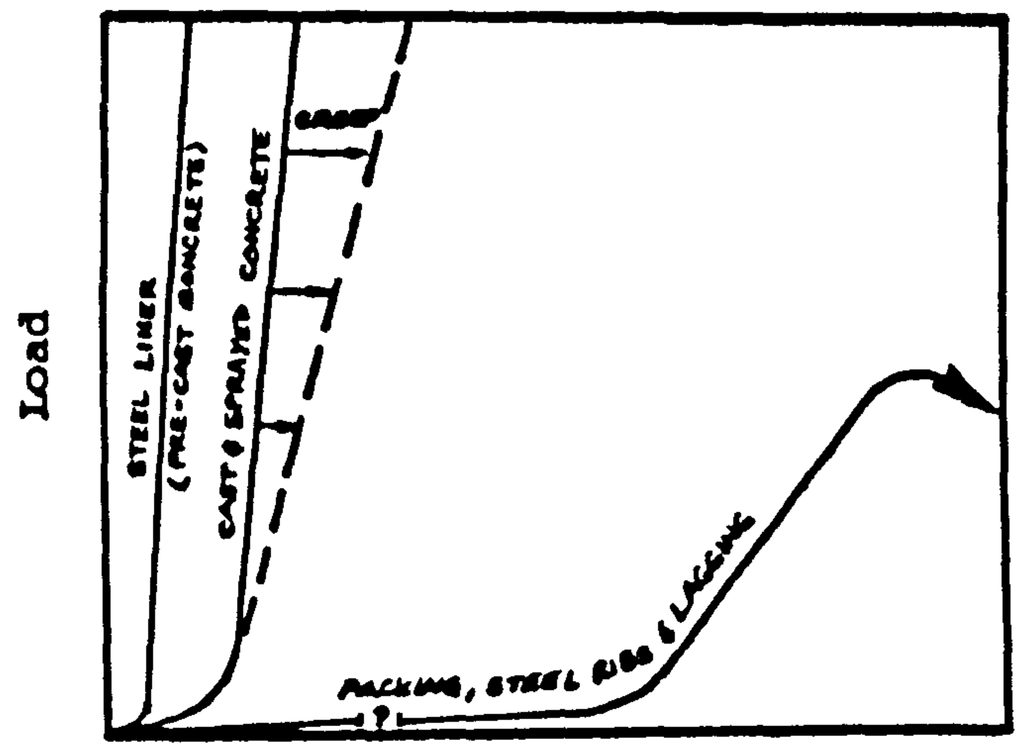

Deformation

(after Ward, 1978)

Fig.11.6 Support Resistance and Deformation

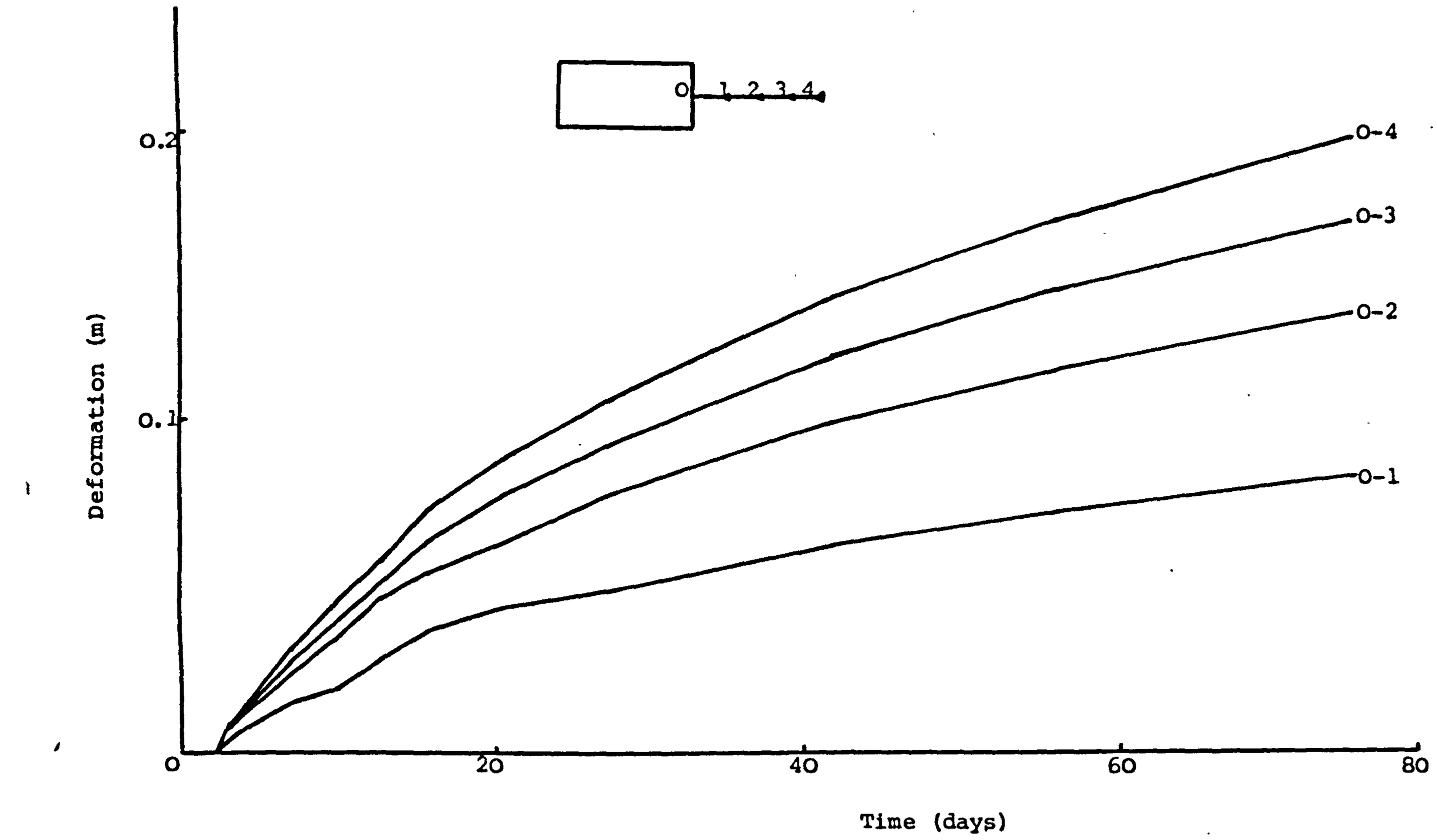

Fig.11.7 Deformation of a Potash Pillar (after Wise, 1978)

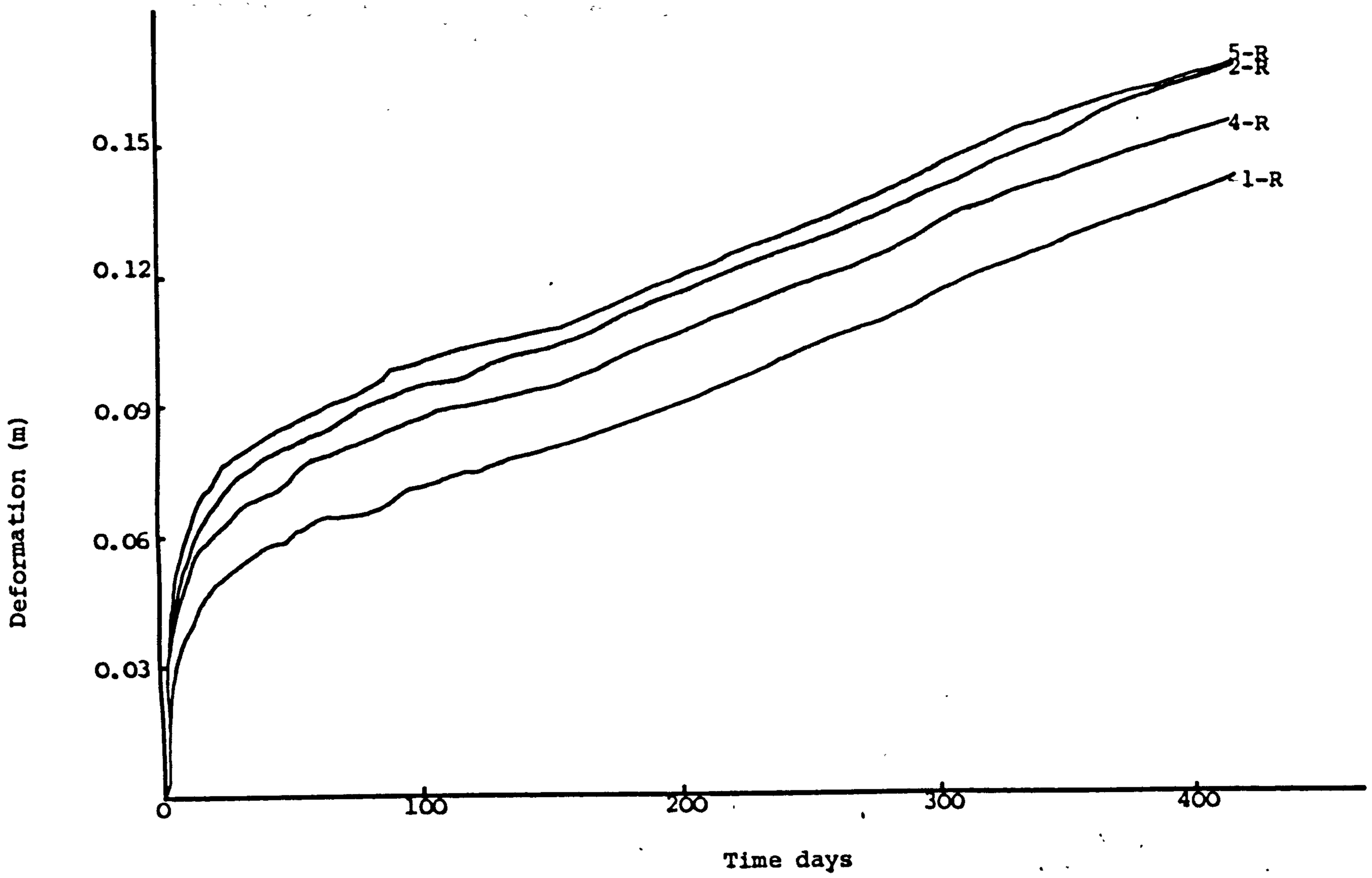

Fig. 11.8 Roof sag measured in Potash by Hebblewhite (1977)

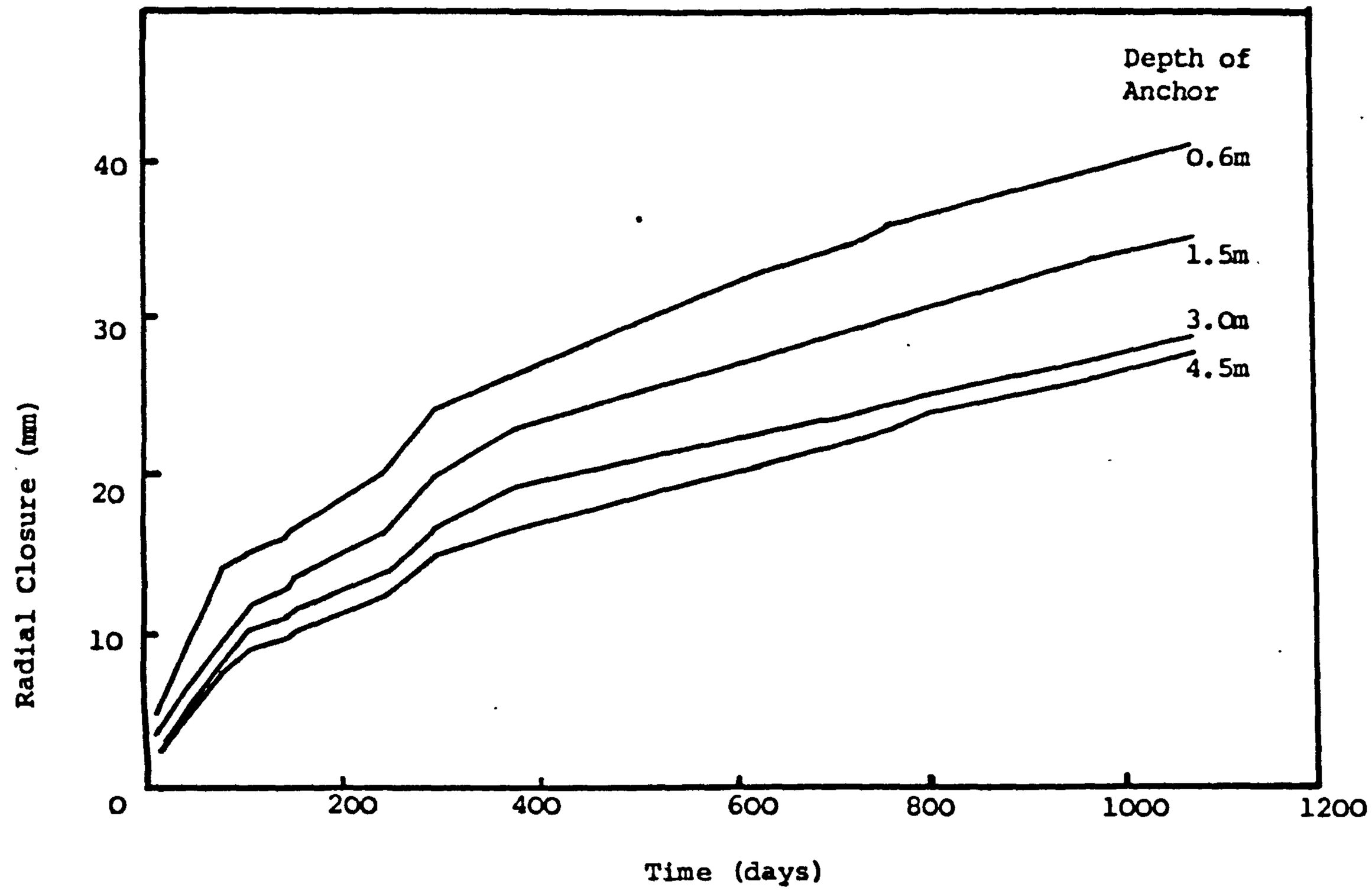

Fig. 11.9 Radial Closure of Shaft in Salt
(after Hebblewhite, Miller and Potts, 1977)

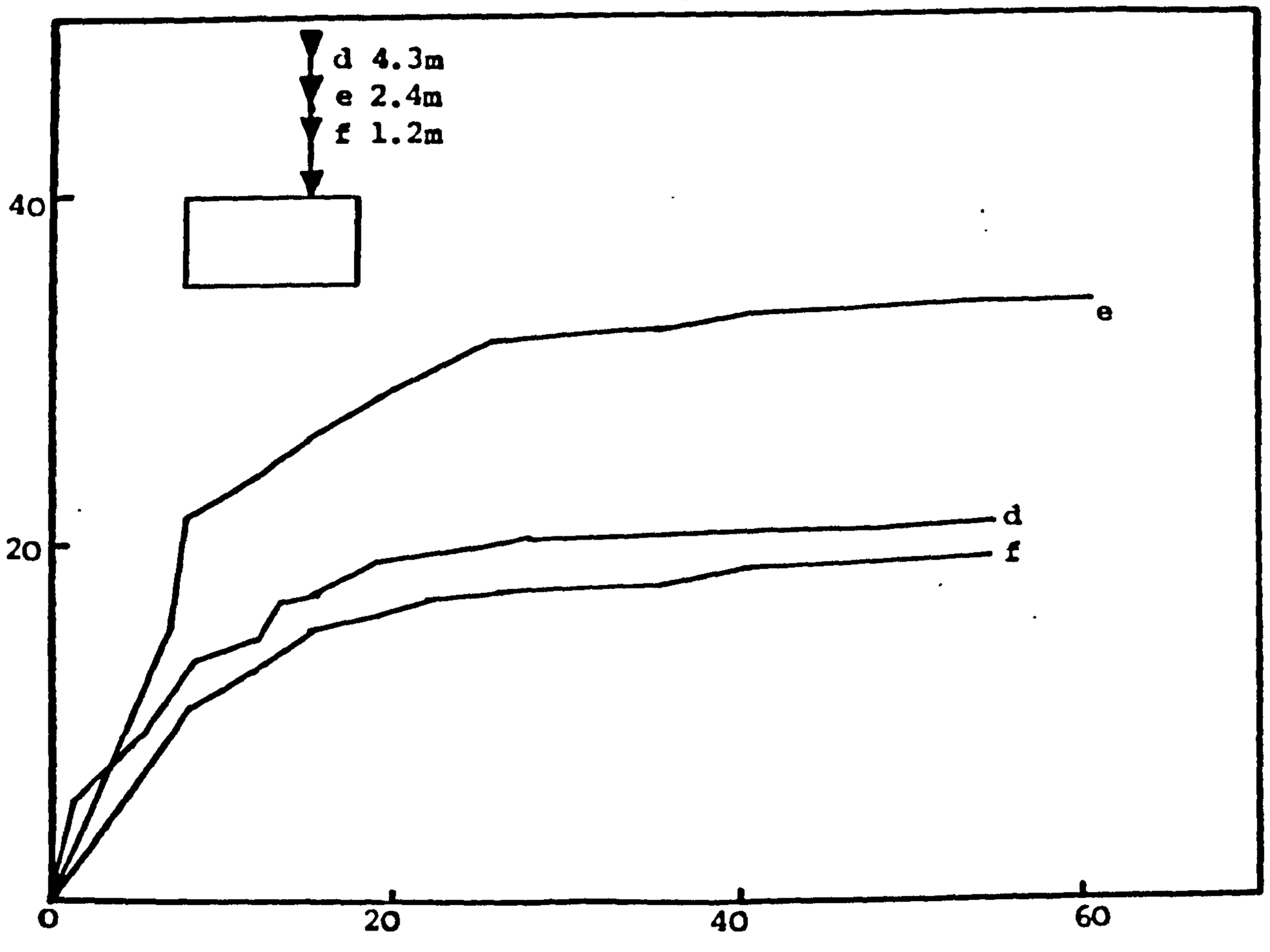

Fig.11.10 Anchor movements in Coal Measures Rocks

(after Kirmani, 1972)

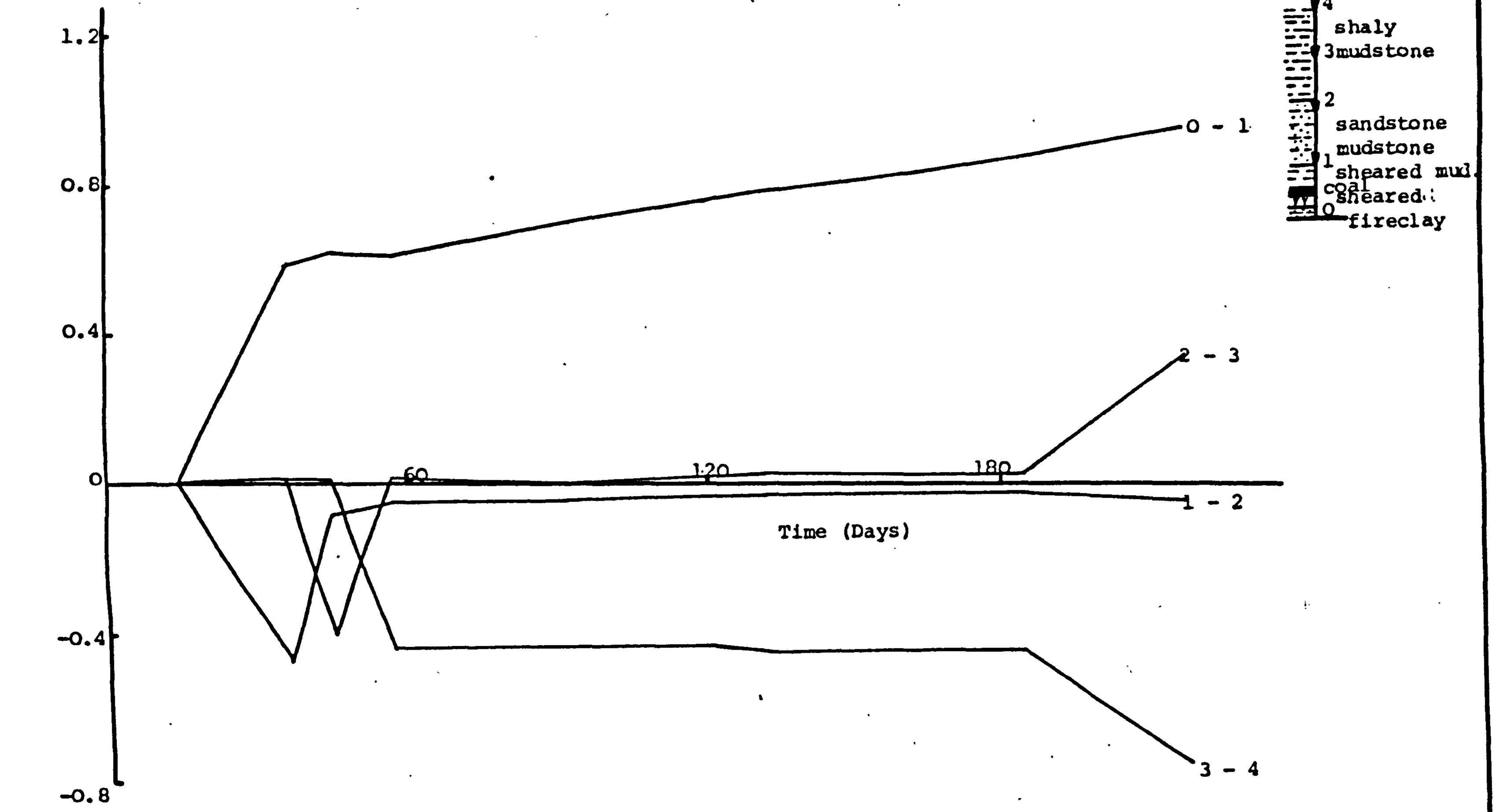

Fig.11.11 Bay Strains in Roof Hole WA3, Woodhorn Colliery

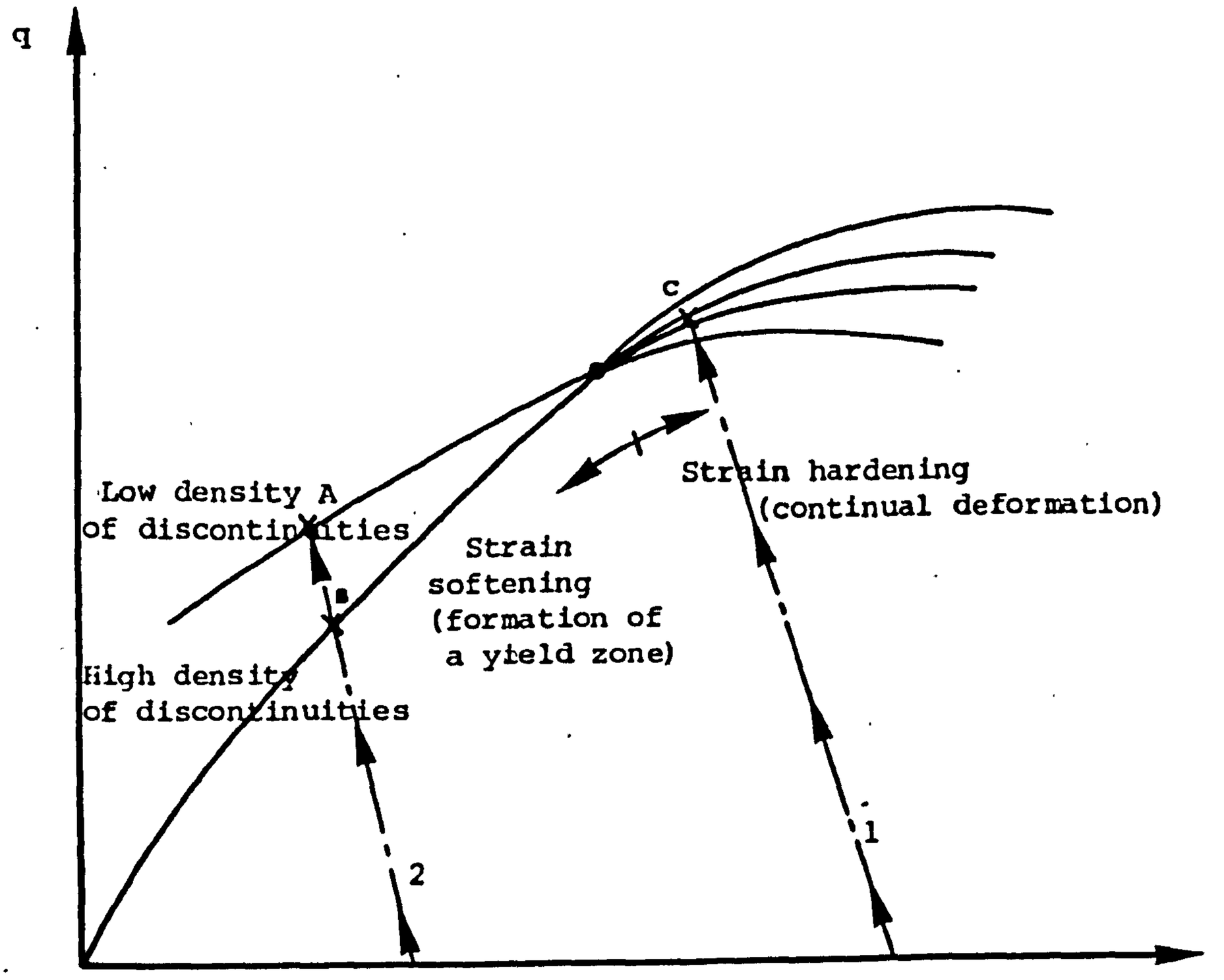

Fig.11.12 Use of the Proposed Critical State Model for determining the stability of an exacavation

CHAPTER TWELVE

CONCLUSIONS AND RECOMMENDATIONS

12.0 Introduction

The work described in this thesis has been concerned with the measurement of volumetric changes in laboratory specimens, compressed triaxially to large axial strains. The results obtained from these experiments have been applied to the calculation of roadway closures and the formulation of a critical state model for rocks. The conclusions reached from these investigations and the recommendations for future work in this area are summarised in the following sections.

12.1 The Servo-Controlled Testing Machine

The Department of Mining Engineering's 500 ton servo-controlled testing machine, its origins and associated units are described. The testing machine, plus the additions expected in the near future, offer a versatile system, complete with automatic logging facilities linked into the Department's Hewlitt Packard mini-computer. Problems have been experienced with unit and system reliability and are still experienced with system stability during long term experiments. However, many of the problems have been slowly eliminated, giving a high degree of short term reliability.

It is recommended that a member of the full-time staff, preferably a technician, be fully acquainted with the design and operation of the available equipment.

12.2 Apparatus for measuring Volumetric Changes

The factors influencing the design of the apparatus, and the existing systems in the literature, were discussed. Apparatus, similar to that originally used by Crouch was described. Crouch's original design involved the use of a pressure intensifier to maintain a constant confining pressure. This was replaced by a relief valve, allowing large and sudden volume changes to be accommodated. The apparatus comprised of four units:

1. a triaxial cell,
2. a relief valve,
3. a pressure gauge and
4. an inlet valve.

Both uniaxial compressive tests and triaxial compressive tests (3.5 to 4.2 MN/m^{-2}), using this equipment, were described and the results presented. Problems were experienced with the reliability of the valve and in maintaining a constant confining pressure, especially at the higher confining pressures. This was attributed to an 'over-release' of oil from the relief valve, due to delays in closing.

It is recommended that the apparatus be redesigned to allow:

(a) the automatic logging of oil displacement,

(b) the confining pressure to be adjusted manually during the experiment without disrupting the results,

(c) more accurate maintenance of the confining pressure and

(d) the oil in the triaxial system to be totally enclosed.

The suggested design, that includes these features, consists of two pressure systems - the triaxial system and the pressure control system, separated by a free moving runner, mounted in a stainless steel tube. The confining pressure would be maintained using a deadweight pressure controller, located in the pressure control system. Such a system would facilitate greater control of the confining pressure since, if the need arose, the confining pressure in the control system could be increased by pump without disrupting the measurement of oil displaced in the triaxial system. The oil displaced in the triaxial system due to the volumetric expansion of the specimen would be reflected in the movement of the runner, which could be logged automatically with the aid of an L.V.D.T.

12.3 Experimental Results

Families of seven rock types were tested under a series of triaxial conditions and their volumetric changes measured. The rock types tested were sandstone, silty sandstone, mudstone, saccharoidal limestone, Portland stone, rock salt and carnallite marl. All the rock types showed a dramatic reduction in volumetric strain between the uniaxial and triaxial compressive tests. Further reductions occurred with increased confining pressure, although the effects diminished as the higher confining pressures were reached. A transition from strain softening to strain hardening was observed for some rocks, in the range of confining pressures used. Another transition, from volumetric expansion to compaction was also noted for certain rock types, as confining pressure increased.

Instantaneous Poisson's ratio decreased rapidly as the confining pressure increased and, for most rocks, approached a value of 0.5, corresponding to zero volume change in the specimen, with deformation. Two exceptions were for the saccharoidal limestone and carnallite marl, which tended towards values of 0.8 and 0.4 respectively. The magnitude of the instantaneous Poisson's ratio approached a near constant value for each confining pressure once frictional sliding occurred.

Lateral strains decreased with increased confining pressure. In all cases the maximum rate of change of lateral straining occurred in the neighbourhood of the peak axial stress, and then reduced to a near constant value.

All the experiments were conducted at a constant strain rate of 21 $\mu\varepsilon$ s^{-1}, except for three conducted on rock salt at various strain rates. The results from the latter tests proved inconclusive due to problems with machine stability. Therefore, it is recommended that further experiments be conducted at various strain rates in order to determine the effects of strain rate on dilatancy. Further tests are also needed on specimens of different volumes, in order to determine the effects of specimen size on dilatancy and the relationship between shear and post failure dilatancy, should also be considered.

12.4 The Critical State Model for Rocks

The critical state model for soils proposed by Schofield and Wroth and described by Atkinson and Bransby is discussed, and a similar model for rocks proposed, based on the evidence obtained from the experimental programme and the literature. The model proposed consists

of a'Hvorslev surface' bounded by the critical state line and stability line, and probably includes a 'Roscoe surface' for specimens deforming stably, and a residual strength surface for those failing unstably. A curve corresponding to the peak differential stresses is also included in the model.

Because of the limitations on pressures imposed by the apparatus, it was impossible to determine the complete model for one particular rock type. Consequently, the model proposed has had to be constructed from the partial models of the different rock types. Therefore, it is recommended that an experimental program be designed, enabling the accurate monitoring of specimen behaviour, and verification of the proposed model. This program should aim to substantiate the 'Roscoe surface' for rocks in particular. The applications of the model to the description of rock behaviour and the design of underground excavations should be pursued further.

12.5 Yield Zone Analysis and Roadway Closure

Various yield zone analyses were reviewed and their predictions of yield zone widths for two hypothetical rocks compared. Two of the analyses were extended to predict roadway closure and the values obtained from these compared with those predicted from the laboratory measurements of dilatancy. The values predicted compared well with those measured in-situ by the author and other workers. The laboratory measurements of dilatancy offered a reasonable estimate of the expected roadway closure. However, the analyses took no account of the effects of stratification and, therefore, the closures calculated from the various analyses should only be regarded as a first estimate.

12.6 Yield in Stratified Deposits

The effects of stratigraphy, rock type and strength, confinement, yielding mechanism and discontinuities upon the prediction of roadway closure, due to volumetric expansion of rock, were discussed and several illustrations, in the form of case studies, presented The need for a greater understanding of the influence of geological conditions upon the stability and dilatancy of the rock mass surrounding an excavation was outlined. However, since the prediction of geological conditions is notoriously uncertain, an approach similar to that of Vick and Einstein's complex decision tree was proposed, and attention was drawn to Farmer and Shelton's design approach.

* * *

ABBREVIATIONS USED IN REFERENCES

AUSTIN (1968)	Proceedings of the 10th Symposium on Rock Mechanics, University of Texas, Austin, 1968.
AUSTIN (1979)	Proceedings of the 20th U.S. Symposium on Rock Mechanics, Austin, Texas, June 4-6, 1979.
BELGRADE (1970)	Proceedings of the 2nd Congress of the International Society Rock Mechanics, Belgrade, 1970.
B.G.S.A.	Bulletin of the Geological Society of America.
BRISBANE (1975)	Proceedings, 2nd Australian, New Zealand Conference on Geomechanics, Brisbane, 1975.
DENVER (1974)	Advances in Rock Mechanics, Proceedings 3rd Congress of the International Society of Rock Mechanics, Denver, 1974, Washington, D.C., Nat. Acad. Sci., 1974.
E.G.	Engineering Geology.
Geo.	Geotechnique.
G.R.L.	Geophysical Research Letters.

I.J.R.M.M.S.	International Journal of Rock Mechanics and Mineral Sciences.
J.A.P.	Journal of Applied Physics.
J.G.R.	Journal of Geophysical Research.
J.S.P.E.	Journal of the Society of Petroleum Engineers.
LISBON (1966)	Proceedings of the 1st Congress of the International Society of Rock Mechanics. Lisbon, 1966.
NEVADA (1978)	Proceedings of the 19th U.S. Rock Mechanics Symposium, University of Nevada, 1978.
NEWCASTLE (1977)	British Geotechnical Society, Conference on Rock Engineering, Newcastle upon Tyne. April, 1977.
P & A.G.	Pure and Applied Geophysics.
PENNSYLVANIA (1975)	Proceedings 1st Conference on Acoustic Emission/microsiesmic activity in Geologic structures and materials. Pens. 1975. H.R. Hardy, Jr. and F.W. Leighton (Eds.)
R.M.	Rock Mechanics.
S.A.M.E.	South African Mechanical Engineer.
Tec.	Tectonophysics.

T.I.M.E. Transactions of the Institute of Mining Engineering.

T.N.Y.A.S. Transactions of the New York Academy of Science.

URBANA (1972) 'Stability of Rock Slopes' - 13th Symposium on Rock Mechanics, University of Illinois, Urbana, 1971, Published by the American Society of Civil Engineers, 1972.

* * *

REFERENCES

ABEL J.F. 'Concrete Shaft lining Design'
DOWIS J.E. and Austin (1979) pp.627-33.
RICHARDS D.P.

ALDRICH M.J. 'Pore Pressure effects on Brea Sandstone subjected to Experimental Deformation' B.G.S.A. 80. pp.1577-86 (1969).

ARMSTRONG J. 'Geotechnical factors affecting tunnelling in Coal Measures Strata' M.Sc. Advanced Course Thesis, University of Newcastle upon Tyne (1978).

A.S.T.M. 'Standard Method of Test for Triaxial Compressive strength of Undrained Rock Core Specimens without Pore Pressure Measurements' D2664-67 (1967).

ATKINSON J.H. and BRANSBY P.L. 'The Mechanics of soils, an introduction to critical state soil mechanics' McGraw Hill, London (1978).

ATTEWELL P.B. and FARMER I.W. 'Fatigue Behaviour of Rock' I.J.R.M.M.S. 10, pp.1-9 (1973).

ATTEWELL P.B. and FARMER I.W. 'Principles of Engineering Geology' Chapman and Hall, London pp.1045 (1976).

BARNARD P.R. 'Researches into the complete stress-strain curve for concrete'. Mag. Conc. Res. 16, pp.203-10 (1964).

BARTON N. 'Review of a new shear-strength criterion for rock joints'. E.G. 7,pp.287-332 (1973).

BARTON N.. 'The shear strength of rock and rock joints'. I.J.R.M.M.S. 13, pp.255-79 (1976).

BIENIAWSKI Z.T. 'Mechanism of Brittle Fracture of Rock. Part 1. Theory of the fracture process; Part 2. Experimental Studies; Part 3. Fracture in Tension and Under long-term loading' I.J.R.M.M.S. 4, pp.395-430 (1967a).

BIENIAWSKI Z.T. 'Stability concept of Brittle Fracture Propagation in Rock' E.G. 2, pp. 149-62 (1967b).

BIENIAWSKI Z.T. 'Time dependent behaviour of fractured rock' R.M. 2, pp. 123-37 (1970).

BIENIAWSKI Z.T. 'Deformational Behaviour of Fractured rock under multiaxial compression' In: 'Structure, Solid Mechanics and Engineering Design' TE'ENI,M. (Ed.). Proc. Southampton 1969 Civil Engineering Materials Conference. London: Wiley-Interscience pp.589-98 (1971).

BIENIAWSKI Z.T. 'Failure of fractured rock'
DENKHAUS H.G. and I.J.R.M.M.S. 6, pp. 323-41 (1969).
VOGLER U.W.

BONNER B.P. 'Shearwave Birefringance in dilating Granite'
G.R.L. 1, pp. 217-20 (1974).

BORDIA S.K. 'The effects of size and stress concentration on the Dilatancy and fracture of rock'
I.J.R.M.M.S. 8, pp. 629-40 (1971).

BORDIA S.K. 'Complete Stress-Volumetric Strain Equation for Brittle Rock up to strength Failure'
I.J.R.M.M.S. 9, pp. 17-24 (1972).

BRACE W.F. 'Laboratory Studies pertaining to Earthquakes'
T.N.Y.A.S. 31, pp. 892-906 (1969).

BRACE W.F. 'Laboratory studies of stick-slip and their application to Earthquakes'
Tec., 14, pp. 189-200 (1972).

BRACE W.F. 'Dilatancy-Related electrical Resistivity Changes in Rocks'
P & A.G. 113 pp. 207-17 (1975).

BRACE W.F. and 'Stick-slip as a mechanism for earthquakes'
BYERLEE J.D. Science, 153, pp. 990-92 (1966).

BRACE W.F. and 'A test of the law of effective stress for
MARTIN R.J. crystalline rocks of low porosity'
I.J.R.M.M.S. 5,pp.415-26 (1968).

BRACE W.F. and ORANGE A.S. 'Electrical Resistivity changes in saturated Rock under Stress' Science, 153, pp. 1525–26 (1966).

BRACE W.F. and ORANGE A.S. 'Electrical resistivity changes in saturated rocks during fracture and frictional sliding' J.G.R. 73, pp. 1433–45 (1968).

BRACE W.F. PAULDING B.W. and SCHOLZ C.S. 'Dilatancy in the Fracture of Crystalline Rocks' J.G.R. 71, pp. 3939–53 (1966).

BRACE W.F. and RILEY D.K. 'Static Uniaxial Deformation of 15 rocks to 30 kB' I.J.R.M.M.S.,9, pp. 271–88 (1972).

BRADY B.T. 'The Nonlinear mechanical behaviour of Brittle Rock. Part 1: stress–strain behaviour during regions I and II. Part 2: stress–strain behaviour during regions III and IV.' I.J.R.M.M.S., 6, pp. 211–25, 301–10 (1969)

BRADY B.T. 'Comment on "Diffusionless Dilating Model for Earthquake Precursors" by W.D. Stuart' G.R.L., 2, pp. 259–61 (1975).

BRADY B.T. DUVALL W.I. and HORINO F.G. 'An experimental Determination of the true Uniaxial stress–strain behaviour of Brittle Rock' R.M., 5, pp. 107–20 (1973).

BRIDGEMAN P.W. 'Volume changes in the plastic stages of simple compression' J.A.P., 20, pp. 1241–51 (1949).

BROWN E.T. and HOEK E. 'Trends in relationships between measured insitu stresses and Depth' I.J.R.M.M.S., 15, pp. 211-15 (1978).

BROWN E.T. HUDSON J.A. 'Controlled Failure of Hollow Rock Cylinders in Uniaxial Compression' R.M., 4, pp. 1-24 (1972).

HARDY M.P. and FAIRHURST C.

BROWN E.T. and MICHELIS P.N. 'A critical state yield criterion for strain hardening rock' Navada (1978) pp. 515-19.

BURDINE N.T. 'Rock Failure under dynamic loading conditions' J.S.P.E., 3, pp. 1-8 (1963).

BYERLEE J.D. and BRACE W.F. 'Stick-slip, stable sliding, and earthquakes - effect of rock type, pressure, strain rate and stiffness' J.G.R., 73, pp. 6031-37 (1968).

BYERLEE J.D. MJACHKIN V. SUMMERS R. and VOEVODA O. 'Structures developed in fault gouge during stable sliding and stick-slip' Tec., 44, pp. 161-71 (1978).

BYERLEE J.D. and SUMMERS R. 'A note on the effect of fault gouge thickness on fault stability' I.J.R.M.M.S., 13, pp. 35-6 (1976).

CAIN P.J.
PENG S.S. and
PODNIEKS E.R.
'Rock fragmentation by high frequency fatigue'
Denver (1974) V.II., P.A. pp.367-72.

CLOOK P.
'Theoretical and Field Investigations into the behaviour of some mine roadway floors associated with longwall extraction'
Ph.D. Thesis, University of Newcastle upon Tyne (1973).

COATES D.F.
'Rock Mechanics Principles'
Mines Branch Monograph 874, Revised (1970).

COGAN J.
'Triaxial Creep Tests on Opohonga limestone and Ophir shale'
I.J.R.M.M.S., 13, pp. 1-10 (1976).

COOK N.G.W.
'The failure of Rock'
I.J.R.M.M.S., 2, pp. 389-403 (1965)

COOK N.G.W.
'An experiment proving that dilatancy is a pervasive volumetric property of Brittle rock loaded to failure'
R.M., 2, pp. 181-88 (1970).

COOK N.G.W. and
HOJEM J.P.M.
'A rigid 50-ton Compression testing machine'
S.A.M.E., 16, pp. 89-92 (1966).

CORNET F.H.
'Pore fluid and the mechanical behaviour of rock'
Urbana (1972), pp. 825-44.

CORNET F.H. and FAIRHURST C. 'Influence of pore pressure on the deformation behaviour of saturated rocks' Denver (1974) V.II.P.A.,pp.634-44.

CROUCH S.L. 'The influence of failed rock on the Mechanical behaviour of Underground Excavations' Ph.D. Thesis, Univ. of Minnesota (1970).

CROUCH S.L. 'The Post-failure behaviour of Norite in Triaxial Compression' Progress report 24, Univ. Minnesota, pp. 83-97: Also in E.G., 6, pp.19-30 (1972).

CULLINGFORD G. LASHINE A.K.S. and PARR G.B. 'Servo-controlled equipment for dynamic triaxial testing of soils' Geo., 22, 3, pp. 526-29 (1972).

DARLEY P. 'Comment on "Apparatus for measuring volume change suitable for automatic logging" by G.A. Rowlands' Geo., 23, 1, pp. 140-41 (1973).

DHIR R.K. and SANGHA C.M. 'Relationship between size, deformation and strength for cylindrical specimens loaded in unaixial compression' I.J.R.M.M.S., 10, pp.699-712 (1973).

DIETERICH J.H. 'Time dependent friction in rocks' J.G.R., 77, pp. 3690-97 (1972).

DONATH F.A. 'Some information squeezed out of rock' Am. Scientist, 58, pp. 54-72 (1970).

DONATH F.A. and FRUTH L.S. 'Dependence of strain-rate effects on deformation mechanism and rock type' J. Geology, 79, pp. 347-71 (1971).

EDMOND J.M. and PATERSON M.S. 'Volume changes during the deformation of rocks at high pressures' I.J.R.M.M.S., 9, pp. 161-82 (1972).

ENGELDER J.T. 'Cataclasis and the generation of fault Gouge' B.G.S.A., 85, pp. 1515-22 (1974).

ENGELDER J.T. 'Microscopic wear grooves on slickensides: Indicators of Paleaseismicity' J.G.R., 79, pp. 4387-92 (1974).

ENGELDER J.T. LOGAN J.M. and HANDIN J. 'The sliding characteristics of sandstone on quartz fault-gouge' P and A.G., 113, pp. 69-86 (1975).

ENGELDER J.T. and SCHOLZ C.S. 'The role of Asperity Indentation and Ploughing in Rock Friction - II: Influence of relative hardness and Normal load' I.J.R.M.M.S., 13, pp. 155-63 (1976).

FAIRHURST C. 'The Mechanical Properties of Rock Masses' National Technical Information Service, Springfield V.A. (1973).

FARMER I.W. and SHELTON P.D. 'Design of Underground Rockbolt Reinforcement' to be published (1979).

FREUDENTHAL A.M. 'Shear dilatancy in rock and Precursory changes in seismic velocities' G.R.L., 2, pp. 517-20 (1975).

GAY N.C. 'The formation of step structures on slickensided shear surfaces' J. Geology, 78, pp. 523-32 (1970).

GEROGIANNOPOULOS N.G. 'A critical state approach to rock mechanics' Ph.D. Thesis, University of London (1976).

GEROGIANNOPOULOS N.G. and BROWN E.T. 'The critical state concept applied to rock' I.J.R.M.M.S., 15, pp. 1-10 (1978).

GOLDSMITH W. SACKMAN J.L. and EWERT C. 'Static and dynamic fracture strength of Barre Granite' I.J.R.M.M.S., 13, pp. 303-09 (1976).

GOODMAN R.E. and DUBOIS J. 'Duplication of dilatancy in analysis of jointed rocks' J. Soil Mech. Found. Div., Proc. Am.Soc.Civ. Engrs., 98, pp. 399-422 (1972).

GOODMAN R.E. and OHNISHI Y. 'Undrained shear testing of jointed rock' R.M., 5, pp. 129-49 (1973).

GRADY D. 'High Strain Rate studies in Rock' G.R.L., 4, pp. 263-66 (1977).

GREEN S.J. LEASIA J.D. PERKINS R.D. and JONES A.H. 'Triaxial stress behaviour of Solenhofen limestone and Westerly Granite at high strain rates' J.G.R., 77, pp. 3711-24 (1972).

GRIFFITH A.A. 'The phenomena of rupture and flow in solids' Phil. Trans. Roy. Soc., London, A. 221. pp. 163-98 (1921).

GRIGGS D.T. TURNER F.J. and HEARD H.C. 'Deformation of rocks at 500° to 800°' In: Rock Deformation, Griggs, D. Handin, J. (eds.). Geol. Soc. Am. Mem., 79, pp.39-104 (1960).

HADLEY K. 'Azimuthal variation of Dilatancy' J.G.R., 80, pp. 4845-50 (1975).

HADLEY K. 'The effect of cyclic stress on dilatancy: Another look' J.G.R., 81, pp. 2471-74 (1976).

HAIMSON B.C. 'Mechanical behaviour of rock under cyclic loading' Denver (1974) V2, P.A., pp.373-78.

HALLBAUER D.K. WAGNER H. and COOK N.G.W. 'Some observations concerning the microscopic and mechanical behaviour of quartzite specimens in stiff, triaxial compression tests' I.J.R.M.M.S., 10, pp. 713-26 (1973).

HANDIN J. HAGER R.V. FRIEDMAN M. and FEATHER J.N. 'Experimental deformation of sedimentary rocks under confining pressure: Pore pressure effects' Bull. Am. Assoc. Petrol. Geol., 47, pp.717-55 (1963).

HARDY H.R. STEFANKO R. and KIMBLE E.J. 'An automated test facility for rock mechanics research' I.J.R.M.M.S., 8, pp. 17-28 (1971).

HAWKES I. and MELLOR M. 'Uniaxial testing in rock mechanics laboratories' E.G., 4, pp. 177-285 (1970).

HEBBLEWHITE B.E. 'Underground Potash Mine design based on rock mechanics principles and measurements' Ph.D. Thesis, University of Newcastle upon Tyne (1977).

HEBBLEWHITE B.E. MILLER H.D.S. and POTTS E.L.J. 'A method for predicting time-dependent deformation in evaporites around a vertical shaft' Newcastle (1977) pp. 529-39.

HOBBS D.W. 'A study of the behaviour of a broken rock under triaxial compression, and its application to mine roadways' I.J.R.M.M.S., 3, pp. 11-43 (1966).

HOBBS D.W. 'Stress-strain behaviour of some coal measure rocks' Coll. Guardian, pp. 200-02 April (1971).

HODKIN D.L. 'Stability of undermined room and pillar workings under the North Sea' Ph.D. Thesis, University of Newcastle upon Tyne (1978).

HOEK E. and BIENIAWSKI Z.T. 'Fracture propagation mechanism in hard rock' Lisbon (1966), 1, p. 243-49.

HOJEM J.P.M. 'A stiff, two meganewton testing machine for
COOK N.G.W. and measuring the work-softening behaviour of
HEINS C. brittle materials'
S.A.M.E., 25, pp. 250-70 (1975).

HORSEMAN S. Private Communication.

HOSHINO K. and 'Process of deformation of the sedimentary
KOIDE H. rocks'
Belgrade (1970), 1, pp. 353-59.

HUDSON J.A. 'Effect of time on the mechanical behaviour
of failed rock'
Nature (London), 232, pp. 185-86 (1971a)

HUDSON J.A. 'Studying time dependent effects in failed
rocks'
Progress report, 24, University of Minnesota,
pp. 104-09 (1971b).

HUDSON J.A. and 'Studying time dependent effects in failed rock'
BROWN E.T. In: New Horizons in Rock Mechanics, Hardy, H.R.,
Stefanko R. (Eds.). Proc. 14th Symp. Rock. Mech.,
Penn. State Univ., 1972, New York: Am.Soc. Civ.
Eng. (1973), pp. 25-34.

HUDSON J.A. 'Optimizing the control of rock failure in
BROWN E.T. and servo-controlled laboratory tests'
FAIRHURST C. R.M., 3, pp. 217-24 (1971).

HUDSON J.A.
BROWN E.T. and
FAIRHURST C.
'Shape of the complete stress-strain curve for rock'
Urbana (1972) pp. 773-95.

HUDSON J.A.
BROWN E.T. and
RUMMEL F.
'The controlled failure of rock discs and rings loaded in diametral compression'
Progress Report 24, Univ. Minnesota, pp. 33-49 (1971); also in I.J.R.M.M.S., 9, pp. 241-48 (1972).

HUDSON J.A.
CROUCH S.L. and
FAIRHURST C.
'SOFT, STIFF and SERVO-controlled testing machines: A review with reference to rock failure'
E.G., 6, pp. 155-89 (1972).

ILLFELDER H.M.J. and
WANG H.F.
'Minicomputer control of servo systems in rock mechanics'
Austin (1979) pp. 293-98.

INGLES O.G.
LEE I.K. and
NEIL R.C.
'The influence of stress History on lateral strain'
R.M., 5, pp. 203-13 (1973).

ISMAIL I.A.H. and
MURRELL S.A.F.
'Dilatancy and the strength of rocks containing pore water under undrained conditions'
Geophys. J.R. Astron.Soc., 44, pp.107-34 (1976).

JACKSON R.E. and
DUNN D.E.
'Experimental sliding friction and cataclasis of foliated rocks'
I.J.R.M.M.S., 11, pp. 235-49 (1974).

JAEGER J.C. 'Rock failures at low confining pressures' Engineering, 189, pp. 283-84 (1960).

JAEGER J.C. 'Rock Mechanics and Hydro-Power Engineering' Water Power, pp. 239-60, September (1961).

JAEGER J.C. 'Elasticity, Fracture and Flow, with Engineering and Geological Applications' Methuen and Co Ltd. and Science Paperbacks (1969).

JAEGER J.C. and COOK N.W.G. 'Fundamentals of Rock Mechanics' Chapman and Hall (London) (1971).

JAMISON W.R. and TEUFEL L.W. 'Pore volume changes associated with failure and frictional sliding of a Porous sandstone' Austin (1972), pp. 163-70.

KAWAMOTO T. and SAITO T. 'The behaviour of rock-like materials in some controlled strain states' Denver (1974) pp. 161-66.

KIRMANI F.A.K. 'Experimental and Theoretical studies of strata conditions around two mine roadways with special reference to fracture phenomena' Ph.D. Thesis, University of Newcastle upon Tyne (1972).

KOVARI K. and TISA A. 'Multiple failure state and strain controlled triaxial tests' R.M., 7, pp. 17-33 (1975).

KUMAR A. 'The effect of stress rate and temperature on the strength of Basalt and Granite' Geophysics, 33, pp. 501-10 (1968).

LADANYI B. 'Use of the long-term strength concept in the determination of ground pressure on tunnel linings' Denver (1974) pp. 1150-56.

LAMBE T.W. and WHITMAN R.V. 'Soil Mechanics' J. Wiley and Sons Inc. (1969).

LANE K.S. 'Pore Pressure Effects on Berea Sandstone subjected to experimental deformation: Discussion' B.G.S.A., 80, pp. 1587-90 (1969).

LEIGH R.D. 'Strata Pressures and rock mass movements by longwall mining' Ph.D. Thesis, University of Durham (1962).

LEWIN P.I. 'Use of servo mechanisms for volume change measurement and k_o Consolidation' Geo. 21, No. 3, pp. 259-62 (1971).

LINDSTROM M. 'Steps facing against the slip direction: A model' Geol. Mag., 111, pp. 71-4 (1974).

LISK R.D. 'The wet and dry strength of "A" Bed Gypsum, Kirkby Thore, Cumbria' M.Sc. Thesis, University of Newcastle upon Tyne (1975).

LIU H.P. and LIVANOS A.C.R. 'Dilatancy and precursory bulging along incipient fracture zones in uniaxial compressed westerly granite' J.G.R., 81, pp. 3495-3510 (1976).

MALONE D. and GARDNER T. 'Study of rock pressures around mining excavations' Final Report of measurements taken at Whitburn/ Wearmouth Collieries, University of Newcastle upon Tyne (1963).

MEAD W.J. 'The geologic role of dilatancy' J. Geol., 33, pp. 685-98 (1925).

MENCL K. 'Dilatancy of Rocks' R.M. and E.G., 3 (1965).

MILLAR P.J. and MARTIN G.R. 'A note on the strength of rock joints in direct shear' Brisbane (1975), pp. 248-52.

MOGI K. 'Some precise measurements of fracture strength of rocks under uniform Compressive stress' Felsmechanik und Ingenieurgeologie, 4, pp. 41-55 (1966).

MONTOTO M. 'Fatigue in rocks: Failure and Internal fissuration of Barre granite under loads cyclically applied' Denver (1974) V.II, p. A., pp. 379-84.

MORGENSTERN N.R. and PHUKAN A.L.T. 'Non-linear deformation of a sandstone' Lisbon (1966) 1, pp. 543-48.

MORGENSTERN N.R. and PHUKAN A.L.T. 'Non-linear stress-strain relations for a homogeneous sandstone' I.J.R.M.M.S., 6, pp. 127-42 (1969).

MUIR WOOD A.M. 'Ground behaviour and support for mining and tunnelling' 14th Sir Julius Wernher Memorial Lecture of I.M.M., Tunnelling '79, Int. Symp. (1979).

MURAYAMA S. and YAGI N. 'Swelling of mudstone due to sucking of water' Lisbon (1966) V.I., T.3, pp. 495-98.

NATIONAL COAL BOARD 'Design of Mine Layouts' Working Party Report (1972).

OHNISHI Y. and GOODMAN R.E. 'Results of laboratory tests on water pressure and flow in joints' Denver (1974), pp. 660-66.

PATERSON M.S. 'Experimental deformation and faulting in Wombeyan Marble' B.G.S.A., 69, pp. 465-76 (1958).

PATERSON M.S. 'Experimental Rock deformation - The brittle field'
Springer-Verlag (1978).

PENG S.S. 'Time-dependent Aspects of rock behaviour as measured by a servo-controlled hydraulic testing machine'
I.J.R.M.M.S., 10, pp. 125-27 (1975).

PENG S.S. 'A note on the fracture propagation and time-dependent behaviour of rocks in uniaxial tension'
I.J.R.M.M.S., 12, pp. 125-27 (1975).

PENG S.S. and PODNIEKS E.R. 'Relaxation and the behaviour of failed rock'
I.J.R.M.M.S., 9, pp. 699-712 (1972).

PRICE A.M. and FARMER I.W. 'Application of Yield Models to Rock'
I.J.R.M.M.S., 16, pp. 157-59 (1979).

RENGERS N. 'Influence of surface roughness on the friction properties of rock planes'
Belgrade (1970), 1, pp. 229-34.

REYNOLDS O. 'On the dilatancy of media composed of rigid particles in contact'
Phil. Mag., 20, pp. 469-81 (1885).

ROGIERS J.C. HUDSON J.A. and FAIRHURST C. 'A note on controlled crack growth in hydraulic facturing of rock'
Progress Report 24, Minnesota, pp.98-103 (1971).

ROSCOE K.H.
SCHOFIELD A.N. and
WROTH C.P.
'On the Yielding of Soils'
Geo., 8, pp. 22-53 (1958).

ROTHMAN R.L.
'Acoustic Emissions in Rock stressed to failure'
Pennsylvania (1975) pp. 109-33.

ROWE P.W.
'The stress-dilatancy relation for static Equilibrium of an assembly of Particles in contact'
Proc. Royal Soc., London, Series A., Vol. 269, pp. 500-27 (1962).

ROWLANDS G.O.
'Apparatus for measuring volume change suitable for automatic logging'
Geo., 22, No.3., pp.525-26 (1972).

RUMMEL F.
'Changes in the P-Wave velocity with increasing inelastic deformation in rock specimens under compression'
Denver (1974) pp. 517-23.

RUMMEL F. and
FAIRHURST C.
'Determination of the Post-failure behaviour of brittle rock using a servo-controlled testing machine'
R.M., 2, pp. 189-204 (1970).

SANGHA C.M. and
DHIR R.K.
'Influence of time on the strength, deformation and fracture properties of a lower devonian sandstone'
I.J.R.M.M.S., 9, pp.343-54 (1972).

SANGHA C.M. and DHIR R.K. 'Strength and deformation of rock subject to multiaxial compressive stresses' I.J.R.M.M.S., 12, pp. 277-82 (1975).

SCHNEIDER H.J. 'Rock-friction - A laboratory Investigation' Denver (1974), V.II., P.A., pp. 311-15.

SCHNEIDER H.J. 'The friction and deformation behaviour of rock joints' R.M., 8, pp. 169-84 (1976).

SCHOCK R.N. 'A constitutive relation describing dilatant behaviour in climax stock granodiorite' I.J.R.M.M.S., 13, pp. 221-23 (1976).

SCHOFIELD A.N. and WROTH C.P. 'Critical State Soil Mechanics' McGraw Hill, London (1958).

SCHOLZ C.H. 'Microfracturing of rocks in Compression' Ph.D. Thesis, Massachusetts Inst. of Technology (1967).

SCHOLZ C.H. 'Microfracturing and the inelastic deformation of rock in compression' J.G.R., 73, pp. 1417-32 (1968a).

SCHOLZ C.H. 'Experimental study of the fracturing Process in Brittle Rock' J.G.R., 73, pp. 1447-54 (1968b).

SCHOLZ C.H. 'Mechanism of creep in brittle rock' J.G.R., 73, pp. 3295-302 (1968c).

SCHOLZ C.H. 'The Role of Microfracturing in Rock deformation' Belgrade (1970) pp.323-27.

SCHOLZ C.H. and KRANZ R. 'Notes on Dilatancy Recovery' J.G.R., 79, pp. 2132-35 (1974).

SCHOLZ C.H. MOLNAR P. and JOHNSON T. 'Detailed studies of frictional sliding of granite and implications for the earthquake mechanism' J.G.R., 77, pp.6392-406 (1972).

SCHOLZ C.H. 'Earthquake prediction: A physical basis' SYKES L.R. and AGGARWAL Y.P. Science, 181, pp. 803-10 (1973).

SERATA S. 'Theory of aggregate rock behaviour based on SAKURAI S. and absolute three-dimensional testing (ATT) of ADACHI T. Rock Salt' Austin (1968) pp. 431-73.

SHELL 'Technical data on Shell Tellus Oils' 2nd Ed. Shell International Petroleum Co Ltd., London (1967).

SHEPHERD J. and 'Faults and their effect on Coal Mine roof FISHER N.I. failure and Mining rate: A case study in a New South Wales Colliery' Mining Engineer, pp.1325-34 (1978).

STACE L.R. 'A Study of Interaction problems in roadways associated with longwall coal mining' Ph.D. Thesis, University of Newcastle upon Tyne (1973).

SPETZLER H. and MARTIN R.J. 'Correlation of strain and velocity during dilatancy' Nature (London) 252, pp. 30-1 (1974).

STARFIELD A.M. and WAWERSIK W.R. 'Pillars as structural components in room and pillar mine design' Progress report 24,Univ. of Minnesota (1971).

STUART W.D. 'Diffusionless dilatancy model for earthquake precursors' G.R.L., 1, pp. 261-64 (1974).

SWANSON S.R. and BROWN W.S. 'The Mechanical response of pre-fractured rock in compression' R.M., 3, pp. 208-16 (1971).

SZECHY K. 'The art of tunnelling' Akadémiaikiadó, Budapest (1973).

UNIVERSITY OF NEWCASTLE UPON TYNE 'Face and Roadway Stability - Geological criteria, Ground deformation Observations - Lynemouth Colliery' Interim Report (1979).

VAUGHAN-THOMAS T. 'Some problems of shaft inset and inset extension roadway construction at Abernant Colliery'
The Mining Engineer, 121, pp. 379-402 (1962).

VICK S.G. and EINSTEIN H.H. 'A probabilistic approach to geologic investigations for hard-rock tunnels'
Denver (1974) pp. 1069-75.

WARD W.H. 'Ground Supports for tunnels in weak rocks'
Geo., 28, pp. 133-171. (1978).

WARD W.H. COATS D.J. and TEDD P. 'Performance of tunnel support systems in the four fathom mudstone'
Tunnelling '76 Symposium, London, May (1976) I.M.M.

WAWERSIK W.R. 'Detailed Analysis of Rock Failure in Laboratory Compression tests'
Ph.D. Thesis, Univ. Minnesota (1968) - taken from Hudson, Crouch and Fairhurst, 1972.

WAWERSIK W.R. 'Time-dependent rock behaviour in uniaxial compression'. In: New horizons in Rock Mechanics. Hardy H.R., Stefanko R. (Eds.). Proc. 14th Symp. Rock Mech., Penn. State Univ., 1972, New York: Am. Soc. Civ. Eng. (1973) pp. 85-106.

WAWERSIK W.R. 'Time dependent behaviour of rock in compression'
Denver (1974) V.II, P.A., pp. 357-63.

WAWERSIK W.R. 'Technique and apparatus for strain measurements on rock in constant confining pressure experiments' R.M., 7, pp. 231-41 (1975).

WAWERSIK W.R. and BRACE W.F. 'Post-failure behaviour of a granite and a diabase' R.M., 3, pp. 61-85 (1971).

WAWERSIK W.R. and FAIRHURST C. 'A study of brittle rock fracture in laboratory compression experiments' I.J.R.M.M.S., 7, pp.561-75 (1970).

WISE N. 'Underground Instrumentation in the Experimental Panel (C0056W) at Boulby Mine' Report, University of Newcastle upon Tyne. (1978).

WHITE J.E. 'Elastic dilatancy, fluid saturation and earthquake dynamics' G.R.L., 3, pp. 747-50 (1976).

WHITTAKER B.N. and SINGH R.N. 'Design and stability of pillars in Longwall Mining' T.I.M.E., pp. 59-73. July (1979).

WHITTAKER B.N. DAWS G. and SEWILSKI A.E. 'Support and lining of mine roadways in the United Kingdom' Denver (1974) pp. 1181-86.

WILSON A.H. 'Expansion in the Yield Zone - Preliminary thoughts' Unpublished (1976a)

WILSON A.H. 'Study of Yield zones around Roadways' Unpublished (1976b)

WILSON A.H. 'The effect of yield zones on the control of ground' 6th Int. Strata Control Conf., Banff Springs, Canada (1977a).

WILSON A.H. 'The stability of tunnels in soft rock at depth' Newcastle (1977b) pp. 511-27.

WILSON A.H. 'A Method of Estimating the closure and strength of lining required in drivages surrounded by a yield zone' Unpublished (1979a).

WILSON A.H. 'Summary of a method of estimating the closure and strength of lining required in drivages surrounded by a yield zone' Unpublished (1979b).

WU F.T. and THOMSEN L. 'Microfracturing and deformation of westerly granite under creep condition' I.J.R.M.M.S., 12, pp. 167-73 (1975).

YOUDAN D.G. 'An appraisal of support requirements for the shaft bottom roadways at North Selby Mine'
M.Sc. Thesis, Univ. Newcastle upon Tyne. (1978).

ZOBACK M.D. and BYERLEE J.D. 'The effect of microcrack dilatancy on the permeability of Westerly granite'
J.G.R., 80, pp. 752-55 (1975a).

ZOBACK M.D. and BYERLEE J.D. 'The effect of cyclic differential stress on dilatancy in Westerly granite under uniaxial and triaxial conditions'
J.G.R., 80, pp. 1526-30 (1975b).

ZOBACK M.D. and BYERLEE J.D. 'A note on the deformational behaviour and permeability of crushed granite'
I.J.R.M.M.S., 13, pp. 291-94 (1976).

* * *

APPENDIX A

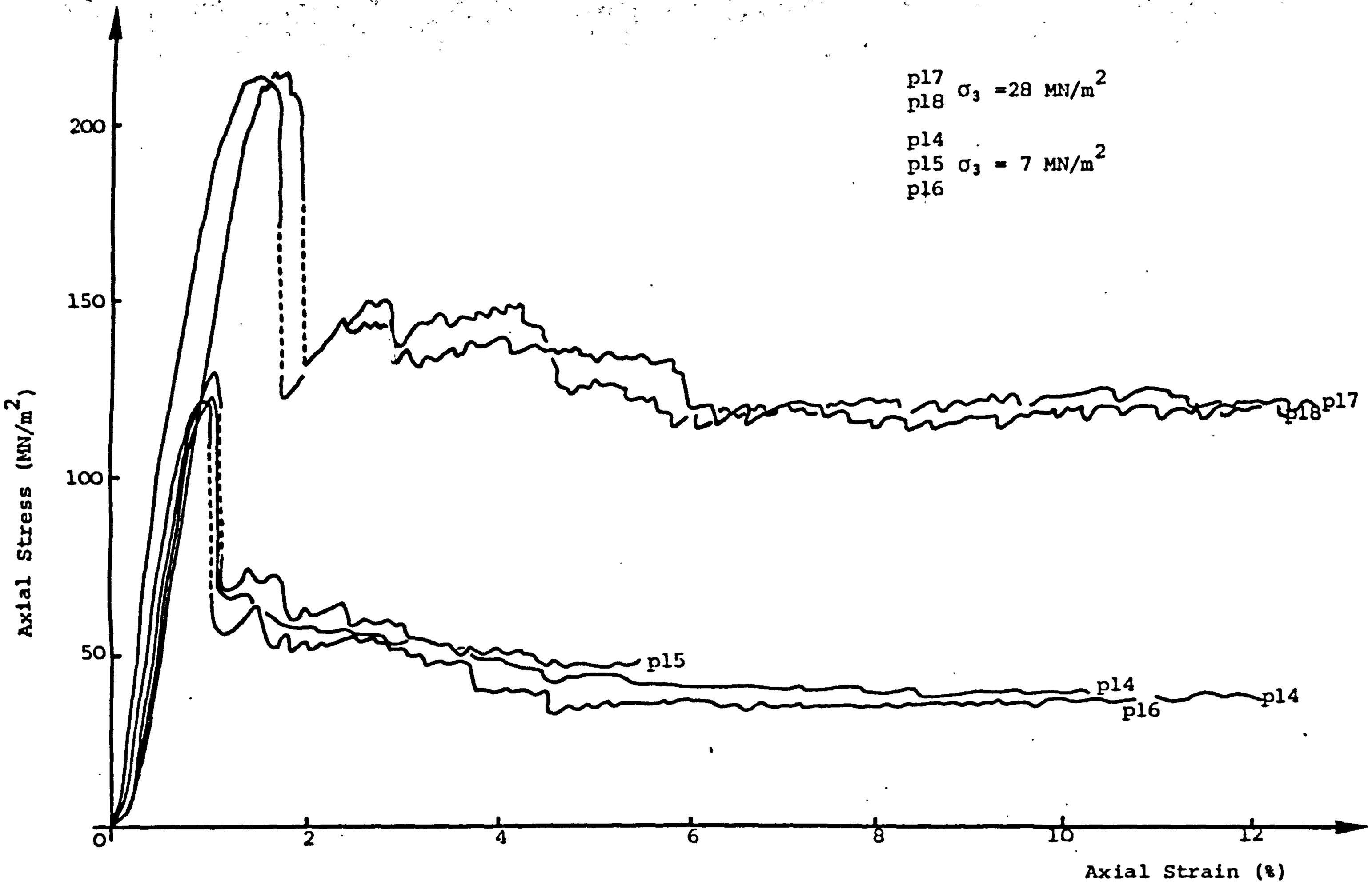

Fig.A.1 Portland Stone: Axial Stress vs Strain for confining pressures of 7 and 28 MN/m^2

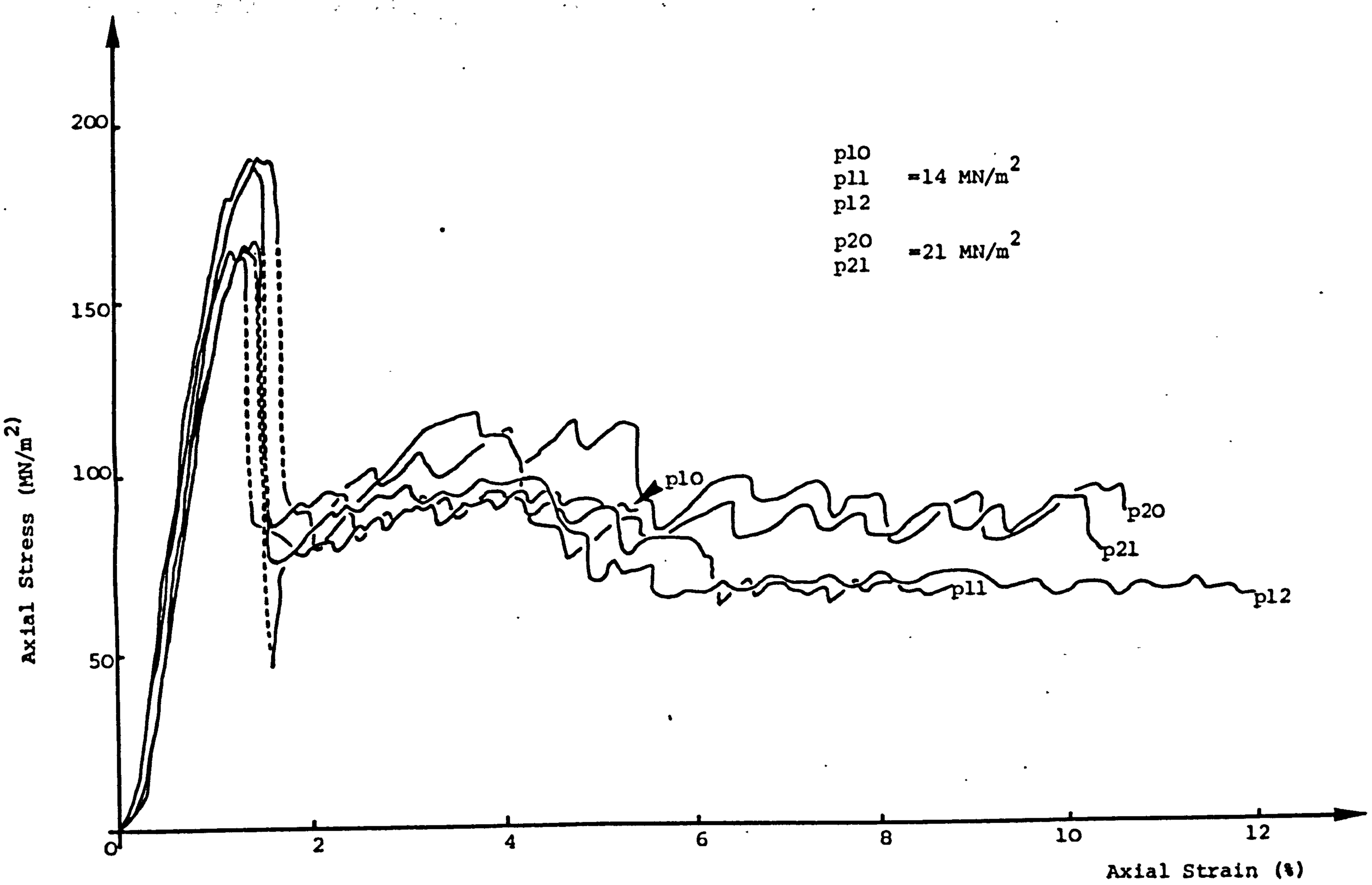

Fig. A.2 Portland Stone: Axial Stress vs Strain for confining pressures of 14 and 21 MN/m^2

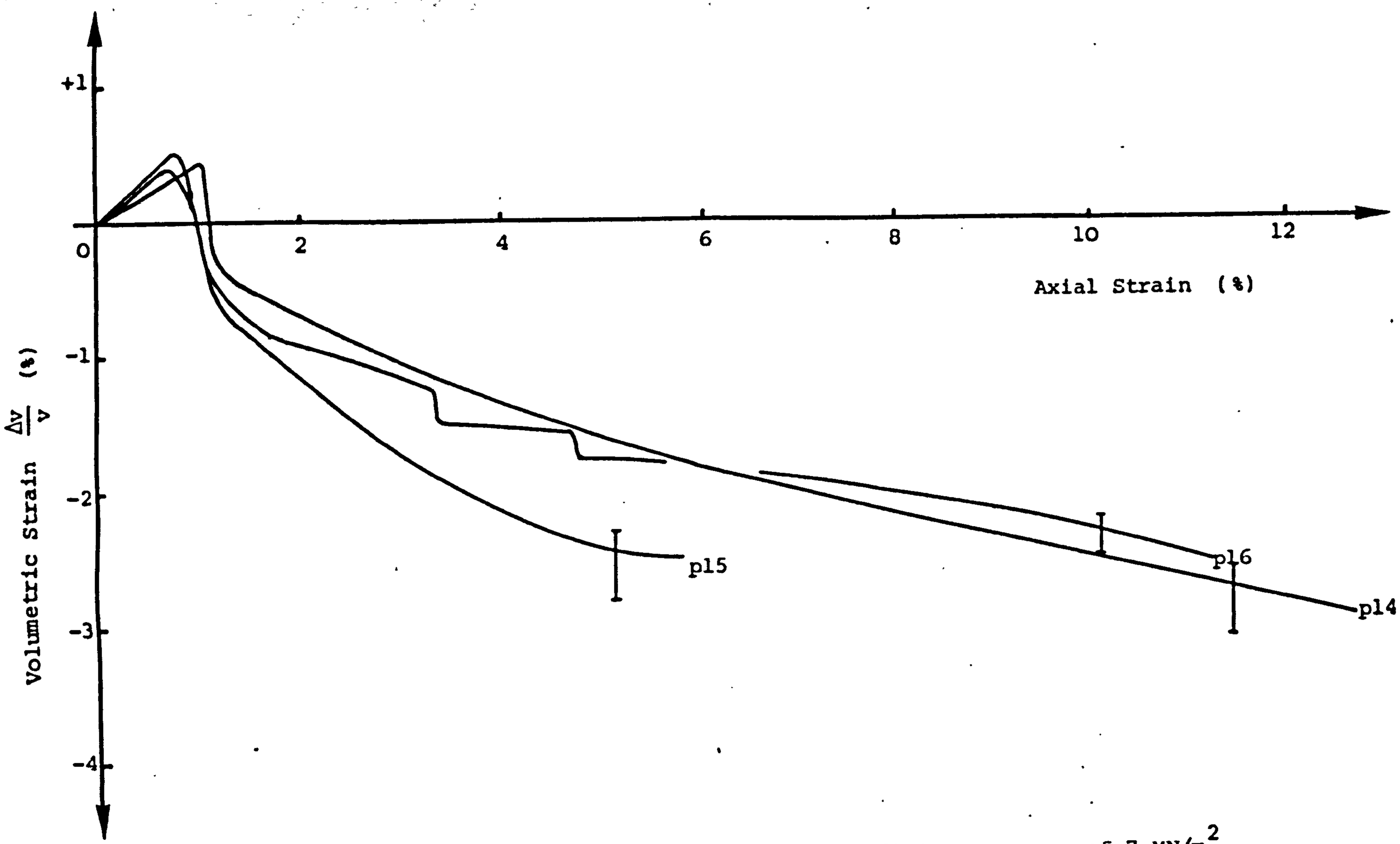

Fig. A.3 Portland Stone: Volumetric vs Axial Strain at a confining pressure of 7 MN/m^2

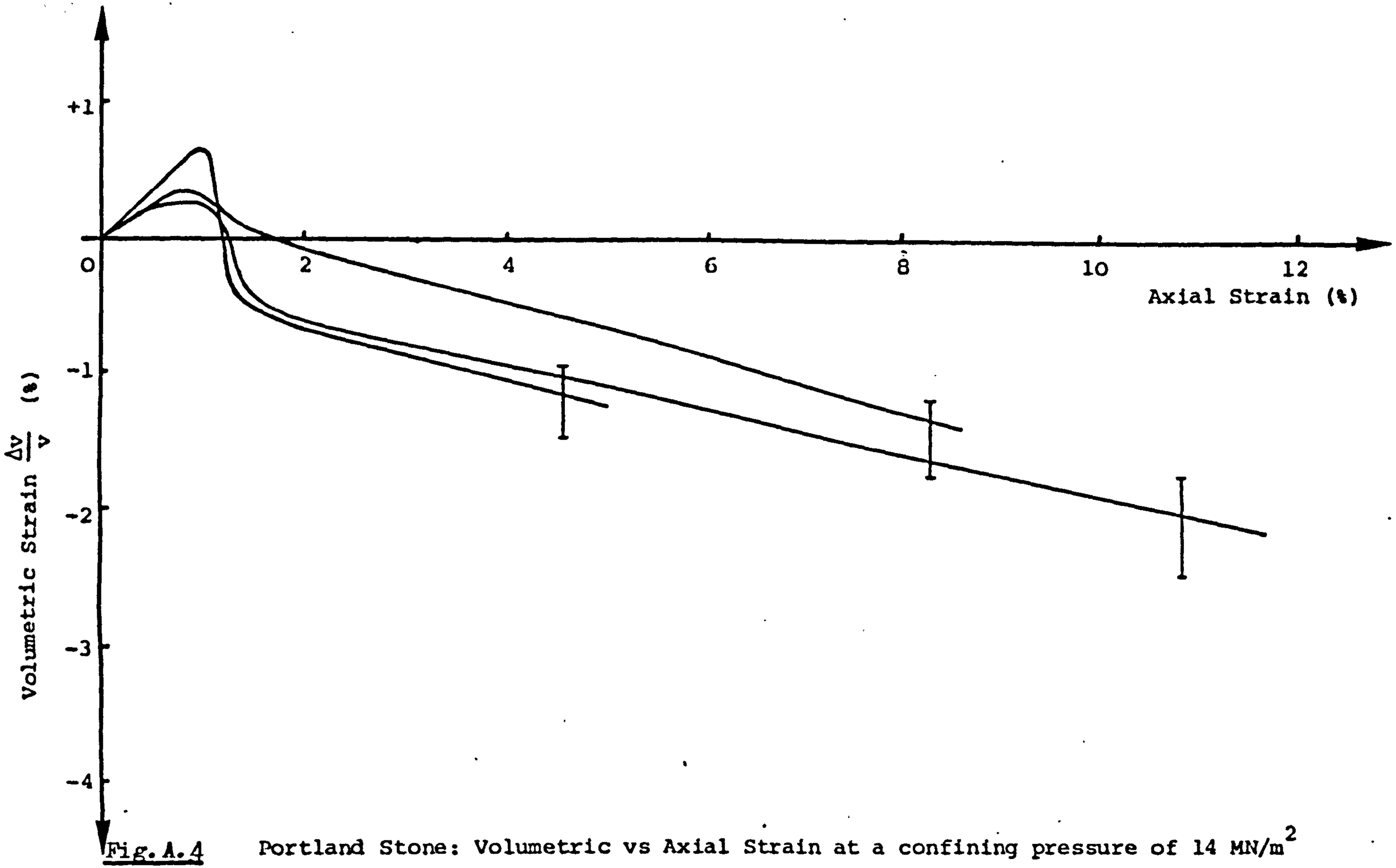

Fig. A.4 Portland Stone: Volumetric vs Axial Strain at a confining pressure of 14 MN/m^2

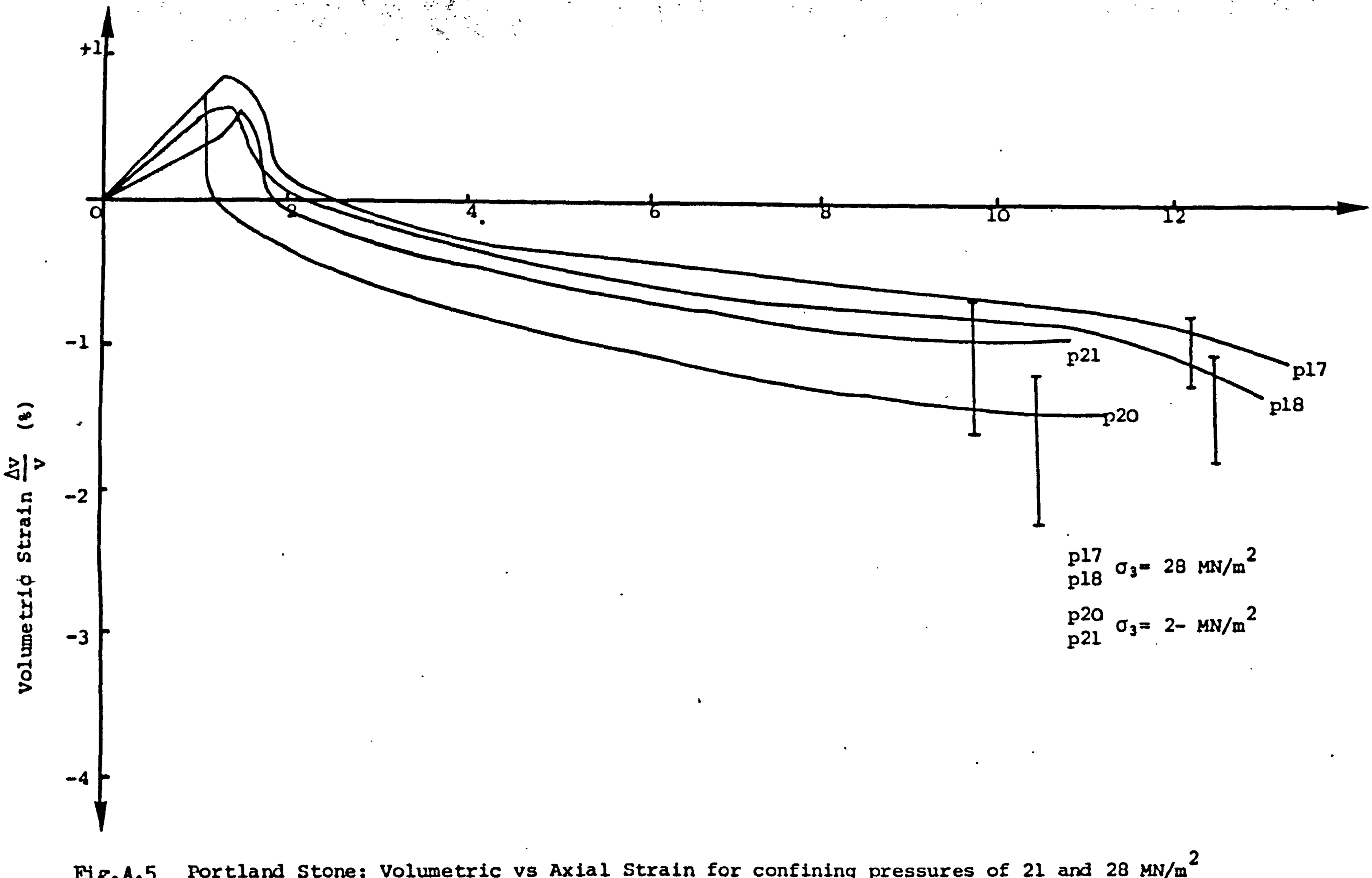

Fig.A.5 Portland Stone: Volumetric vs Axial Strain for confining pressures of 21 and 28 MN/m^2

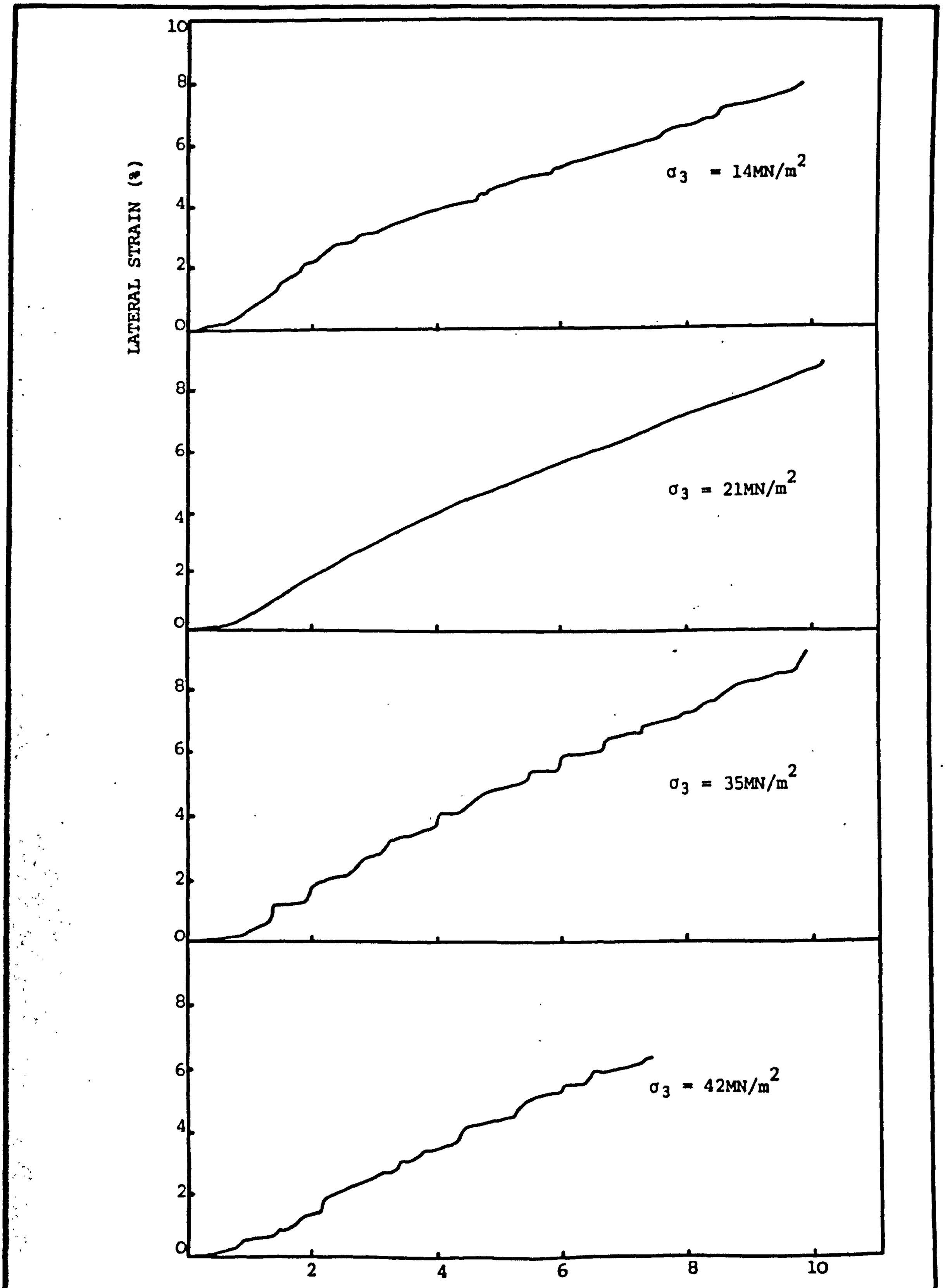

Fig. A.6 SACROIDAL LIMESTONE: Comparison of Lateral vs Axial Strains for different confining pressures.

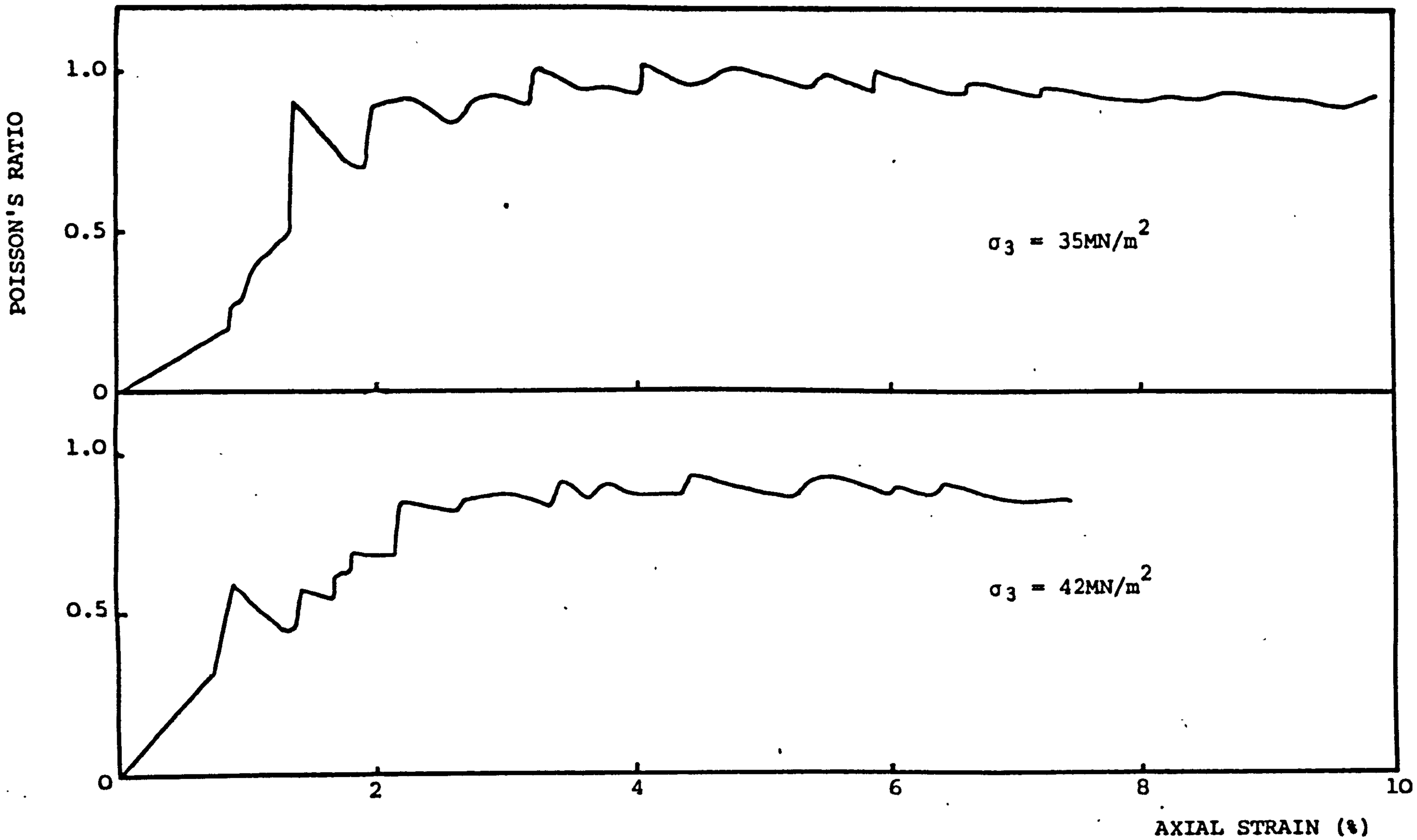

Fig. A.7. SACROIDAL LIMESTONE: Comparison of Poisson's Ratio vs Axial Strain for Confining Pressures of 35 and 42MN/m^2

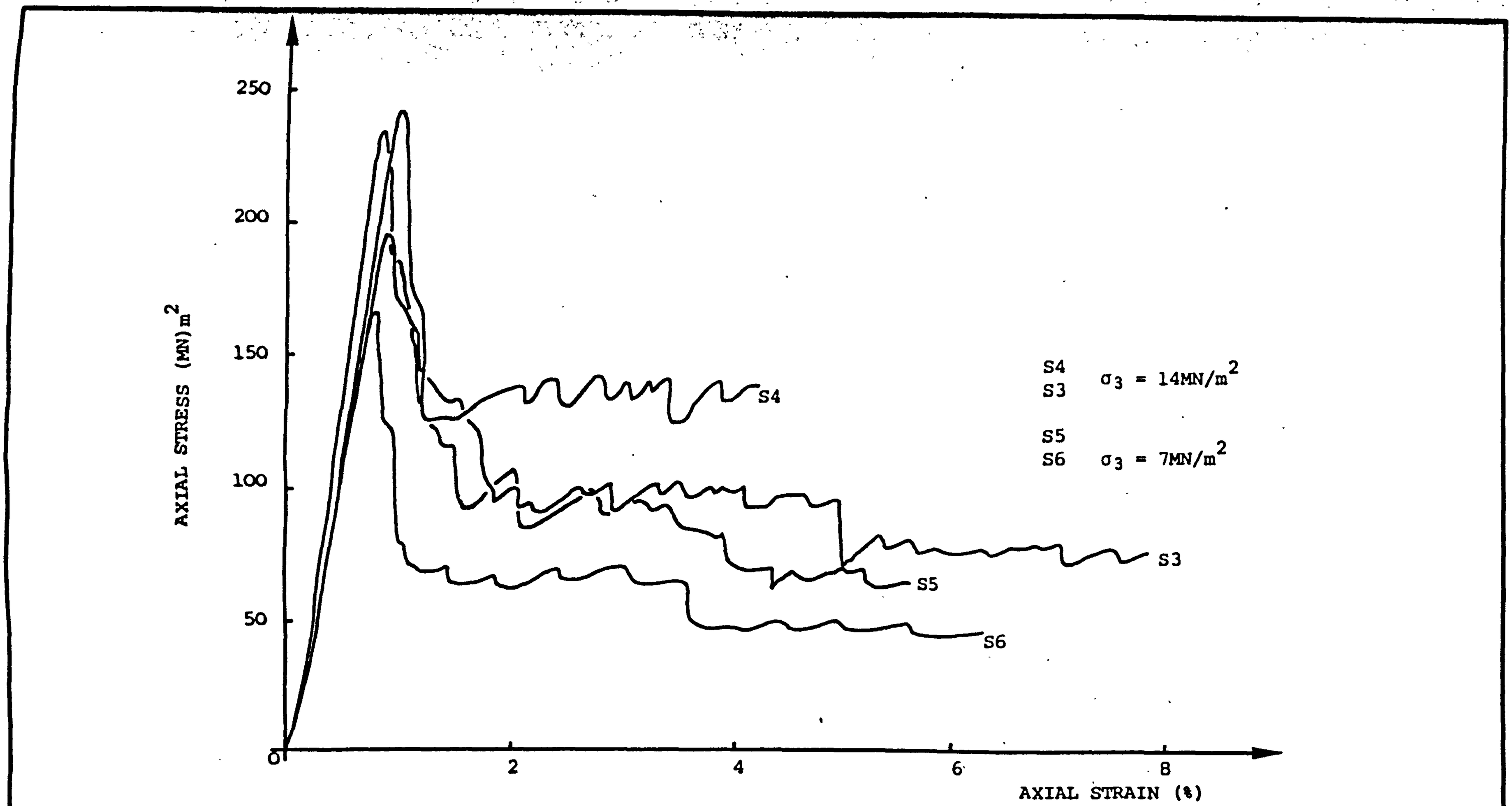

Fig. A.8 SANDSTONE: Comparison of Axial Stress vs Strain for Confining Pressure of 7 and 14MN/m^2

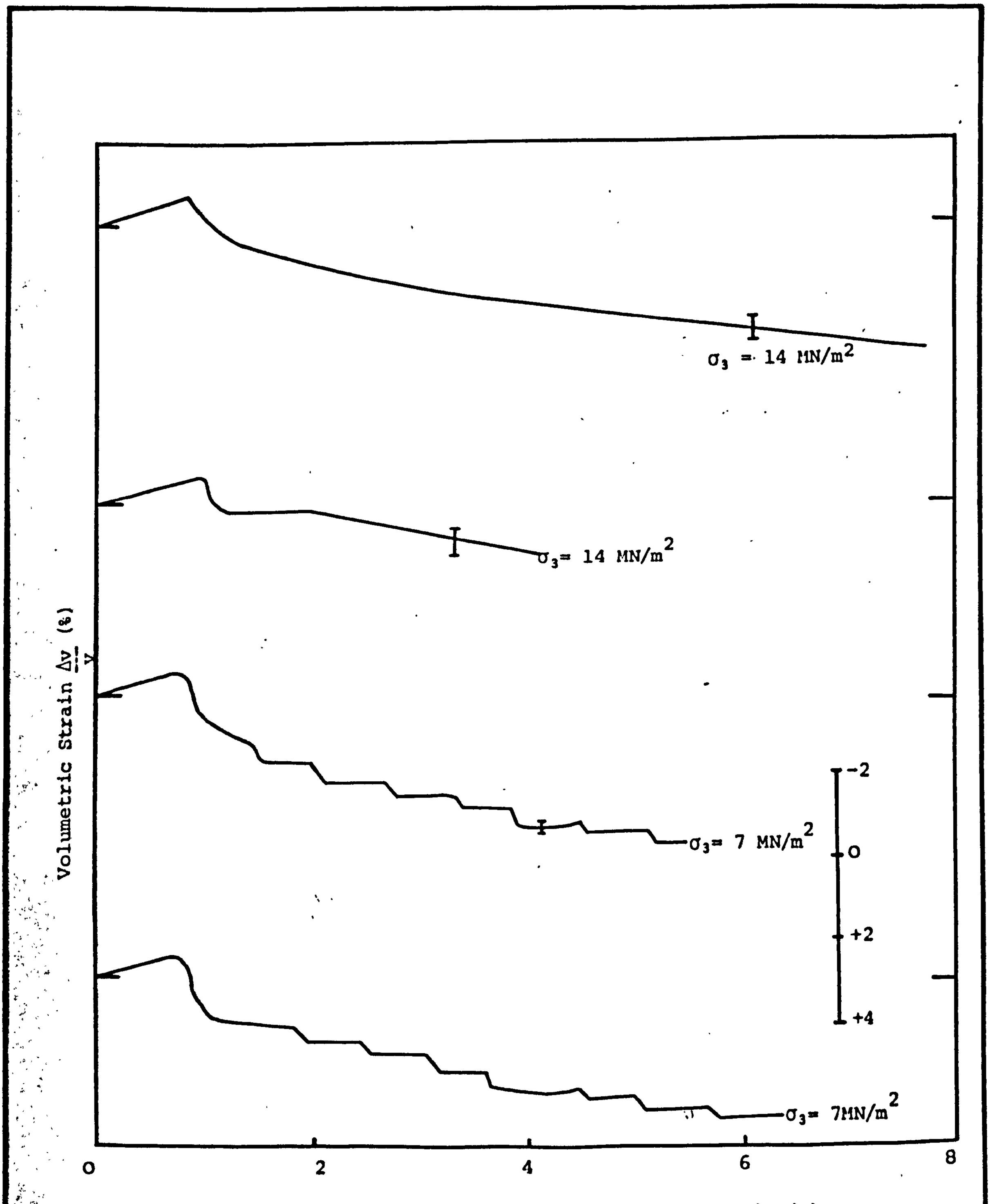

Fig. A.9 Sandstone: Comparison of volumetric vs Axial Strain for confining pressures of 7 and 14 MN/m^2

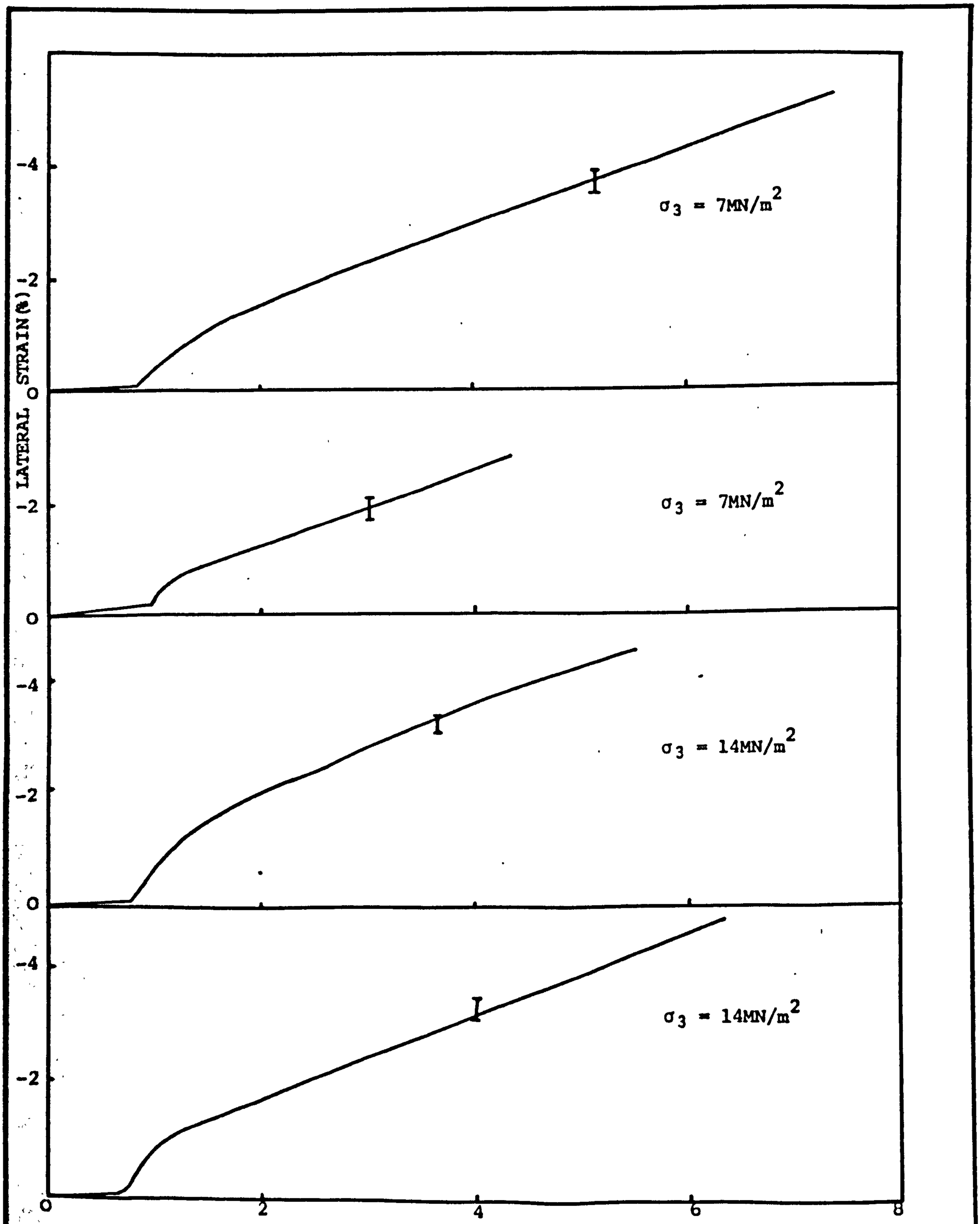

Fig.A.10SANDSTONE: Comparison of lateral vs Axial strain for confining pressures of 7 and 14 MN/m^2

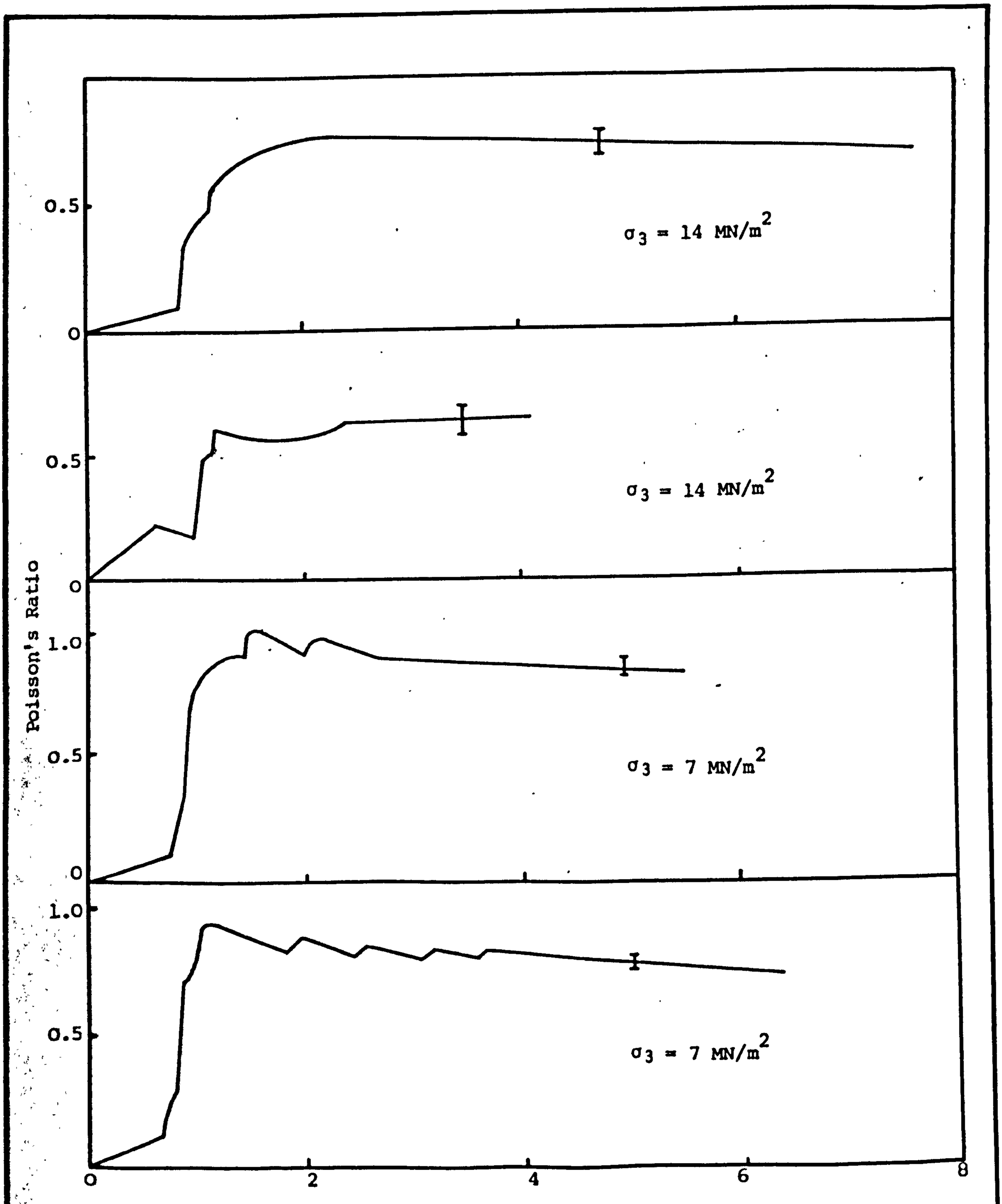

Fig.A.11 Sandstone: Comparison of Poisson's Ratio vs Axial Strain for confining pressures of 14 and 7 MN/m^2

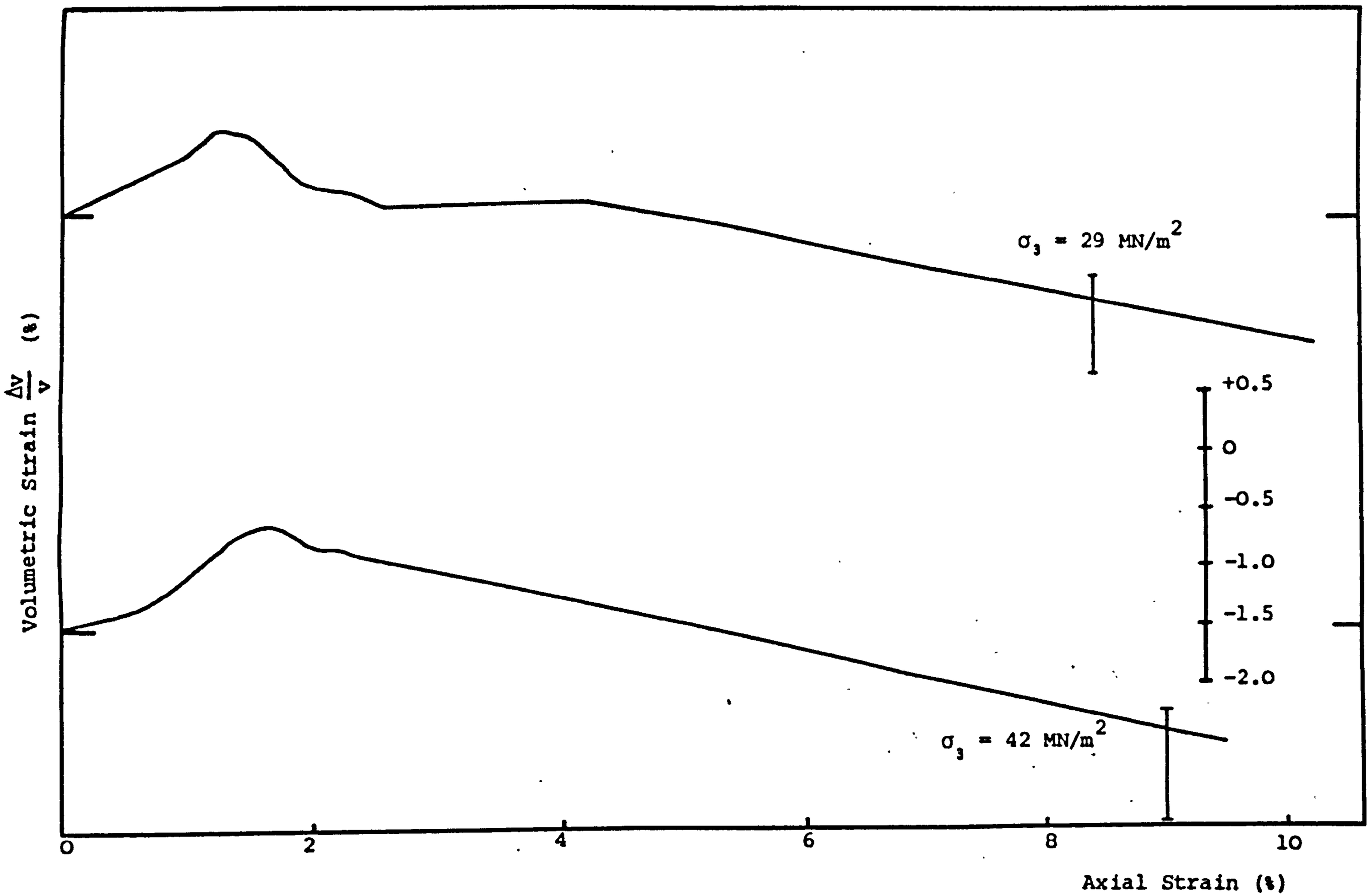

Fig. A.12 Silty Sandstone: Comparison of volumetric vs Axial Strain for confining pressures of 29 and 42 MN/m^2

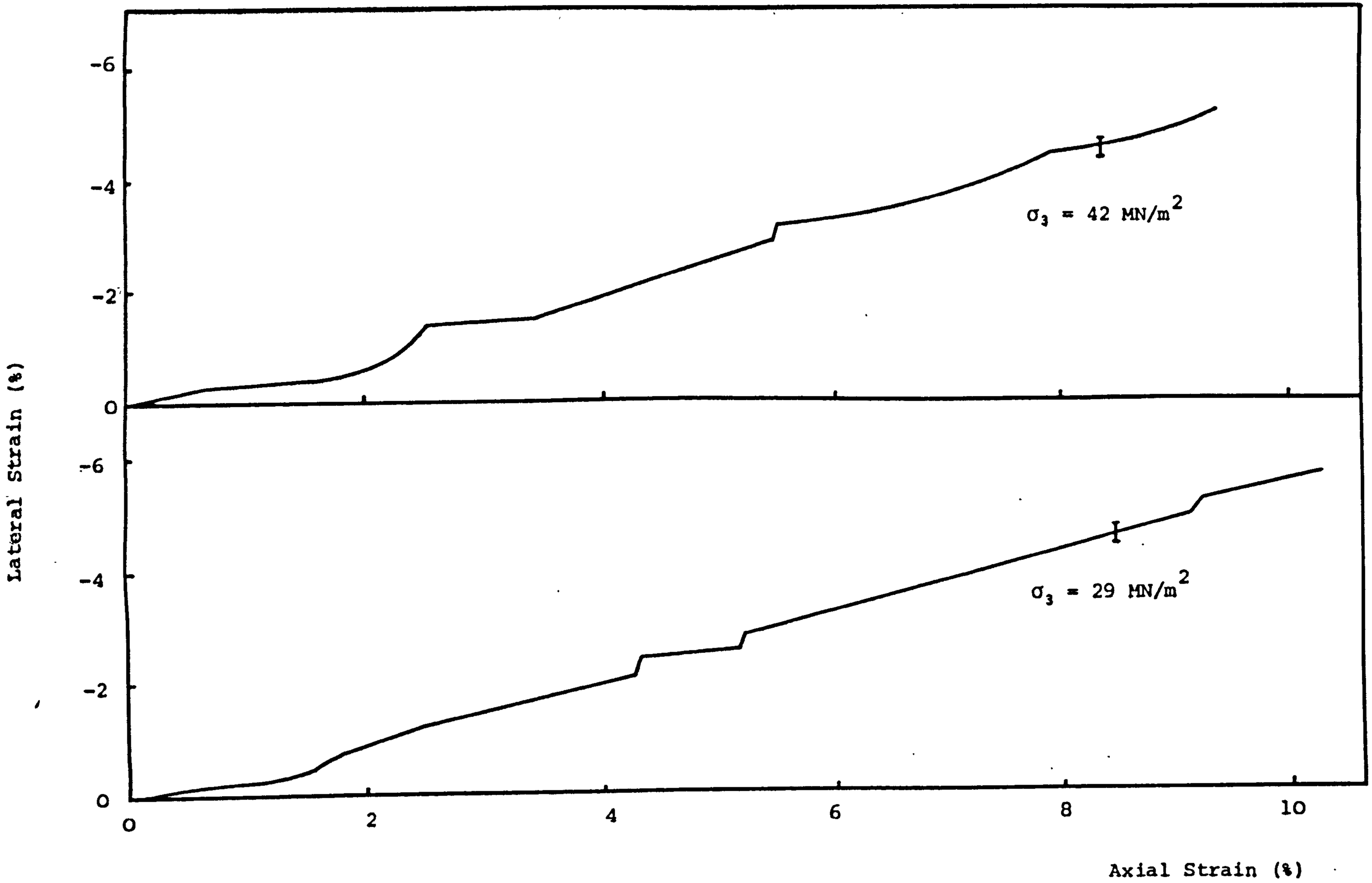

Fig. A.13 Silty Sandstone: Comparison of lateral vs axial strain for confining pressures of 42 and 29 MN/m^2

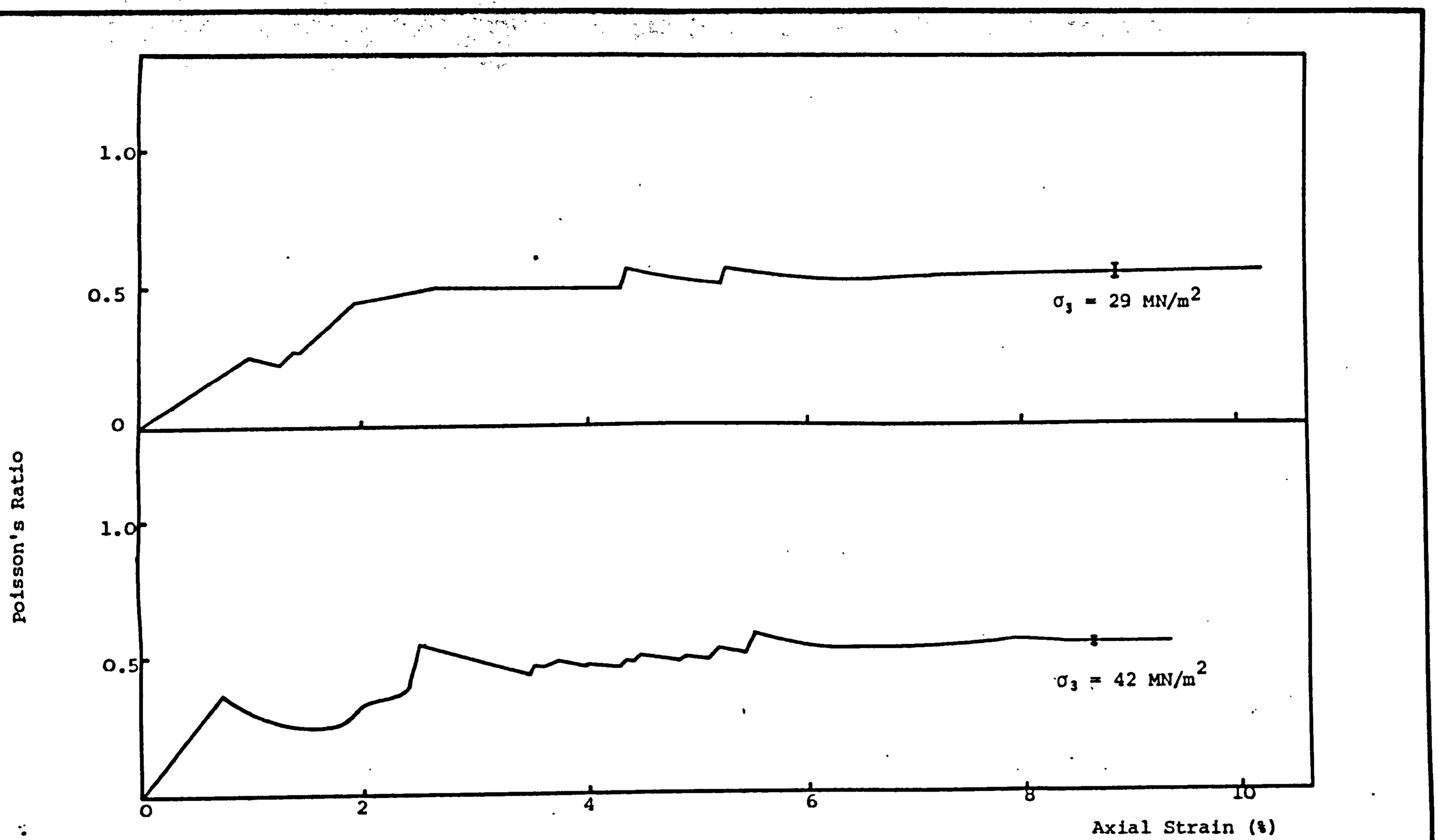

Fig. A.14 Silty Sandstone: Comparison of Poisson's ratio vs Axial Strain for confining pressures 29 and 42 MN/m^2

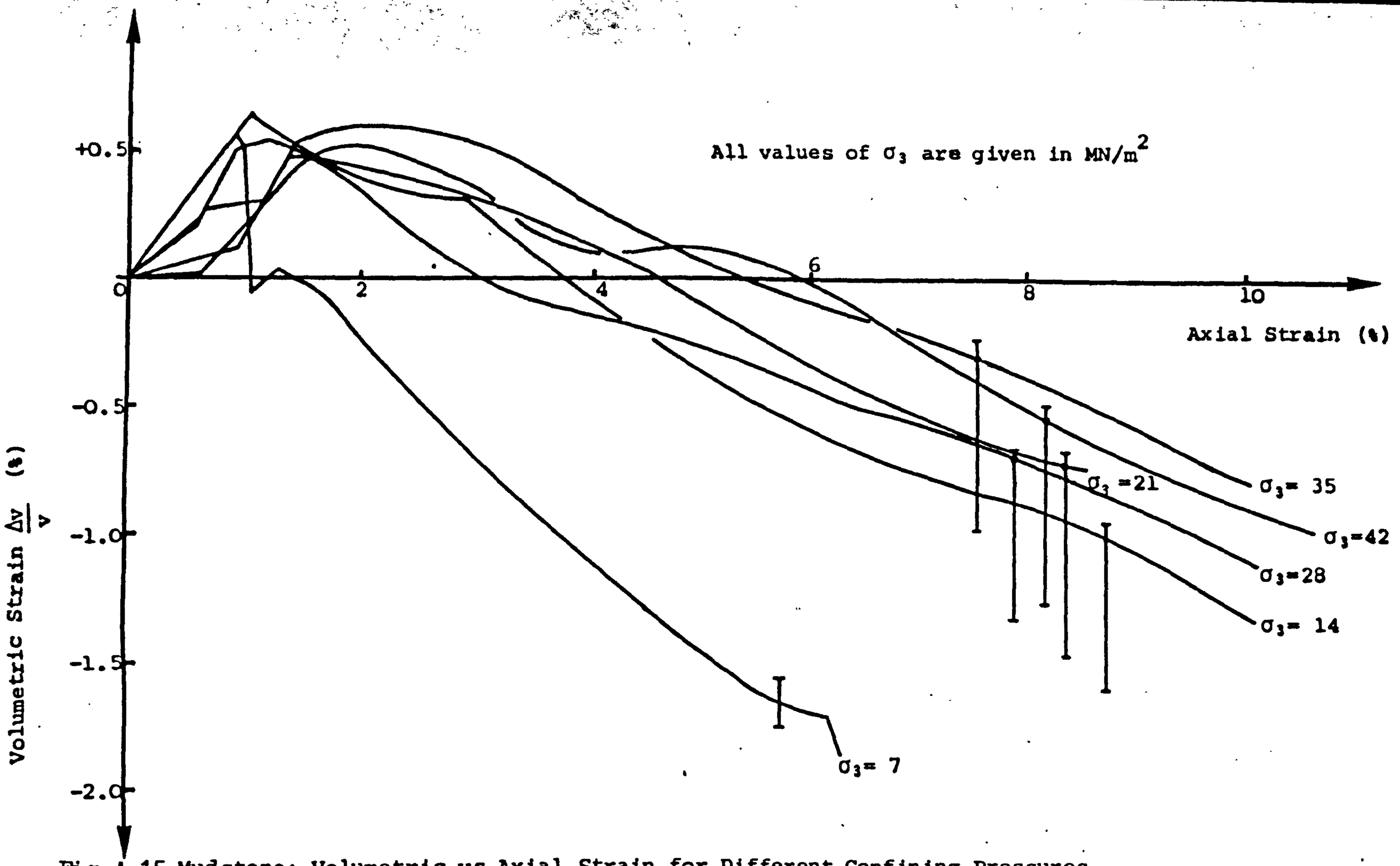

Fig.A.15 Mudstone: Volumetric vs Axial Strain for Different Confining Pressures

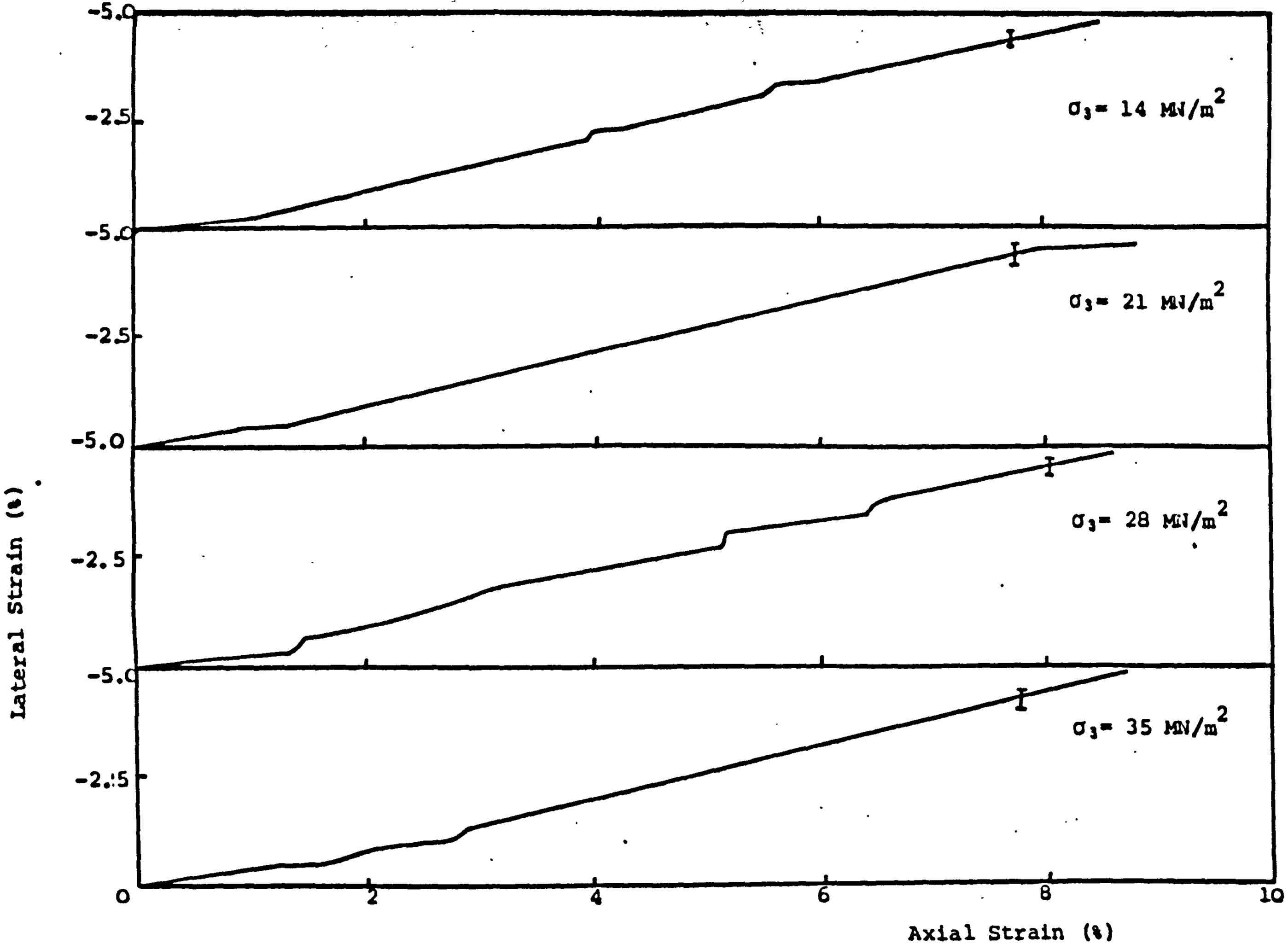

Fig.A.16 Mudstone: Comparison of Lateral vs Axial Strain for different confining pressures

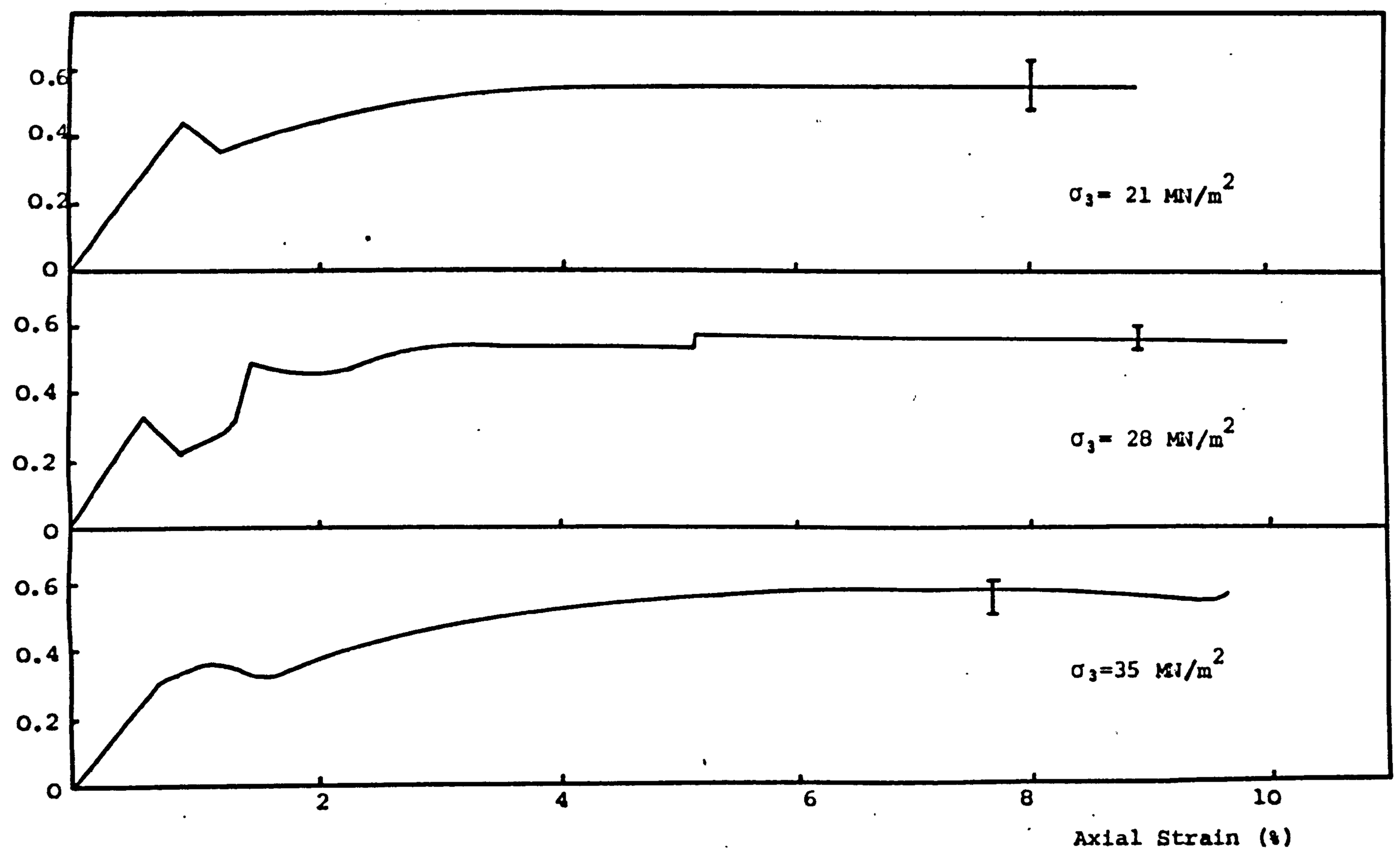

Fig. A.17 Mudstone: Comparison of Poisson's Ratio vs Axial Strain for confining pressures of 21, 28 and 35 MN/m^2

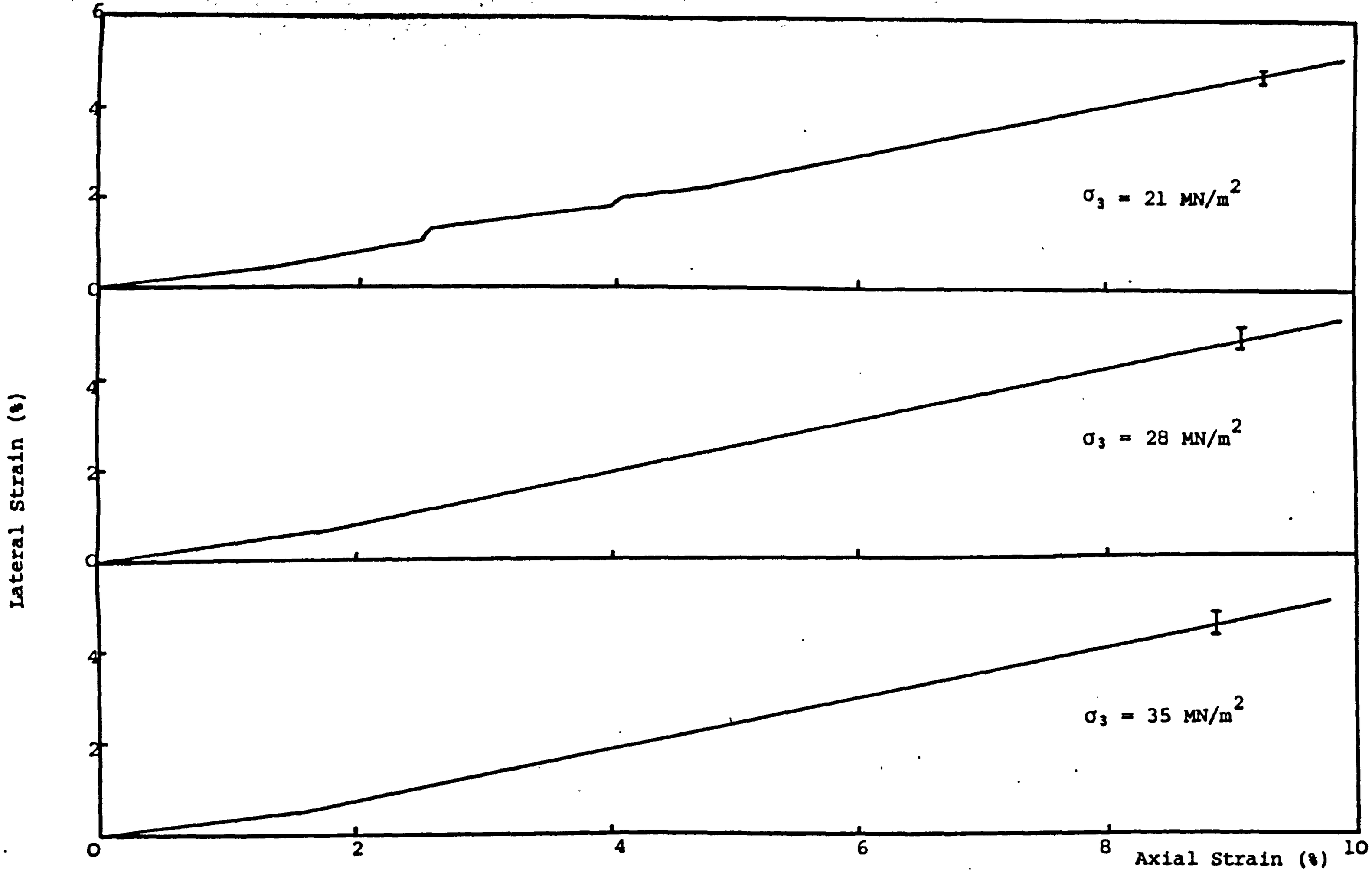

Fig. A.18 Rock Salt: Comparison of Lateral vs Axial Strains for confining pressures of 21, 28 and 35 MN/m^2

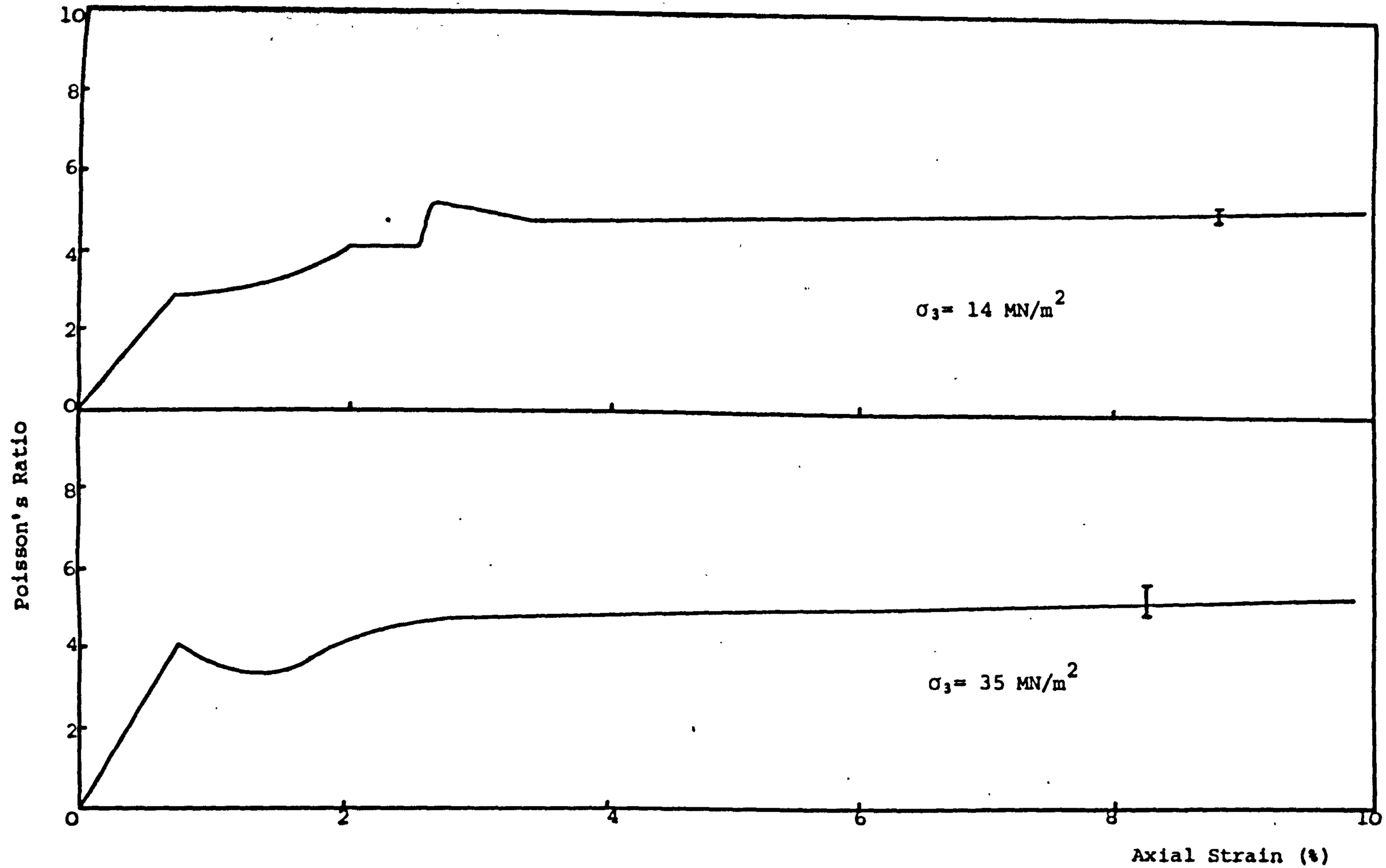

Fig. A.19 Rock Salt: Posson's Ratio vs Axial Strain for Confining Pressures of 14 and 35 MN/m^2